CIPM MRA
Comparison reports

CCEM-K5.2017

Active power at 53 Hz

KEY COMPARISON

Any further distribution of this Report must be cited as:
G. Kok *et al* 2026 *CIPM MRA Comparison reports* **01005**

https://doi.org/10.59161/TYLY6391

CCEM-K5.2017

Key Comparison of 50/60 Hz Power

Final Report

Date: 8 January 2026

Gertjan Kok (VSL)

Gert Rietveld (VSL)

Rene Caranza (CENAM)

Matthias Schmidt (PTB)

Table of Contents

This report contains five annexes:

- Annex A - Reported measurement values
- Annex B - Comparison protocol
- Annex C - Participant Reports
- Annex D - Read-me file to digital supplement
- Annex E - Digital supplement

Annex E is in the form of a separate .json file

1. Introduction

Committed to underpin the Mutual Recognition Arrangement (MRA) as proposed by the International Committee of Weights and Measures (CIPM), a key comparison of 50/60 Hz power standards has been organized under the auspices of the Consultative Committee of Electromagnetism (CCEM).

The last CCEM key comparison of power standards was organized by NIST between the years 1996 to 1999, NIST being the pilot laboratory. The results of this comparison were reported in 2002 [1]. Since the completion of this comparison is already more than 20 years ago, significant technical updates have been made to the primary power reference setups of many NMIs, and improved travelling standards have become available, the present comparison was agreed upon.

In this key comparison the current state of the art is assessed with respect to the comparability of power measurements at the highest possible accuracy by National Metrology Institutes (NMIs). The comparison protocol was based on the procedures used during the last international comparison CCEM-K5 [2] and followed the CCEM Guidelines for Planning, Organizing, Conducting and Reporting Key, Supplementary and Pilot Comparisons [3].

This report presents the outcomes of the key comparison. The analysis of the comparison results with respect to the CMC claims of the participating institutes and the measures to be taken in the case of inconsistencies are not within the scope of this report.

2. Participating laboratories and time schedule

At the outset of the comparison eleven laboratories participated in the comparison. The coordination of the comparison was shared by three NMIs: CENAM, Mexico, was responsible for the technical protocol and for the practical organization of the comparison; PTB, Germany, was the central pilot laboratory (PL) which performed repeated measurements of the travelling standards; finally, VSL, Netherlands, was responsible for the general coordination and the final report.

The comparison was organized such that each of the laboratories measured the power errors of the same two standards at ten different operating or test points with the pilot lab re-measuring the travelling standards at distinct points in time during the comparison in order to determine any instabilities the standards might have.

During the comparison several changes to the original plan occurred. The most important changes were:

- One of the two RD22s initially provided by NIST as travelling standards broke down during the initial stability check for unexplainable reasons and the RD22 could not be repaired. Therefore, there are different long histories of the two standards since the replacement unit was added later. This can also be seen in section 6.3.1.
- There were considerable delays due to issues with customs both in China (NIM) and Russia (VNIIM).
- The Covid-19 pandemic took place from 2020 till 2022. This caused significant delays in addition to the delays at customs. In the end the measurements, including the characterization of the travelling standards at PTB, were performed in the period from August 2016 till August 2022 (6 years), whereas originally the period from January 2017 to November 2019 (3 years) was foreseen. Preparation of Draft A also took longer than originally expected.
- VSL discovered a possible error in its measurement setup after submitting its measurement results, but before the comparison data was completed. VSL re-measured the travelling standards at the end of the comparison, before the last stability measurement, and provided new results.
- NIST was asked to recheck the provided data due to some discrepancies that showed up in an initial analysis of the data. NIST discovered a possible error in its measurement setup, re-measured the travelling standards at the very end of the comparison, after the last stability measurement, and provided new results.
- Given the low uncertainties claimed by NMIA, resulting in a large weight in the determination of the KCRV, and due to some discrepancies that showed up in an initial analysis of the data, NMIA was asked to double check their measurement results. The review by NMIA of their results resulted in a slightly changed set of estimates (1.2 μW/VA at zero power factor, 0.6 μW/VA at power factor of 0.5 and no change at unity power factor), together with slightly increased measurement uncertainties (increase between 0.1 μW/VA and 0.3 μW/VA depending on the power factor).
- For geopolitical reasons, the results of VNIIM, the Russian NMI, were not taken into consideration in this report.

Table 1 lists the ten retained participating laboratories in chronological order and the mean dates of their measurements of the travelling standards, along with the dates of the measurements performed by the pilot lab PTB.

Table 1: List of participating laboratories and measurement dates. The last column indicates which measurement results have been used as the 'submitted values' in the intercomparison analysis.

Acronym	**Institute Name and Contact Person**	**Country**	**Region**	**Mean date of measurements**	
PTB	Physikalisch-Technische Bundesanstalt	Germany	EURAMET	25/08/2016, 30/09/2016, 24/10/2016, 23/02/2017, 01/12/2017, 11/01/2018 *(stability)*	
CENAM	Centro Nacional de Metrología	Mexico	SIM	12/03/2018	✓
NIST	National Institute of Standards and Technology	USA	SIM	29/05/2018 *(withdrawn)*	
PTB	Physikalisch-Technische Bundesanstalt	Germany	EURAMET	09/08/2018 *(stability)*	
LNE	Laboratoire National d'Essais	France	EURAMET	12/09/2018	✓
RISE	Research Institute of Sweden	Sweden	EURAMET	23/10/2018	✓
VSL	Dutch National Metrology Institute	Netherlands	EURAMET	19/11/2018 *(withdrawn)*	
PTB	Physikalisch-Technische Bundesanstalt	Germany	EURAMET	09/01/2019 *(stability)*	
NMIA	National Measurement Institute Australia	Australia	APMP	21/03/2019	✓
NIM	National Institute of Metrology	China	APMP	16/06/2019	✓
PTB	Physikalisch-Technische Bundesanstalt	Germany	EURAMET	07/01/2020 (stability and participant value)	✓
NMISA	National Metrology Institute of South Africa	South Africa	AFRIMET	18/03/2020	✓
INMETRO	Instituto Nacional de Metrologia, Qualidade e Tecnologia	Brazil	SIM	09/11/2020	✓
VSL	Dutch National Metrology Institute	Netherlands	EURAMET	26/02/2021	✓
PTB	Physikalisch-Technische Bundesanstalt	Germany	EURAMET	31/05/2021 *(stability)*	
NIST	National Institute of Standards and Technology	USA	SIM	16/08/2022	✓

3. Travelling standards

3.1. Description of the travelling standards

Two travelling standards (TSs) of the type RADIAN RD-22-332S were used in this key comparison. These standards were adapted to measure active power at 120 V and 240 V and 5 A with outstanding stability in time. These standards were provided by NIST, which is gratefully acknowledged. The serial numbers of the provided standards were 206 816, denoted by TS A in this report, and 203 409, denoted by TS B. The TS with serial number 206 816 is the replacement of a RD-22 with serial number 206 815 that was initially provided. This latter standard broke down during initial stability tests, as mentioned in section 2. The travelling standards were powered using a 24 V DC power supply delivered with the standards. More details on the travelling standards, including some pictures, are provided in the comparison protocol, see Annex B of this report.

As the two travelling standards were of the same make, it was expected that their behaviour could be similar. In particular, their drift behaviour might be similar. This aspect will be discussed in more detail in section 6.3 that discusses the stability of the TSs. As these travelling standards presently seem the best available standards for this type of comparison measurements, it was nevertheless decided to use these two standards rather than two standards of different makes and operating principles.

A further important note is that the RD-22 standards typically have very small measurement errors. In order to prevent usage of this knowledge by the comparison participants, the two travelling standards in this comparison were intentionally given large offsets in the internal firmware (not accessible by the comparison participants).

3.2. Quantity to be measured

The quantity to be reported is the error of the travelling standard when measuring active power, which was expressed as a ratio of power error divided by apparent power with unit µW/VA. This quantity will be called the 'calibration error' in subsequent sections. Both the value and its associated expanded uncertainty for a level of confidence of 95.45 % (i.e. $k = 2$ for a normal distribution) were to be reported. The total estimated expanded uncertainty stated in the reports provided by the NMIs encompassed both the Type A uncertainty and the Type B uncertainty of the corresponding NMI calibration system. Ten test points were measured as listed in Table 2 and for each of them a single measurement result was submitted by the participating laboratories.

Table 2: Parameters of the 10 test points. All combinations of the 2 RMS voltages and the 5 power factors were measured at an RMS current of 5 A. The "lead" in the power factor is defined as the current phase leading the voltage phase, and "lag" as the current phase lagging the voltage phase. The corresponding phase angle is shown for clarity.

Parameter	Voltage	Current	Power factor	Phase angle [deg]	Frequency [Hz]
Value(s)	120 V	5 A	1.0, 0.5 lead, 0.5 lag, 0 lead, 0 lag	0, 60, 90, -60, -90	53
	240 V	5 A	1.0, 0.5 lead, 0.5 lag,	0, 60, 90, -60, -90	53

			0 lead, 0 lag		

There were no explicit requirements on ambient temperature and ambient relative humidity during the measurement. In practice, the ambient temperature during the measurements varied between 22.2 °C and 24.5 °C and the relative humidity between 30 % and 57 %. Inspection of the results did not indicate that a temperature or humidity correction would be needed.

There were no detailed requirements related to the earthing of the devices. The laboratories were requested to use the same method that they use during normal calibrations of such devices.

4. Measurement procedures

A comparison protocol was prepared following the CCEM Guidelines for Planning, Organizing, Conducting and Reporting Key, Supplementary and Pilot Comparisons [3], detailing the procedure to be followed for measuring and transporting the travelling standards. The full protocol has been included in Annex B. Below the main part of the procedure has been reproduced.

The measurement method is the one that is used by the participating laboratory for the provision of a regular calibration. The prescribed method for the measurements was as follows:

1. Upon arrival, allow the reference standard to warm up at least 4 hours after powering it with the 24 V DC power supply. Then switch the unit off and on in order for its internal DC voltage reference to correct according to its internal temperature.
2. For the voltage and current sources, make sure that their frequency is set at 53 Hz, according to the test points shown in Table 2.
3. Make sure that test voltage and current are within at most 0.2 % of the values shown in Table 2.
4. At every power factor (phase angle) shown in Table 2, make as many independent measurements as stated in the calibration procedures of your laboratory.
5. Record the readings of active power, voltage, current, power factor/phase angle and frequency displayed on the backlit LCD of the travelling standard.
6. Calculate the error of the travelling standard at the test points shown in Table 2. The error is defined as the difference between the measured power as indicated by the travelling standard and the power applied to it, and divided by the applied apparent power. The error should be expressed in the unit µW/VA. The error is positive if the travelling standard's indication is larger than the power applied to it, as measured by the participating laboratory.
7. The average of at least five sets of measurements should be reported. The travelling standard should be de-energized between each set of measurements for 1 minute, followed by at least 15 minute warm-up period.
8. The total estimated expanded uncertainty quoted in the laboratory's report should encompass the Type A and Type B uncertainties of the corresponding NMI calibration service. The expanded uncertainty should be estimated for a level of confidence of 95.45 %.
9. Report the mean value and spread of the ambient temperature, and the relative humidity of the laboratory.
10. The measurement report of the participant may be completed according to the "Layout of the measurement report", as shown in section A4 of Annex B.

5. Measurement method

The reference measurement setups used by the participants in this comparison to calibrate the travelling power meters show great similarities (see Annex C). A typical approach is given in Figure 1, where the schematic diagram of the power reference measurement system of CENAM is given.

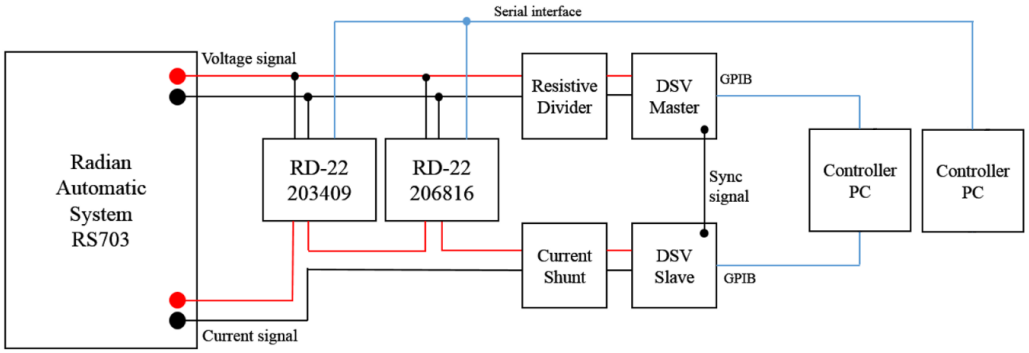

Figure 1: Schematic diagram of CENAM's power reference measurement system, using a resistive (voltage) divider, a current shunt and two digital sampling voltmeters (DSV).

For generation of the calibration signals, a phantom power approach is used where voltage and current are generated in two separate circuits. The generation is done with a power calibrator that is able to directly generate the voltage and current signals under test, such as shown in Figure 1, or with a function generator together with transimpedance and transconductance amplifiers.

The calibration signals are applied simultaneously to the device(s) under test and the reference setup. The reference setup consists of voltage and current scaling devices and two digital sampling voltmeters (DSVs, see Figure 1). One DSV is used to measure the voltage output of the voltage scaling device which is around the 0.8 V level, and the other DSV is used to measure the current which is converted to a similar 0.8 V voltage by the current scaling device. The phase relation between the voltage and current measurement is created by an external trigger ("sync signal" in Figure 1) which is supplied to both DSVs. This trigger can either originate from the power calibrator or from a separate trigger unit.

The typical DSV used by the comparison participants is the HP 3458A digital multimeter. AC voltage traceability of the DSVs is realised via AC/DC transfer standards or a programmable Josephson voltage standards (PJVS). Both NIM and NIST have incorporated a PJVS directly into their primary power measurement reference setup.

Voltage scaling is either done using a resistive divider (CENAM, NMISA, RISE, NIST) or an inductive voltage divider (INMETRO, LNE, NIM, NMIA, PTB, VSL). NIST uses a special approach for voltage scaling where traceability is realised with a permuting voltage divider, consisting of an 11-element relay-switched array of 1 MΩ thin-film resistors with low temperature and voltage coefficients.

The current to voltage conversion is either done with a current shunt (CENAM, LNE, NIST, NMISA, RISE, VSL) or with a current transformer together with a current shunt (INMETRO, NIM, NMIA, PTB). The major advantage of the latter approach is that the power dissipated in the current shunt is much less,

which limits the impact of the power coefficient of the shunt to the total uncertainty budget. Typically wideband current shunts are used with minimal or even negligible phase error at 53 Hz.

6. Measurement results and data analysis

This section describes the data analysis for the CCEM-K5.2017 key comparison. It follows the mainstream approach which is presented in [4] for the one-dimensional case and in [5] for the more general, multi-dimensional case. As there are two travelling standards used in this comparison, the approach outlined in [5] is used in this document. The main ingredient of this approach is a least-squares fit using all the supplied measurement results to find the Key Comparison Reference Values (KCRVs).

In the next sections, the performed data analysis are described in detail. After introducing the notation, the relevant mathematical equations are presented. Next, the stability of the TSs is assessed, whereafter the KCRVs and unilateral degrees of equivalence (DoEs) are calculated. In a first step, the DoEs are calculated for each TS separately (called DoE-TSs) whereafter they are merged to a single DoE per laboratory. Normalized DoEs, i.e. En-values, are also computed. As an additional analysis, the consistency between the two DoE-TSs provided by each laboratory for TS A and TS B is assessed. To this purpose, an Fn-value is introduced, mimicking the well-known En-value. The main reason for introducing this additional number is to identify laboratories that have DoE-TSs with a larger mutual difference than to be expected based on the mathematical model. Such a laboratory could possibly end up with an En value close to zero while one DoE-TS might be a very large positive number while the other DoE-TS could be a very large negative number. This situation would not be satisfactory and therefore such results have been marked in this report. The analysis finishes with a brief discussion.

6.1. Symbols and Abbreviations

The mathematical model and data analysis method have been implemented for each of the ten test points separately. In order not to make the notation too complex, the test point is not explicitly indexed as a parameter in the notation. The test points are specified by the required voltage, current and PF values and are listed in Table 2. Where relevant, the travelling standard is indicated with superscript A or B. The notation here below is introduced for travelling standard TS A. The notation for travelling standard TS B is defined in an analogous way. Vectors of scalar quantities are printed in bold face with the same symbol. Vector quantities are introduced in the text, but not included in this list of symbols.

TS Travelling Standard: artefact that has been sent around to the participating laboratories

$.^{A}$ Superscript that indicates that the quantity relates to the travelling standard with serial number 206 816

$.^{B}$ Superscript that indicates that the quantity relates to the travelling standard with serial number 203 409

PL Pilot Laboratory: laboratory where the standards have been repeatedly measured (in this case PTB)

KCRV Key Comparison Reference Value

DoE Degree Of Equivalence

n number of participating laboratories

k coverage factor for the expanded uncertainty

y_0^A true value of TS A: the unknown value of the calibration error of TS A

y_{ref}^A key-comparison reference value for TS A: the best estimate of y_0^A

y_i^A measured value by laboratory i for the calibration error of TS A

s_i^A estimated systematic drift of TS A at the time of measurements at laboratory i

δ_i^A random instrument instability of TS A measured at laboratory i (mean zero)

η_i^A measurement error of laboratory i for TS A (mean zero)

y'^A_i drift corrected value of laboratory i for TS A, corrected for the drift s_i^A of the TS A

u_i^A standard uncertainty of η_i^A provided by laboratory i, characterizing the uncertainty of the provided value y_i^A

r correlation coefficient between the measurement errors η_i at laboratory i when measuring different TSs at the same test point, i.e. the correlation between η_i^A and η_i^B. The value of the correlation coefficient is assumed to be the same for all laboratories.

u_{TS}^A standard uncertainty of δ_i^A, i.e. uncertainty due to random instrument instability of the TS. This value is the same for all laboratories.

$u(s_i^A)$ standard uncertainty of s_i^A, i.e. uncertainty of the performed systematic drift correction

$u(y'^A_i)$ standard uncertainty of y'^A_i, combining the provided laboratory uncertainty u_i^A, the instrument instability uncertainty u_{TS}^A and the uncertainty of the drift correction $u(s_i^A)$

$V_{\boldsymbol{y}'}$ covariance matrix of $\boldsymbol{y}'$, the vector containing the y'^A_i and y'^B_i

d_i^A degree of equivalence of laboratory i with the key-comparison reference value for TS A (DoE-TS)

d'_i merged degree of equivalence of laboratory i with the key-comparison reference values (DoE), combining the individual DoE-TSs for the different TSs

En En-value, normalized degree of equivalence

Fn Fn-value, degree of consistency for the calculated DoE-TSs d_i^A and d_i^B in view of the uncertainties and the assumed correlation

6.2. Mathematical model

The measured value y_i^A (i.e. the calibration error) for TS A by laboratory i at a specific test point can be modelled as a sum of the true value y_0^A, the systematic drift s_i^A at the time of measurement, the random instrument instability δ_i^A, and the measurement error η_i^A of the laboratory in the following way (using a similar notation for TS B):

$$y_i^A = y_0^A + s_i^A + \delta_i^A + \eta_i^A \qquad 1 \le i \le n \qquad (1)$$

$$y_i^B = y_0^B + s_i^B + \delta_i^B + \eta_i^B \qquad 1 \le i \le n \tag{2}$$

where there are n laboratories which all have measured both TS A and TS B.

The standard uncertainty u_i of the mean-zero measurement errors η_i^A and η_i^B are provided by laboratory i itself:

$$u(\eta_i^A) = u_i^A,$$
$$u(\eta_i^B) = u_i^B.$$

These uncertainties cover both any possible, unknown systematic biases as well as all random, repeatability uncertainties for a specific laboratory, and are determined and provided by the laboratories themselves. In this analysis, based on expert judgement, it is assumed that the measurement errors η_i^A and η_i^B of the same laboratory for different TSs are substantially correlated due to laboratory dependent systematic effects, but not completely, i.e. it is assumed that

$$r = r_i = r(\eta_i^A, \eta_i^B) = 0.8 \text{ for } 1 \le i \le n. \tag{3}$$

This correlation coefficient is assumed to be the same for each laboratory. This is based on the expectation that the ratio of type A and type B uncertainties is comparable for the participating laboratories, and that the type B uncertainties for the participating laboratories have similar correlations. The non-zero correlation coefficient of (3) links the results involving TS A and the results involving TS B to each other for each single test point. On the other hand, the results of all ten test points have been completely independently analyzed, i.e. no between-test-point-correlation has been assumed.

The standard uncertainties u_{TS}^A and u_{TS}^B of the travelling standards are determined based on the repeated measurements by the pilot laboratory and are the same for each laboratory. This calculation will be presented in section 6.3. These values only depend on the TS and not on the laboratory i:

$$u(\delta_i^A) = u_{\mathrm{TS}}^A$$
$$u(\delta_i^B) = u_{\mathrm{TS}}^B.$$

The correction for systematic drift of TS A and TS B for laboratory i is given by s_i^A and s_i^B, with associated covariance matrices given by $V_{\boldsymbol{s}^A}$ and $V_{\boldsymbol{s}^B}$. The diagonal entries of these covariance matrices contain the squares of the uncertainties of the estimated drifts, i.e. the squares of $u(s_i^A)$ and $u(s_i^B)$. The drift estimates s_i^A and s_j^A for different laboratories i and j are correlated due to the uncertainty in the common linear drift coefficient. The drift corrected measurement results are called y'^A_i (resp. y'^B_i) and are given by

$$y'^A_i = y_i^A - s_i^A \qquad 1 \le i \le n \tag{4}$$
$$y'^B_i = y_i^B - s_i^B \qquad 1 \le i \le n \tag{5}$$

The combined uncertainty $u(y'^{A}_i)$ (resp. $u(y'^{B}_i)$) of the corrected measurement results y'^{A}_i (resp. y'^{B}_i) follows from combining the laboratory uncertainty u^A_i (resp. u^B_i) with the instrument instability uncertainty u^A_{TS} (resp. u^B_{TS}) and with the uncertainty of the estimated drift $u(s^A_i)$ (resp. $u(s^B_i)$). Component-wise this yields:

$$u(y'^{A}_i) = \sqrt{u^2(s^A_i) + (u^A_i)^2 + (u^A_{TS})^2} \qquad 1 \le i \le n \tag{6}$$

$$u(y'^{B}_i) = \sqrt{u^2(s^B_i) + (u^B_i)^2 + (u^B_{TS})^2} \qquad 1 \le i \le n \tag{7}$$

The pilot laboratory is taking part in the comparison with the results of a single measurement date, and not with the mean results of measurements taken at several dates (cf. Table 1). Therefore equations (6) and (7) hold for the pilot laboratory as well.

The equations (1) and (2) above can be written in matrix notation in the following way:

$$\boldsymbol{y'} = \boldsymbol{y} - \boldsymbol{s} = X\,\boldsymbol{y}_0^{AB} + \boldsymbol{\delta} + \boldsymbol{\eta} \tag{8}$$

with

$$\boldsymbol{y} = \begin{pmatrix} y_1^A \\ y_1^B \\ y_2^A \\ y_2^B \\ \vdots \\ y_n^A \\ y_n^B \end{pmatrix}, \quad X = \begin{pmatrix} 1 & 0 \\ 0 & 1 \\ 1 & 0 \\ 0 & 1 \\ \vdots & \vdots \\ 1 & 0 \\ 0 & 1 \end{pmatrix}, \quad \boldsymbol{y}_0^{AB} = \begin{pmatrix} y_0^A \\ y_0^B \end{pmatrix}, \quad \boldsymbol{s} = \begin{pmatrix} s_1^A \\ s_1^B \\ s_2^A \\ s_2^B \\ \vdots \\ s_n^A \\ s_n^B \end{pmatrix}, \quad \boldsymbol{\delta} = \begin{pmatrix} \delta_1^A \\ \delta_1^B \\ \delta_2^A \\ \delta_2^B \\ \vdots \\ \delta_n^A \\ \delta_n^B \end{pmatrix}, \quad \boldsymbol{\eta} = \begin{pmatrix} \eta_1^A \\ \eta_1^B \\ \eta_2^A \\ \eta_2^B \\ \vdots \\ \eta_n^A \\ \eta_n^B \end{pmatrix}$$

and associated covariance matrix $V_{\boldsymbol{y}'}$ of $\boldsymbol{y'}$ given by

$$V_{\boldsymbol{y}'} = \begin{pmatrix} v_{1,1} & \cdots & v_{1,2n} \\ \vdots & \ddots & \vdots \\ v_{2n,1} & \cdots & v_{2n,2n} \end{pmatrix} \tag{9}$$

In the absence of drift, the only non-zero entries $v_{j,k}$ of the covariance matrix $V_{\boldsymbol{y}'}$ are given by the diagonal entries $v_{j,j}$ and the entries resulting from the covariance of the measurements performed by the same laboratory pilot laboratory:

$$v_{j,j} = u^2(y_i^A) \qquad \text{for } j \text{ uneven and } j = 2i-1,$$

$$v_{j,j} = u^2(y_i^B) \qquad \text{for } i \text{ even and } j = 2i,$$

$$v_{j,j+1} = v_{j+1,j} = r\,u_i^A u_i^B \qquad \text{for } j \text{ uneven and } j = 2i-1.$$

In the case of a non-zero drift $\boldsymbol{s}$ for TS A all uneven entries of $\boldsymbol{s}$ are correlated, i.e. the entries $v_{j,k}$ with both j and k uneven are non-zero, and similarly if there is a non-zero for TS B the entries $v_{j,k}$ with both j and k even are non-zero. As the measurements of the pilot laboratory for TS A and TS B are correlated

in virtue of equation (3), the drift coefficients for both TSs are also correlated. However, as the drift corrections and associated uncertainties are small, these latter correlations have been neglected in this analysis and independent covariance matrices $V_{\boldsymbol{s}^A}$ and $V_{\boldsymbol{s}^B}$ have been included into $V_{\boldsymbol{y}'}$.

The system of equations given by equations (8) and (9) has been solved for $\boldsymbol{y}_0^{AB}$ in a weighted least squares sense, minimizing the sum of the residuals $\boldsymbol{\delta} + \boldsymbol{\eta}$ of the TS instabilities and the laboratory measurements, which corresponds to the maximum likelihood solution for $\boldsymbol{y}_0^{AB}$. Solving this system can be performed by minimizing the function

$$\boldsymbol{a} \mapsto (\boldsymbol{y}' - X\boldsymbol{a})^{\mathrm{T}}\, V_{\boldsymbol{y}'}{}^{-1}\, (\boldsymbol{y}' - X\boldsymbol{a}).$$

The solution $\widehat{\boldsymbol{a}} = \boldsymbol{y}_{\mathrm{ref}}^{AB} = \left(y_{\mathrm{ref}}^{A}, y_{\mathrm{ref}}^{B}\right)^{\mathrm{T}}$ constitutes the KCRV estimates for y_0^A and y_0^B of equations (1) and (2). $\boldsymbol{y}_{\mathrm{ref}}^{AB}$ and its associated covariance matrix $V_{\boldsymbol{y}_{\mathrm{ref}}^{AB}}$ are given by [5]:

$$\boldsymbol{y}_{\mathrm{ref}}^{AB} = V_{\boldsymbol{y}_{\mathrm{ref}}^{AB}}^{-1} X^{\mathrm{T}}\, V_{\boldsymbol{y}'}^{-1}\, \boldsymbol{y}' \quad \text{and} \quad V_{\boldsymbol{y}_{\mathrm{ref}}^{AB}} = \left(X^{\mathrm{T}} V_{\boldsymbol{y}'}^{-1} X\right)^{-1} \tag{10}$$

Before merging, the degrees of equivalence per TS (DoE-TSs) d_i^A and d_i^B of the comparison are computed per laboratory and per TS separately, i.e.:

$$d_i^A = y'^A_i - y_{\mathrm{ref}}^A \qquad \text{for } 1 \le i \le n$$

$$d_i^B = y'^B_i - y_{\mathrm{ref}}^B \qquad \text{for } 1 \le i \le n$$

or in vector notation

$$\boldsymbol{d} = \boldsymbol{y}' - \boldsymbol{y}_{\mathrm{ref}} \quad \text{with} \quad \boldsymbol{y}_{\mathrm{ref}} = X\, \boldsymbol{y}_{\mathrm{ref}}^{AB}, \tag{11}$$

$$d_j = d_i^A \qquad \text{for } j \text{ uneven and } j = 2i - 1,$$

$$d_j = d_i^B \qquad \text{for } i \text{ even and } j = 2i.$$

These DoE-TSs are affected by the uncertainties of the drift corrections s_i^A, s_i^B, the TS instabilities δ_i^A, δ_i^B and the laboratory measurement errors η_i^A, η_i^B. A large DoE-TS indicates a large realization of the laboratory measurement error, and/or a large realization of the random TS instability, and/or a large realization of the random part of the drift correction.

The uncertainty of the DoE-TSs are given by the covariance matrix [5]

$$V_{\boldsymbol{d}} = V_{\boldsymbol{y}'} - V_{\boldsymbol{y}_{\mathrm{ref}}} \text{ where } V_{\boldsymbol{y}_{\mathrm{ref}}} = X\, V_{\boldsymbol{y}_{\mathrm{ref}}^{AB}}\, X^{\mathrm{T}} \tag{12}$$

Component-wise this corresponds to

$$u\left(d_i^A\right) = \sqrt{u^2(y'^A_i) - u^2(y_{\mathrm{ref}}^A)} \qquad \text{for } 1 \le i \le n$$

$$u\left(d_i^B\right) = \sqrt{u^2(y'^B_i) - u^2(y_{\mathrm{ref}}^B)} \qquad \text{for } 1 \le i \le n$$

where $u(y'^{A}_{i})$ and $u(y'^{B}_{i})$ are given by equations (6) and (7), and $u^2\left(y^{A}_{\mathrm{ref}}\right)$ and $u^2(y^{B}_{\mathrm{ref}})$ are given by entries (1,1) and (2,2) of the 2 × 2 matrix $V_{\boldsymbol{y}^{AB}_{\mathrm{ref}}}$.

Bilateral DoE-TSs between a pair of two laboratories for a given TS can be easily computed by calculating appropriate differences, e.g. $d^{A}_{ij} = d^{A}_{i} - d^{A}_{j}$. For calculating the uncertainty of d^{A}_{ij} the covariance between d^{A}_{i} and d^{A}_{j} is needed, which is not included in this report to save some space. Nevertheless, the covariance matrix of the unilateral DoE-TSs, as well as the bilateral DoE-TSs and their standard uncertainties have been included in the digital supplement to this report, see Annex D for more information.

In order to present a single DoE d'_i with uncertainty $u(d'_i)$ per laboratory i, the DoE-TSs d^{A}_{i} and d^{B}_{i} have been combined or 'merged' in the following way, where $\boldsymbol{e} = (1,1)^{\mathrm{T}}$, $\boldsymbol{d}_i = (d^{A}_{i}, d^{B}_{i})^{\mathrm{T}}$ and $V_{\boldsymbol{d}_i}$ denotes the covariance matrix of $\boldsymbol{d}_i$:

$$u(d'_i) = \left(\boldsymbol{e}^{\mathrm{T}}\, {V_{\boldsymbol{d}_i}}^{-1}\, \boldsymbol{e}\right)^{-1/2} \tag{13}$$

$$d'_i = (\boldsymbol{e}^{\mathrm{T}}\, {V_{\boldsymbol{d}_i}}^{-1} \boldsymbol{d}_i)\, u^2(d_i) \tag{14}$$

If $V_{\boldsymbol{d}_i}$ is diagonal, this corresponds to the usual uncertainty weighted average. In the case of non-diagonal $V_{\boldsymbol{d}_i}$ the correlations are properly taken into account by these formulae, such that d'_i has lowest possible uncertainty. Note that by virtue of this averaging and the fact that d^{A}_{i} and d^{B}_{i} are not fully correlated, the uncertainty $u(d'_i)$ of the combined DoE d'_i is lower than those of the individual DoE-TSs d^{A}_{i} and d^{B}_{i} and this increases the merged normalized errors $d'_i/(2\,u(d'_i))$ compared to those calculated for both TSs individually.

In order to compute the covariances between different DoEs d'_i, which are needed for computing the uncertainties of bilateral DoEs, it is convenient to take a matrix-vector based approach in the following way:

$$\begin{gathered}
\boldsymbol{d} = \begin{pmatrix} \boldsymbol{d}_1 \\ \vdots \\ \boldsymbol{d}_n \end{pmatrix} \\
\boldsymbol{w}_i^{\mathrm{T}} = (\boldsymbol{e}^{\mathrm{T}}\, {V_{\boldsymbol{d}_i}}^{-1})\, u^2(d_i) \\
W = \begin{pmatrix} \boldsymbol{w}_1^{\mathrm{T}} & \boldsymbol{0} & \boldsymbol{0} \\ \boldsymbol{0} & \ddots & \boldsymbol{0} \\ \boldsymbol{0} & \boldsymbol{0} & \boldsymbol{w}_n^{\mathrm{T}} \end{pmatrix} \\
\boldsymbol{d}' = W\, \boldsymbol{d}
\end{gathered} \tag{15}$$

$$V_{\boldsymbol{d}'} = W\, V_{\boldsymbol{d}}\, W^{\mathrm{T}} \tag{16}$$

Bilateral DoEs d'_{ij} between laboratories i and j and their uncertainties $u(d'_{ij})$ can now be calculated using the vector $\boldsymbol{e}_{ij} = (0, \ldots, 0, 1, 0, \ldots, 0, -1, 0, \ldots 0)^{\mathrm{T}}$, whereby the 1 is at position i and the -1 is at position j, in the following way:

$$d'_{ij} = \boldsymbol{e}_{ij}^{\mathrm{T}}\, \boldsymbol{d}' = d'_i - d'_j \tag{17}$$

$$u\left(d'_{ij}\right) = \sqrt{\boldsymbol{e}_{ij}^{\mathrm{T}}\, V_{\boldsymbol{d}'}\, \boldsymbol{e}_{ij}} = \sqrt{u^2(d'_i) + u^2\left(d'_j\right) - 2\, u(d'_i, d'_j)}, \tag{18}$$

where $u(d'_i, d'_j)$ denotes the covariance between d'_i and d'_j, corresponding to entry (i, j) from $V_{\boldsymbol{d}'}$.

The bilateral DoEs have not been reported in this document, but are part of the digital supplement, see Annexes D and E. This digital supplement is added to allow for verification of the calculations performed in the analysis of the comparison results.

Based on the merged DoEs and their expanded uncertainties, the normalized DoEs or so-called (signed) En-values En have been calculated according to

$$En = \frac{d'_i}{2\, u(d'_i)} \tag{19}$$

En-values with absolute value larger than 1 are usually interpreted as suspicious values. If the model, including the provided and calculated uncertainties and correlations, fits the data well, it should hold that $|En| \leq 1$ for around 95 % of the results.

By applying the averaging procedure of DoE-TSs of Equation (14) a laboratory having a large positive d_i^A and a similarly large negative d_i^B (or vice versa) can end up with a merged DoE d'_i close to 0 and an En-value with absolute value well below 1. To study and highlight this effect, the differences

$$f_i = d_i^A - d_i^B$$

have been computed and compared with their uncertainties $u(f_i)$. Similar to En-values, a (signed) Fn-value Fn has been defined according to

$$Fn = \frac{f_i}{2\, u(f_i)} \tag{20}$$

If the model, including the provided and calculated uncertainties and correlations, fits the data well, it should hold that $|Fn| \leq 1$ for around 95 % of the results. Actually, since d_i^A and d_i^B are typically dominated by systematic (type B) uncertainties, the value $f_i = d_i^A - d_i^B$ is expected to be small compared to d_i^A and d_i^B individually, and $u(f_i)$ is typically dominated by the remaining random uncertainties. If systematic and random uncertainties have been assessed properly, $|Fn|$ is statistically expected to be smaller than 1 for 95 % of the results. Put differently, a systematic deviation in the measurement setup of the laboratory will provide the same offset to both d_i^A and d_i^B, so will not contribute to f_i.

Laboratories providing two strongly different DoE-TSs will end up with a $|Fn| > 1$ and can be marked as presenting suspicious results with respect to the model assumptions.

It is noted that in the calculation procedure, all results are contributing to the calculation of the KCRV, although calculations involving the chi-squared test as suggested in [4] and [5] did not indicate fully consistent results for each test point. However, there were no major inconsistencies and it was preferred to prevent somewhat arbitrary decisions regarding how to exclude results from contributing to the calculation of the KCRV (e.g. excluding single measurement results only or excluding all results of a laboratory as a whole) or how to increase uncertainties of the traveling standards to make all results mathematically consistent.

It finally has been decided to keep the analysis as simple and clean as possible. Based on a first evaluation of the results, there was also the impression that instability of TS B was larger than what could be mathematically established based on the repeated measurements of TS B at the pilot laboratory, notably for the phase uncertainty. Furthermore, some exploratory investigations in the direction of excluding results and increasing uncertainties did not yield significant improvements or new insights. At the end it was therefore decided that all provided results were allowed to contribute to the KCRV and that no uncertainties were artificially increased.

6.3. Calculation of the travelling standard instabilities and drifts

6.3.1. Drift assessment

In order to assess the stability of the TSs, the pilot laboratory has measured two representative points, i.e. point 6 (240 V, 5 A, PF 1) and point 10 (240 V, 5A, 0 lag), several times over the time span of the intercomparison, i.e. six times TS A and ten times TS B. As already noted in sections 2 and 3, the instrument originally taken as TS A broke down during the initial stability tests and was replaced by another device. Therefore the histories are not equally long for TS A and TS B. The measured values can be found in Table 3 and Table 4 and plotted in Figure 2.

Table 3: Measured TS errors in ppm over time as found by the pilot laboratory for TS A. The expanded uncertainty of each measurement is 10 ppm (k = 2).

Measurement date	01/12/ 2017	11/01/ 2018	09/08/ 2018	09/01/ 2019	07/01/ 2020	31/05/ 2021
pnt 6: 240 V, 5 A, PF = 1	-54.0	-54.3	-51.3	-52.6	-52.5	-47.6
pnt 10: 240 V, 5 A, PF = 0 lag	43.0	40.9	41.3	41.8	41.5	41.5

Table 4: Measured TS errors in ppm over time as found by the pilot laboratory for TS B. The expanded uncertainty of each measurement is 10 ppm (k = 2).

Measurement date	25/08/ 2016	30/09/ 2016	24/10/ 2016	23/02/ 2017	01/12/ 2017	11/01/ 2018	09/08/ 2018	09/01/ 2019	07/01/ 2020	31/05/ 2021
pnt 6: 240 V, 5 A, PF = 1	85.8	87.8	86.7	86.7	90.0	88.5	89.2	91.2	87.5	95.3
pnt 10: 240 V, 5 A, PF = 0 lag	-31.5	-34.1	-33.9	-32.0	-31.0	-31.2	-30.4	-36.1	-30.8	-33.2

For each of these four cases it was determined if there is a small, but significant linear drift by fitting the equation $y = a_y + b_y\ (t\ -\ t_{\mathrm{PL}})$ to the measurement results y and the measurement time points t and by testing if the value of the coefficient b was significant in view of its uncertainty $u(b)$ using a t-test. In this equation t_{PL} denotes the time point at which the pilot laboratory reported its measurement results to be used for the comparison, i.e. $t_{\mathrm{PL}} = 07/01/2020$. In Table 5 the results of the drift assessment is shown. In Figure 2 the stability measurements and the results of the drift assessment have been plotted.

Table 5: Results of tests for linear drift for the four repeatedly measured test points by the pilot laboratory

Case	b_y / (ppm/y)	$u(b_y)$ / (ppm/y)	$\lvert b_y \rvert / u(b_y)$	degrees of freedom	critical value at $\alpha = 0.05$	significant linear drift
TS A, pnt 6	1.60	0.43	3.7	4	2.8	yes
TS A, pnt 10	-0.11	0.26	0.4	4	2.8	no
TS B, pnt 6	1.42	0.37	3.8	8	2.3	yes
TS B, pnt 10	0.02	0.42	0.05	8	2.3	no

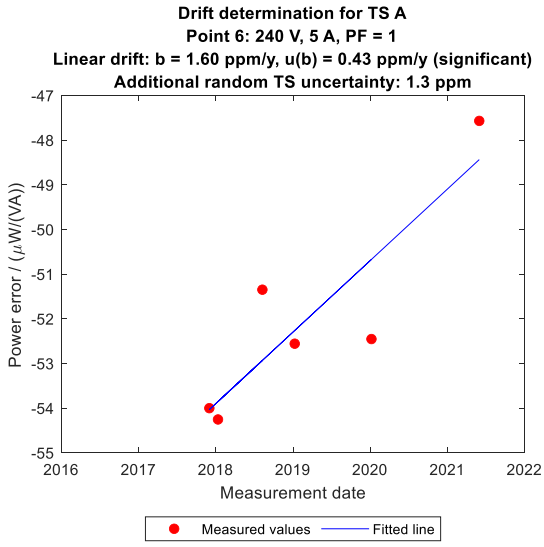

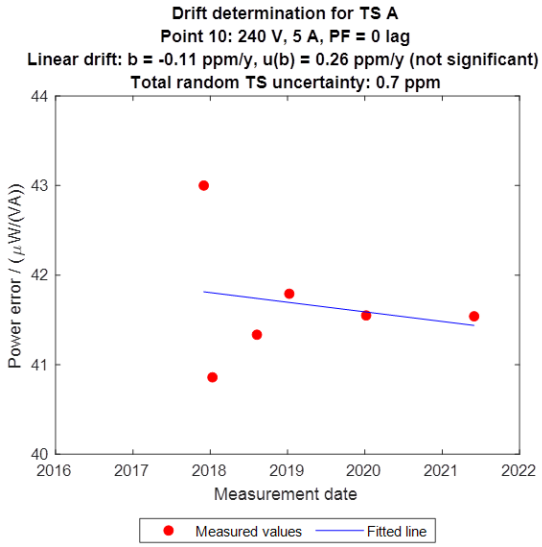

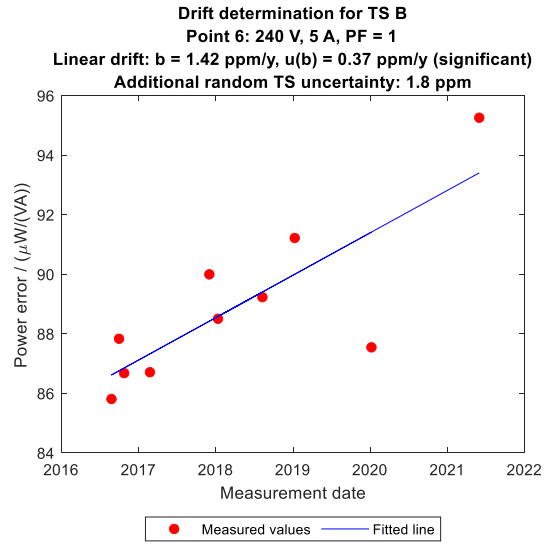

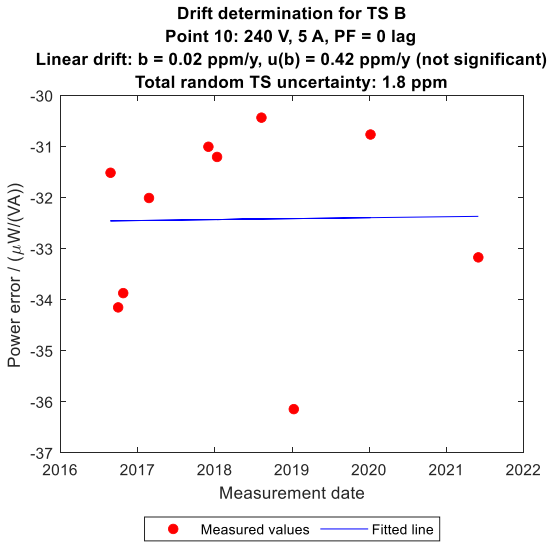

Figure 2: Plot of the repeated measurements at pilot laboratory for TS A and TS B at test points 6 and 10.

6.3.2. Drift of TS versus drift of pilot laboratory

For both travelling standards a similar linear drift was observed at test point 6 (PF = 1), but not at test point 10 (PF = 0). The drift at PF = 1 is likely caused by drifts in the internal Zener voltage reference, that are similar in both travelling standards. The essentially zero drift at PF = 0 can be understood by the fact that phase errors in power meters are caused by internal time delays and parasitic impedance effects, which are expected not to change over time.

It might be argued that there could have been a drift at the pilot laboratory for the data at PF = 1, rather than a common drift of the two TS. However, it was already noted in section 3.1 that the two TS are not two independent instruments with different measurement principles and of different makes. They are rather closely related and a similar drift behaviour is not unexpected. Furthermore, the pilot laboratory did not detect similar effects in the Euramet comparison that took place in the same period of time and in which a similar TS was used, nor in the calibration results of other secondary standards.

A closer analysis revealed that mainly the voltage measurement of the TS had changed with respect to the pilot laboratory, while the current measurement had only changed a little. Since the pilot laboratory measures voltage and current sequentially and uses the same ADC for current and voltage with comparable amplitude, it is improbable that there is an amplitude drift at the pilot laboratory, as in that case most probably both current and voltage amplitudes would have been different between TS and pilot laboratory.

It thus is concluded that both TSs were drifting and not the reference setup at the pilot laboratory.

6.3.3. Interpolation of drift to other test points

As only two of the ten test points were repeatedly measured, some assumptions were needed to calculate the drift and TS instability uncertainty at the other eight test points. The assumptions used are:

1. The TSs measure active power P by measuring the amplitudes of the voltage V and of the current I, and the phase difference φ between them, i.e. $P = VI\cos\varphi$.
2. The voltage and current amplitude errors of a TS are the same at different test points for a certain test voltage.
3. The phase errors of a TS are the same at different test points for a certain test voltage.
4. The drift in amplitude and phase errors are the same at 120 V and at 240 V.

Using these assumptions the calibration error ε (which is called y in other parts of this report) can be written as $\varepsilon = dP/(VI)$, where dP indicates the error in measured power P. It now follows that

$$\varepsilon(\varphi) = \frac{dP}{VI} = \frac{d(VI\cos\varphi)}{VI} = \cos\varphi\,\frac{d(VI)}{VI} + \sin\varphi\,d\varphi$$

$$\varepsilon(\varphi = 0) = \frac{d(VI)}{VI}$$

$$\varepsilon\left(\varphi = -\frac{\pi}{2}\right) = -d\varphi$$

$$\varepsilon(\varphi) = \cos\varphi\,\varepsilon(\varphi = 0) - \sin\varphi\,\varepsilon(\varphi = -\tfrac{\pi}{2}) \qquad (21)$$

By means of equation (21) the measured error in any test point can be predicted from the errors found in test points 6 and 10. This relationship will be used for the estimation of the systematic drift in the other eight test points.

6.3.4. Calculated drift coefficients

In this section the drift $s(t) = a_s + b_s\ (t - t_{\mathrm{PL}})$ that will be retained in the main part of the analysis will be presented, where t_{PL} is the time of measurement of the pilot laboratory. For the linear drift coefficient b_s the fitted value b_y is taken. However a decision needs to be made with respect to the value of the constant a_s. If the fitted value a_y would be used, then the fitted mean TS error would be interpreted in the model as a constant instrument instability and this would result in a KCRV $y_{\mathrm{ref}} \approx 0$ ppm. For the calculation of the degrees of equivalence and the normalized deviations this choice is not relevant, but it would be a somewhat strange KCRV if compared with the measurement data, and not be representative for the underlying 'true' SI value. As arbitrary choice it has been decided that the instrument drift is 0 ppm at the reporting date of the pilot laboratory, i.e., at $t_{\mathrm{PL}} =$ 07/01/2020. This results in setting $a_s = 0$ ppm. The estimated drift at time point t_i is thus

$$s(t_i) = b\ (t_i - t_{\mathrm{PL}}) \tag{22}$$

with standard uncertainty

$$u(s(t_i)) = |t_i - t_{\mathrm{PL}}|\ u(b).$$

The covariance in estimated drift at time points t_i and t_j is given by

$$u\big(s(t_i), s(t_j)\big) = |t_i - t_{\mathrm{PL}}|\ \big|t_j - t_{\mathrm{PL}}\big|\ u^2(b). \tag{23}$$

The values calculated according to these equations have been used in equations (4) and (5).

In Table 5 the calculated values for the drift coefficients for test point 6 (i.e. 240 V, 5 A, PF = 1) and test point 10 are shown (i.e. 240 V, 5 A, PF = 0) for both TSs. Using equation (21), which follows from the assumptions mentioned at the start of this section, and the fact that $b\left(\varphi = -\frac{\pi}{2}\right) = 0$ as the drift coefficients are insignificant for test point 10 for both TSs, the following expression is found for drift coefficients $b(\varphi)$ at other test points as function of the phase difference φ:

$$b(\varphi) = \cos\varphi\ \ b(\varphi = 0)$$

For the uncertainty $u(b(\varphi))$ of the drift coefficient it is analogously found that

$$u(b(\varphi)) = |\cos\varphi\,|\ u(b(\varphi = 0))$$

The drift coefficients for each of the ten test points calculated in this way are shown in Table 6.

Table 6: Retained drift coefficients per test point in ppm/y, with standard uncertainty in parentheses. The values for TP-1 to TP-5 are copies of the values for TP-6 to TP-10.

Test point	TP-1	TP-2	TP-3	TP-4	TP-5	TP-6	TP-7	TP-8	TP-9	TP-10
TS A	1.60 (0.43)	0.80 (0.22)	0.00 (0.00)	0.80 (0.22)	0.00 (0.00)	1.60 (0.43)	0.80 (0.22)	0.00 (0.00)	0.80 (0.22)	0.00 (0.00)
TS B	1.42 (0.37)	0.71 (0.19)	0.00 (0.00)	0.71 (0.19)	0.00 (0.00)	1.42 (0.37)	0.71 (0.19)	0.00 (0.00)	0.71 (0.19)	0.00 (0.00)

6.3.5. TS standard uncertainty

In addition to the calculated drift and drift uncertainty as presented in the last section, an uncertainty component representing the standard (type A) uncertainty of the TS was calculated, denoted by u_{TS}^{A} and u_{TS}^{B}. For test point 6 this was done based on the standard deviation of the residuals of the line fit used for the drift calculation, and for test point 10 the standard deviation of the repeated measurement results was used. For points TP-7 to TP-9 an interpolation was performed based on equation (21), and the values for points TP-1 and TP-5 are taken identical to those found for TP-6 to TP-10. The resulting values are shown in Table 7. It can be seen that TS B has a larger instability standard uncertainty than TS A. The instability standard uncertainty for TS B is (almost) constant due to the fact that (almost) the same value was found for both point 6 and point 10.

Table 7: Standard (type A) uncertainty in ppm associated with the TSs after correction for the systematic drift (if significant). TP-7, TP-8 and TP-9 are interpolated between TP-6 and TP-10. The values for TP-1 to TP-5 are copies of the values of TP-6 to TP-10.

Test point	TP-1	TP-2	TP-3	TP-4	TP-5	TP-6	TP-7	TP-8	TP-9	TP-10
TS A	1.3	0.9	0.7	0.9	0.7	1.3	0.9	0.7	0.9	0.7
TS B	1.8	1.8	1.8	1.8	1.8	1.8	1.8	1.8	1.8	1.8

6.3.6. Correlations

The calculated drift corrections result in some covariance contributions to the covariance matrix $V_{\boldsymbol{y}'}$ of equation (9). The most important correlation contribution is the correlation between $s(t_i)$ and $s(t_j)$ due to the common dependence on b, as presented in equation (23). This correlation is fully accounted for and has been included in $V_{\boldsymbol{y}'}$.

Some other, rather insignificant correlations have been neglected in the construction of the covariance matrix $V_{\boldsymbol{y}'}$. First of all, it can be shown that the correlation between b and the reported value y_{PL} is small, and it will thus have a negligible effect on the final results. Therefore this correlation has not been included in the calculations. Another correlation that has been neglected is the correlation between the drift coefficients b^A and b^B for TS A and TS B which is due to the correlation between all measurements performed at the pilot laboratory, cf. equation (3). Again, the effect of not including this correlation is deemed to be negligible.

6.4. Key comparison reference values

Having analyzed the drift and instability of the TSs, the model for the KCRVs can now be solved. Table 8 and Table 9 for each test point show the calculated key comparison reference value y_{ref}^{A} and y_{ref}^{B} with expanded uncertainty ($k = 2$) and the drift corrected values of each laboratory for TS A and TS B respectively, together with the expanded combined uncertainties which include a component for drift and instability of the TSs. In Figure 3 the DoE-TSs are visualized, whereby the results for TS A have been plotted in blue, and for TS-B in red. The reported measurement results together with the reported expanded uncertainties by the laboratories themselves can be found in appendix A.

Table 8: Key comparison reference values and reported values after drift correction of the TS with expanded combined uncertainties (k = 2) in parentheses for TS A.

Test point / Lab	120 V 5 A PF = 1	120 V 5 A 0.5 lead	120 V 5 A 0 lead	120 V 5 A 0.5 lag	120 V 5 A 0 lag	240 V 5 A PF = 1	240 V 5 A 0.5 lead	240 V 5 A 0 lead	240 V 5 A 0.5 lag	240 V 5A 0 lag
KCRV-A	-57.2 (3.0)	-66.0 (2.4)	-43.6 (2.3)	9.4 (2.4)	41.8 (2.3)	-54.9 (3.1)	-65.3 (2.5)	-44.4 (2.4)	11.5 (2.5)	42.5 (2.4)
CENAM-A	-60.1 (7.7)	-58.4 (9.9)	-32.3 (10.6)	-1.9 (9.9)	31.7 (10.6)	-60.8 (7.7)	-58.9 (9.9)	-34.1 (10.6)	-2.0 (9.9)	32.0 (10.6)
LNE-A	-54.6 (26.2)	-66.1 (16.1)	-45.0 (11.1)	12.7 (16.1)	43.5 (11.1)	-53.5 (26.2)	-66.1 (16.1)	-44.6 (12.1)	15.3 (17.1)	45.0 (11.1)
RISE-A	-51.4 (10.3)	-62.4 (9.3)	-40.8 (9.2)	10.3 (9.3)	40.4 (9.2)	-49.9 (10.3)	-62.7 (9.3)	-43.7 (9.2)	12.9 (9.3)	42.1 (9.2)
NMIA-A	-55.5 (5.4)	-65.8 (3.4)	-44.3 (3.4)	10.7 (3.4)	42.5 (3.4)	-50.7 (5.4)	-64.2 (3.4)	-44.9 (3.4)	13.5 (3.4)	43.2 (3.4)
NIM-A	-59.8 (12.3)	-70.0 (12.1)	-46.2 (10.1)	10.2 (12.1)	44.8 (10.1)	-54.2 (12.3)	-68.0 (12.1)	-46.9 (10.1)	13.8 (12.1)	45.4 (10.1)
PTB-A	-56.2 (10.3)	-64.6 (10.2)	-42.2 (10.1)	8.8 (10.2)	40.5 (10.1)	-52.5 (10.3)	-63.9 (10.2)	-43.1 (10.1)	11.7 (10.2)	41.5 (10.1)
NMISA-A	-60.3 (55.1)	-33.2 (39.0)	-8.0 (39.0)	-3.2 (39.0)	5.0 (39.0)	-44.3 (60.1)	-29.2 (42.0)	-23.0 (37.0)	3.8 (42.0)	32.0 (37.0)
INMETRO-A	-51.3 (26.1)	-63.7 (26.1)	-44.0 (26.0)	11.3 (26.1)	41.0 (26.0)	-37.3 (26.1)	-54.7 (26.1)	-41.0 (26.0)	16.3 (26.1)	40.0 (26.0)
VSL-A	-66.7 (10.6)	-70.9 (8.1)	-44.1 (6.9)	3.7 (8.3)	41.0 (6.5)	-65.8 (10.0)	-71.5 (7.5)	-44.9 (6.3)	5.0 (7.4)	41.6 (6.4)
NIST-A	-57.4 (7.2)	-68.4 (6.7)	-45.8 (6.6)	11.3 (6.7)	44.2 (6.6)	-58.1 (10.4)	-69.2 (9.6)	-46.2 (9.1)	10.1 (9.4)	43.2 (9.1)

Table 9: Key comparison reference values and reported values after drift correction of the TS with expanded combined uncertainties (k = 2) in parentheses for TS B.

Test point / Lab	120 V 5 A PF = 1	120 V 5 A 0.5 lead	120 V 5 A 0 lead	120 V 5 A 0.5 lag	120 V 5 A 0 lag	240 V 5 A PF = 1	240 V 5 A 0.5 lead	240 V 5 A 0 lead	240 V 5 A 0.5 lag	240 V 5A 0 lag
KCRV-B	81.6 (3.2)	68.9 (2.8)	32.1 (2.8)	12.7 (2.8)	-34.4 (2.7)	85.8 (3.3)	74.5 (2.9)	36.3 (2.8)	12.1 (2.9)	-38.8 (2.8)
CENAM-B	79.4 (8.0)	74.0 (10.4)	39.9 (11.1)	5.0 (10.4)	-41.0 (11.1)	80.6 (8.0)	76.5 (10.4)	40.4 (11.1)	3.9 (10.4)	-43.1 (11.1)
LNE-B	88.4 (26.3)	71.8 (16.4)	29.6 (11.6)	17.7 (16.4)	-32.2 (11.6)	90.8 (26.3)	74.7 (16.4)	33.8 (12.6)	17.1 (16.4)	-35.9 (11.6)
RISE-B	90.0 (10.5)	71.9 (9.8)	32.6 (9.8)	16.7 (9.8)	-33.2 (9.8)	92.6 (10.5)	76.1 (9.8)	34.4 (9.8)	16.1 (9.8)	-35.9 (9.8)
NMIA-B	82.4 (5.9)	66.8 (4.7)	29.2 (4.8)	15.8 (4.7)	-31.7 (4.8)	87.3 (5.9)	71.4 (4.7)	32.0 (4.8)	15.7 (4.7)	-34.3 (4.8)
NIM-B	70.5 (16.4)	62.4 (16.4)	31.0 (10.7)	8.1 (16.4)	-33.2 (10.7)	82.8 (16.4)	75.9 (16.4)	40.0 (10.7)	6.6 (16.4)	-42.3 (10.7)
PTB-B	81.8 (10.6)	64.4 (10.6)	27.2 (10.7)	17.4 (10.6)	-29.7 (10.7)	87.5 (10.6)	68.2 (10.6)	28.6 (10.7)	19.7 (10.6)	-30.8 (10.7)
NMISA-B	102.7 (55.1)	97.9 (39.2)	69.0 (39.2)	-24.1 (39.2)	-56.0 (39.2)	102.7 (60.1)	112.9 (42.2)	78.0 (37.2)	6.9 (42.2)	-83.0 (37.2)
INMETRO-B	81.8 (26.2)	64.4 (26.3)	28.0 (26.3)	16.4 (26.3)	-30.0 (26.3)	100.8 (26.2)	83.4 (26.3)	38.0 (26.3)	17.4 (26.3)	-39.0 (26.3)
VSL-B	71.6 (10.9)	65.3 (8.7)	33.9 (7.9)	5.1 (8.6)	-37.3 (7.3)	77.4 (10.2)	72.8 (8.0)	39.0 (7.2)	4.1 (8.1)	-41.5 (7.2)
NIST-B	83.4 (7.5)	74.6 (7.4)	37.9 (7.4)	8.7 (7.4)	-40.0 (7.4)	84.9 (10.6)	83.9 (10.3)	47.9 (9.7)	-0.5 (9.9)	-51.7 (9.7)

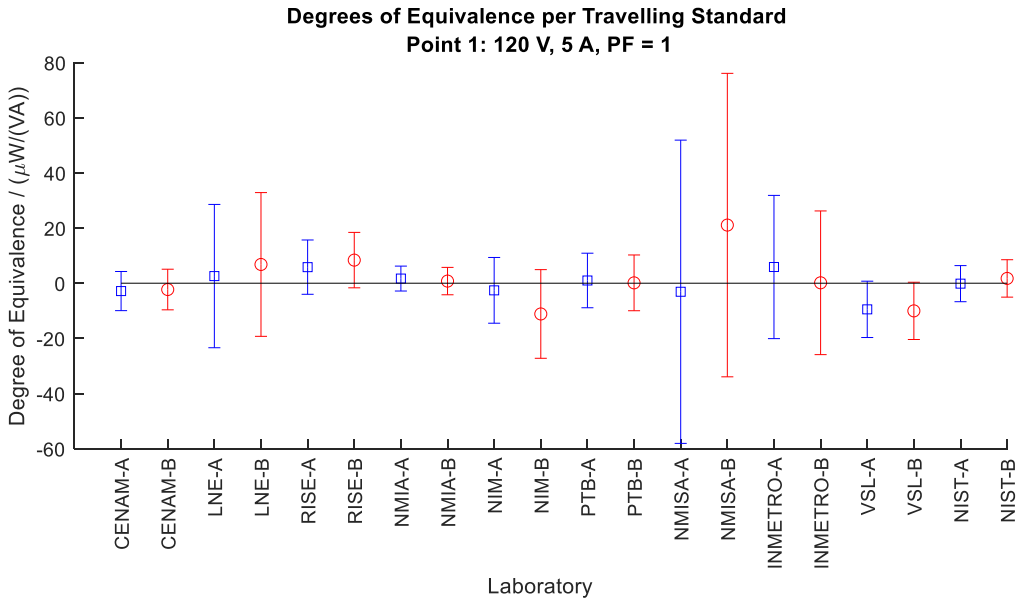

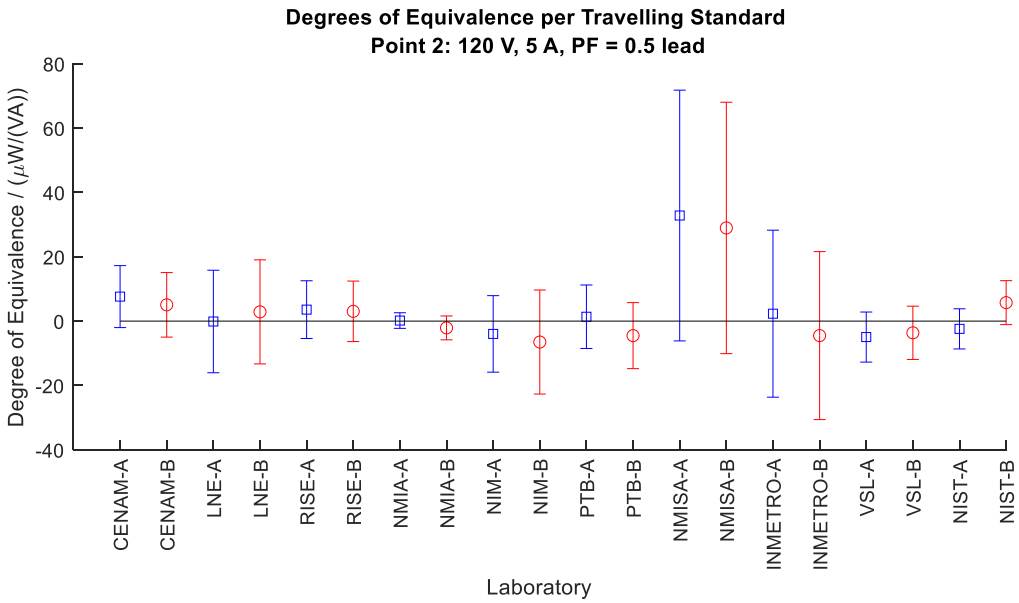
Degrees of Equivalence per Travelling Standard
Point 2: 120 V, 5 A, PF = 0.5 lead
Degree of Equivalence / (μW/(VA))
80
60
40
20
0
-20
-40
CENAM-A
CENAM-B
LNE-A
LNE-B
RISE-A
RISE-B
NMIA-A
NMIA-B
NIM-A
NIM-B
PTB-A
PTB-B
NMISA-A
NMISA-B
INMETRO-A
INMETRO-B
VSL-A
VSL-B
NIST-A
NIST-B
Laboratory

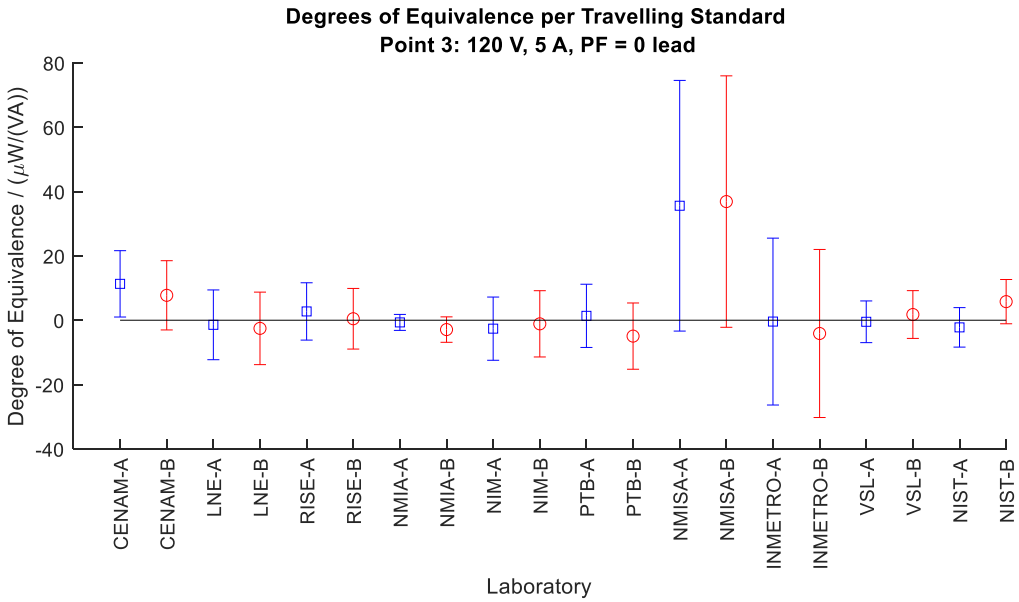
Degrees of Equivalence per Travelling Standard
Point 3: 120 V, 5 A, PF = 0 lead
Degree of Equivalence / (μW/(VA))
80
60
40
20
0
-20
-40
CENAM-A
CENAM-B
LNE-A
LNE-B
RISE-A
RISE-B
NMIA-A
NMIA-B
NIM-A
NIM-B
PTB-A
PTB-B
NMISA-A
NMISA-B
INMETRO-A
INMETRO-B
VSL-A
VSL-B
NIST-A
NIST-B
Laboratory

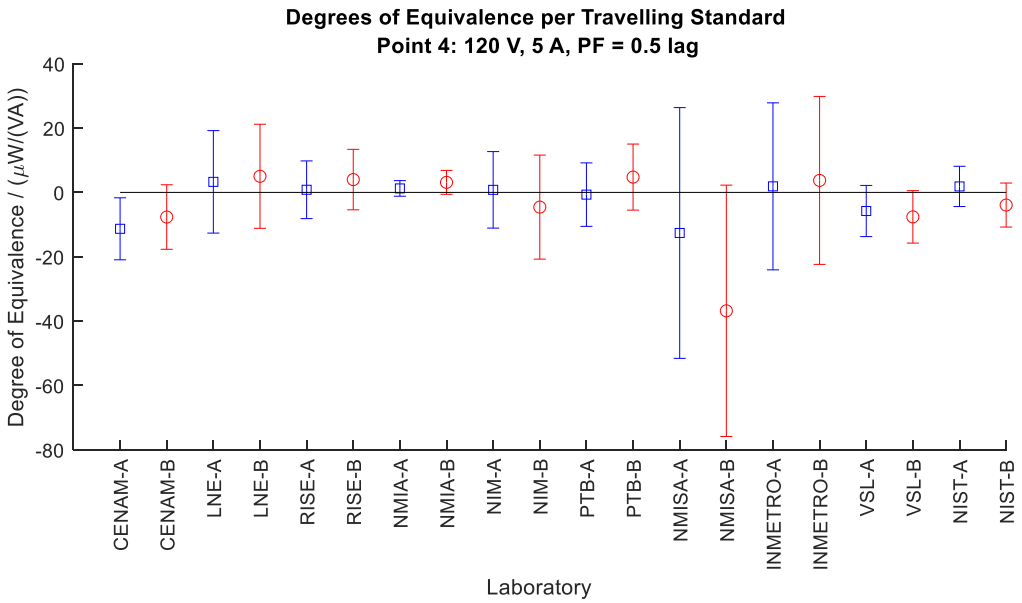
Degrees of Equivalence per Travelling Standard
Point 4: 120 V, 5 A, PF = 0.5 lag
Degree of Equivalence / (μW/(VA))
40
20
0
-20
-40
-60
-80
CENAM-A
CENAM-B
LNE-A
LNE-B
RISE-A
RISE-B
NMIA-A
NMIA-B
NIM-A
NIM-B
PTB-A
PTB-B
NMISA-A
NMISA-B
INMETRO-A
INMETRO-B
VSL-A
VSL-B
NIST-A
NIST-B
Laboratory

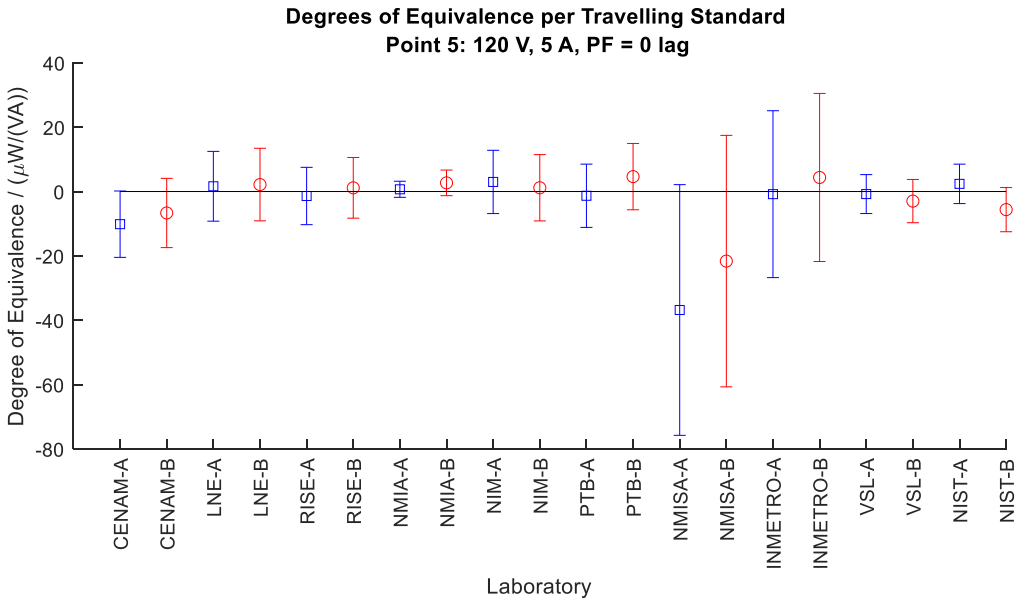
Degrees of Equivalence per Travelling Standard
Point 5: 120 V, 5 A, PF = 0 lag
Degree of Equivalence / (μW/(VA))
40
20
0
-20
-40
-60
-80
CENAM-A
CENAM-B
LNE-A
LNE-B
RISE-A
RISE-B
NMIA-A
NMIA-B
NIM-A
NIM-B
PTB-A
PTB-B
NMISA-A
NMISA-B
INMETRO-A
INMETRO-B
VSL-A
VSL-B
NIST-A
NIST-B
Laboratory

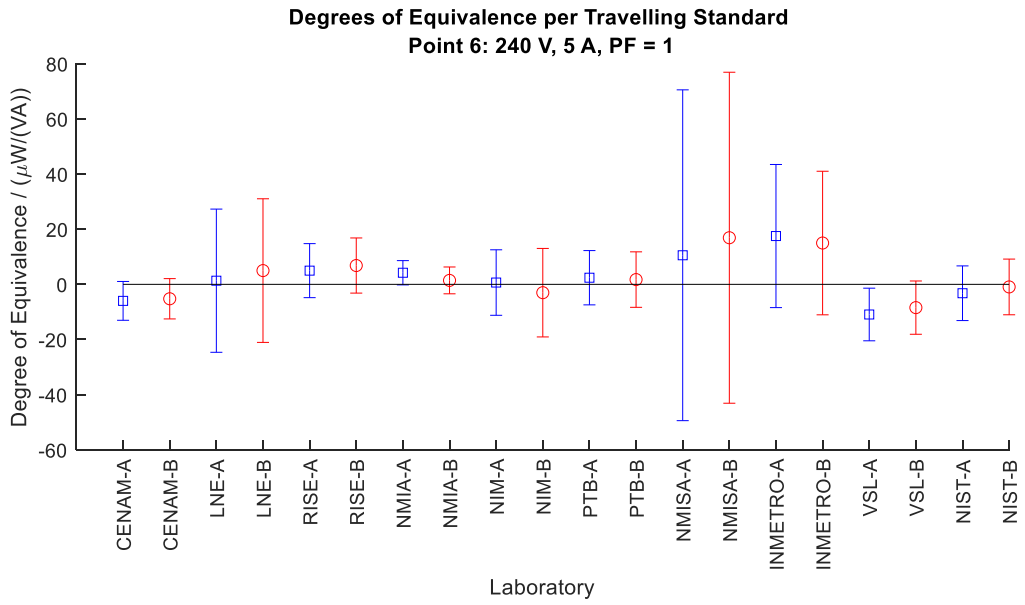
Degrees of Equivalence per Travelling Standard
Point 6: 240 V, 5 A, PF = 1
Degree of Equivalence / (μW/(VA))
80
60
40
20
0
-20
-40
-60
CENAM-A
CENAM-B
LNE-A
LNE-B
RISE-A
RISE-B
NMIA-A
NMIA-B
NIM-A
NIM-B
PTB-A
PTB-B
NMISA-A
NMISA-B
INMETRO-A
INMETRO-B
VSL-A
VSL-B
NIST-A
NIST-B
Laboratory

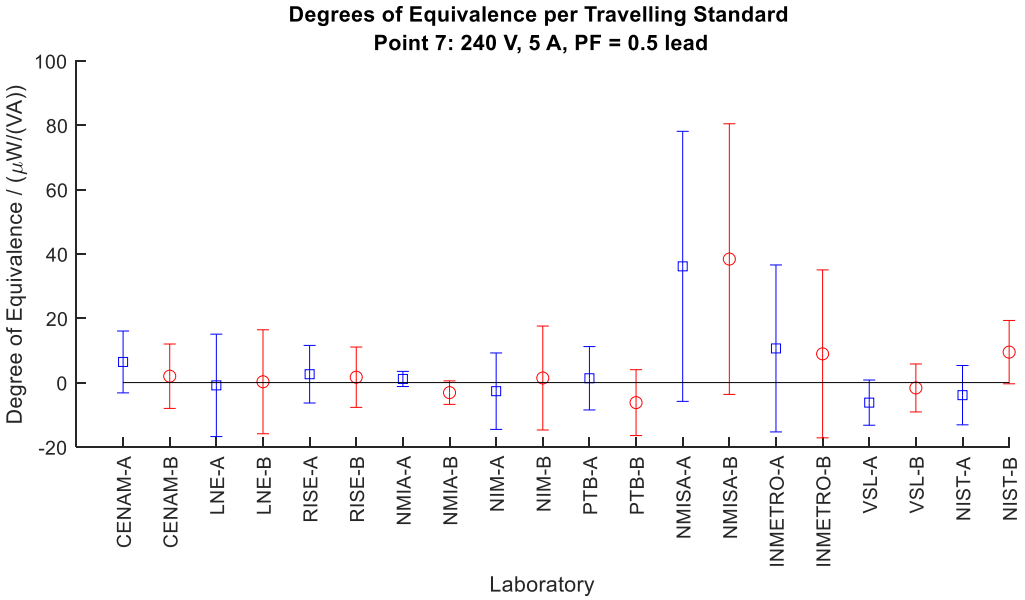
Degrees of Equivalence per Travelling Standard
Point 7: 240 V, 5 A, PF = 0.5 lead
Degree of Equivalence / (μW/(VA))
100
80
60
40
20
0
-20
CENAM-A
CENAM-B
LNE-A
LNE-B
RISE-A
RISE-B
NMIA-A
NMIA-B
NIM-A
NIM-B
PTB-A
PTB-B
NMISA-A
NMISA-B
INMETRO-A
INMETRO-B
VSL-A
VSL-B
NIST-A
NIST-B
Laboratory

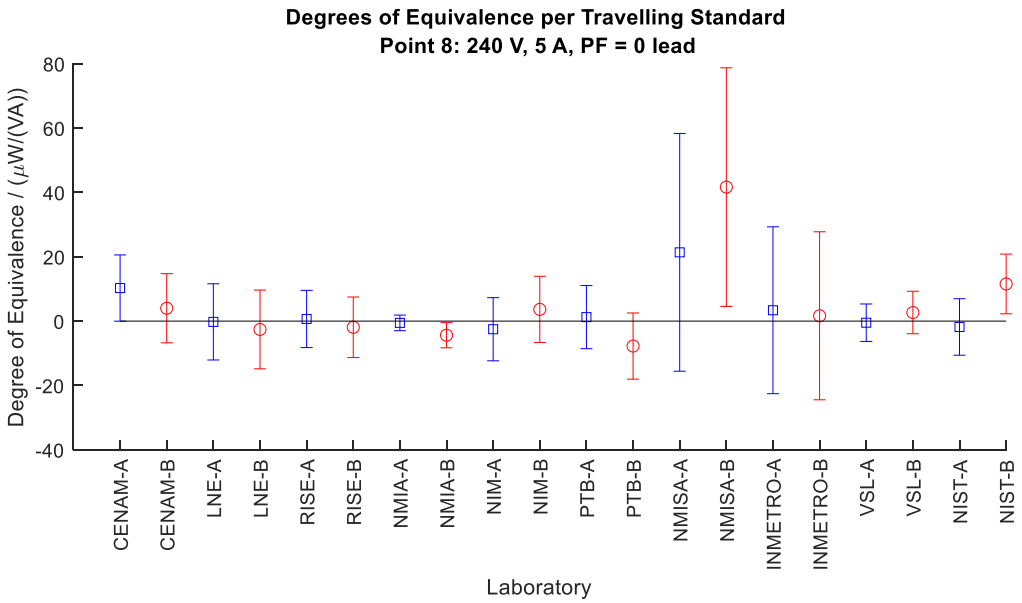
Degrees of Equivalence per Travelling Standard
Point 8: 240 V, 5 A, PF = 0 lead
Degree of Equivalence / (μW/(VA))
80
60
40
20
0
-20
-40
CENAM-A
CENAM-B
LNE-A
LNE-B
RISE-A
RISE-B
NMIA-A
NMIA-B
NIM-A
NIM-B
PTB-A
PTB-B
NMISA-A
NMISA-B
INMETRO-A
INMETRO-B
VSL-A
VSL-B
NIST-A
NIST-B
Laboratory

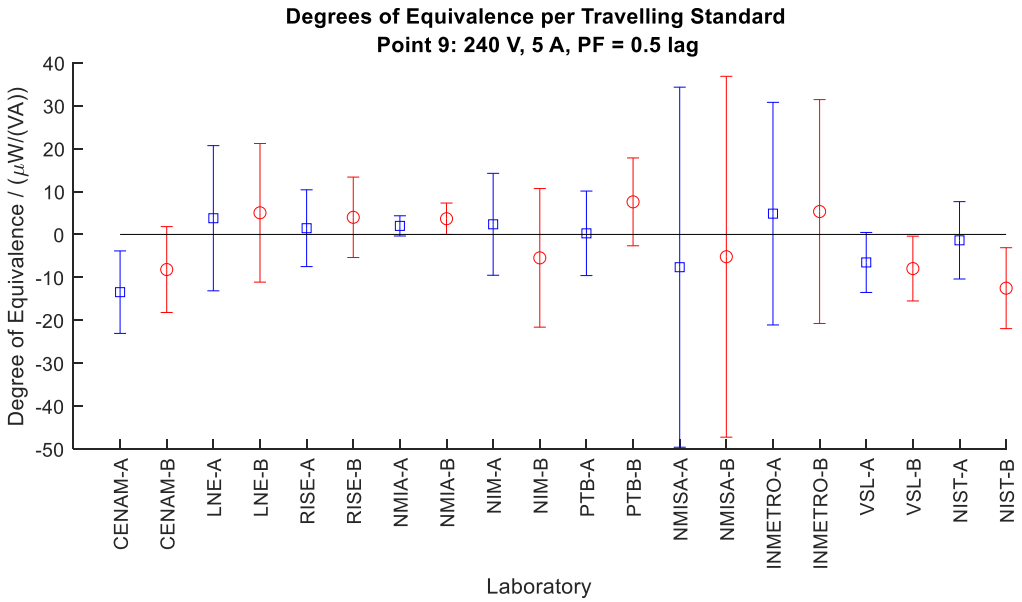
Degrees of Equivalence per Travelling Standard
Point 9: 240 V, 5 A, PF = 0.5 lag
Degree of Equivalence / (μW/(VA))
40
30
20
10
0
-10
-20
-30
-40
-50
CENAM-A
CENAM-B
LNE-A
LNE-B
RISE-A
RISE-B
NMIA-A
NMIA-B
NIM-A
NIM-B
PTB-A
PTB-B
NMISA-A
NMISA-B
INMETRO-A
INMETRO-B
VSL-A
VSL-B
NIST-A
NIST-B
Laboratory

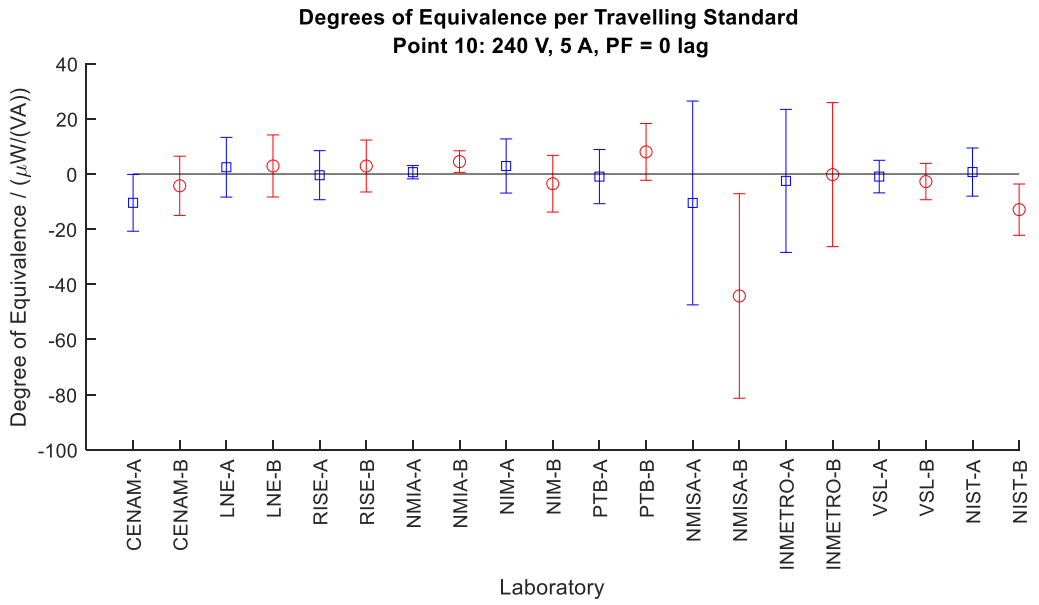

Figure 3: Degrees of equivalence (DoE-TSs) for the 10 laboratories and the two TSs.

6.5. Merged degrees of equivalence

For each test point and each laboratory, the merged degree of equivalence (DoE) d'_i calculated according to equations (13) and (14) is listed in Table 10 and shown in Figure 4.

Table 10: Merged degrees of equivalence with expanded combined uncertainties (k = 2).

Test point / Lab	120 V 5 A PF = 1	120 V 5 A 0.5 lead	120 V 5 A 0 lead	120 V 5 A 0.5 lag	120 V 5 A 0 lag	240 V 5 A PF = 1	240 V 5 A 0.5 lead	240 V 5 A 0 lead	240 V 5 A 0.5 lag	240 V 5A 0 lag
CENAM	-2.60 (6.55)	6.53 (9.16)	9.84 (9.84)	-9.76 (9.16)	-8.71 (9.85)	-5.65 (6.50)	4.54 (9.14)	7.68 (9.83)	-11.23 (9.14)	-7.89 (9.83)
LNE	4.66 (24.61)	1.28 (15.13)	-1.89 (10.35)	4.09 (15.13)	1.86 (10.35)	3.13 (24.59)	-0.34 (15.12)	-1.25 (11.30)	4.54 (15.56)	2.66 (10.34)
RISE	7.00 (9.24)	3.35 (8.53)	1.84 (8.52)	2.13 (8.53)	-0.40 (8.53)	5.82 (9.20)	2.22 (8.52)	-0.35 (8.51)	2.50 (8.52)	0.88 (8.51)
NMIA	1.31 (4.09)	-0.36 (2.26)	-1.07 (2.39)	1.67 (2.25)	1.05 (2.40)	3.08 (3.98)	0.15 (2.19)	-1.22 (2.33)	2.37 (2.19)	1.34 (2.34)
NIM	-2.17 (11.91)	-3.78 (11.87)	-2.01 (9.39)	1.21 (11.87)	2.25 (9.39)	0.84 (11.86)	-2.99 (11.85)	-0.01 (9.38)	2.97 (11.85)	0.30 (9.38)
PTB	0.59 (9.31)	-1.12 (9.39)	-1.20 (9.39)	1.61 (9.39)	1.10 (9.39)	2.09 (9.27)	-1.86 (9.38)	-2.42 (9.38)	3.36 (9.38)	2.71 (9.38)
NMISA	8.94 (52.15)	30.91 (36.98)	36.22 (36.98)	-24.55 (36.98)	-29.34 (36.98)	13.71 (56.89)	37.24 (39.82)	31.34 (35.08)	-6.43 (39.82)	-27.06 (35.08)
INMETRO	3.06 (24.61)	-1.00 (24.64)	-2.21 (24.64)	2.78 (24.64)	1.69 (24.64)	16.27 (24.59)	9.79 (24.63)	2.54 (24.63)	5.09 (24.63)	-1.39 (24.63)
VSL	-9.74 (9.58)	-4.44 (7.41)	0.15 (6.30)	-6.61 (7.45)	-1.53 (5.79)	-9.74 (8.91)	-4.39 (6.65)	0.49 (5.60)	-7.06 (6.67)	-1.54 (5.65)
NIST	0.71 (5.91)	0.60 (5.91)	0.36 (5.90)	-0.28 (5.92)	-0.22 (5.89)	-2.15 (9.22)	1.15 (8.84)	3.44 (8.39)	-6.03 (8.56)	-4.48 (8.36)

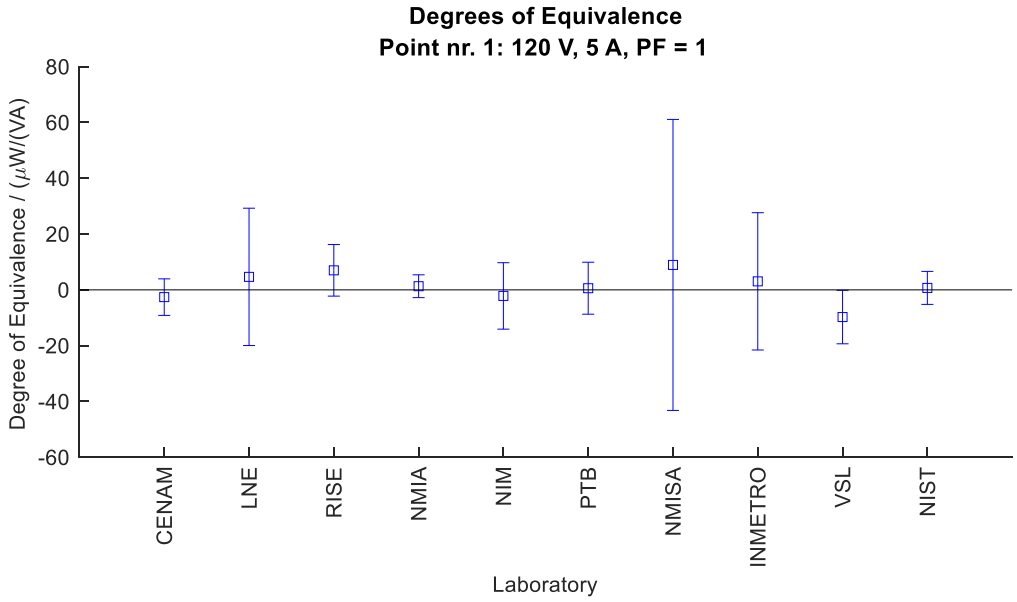
Degrees of Equivalence
Point nr. 1: 120 V, 5 A, PF = 1
Degree of Equivalence / (μW/(VA)
80
60
40
20
0
-20
-40
-60
CENAM
LNE
RISE
NMIA
NIM
PTB
NMISA
INMETRO
VSL
NIST
Laboratory

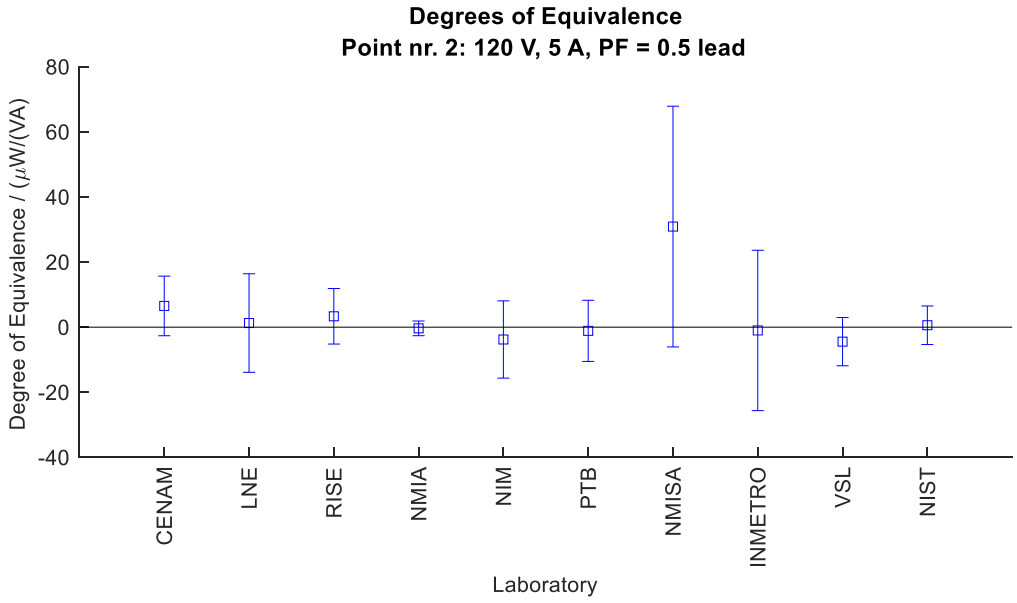
Degrees of Equivalence
Point nr. 2: 120 V, 5 A, PF = 0.5 lead
Degree of Equivalence / (μW/(VA)
80
60
40
20
0
-20
-40
CENAM
LNE
RISE
NMIA
NIM
PTB
NMISA
INMETRO
VSL
NIST
Laboratory

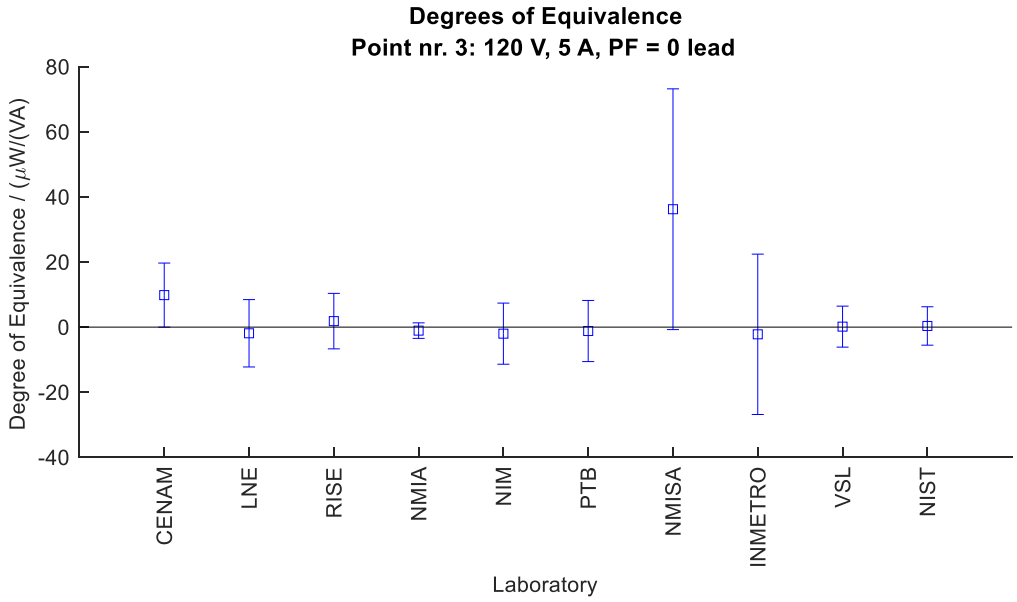
Degrees of Equivalence
Point nr. 3: 120 V, 5 A, PF = 0 lead
Degree of Equivalence / (μW/(VA)
80
60
40
20
0
-20
-40
CENAM
LNE
RISE
NMIA
NIM
PTB
NMISA
INMETRO
VSL
NIST
Laboratory

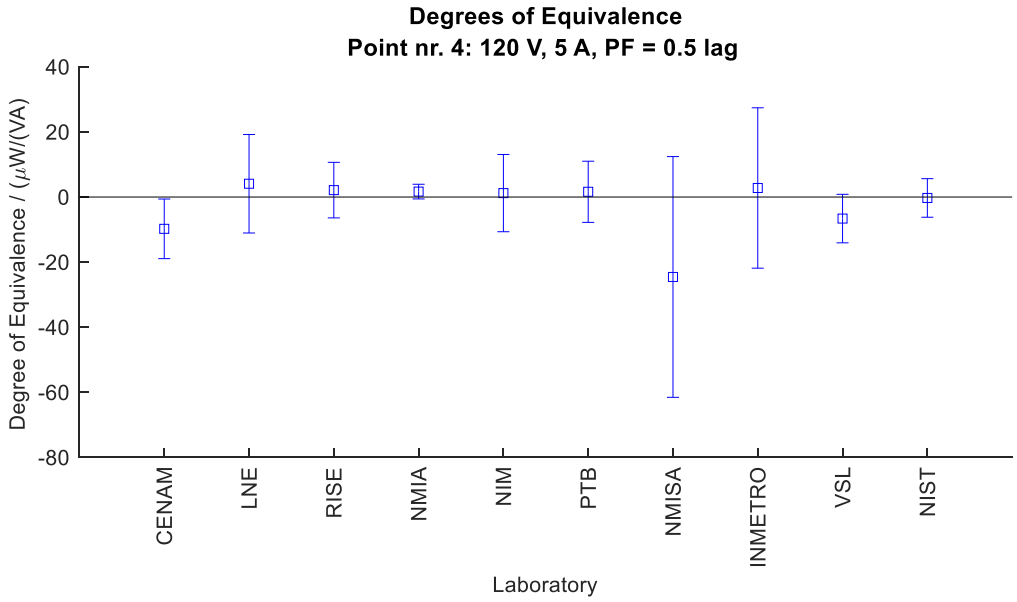
Degrees of Equivalence
Point nr. 4: 120 V, 5 A, PF = 0.5 lag
Degree of Equivalence / (μW/(VA)
40
20
0
-20
-40
-60
-80
CENAM
LNE
RISE
NMIA
NIM
PTB
NMISA
INMETRO
VSL
NIST
Laboratory

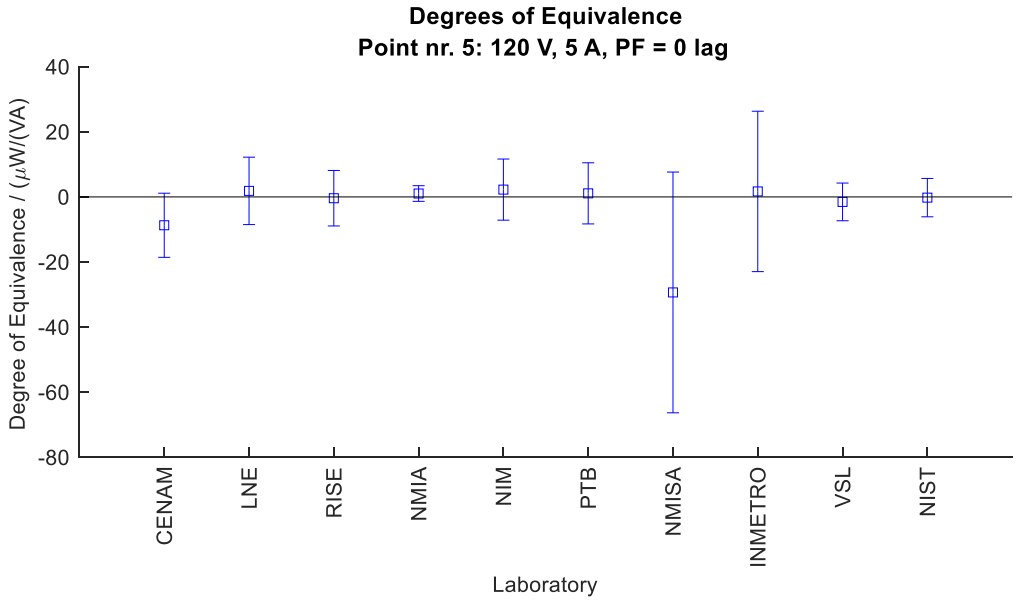
Degrees of Equivalence
Point nr. 5: 120 V, 5 A, PF = 0 lag
Degree of Equivalence / (μW/(VA)
40
20
0
-20
-40
-60
-80
CENAM
LNE
RISE
NMIA
NIM
PTB
NMISA
INMETRO
VSL
NIST
Laboratory

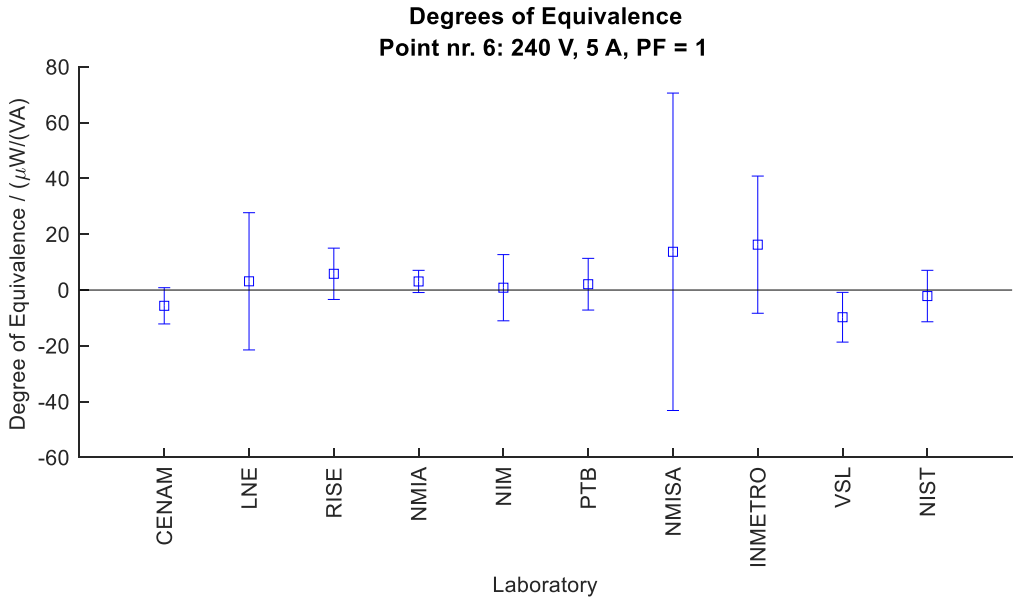
Degrees of Equivalence
Point nr. 6: 240 V, 5 A, PF = 1
Degree of Equivalence / (μW/(VA)
80
60
40
20
0
-20
-40
-60
CENAM
LNE
RISE
NMIA
NIM
PTB
NMISA
INMETRO
VSL
NIST
Laboratory

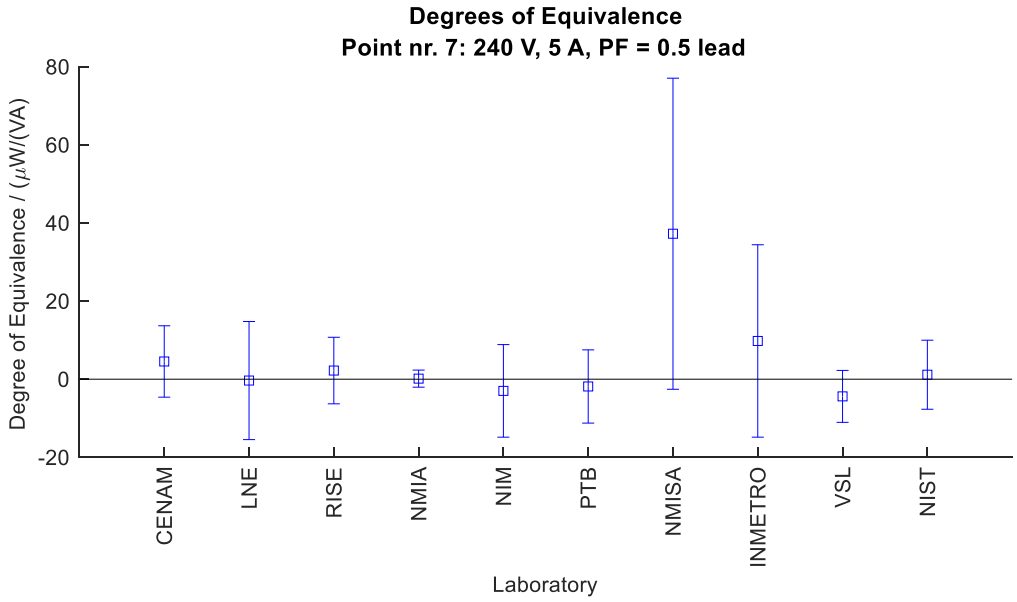
Degrees of Equivalence
Point nr. 7: 240 V, 5 A, PF = 0.5 lead
Degree of Equivalence / (μW/(VA)
80
60
40
20
0
-20
CENAM
LNE
RISE
NMIA
NIM
PTB
NMISA
INMETRO
VSL
NIST
Laboratory

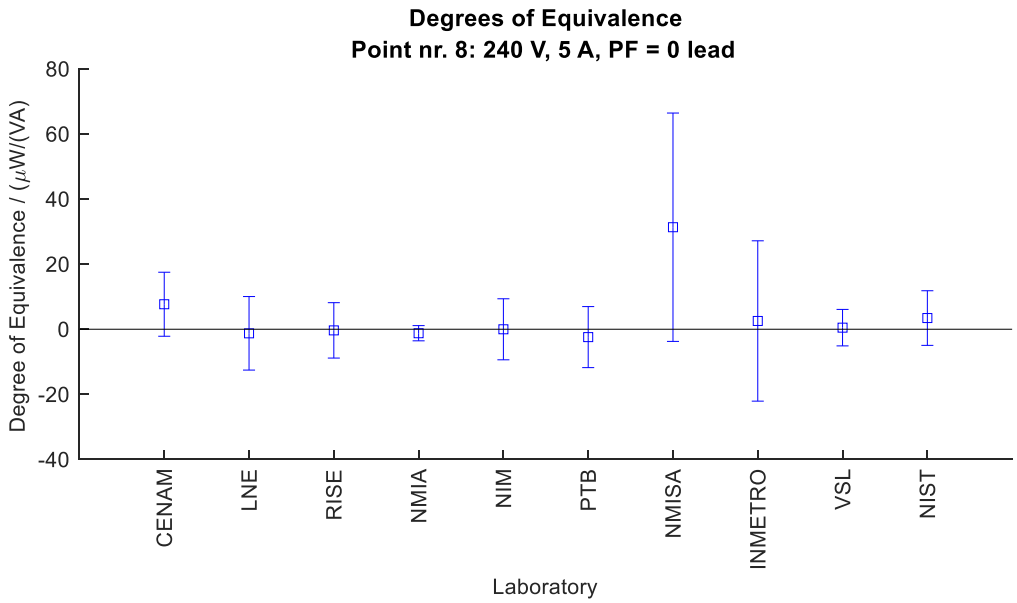
Degrees of Equivalence
Point nr. 8: 240 V, 5 A, PF = 0 lead
Degree of Equivalence / (μW/(VA)
80
60
40
20
0
-20
-40
CENAM
LNE
RISE
NMIA
NIM
PTB
NMISA
INMETRO
VSL
NIST
Laboratory

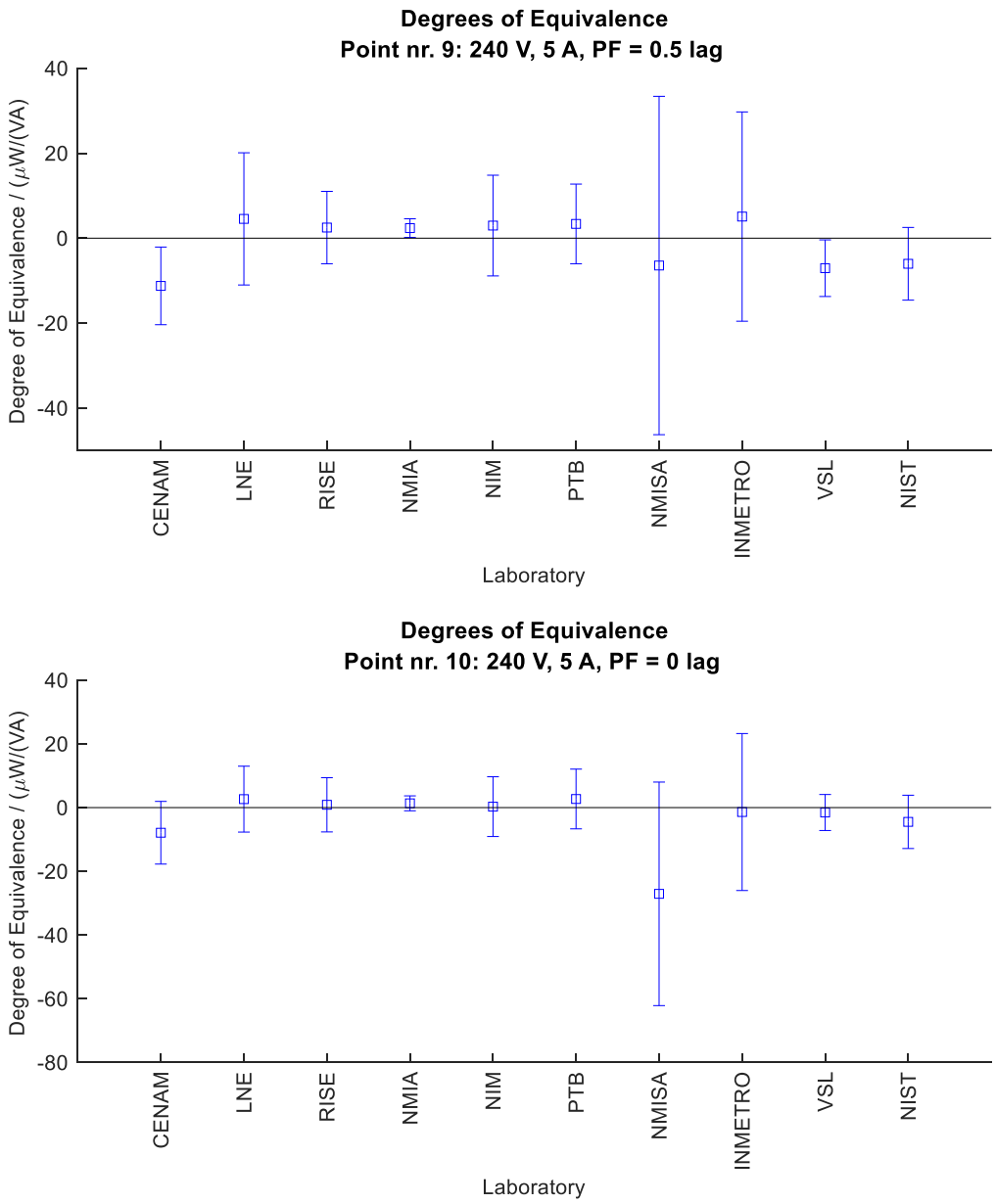

Figure 4: Merged degrees of equivalence for the 10 laboratories for all ten test points.

Based on the merged DoEs and their expanded uncertainties, the normalized DoEs or so-called (signed) En-values have been calculated according to equation (19), as well as Fn-values according to equation (20). The resulting En-values are shown in Table 11. The six values with absolute En-value (slightly) larger than 1 have been printed in bold face, whereas value with an absolute Fn-value larger than 1 have been printed with a shaded background.

Table 11: Normalized DoEs or (signed) En-values. Cells with a shaded background correspond to entries for which the individual DoEs for TS A and TS B were significantly different.

Test point / Lab	120 V 5 A PF = 1	120 V 5 A 0.5 lead	120 V 5 A 0 lead	120 V 5 A 0.5 lag	120 V 5 A 0 lag	240 V 5 A PF = 1	240 V 5 A 0.5 lead	240 V 5 A 0 lead	240 V 5 A 0.5 lag	240 V 5A 0 lag
CENAM	-0.40	0.71	1.00	**-1.07**	-0.88	-0.87	0.50	0.78	**-1.23**	-0.80
LNE	0.19	0.08	-0.18	0.27	0.18	0.13	-0.02	-0.11	0.29	0.26
RISE	0.76	0.39	0.22	0.25	-0.05	0.63	0.26	-0.04	0.29	0.10
NMIA	0.32	-0.16	-0.45	0.74	0.44	0.78	0.07	-0.52	**1.08**	0.57
NIM	-0.18	-0.32	-0.21	0.10	0.24	0.07	-0.25	-0.00	0.25	0.03
PTB	0.06	-0.12	-0.13	0.17	0.12	0.23	-0.20	-0.26	0.36	0.29
NMISA	0.17	0.84	0.98	-0.66	-0.79	0.24	0.94	0.89	-0.16	-0.77
INMETRO	0.12	-0.04	-0.09	0.11	0.07	0.66	0.40	0.10	0.21	-0.06
VSL	**-1.02**	-0.60	0.02	-0.89	-0.26	**-1.09**	-0.66	0.09	**-1.06**	-0.27
NIST	0.12	0.10	0.06	-0.05	-0.04	-0.23	0.13	0.41	-0.70	-0.54

6.6. Model fit

In this section, some comments are made to how well the model fits the data from a mathematical perspective.

In Table 11, six En-values have an absolute value larger than 1, indicating that the model does not perfectly fit the data. A possibility to amend the fit of the data to the model would be to apply a chi-squared consistency test of the provided results, and exclude specific laboratories from contributing to the KCRV value in the case of a statistical inconsistency, as proposed in [4] and [5]. Such a procedure would implicitly assume that specific laboratories have underestimated their provided uncertainties. If this procedure is followed, the following results would be removed from contributing to the KCRV value: TS-B: NIST points 7, 8, 9, 10 and NMISA point 10. For TS A all points could be kept. This is another indication that the model does not perfectly fit the data, especially not for TS B. As the inconsistency did not seem to be major based on a first evaluation of the data, and as it may have been caused by the low claimed uncertainties of some other laboratories, it was finally decided not to exclude any points from contributing to the KCRV calculation.

In equation (3), a large correlation has been assumed between the uncertainties of y_i^A and y_i^B. Therefore, the individual DoE-TSs d_i^A and d_i^B are generally expected to be similar in size as well, which is mathematically expressed by means of the Fn-value defined in equation (20). As there are sixteen entries in Table 11 for which the Fn-value is larger than 1, this indicates that the model also in this aspect does not perfectly fit the data.

It has been explored what the effect of the correlation coefficient of equation (3) has on the model fit, and if there is a value for which the results are significantly better. This turns out not to be the case. The correlation coefficient is based on expert judgement and is believed to be generally correct. In general, reducing the correlation coefficient leads to more laboratories with high En-values as it leads to a reduction of the uncertainty of the merged DoEs, whereas increasing the correlation coefficients leads to more results with high Fn-values. The value of 0.8 seems to be a good compromise solution, leading to the lowest number of results with high En-value. Note that there was not enough information present to justify the definition and usage of laboratory specific correlation coefficients in the analysis.

If no correlation is assumed in equation (3) and if the comparison is analysed as two separate comparisons, then still for both TSs there will be laboratories with En-value (based on the DoE-TS values) larger than 1. So also in the case of analysing the comparison as two independent sub-comparisons, there is no single sub-comparison or TS for which all laboratories are fully consistent with each other.

A possible approach to make the data fit the model and to make all results consistent is to considerably increase the instability uncertainty of the TSs. However, good technical arguments should be found before doing so, as it may mask actual existing problems. A possibility is that the TSs, especially TS B, are sensitive to earthing and other installation effects. As both TSs are of the same make (cf. the discussion on the drift), a considerably different instability uncertainty does not seem to be justified on purely theoretical grounds only. Linearly adding 1 ppm of TS instability uncertainty to both u_{TS}^{A} and u_{TS}^{B} did not make all results consistent, and adding even more uncertainty does not seem to be technical justifiable.

Another possible reason for imperfect model fit is that one or more laboratories underestimated their measurement uncertainty. Each laboratory should carefully assess if the provided uncertainties are realistic. This is in particular true for the laboratories claiming the lowest uncertainties, as they most heavily influence the KCRVs.

Some further analyses have been performed which are not reported in detail in this report. A check has been performed regarding correlation between the reported calibration error and the realized value of the nominal quantities specifying each test point (voltage amplitude, current amplitude, phase difference, frequency) and the realized ambient conditions (temperature, pressure). No significant correlation has been found, indicating that the error of the TSs is not sensitive to small variations of the test point and to fluctuations of the ambient conditions.

7. Summary

In the CCEM-K5.2017 comparison, two traveling standards for evaluation of electrical power measurement CMCs (TS A and TS B) were sent around and measured by ten laboratories. The devices were calibrated by the comparison participants at ten test points, for five different power factors at both at 120 V – 5 A and 240 V – 5 A, and the calibration results were reported to VSL. The total measurement period spanned from March 2018 until August 2022, and was affected by customs issues, the outbreak of the covid pandemic, and the request for re-measurements by VSL and NIST.

PTB performed extensive characterisations of the two travelling standards before the start of the comparison. In order to detect a possible drift of the traveling standards during the comparison measurements, PTB also measured the travelling standards after each regional loop. In total, PTB has measured TS A six times and TS B ten times, both at two representative test points. The two travelling standards turned out to show a very small systematic drift of only 1.5 ppm/y for the magnitude error and no significant drift for the phase error. The random standard uncertainty of the TSs in the PTB stability measurements was between 0.7 ppm and 1.3 ppm for TS A and around 1.8 ppm for TS B.

The method of least squares was used to calculate KCRVs and DoEs. This method is a well-known, transparent method for analysing comparisons. All laboratories were included in the calculation of the two KCRVs. The two resulting DoE-TSs for the two TSs and for each laboratory were combined to a single, merged DoE based on weighing with the inverse of the covariance matrix of the DoE-TSs. Here, a correlation coefficient of 0.8 was assumed for measurements performed by the same laboratory for the two standards. Normalized DoEs, i.e. En-values, were calculated as well. Furthermore, the laboratory results were assessed by means of Fn-values, that give an indication of the consistency in the measurement results of TS A and TS B.

It turned out that the provided measurement results are not fully consistent with each other for all participants given the employed mathematical analysis method. This was both observed during the calculation of the KCRVs as well as while merging the DoE-TSs obtained for TS A and TS B into a single DoE per laboratory. Changing or slightly relaxing some of the model assumptions in the mathematical analysis could not resolve this issue. This indicates that the main reason for this inconsistency seems to be underestimated systematic effects that have resulted in underestimated uncertainties reported by some participants. The somewhat larger scatter in the measurement results for TS B indicate that there may be an unknown effect from the different measurement setups used by the participants on the TS B reading as well, but this effect cannot explain the inconsistencies found.

Analysis of the comparison results with respect to the CMC claims of the participating institutes and the measures to be taken in the case of inconsistencies are not within the scope of this report. Still, the NMIs participated in this comparison are urged to carefully (re)consider their measurement uncertainties and corresponding CMC claims, given the slightly inconsistent comparison results. The present comparison results, and the need for re-measurements and re-evaluation of results by three participants, also underline the need in future comparisons to carefully assess if the uncertainties provided are realistic prior to submitting the measurement results.

8. References

[1] N. Oldham, T. Nelson. R. Bergeest. G. Ramm, R. Carranza. A. C. Corney, M. Gibbes, G. Kyriazis, H. Laiz, L. Liu, Z. Lu, U. Pogliano, K. Rydler, E. Shapiro, E. So, M. Temba, and P. Wright, "An International Comparison of 50/60 Hz Power (1996-1999), IEEE Trans. Instr. and Meas., Vol. 50, Num. 2, pp. 356-360, Apr. 2001.

[2] N. Oldham, T. Nelson, T. N. F. Zhang and H. K. Liu, "CCEM-K5 Comparison of 50/60 Hz Power. Final Report", Metrologia 40, Technical Supplement 01003.

[3] CCEM Guidelines for Planning, Organizing, Conducting and Reporting Key, Supplementary and Pilot Comparisons. CCEM, 21 March 2007.

[4] M G Cox, The evaluation of key comparison data, Metrologia 39, 589, 2002

[5] L Nielsen, Evaluation of measurement intercomparisons by the method of least squares, DFM Technical Report, 2000, DOI: 10.13140/RG.2.2.12239.02728

CCEM-K5.2017 Key Comparison of 50/60 Hz Power

Report Draft B

Annex A

-

Reported measurement values

Annex A: Reported measurement values

In Table 1 and Table 2, the measurement values y_i with expanded uncertainties $2u_i$ reported by each laboratory are shown for respectively TS A and TS B.

The large deviations from nominal value of around -60 μW/VA and +80 μW/VA at PF = 1 were intentionally programmed into the firmware of the two travelling standards (see Section 3.1).

Table 1: Reported measurement values with reported expanded uncertainties for TS A.

Laboratory name	Approximate test date	120 V 5 A PF = 1	120 V 5 A 0.5 lead	120 V 5 A 0 lead	120 V 5 A 0.5 lag	120 V 5 A 0 lag	240 V 5 A PF = 1	240 V 5 A 0.5 lead	240 V 5 A 0 lead	240 V 5 A 0.5 lag	240 V 5 A 0 lag
CENAM-A	12/03/18	-63.0 (7.1)	-59.8 (9.7)	-32.3 (10.5)	-3.3 (9.7)	31.7 (10.5)	-63.8 (7.1)	-60.3 (9.7)	-34.1 (10.5)	-3.4 (9.7)	32.0 (10.5)
LNE-A	10/09/18	-56.7 (26.0)	-67.1 (16.0)	-45.0 (11.0)	11.7 (16.0)	43.5 (11.0)	-55.7 (26.0)	-67.2 (16.0)	-44.6 (12.0)	14.2 (17.0)	45.0 (11.0)
RISE-A	20/10/18	-53.3 (9.9)	-63.4 (9.1)	-40.8 (9.1)	9.3 (9.1)	40.4 (9.1)	-51.8 (9.9)	-63.7 (9.1)	-43.7 (9.1)	12.0 (9.1)	42.1 (9.1)
NMIA-A	23/03/19	-56.8 (4.7)	-66.4 (2.9)	-44.3 (3.1)	10.1 (2.9)	42.5 (3.1)	-51.9 (4.7)	-64.8 (2.9)	-44.9 (3.1)	12.8 (2.9)	43.2 (3.1)
NIM-A	16/06/19	-60.7 (12.0)	-70.4 (12.0)	-46.2 (10.0)	9.8 (12.0)	44.8 (10.0)	-55.1 (12.0)	-68.4 (12.0)	-46.9 (10.0)	13.4 (12.0)	45.4 (10.0)
PTB-A	07/01/20	-56.2 (10.0)	-64.6 (10.0)	-42.2 (10.0)	8.8 (10.0)	40.5 (10.0)	-52.5 (10.0)	-63.9 (10.0)	-43.1 (10.0)	11.7 (10.0)	41.5 (10.0)
NMISA-A	18/03/20	-60.0 (55.0)	-33.0 (39.0)	-8.0 (39.0)	-3.0 (39.0)	5.0 (39.0)	-44.0 (60.0)	-29.0 (42.0)	-23.0 (37.0)	4.0 (42.0)	32.0 (37.0)
INMETRO-A	07/11/20	-50.0 (26.0)	-63.0 (26.0)	-44.0 (26.0)	12.0 (26.0)	41.0 (26.0)	-36.0 (26.0)	-54.0 (26.0)	-41.0 (26.0)	17.0 (26.0)	40.0 (26.0)
VSL-A	26/02/21	-64.9 (10.3)	-70.0 (7.9)	-44.1 (6.7)	4.6 (8.1)	41.0 (6.3)	-64.0 (9.7)	-70.6 (7.2)	-44.9 (6.1)	5.9 (7.2)	41.6 (6.2)
NIST-A	16/08/22	-53.2 (6.3)	-66.3 (6.4)	-45.8 (6.4)	13.4 (6.4)	44.2 (6.4)	-53.9 (9.8)	-67.1 (9.3)	-46.2 (9.0)	12.2 (9.1)	43.2 (8.9)

Table 2: Reported measurement values with reported expanded uncertainties for TS B.

Laboratory name	Approximate test date	120 V 5 A PF = 1	120 V 5 A 0.5 lead	120 V 5 A 0 lead	120 V 5 A 0.5 lag	120 V 5 A 0 lag	240 V 5 A PF = 1	240 V 5 A 0.5 lead	240 V 5 A 0 lead	240 V 5 A 0.5 lag	240 V 5 A 0 lag
CENAM-B	12/03/18	76.8 (7.1)	72.7 (9.7)	39.9 (10.5)	3.7 (9.7)	-41.0 (10.5)	78.0 (7.1)	75.2 (9.7)	40.4 (10.5)	2.6 (9.7)	-43.1 (10.5)
LNE-B	12/09/18	86.6 (26.0)	70.8 (16.0)	29.6 (11.0)	16.7 (16.0)	-32.2 (11.0)	88.9 (26.0)	73.8 (16.0)	33.8 (12.0)	16.2 (16.0)	-35.9 (11.0)
RISE-B	23/10/18	88.3 (9.9)	71.1 (9.1)	32.6 (9.1)	15.8 (9.1)	-33.2 (9.1)	90.9 (9.9)	75.3 (9.1)	34.4 (9.1)	15.2 (9.1)	-35.9 (9.1)
NMIA-B	21/03/19	81.3 (4.7)	66.2 (2.9)	29.2 (3.1)	15.2 (2.9)	-31.7 (3.1)	86.1 (4.7)	70.8 (2.9)	32.0 (3.1)	15.2 (2.9)	-34.3 (3.1)
NIM-B	16/06/19	69.7 (16.0)	62.0 (16.0)	31.0 (10.0)	7.7 (16.0)	-33.2 (10.0)	82.0 (16.0)	75.5 (16.0)	40.0 (10.0)	6.2 (16.0)	-42.3 (10.0)
PTB-B	07/01/20	81.8 (10.0)	64.4 (10.0)	27.2 (10.0)	17.4 (10.0)	-29.7 (10.0)	87.5 (10.0)	68.2 (10.0)	28.6 (10.0)	19.7 (10.0)	-30.8 (10.0)
NMISA-B	18/03/20	103.0 (55.0)	98.0 (39.0)	69.0 (39.0)	-24.0 (39.0)	-56.0 (39.0)	103.0 (60.0)	113.0 (42.0)	78.0 (37.0)	7.0 (42.0)	-83.0 (37.0)
INMETRO-B	09/11/20	83.0 (26.0)	65.0 (26.0)	28.0 (26.0)	17.0 (26.0)	-30.0 (26.0)	102.0 (26.0)	84.0 (26.0)	38.0 (26.0)	18.0 (26.0)	-39.0 (26.0)
VSL-B	26/02/21	73.2 (10.2)	66.1 (7.9)	33.9 (7.0)	5.9 (7.8)	-37.3 (6.2)	79.0 (9.6)	73.6 (7.1)	39.0 (6.2)	4.9 (7.2)	-41.5 (6.1)
NIST-B	16/08/22	87.1 (6.3)	76.5 (6.4)	37.9 (6.4)	10.6 (6.4)	-40.0 (6.4)	88.6 (9.8)	85.8 (9.5)	47.9 (9.0)	1.4 (9.1)	-51.7 (9.0)

CCEM-K5.2017 Key Comparison of 50/60 Hz Power

Report Draft B

Annex B

-

Comparison Protocol

CCEM-K5.2017

Key comparison of 50/60 Hz power

TECHNICAL PROTOCOL

December 2017

Organizing laboratories: CENAM, PTB, VSL

TABLE OF CONTENTS

1. INTRODUCTION

Committed to underpin the Mutual Recognition Arrangement as proposed by the Committee International of Weights and Measures, CIPM, a key comparison of 50/60 Hz of power standards is currently being organized under the auspices of the Consultative Committee of Electromagnetism, CCEM.

The last CCEM key comparison of power standards was organized by NIST between years 1996 to 1999, NIST being the pilot laboratory. Fifteen national metrology institutes from different regional metrology organizations did take part. The results of this comparison were reported in 2002 [1].

Since the completion of this comparison already is more than 15 years ago, and significant technical updates have been made to the primary power reference setups of many NMIs, the present comparison was agreed upon. Participating NMIs will be responsible for conducting the tests in their respective laboratories and submitting their test data in the format prepared for this comparison.

The comparison will follow the test procedure and data analysis method [2] used during the last international comparison CCEM-K5. This protocol has been prepared following the CCEM Guidelines for Planning, Organizing, Conducting and Reporting Key, Supplementary and Pilot Comparisons [3].

Coordinating laboratory: VSL, Netherlands (writing report)
Pilot laboratory: PTB, Germany (measurement of the travelling standards)
Assisting laboratory: CENAM, México (organization)

2. REFERENCE STANDARDS

2.1 Description of the reference standards

Two reference standards, of the type RADIAN RD-22-332S, will be used in this key comparison. These standards have been adapted to measure active power at 120 V and 240 V and 5 A with outstanding stability in time.

CCEM is grateful to NIST for having provided the reference standards for this key comparison.

Figure 1: reference standard: RD-22-332S, serial number: 206 815

Figure 2: reference standard: RD-22-332S, serial number: 203 409

Special connections on the reference standards.

<u>24 V DC Power Supply:</u>

The travelling standards should be powered using a 24 V DC power supply delivered with the standards. See Figure 4 for the location of the connections.

> **MAKE SURE that the voltage input selector of the 24 V DC power supply is set to the correct value – 120 V or 240 V – before connecting the power supply to the AC mains.**

<u>AC current measurements</u>:

As shown in Figure 3, the reference standards have been fitted to provide high accuracy measurements of 5 A current. As shown in the picture below, a couple of posts out of the reference standard allow for the measurement of 5 A current. This allows for the connection of cables with either banana plugs or spades.

To ensure that the standard reference correctly measures the phase angle between the applied voltage and current, take post in red as the HIGH side of the 5 A current measurement circuit.

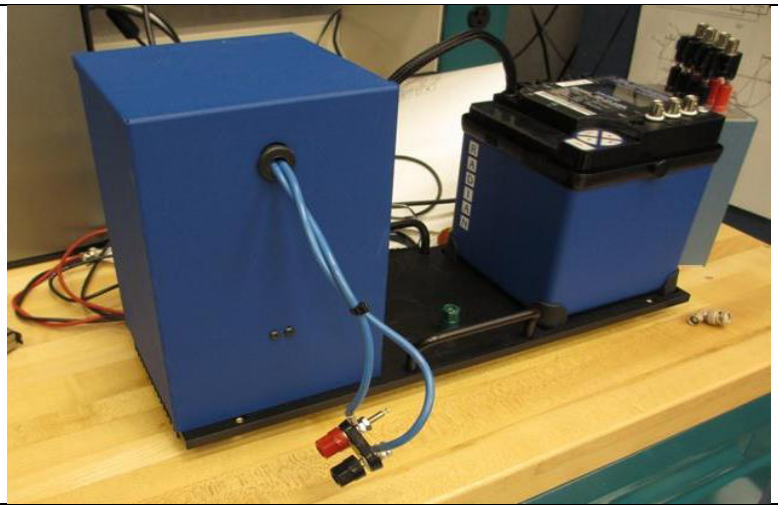

Figure 3. Special connection for current measurements on the reference standard.

<u>AC voltage measurements:</u>

As shown in Figure 4, the V_{CA} input voltage of the reference standards are on the left hand side of the panel of the references. Be aware of the connection of the auxiliary power input of 24 V_{DC}, which is located below the V_{CA} posts.

Figure 4: The V_{CA} input posts on the reference standards. The 24 V DC auxiliary power input is below the V_{CA} input posts.

2.2 Measurement Quantity

The quantity to be reported is the calibration error of the travelling standard when measuring active power; the calibration error will be expressed in μW/VA.

The participating laboratory should report a single measurement result and its uncertainty for each of the testing points as given in Table 2.

Table 2. Testing points for the measurement of Active Power.

Parameter	Value
RMS voltages	**120 V** **240 V**
RMS current	**5 A**
power factor	**1.0** **0.5 lead** **0.5 lag** **0 lead** **0 lag**
testing frequency	**53 Hz**
Total amount of testing points	**10**

Notes:

1. The "lead" is defined as the current phase leading the voltage phase, and "lag" as the current phase lagging the voltage phase.

2. The measurement result to be reported is the calibration error of the travelling standard, defined as the difference between the measured quantity indicated by the travelling standard and the quantity applied to it, and divided by the nominal apparent power VA.
3. The error and uncertainty of the calibration should be expressed in terms of μW/VA.
4. The travelling standard should be de-energized between each set of measurements for 1 minute, followed by at least 15 minute warm-up period.
5. The total estimated expanded uncertainty quoted in the report shall encompass the Type A uncertainty and the Type B uncertainty of the corresponding NMI calibration system. The expanded uncertainty should be estimated for a level of confidence of 95.45 %.

2.3 Relevant parameters

The values of RMS voltage, RMS current, PF (power factor/phase angle) and frequency are relevant parameters to the 50/60 Hz key comparison power. As indicated in Annex A4 *Layout of the Measurement Report*, participants must record the mean value of voltage, current, PF (power factor/phase angle) and frequency for each of the testing points in Table 1. As shown in Annex A3 *Typical scheme of an uncertainty budget*, the participant laboratory must report all uncertainty sources pertinent to the measurement of power.

2.4 Software for data logging the power readings from the reference standards

The CCEM is grateful to Radian Research Inc. for supporting the CCEM-K5 key comparison of power for the provision of a software package that the participating laboratories may download.

Laboratories may download the following two ftp sites where versions of PC Suite software can be found.

Note that the first file 02.00.13 is for Microsoft XP, whereas version 04.00.04.zip is for Microsoft WIN 7 platform.

PC suit software	**platform**
www.radianresearch.com/upgrade/PCSuite_02_00_13.zip	Microsoft XP
www.radianresearch.com/upgrade/PC_Suite_Release_04.00.04.zip	Microsoft WIN 7

2.5 The key comparison reference value and the degrees of equivalence

This protocol has been prepared following the guidelines of the CCEM as given in [3]. The principles of the method of computation of the reference value are as follows:

i. The key comparison reference value (KCRV) and the degrees of equivalence among the participants for the CCEM.EM-K5 key comparison shall be determined according to the procedure agreed upon by the CCEM for the CCEM-K5 Comparison 50/60 Hz Power (1996-1999) [1].
ii. For the calculation of the KCRV, the weighted mean over the participating laboratories will be used. If the uncertainty contribution of a participant due to the traceability to another NMI participating in this comparison amounts to a substantial part of the overall uncertainty value, the result will not be taken into account in the calculation of the KCRV.
iii. The degree of equivalence among the participating laboratories shall be expressed quantitatively by two terms:
    - the difference of the participating laboratory from the key comparison reference value

- the uncertainty of this difference at a 95.45 % level of confidence.

iv. In order to compare the results of the different participants, including the pilot laboratory, each of the participants should report a single measurement result for each of the testing points shown in Table 2.

v. The bilateral degrees of equivalence. As requested per the CCEM, the bilateral degrees of equivalence among the participating laboratories in a key comparison will not be explicitly shown, but the formula for obtaining them will be included, thus allowing the participating laboratories to calculate their bilateral degree of equivalence from the data resulting from the difference between the participating laboratories and the KCRV.

2.6 Preparation of Drafts A and B of this key comparison.

As stated in the CCEM Guidelines [3], for this key comparison, the following information shall be considered in preparing Drafts A and B with the results of the comparison:

- individual values for each institute together with their declared uncertainties;
- the key comparison reference value with its associated uncertainty;
- for each institute, the deviation from the key comparison reference value and the uncertainty in that deviation (at a 95.45 % level of confidence), i.e. its degree of equivalence.

3. ORGANIZATION

3.1 Coordinator and members of the support group

The organization of the comparison is shared between three institutes: CENAM, PTB and VSL. CENAM is responsible for the organization of the comparison, including the technical protocol, PTB is performing multiple measurements during the comparison in order to determine the stability of the standards, and VSL is doing the general coordination and is responsible for the final report.

Name	Organization	Address	e-mail address
Gert Rietveld	VSL	Thijsseweg 11, 2629 JA Delft The Netherlands	grietveld@vsl.nl
Rene Carranza	CENAM	km. 4.5 Carretera los Cues, El Marques, 76246 Queretaro, Mexico phone: 52 442 2 11 05 94	rene.carranza@cenam.mx
Matthias Schmidt	PTB	Bundesallee 100, 38116 Braunschweig Germany	Matthias.Schmidt@ptb.de

3.2 Participants

(see also Annex A1 Detailed list of participants)

	Participating NMI	Contact person	e-mail address	phone
1	CENAM	René Carranza	rcarranz@cenam.mx	+52 44 22 11 05 94
2	INMETRO	Rodrigo Simões Ribeiro	rsribeiro@inmetro.gov.br	+55 21 26 79 90 80
3	LNE	Daniela Istrate	Daniela.istrate@lne.fr	+3 31 30 69 32 05
4	NIM	Lei Wang	wl@nim.ac.cn	
5	NIST	Tom Nelson	thomas.nelson@nist.gov	
6	NMIA	Ilya Budovsky	ilya.budovsky@measurement.gov.au	

7	NMISA	Flippie Prinsloo	fprinsloo@nmisa.org	+2 71 28 41 30 13
8	PTB	Matthias Schmidt	Matthias.Schmidt@ptb.de	
9	SP	Stefan Svensson	stefan.svensson@sp.se	
10	VNIIM	Gleb Gubler	g.b.gubler@vniim.ru	+7 81 22 51 74 44
11	VSL	Gert Rietveld	grietveld@vsl.nl	+3 11 52 69 16 45

3.3 Time Schedule

Table 2 shows the Time Schedule of the comparison. So far, the time schedule is related only to the metrology regional organization. The final schedule with precise information of allocated times to each laboratory will be delivered later by CENAM and included in annex A2 of this protocol. If a delay occurs with either travelling standards, in such a way that it affects the overall schedule time, the time schedule will be revised and all the participants will be informed by CENAM of any change to the schedule.

Table 2. Time schedule of the comparison

	activities	Time Schedule
1	Characterization of reference standards at PTB	Jan 2017 – Jan 2018
2	SIM (NIST, CENAM, INMETRO)	Feb 2018 – May 2018
3	PTB	Jun 2018 - Jul 2018
4	EURAMET (VSL, LNE, SP)	Aug 2018 – Nov 2018
5	PTB	Dec 2018 - Jan 2019
6	APMP (VNIIM, NIM, NMIA)	Feb 2019 – May 2019
7	PTB	Jun 2019 - Jul 2019
8	AFRIMET (NMISA)	Aug 2019 – Sep 2019
9	PTB	Oct 2019 – Nov 2019
10	Draft A	Jan 2020

NOTE: It is recommended that the time of measurement at the participating laboratory should be not more than two weeks in order to comply with the planned schedule.

3.4 "Door-to-door delivery scheme"

In order to reduce delay times at customs, the travelling standards shall be sent directly to the address of the following laboratory according to the schedule program given in Table 2. Make sure that the address of the following laboratory is as given in Annex 1.

The standards will be provided with an individual rugged plastic container, suitable for shipping the standards on airplane. The standards and accompanying accessories, like connectors and 24 V_{DC} power supply are to be transported inside the rugged plastic container.

The standards are packaged along with a temperature/humidity miniature logger. During measurements at the participant's laboratory, make sure that the logger remains on the top surface of the travelling standard, mainly close to the backlit LCD of the travelling standard, in order to log

measurements of ambient temperature and humidity. There is no need for the participating laboratory trying to gain access to the logger; its contents will be downloaded at PTB in order to keep track of the changes of temperature or humidity which may have occurred during transportation or while staying at the participating laboratory.

IMPORTANT: In order to have the final time schedule of the comparison, all the participants should inform CENAM whether they agree to send the travelling standard by a customs agency or may want to be responsible of a different way to transport the travelling standard.

The contact person of the participant laboratory must inform CENAM of all the pertinent information when sending the travelling standards to the destine customs agency.

Costs involved with sending the travelling standard either to PTB or to the next participant, should be paid by the participant laboratory.

3.5 Unpacking, handling and packing

Unpacking:

1. Upon arrival, the participant laboratory must carefully inspect the travelling standard before it is removed from the plastic rugged container. In case of damage to the travelling standard, please take a photograph and send it to the pilot laboratory.
2. For removing the travelling standards from their containers, please refer below to the handling instructions.
3. Fill the *Confirmation note of receipt* (Annex A5) and send it to the pilot laboratory.

Handling:

Extreme care should be taken to remove the travelling standards out the rugged plastic container.

For removing the RD-22 from the container, the metal handlers located at both sides of its platform must be used.

Packing:

1. For packing the travelling standards, make sure that the travelling standard is comfortably put inside the container. For maneuvering the travelling standards, please refer to the above handling instructions.
2. **All accompanying accessories should be put inside the container**. Make sure that the **miniature data logger** is put along the standards in the container.
3. Inform the pilot laboratory of pertinent details regarding the clearance of customs, shipping and flights. If the travelling standards should be sent to another participant, make sure that both the recipient and the pilot laboratories are informed about travelling details.
4. Fill the *Confirmation note of shipment* (Annex A6) and send it to the pilot laboratory.

3.6 Failure of the travelling standard

In case of failure:

1. Unplug the travelling standard.
2. Write immediately to the pilot laboratory describing the behavior of the travelling standard. Send along any message displayed on the backlit LCD. Take photographs of the measuring system and of the connecting cables to the travelling standard.
3. Wait for instructions from the pilot laboratory on the way to proceed.

3.7 Financial aspects, insurance, customs

In every case, the participant laboratory should ensure that its organization covers insurance for any defect to the travelling standards while they are in its premises.

All the participants will be responsible for expenses related with sending the travelling standards either to the next participant or to the pilot laboratory.

4. MEASUREMENT INSTRUCTIONS

4.1 General instructions

There are no performance tests on the reference standard to be performed before measurements at the participant's laboratory.

4.2 Particular requirements for energizing and connecting the travelling standards

4.2.1 Energizing the reference standards at 24 V_{DC}.

The reference standards are provided with a 24 V_{DC} power supply, which shall be connected to the mains at either 120 V or 240 V, 45 Hz or 65 Hz.

Before connecting the 24 V_{DC} power supply to the mains:

1. **MAKE SURE that the voltage input selector of the 24 V DC power supply is set to the correct value – 120 V or 240 V.**

2. Make sure that this supply is properly connected to the Auxiliary Power input port of the reference standard as shown in Figure 5.

3. Then, plug the 24 V_{DC} power supply to the mains power.

The auxiliary power to the travelling standard should be applied at least 4 hours before starting the tests.

> **IMPORTANT: In order to achieve the best measurement capability of the travelling standard, allow it to warm up at least 4 hours at room temperature. Then, switch the reference standard off and on again. This action will set the internal DC voltage reference of the standard being corrected at its current internal temperature.**

4.2.2 Connecting the reference standards

Make sure that the testing voltage and current sources are properly connected to the input terminals of the reference standard. Refer to Figure 5 for details.

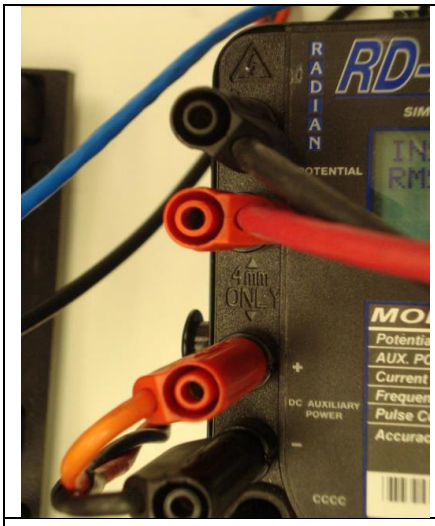	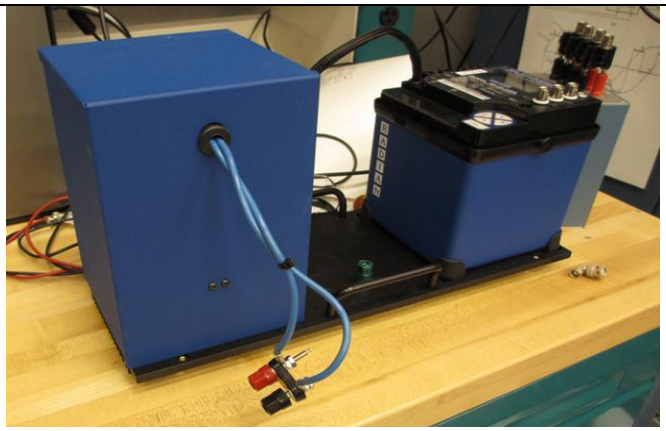
V_{CA} input for 120 and 240 V_{CA} DC auxiliary power = 24 V_{DC}	**I_{CA} input for 5 A**

Figure 5. Connecting the reference standard for V_{CA} = 120 V and 240 V, I_{CA} = 5 A, and auxiliary power of 24 V_{DC}.

4.3 Method of measurement of active power

The measurement method is that used by the participating laboratory for the provision of a calibration. Make sure that testing voltage and current are within at least 0.2% of the values shown in Table 1.

1. Upon arrival, allow the reference standard to warm up at least 4 hours after powering it with the 24 V DC power supply. Then switch the unit off and on in order for its internal DC voltage reference to correct according to its internal temperature.
2. For the voltage and current sources, make sure that their frequency is set at 53 Hz, according to the testing points shown in Table 1.
3. At every power factor/phase angle shown in Table 1, make as many independent measurements as stated on the calibration procedures of your laboratory.
4. Record the readings of active power, voltage, current, power factor/phase angle and frequency displayed on the backlit LCD of the travelling standard.
5. Calculate the calibration error of the travelling standard at the testing points shown in Table 1. The calibration error is defined as the difference between the measured quantity indicated by the reference standard and the quantity applied to it, and divided by the applied VA. The calibration error should be expressed in µW/VA for active power. The error is positive if the reference standard's indication is more positive than the applied quantity.
6. The average of at least five sets of measurements should be reported. The reference standard should be de-energized between each set of measurements for 1 minute, followed by at least 15 minute warm-up period.
7. The total estimated expanded uncertainty quoted in the laboratory's report should encompass the Type A and Type B uncertainties of the corresponding NMI calibration service. The expanded uncertainty should be estimated for a level of confidence of 95.45 %.
8. Report the mean value and spread of the ambient temperature and relative humidity of the laboratory.
9. The measurement report of the participant may be completed according to Annex A4 *Layout*

of the measurement report.

5. UNCERTAINTY OF MEASUREMENT

(See Annex A3 *Typical scheme of uncertainty budget*)

The uncertainty of measurement must be determined following the Guide for the Expression of Uncertainty in Measurement [4].

Participant laboratories are requested to report the main uncertainty components of their measurement systems, identifying all the pertinent uncertainty sources and quantifying their contribution to the expanded uncertainty.

In order to have a comparable uncertainty evaluation, each laboratory is asked to report the following information in the form of an uncertainty budget:

i. The result of the type A method of uncertainty estimation which yields the standard deviation of the mean values of data sets recorded by the participant in order to calculate its final report value.
ii. The result of the type B method of uncertainty estimation.
iii. The expanded uncertainty estimated at a 95.45 % level of confidence.
iv. The degrees of freedom for the estimation of the expanded uncertainty at a 95.45 % level of confidence.

6. MEASUREMENT REPORT

(See Annex A4 *Layout of the measurement report* and the template Excel reporting file)

The participant laboratory should report the following information within 2 (two) months from the end of measurements:

1. The mean of the calibration error of the travelling standard. The calibration error should be expressed in terms of μW/VA.
2. The expanded uncertainty of the calibration error of the travelling standard should be estimated at a 95.45 % level of confidence. The expanded uncertainty should be expressed in terms of μW/VA.
3. The uncertainty components coming out from the Type A and B methods of uncertainty estimation of the calibration error of the travelling standard.
4. The mean value and standard uncertainty of the relevant parameters of the active power value, such as: RMS voltage, RMS current, power factor / phase angle, frequency. The standard uncertainty of the relevant parameters should be determined for a 95.45 % level of confidence ($k = 2$ for a normal distribution).
5. The final results for all 10 test points must also be reported using the Excel template file associated with the comparison.
6. Measurement uncertainty estimation shall comply with the Guide to the Expression of Uncertainty in Measurement [4].
7. A complete uncertainty budget and any additional information must be reported as shown in Annex A3.

All participants must report the results of the comparison to the VSL as soon as possible, in every case, not later than 2 (two) months after the measurements are completed.

7. REFERENCES

1. N. Oldham, T. Nelson. R. Bergeest. G. Ramm, R. Carranza. A. C. Corney, M. Gibbes, G. Kyriazis, H. Laiz, L. Liu, Z. Lu, U. Pogliano, K. Rydler, E. Shapiro, E. So, M. Temba, and P. Wright, "An International Comparison of 50/60 Hz Power (1996-1999), IEEE Trans. Instr. and Meas., Vol. 50, Num. 2, pp. 356-360, Apr. 2001.
2. N. Oldham, T. Nelson, T. N. F. Zhang and H. K. Liu, "CCEM-K5 Comparison of 50/60 Hz Power. Final Report", Metrologia 40, Technical Supplement 01003.
3. CCEM Guidelines for Planning, Organizing, Conducting and Reporting Key, Supplementary and Pilot Comparisons. CCEM, 21 March 2007.
4. Guide to the Expression of Uncertainty in Measurement, 1999. International Organization of Standards, Geneva, Switzerland. ISO ENV 13005:1999.

A1. DETAILED LIST OF PARTICIPANTS

The indicated NMI addresses are the shipping addresses.

	Participating NMI	Contact person	NMI address (shipping address)	e-mail address	phone
1	CENAM	René Carranza	km 4.5 Carretera Los Cues, El Marques, CP 76246 Queretaro, Mexico	rcarranz@cenam.mx	+52 442 2 11 05 95
2	INMETRO	Rodrigo Simões Ribeiro	Laboratório de Metrologia em Energia Elétrica – Lamel Divisão de Metrologia Elétrica Inmetro-Instituto Nacional de Metrologia, Qualidade e Tecnologia Av. Nossa Senhora das Graças, 50 - Prédio 2 CEP: 25.250-020 - Xerém - Duque de Caxias Rio de Janeiro - RJ - Brasil	rsribeiro@inmetro.gov.br	++55 21 26 79 90 80
3	LNE	Daniela Istrate		Daniela.istrate@lne.fr Michel.Massault@lne.fr christel.constantino@lne.fr	+33 1 30 69 32 05
4	NIM	Lei Wang		wl@nim.ac.cn	
5	NIST	Tom Nelson	National Institute of Standards and Technology 100 Bureau Drive, Stop 8170 Gaithersburg, MD 20899-8170	Thomas.nelson@nist.gov	
6	NMIA	Ilya Budovsky		ilya.budovsky@measurement.gov.au leigh.johnson@measurement.gov.au	
7	NMISA	Flippie Prinsloo	CSIR Campus, Building 5 Meiring Naudé Road, Brumeria Pretoria, 0184 South Africa	fprinsloo@nmisa.org	+2 71 28 41 30 13
8	PTB	Matthias Schmidt	Working Group 2.33 Bundesallee 100 38116 Braunschweig Germany	Matthias.Schmidt@ptb.de	+49 531 592 2330
9	SP	Stefan Svensson		stefan.svensson@sp.se	
10	VNIIM	Gleb Gubler		g.b.gubler@vniim.ru g.B.gubler@vnim.ru	+7 812 2517444
11	VSL	Gert Rietveld	Thijsseweg 11 2629 JA Delft, The Netherlands	grietveld@vsl.nl	+31 15 2691645

A2. SCHEDULE OF THE MEASUREMENTS

Table A.2.1. Circulation schedule of the reference standard

Laboratory		Allocated time	
		receiving day	sending day
1			
2			
3			
4			
5			
6			
7			
8			

A3. TYPICAL SCHEME OF AN UNCERTAINTY BUDGET

The uncertainty of measurement must be determined following the Guide for the Expression of Uncertainty in Measurement [4]. Information of the uncertainty of measurements must be provided in this form.

Participant laboratories are requested to report the main uncertainty components of their measurement systems, identifying all the pertinent uncertainty sources and quantifying their contribution to the expanded uncertainty.

In order to have a comparable uncertainty evaluation, each laboratory is asked to report the following information in the form of an uncertainty budget:

i. The result of the type A method of uncertainty estimation which yields the standard deviation of the mean values of data sets recorded by the participant in order to calculate its final report value.
ii. The result of the type B method of uncertainty estimation.
iii. The expanded uncertainty estimated at a 95.45 % level of confidence.
iv. The degrees of freedom for the estimation of the expanded uncertainty at a 95.45 % level of confidence.

Main uncertainty components y_i	Standard uncertainty $u(y_i)$	Type method A or B of evaluation/probability distribution function	Sensitivity coefficient c_i	Uncertainty contribution $u(R_i)$	Degrees of freedom n_i
1) Standard deviation of the calibration error of the travelling standard		Type A pdf: Normal			
2) uncertainty components of the reference standard of the participant					
3) Ambient conditions					
3.1) temperature 3.2) humidity					
Root square sum of Type A standard uncertainties and effective degrees of freedom					
Root square sum of Type B standard uncertainties and effective degrees of freedom					
Combined standard uncertainty and effective degrees of freedom					
Expanded uncertainty (95.45 % coverage factor)					

A4. LAYOUT OF THE MEASUREMENT REPORT

1. Identification of the travelling standard: RD-22
2. Identification of the participant laboratory and its representative
3. Measurement set-up and traceability scheme
4. Measurement procedure
5. Results:
   a. Mean value of the calibration error of reference standard at the active power values shown in Table 1, expressed in μW/VA.
   b. Expanded uncertainty estimated at a 95.45 % confidence level and the degrees of freedom of the calibration error of the travelling standard at active power.
   c. Mean value of the relevant parameters measured by the reference standard: voltage, current, power factor, frequency.
   d. Mean date of measurement.
   e. Ambient conditions: mean value and spread of temperature and humidity measurements.

   These measurement results must (also) be reported using the template xls file that comes with this protocol
6. Detailed uncertainty budget as in *Annex 3*.
7. Report the date and time when the reference standard is de-energized and energized.
8. Signature and title of the laboratory representative.

A5. CONFIRMATION NOTE OF RECEIPT

To: René Carranza, rcarranz@cenam.mx
CENAM, Mexico

CC: ……
(previous participating laboratory)

From: …….
(participating laboratory)

Re: CCEM-K5 Receipt of travelling standard (identification of the travelling standard: RD-22

We confirm having received the travelling standard of the CCEM-K5 key comparison 50/60 Hz power on (date)….

After visual inspection:

No damage of the transport package and the travelling standard has been noticed.

Or

The following damage(s) are reported. In such a case, please add pictures of damages.

Date: …….

A6. CONFIRMATION NOTE OF SHIPMENT

To: René Carranza, rcarranz@cenam.mx
CENAM, Mexico

CC: ……
(next participating laboratory)

From: ……..
(participating laboratory)

Re: CCEM-K5 Dispatch of travelling standard (identification of the travelling standard: RD-22)

We confirm having shipped the travelling standard of the CCEM-K5 key comparison 50/60 Hz power on (date)…. to the following address**:**

a) if the travelling standard will be sent to the pilot laboratory:
PTB Braunschweig
Matthias Schmidt
Working Group 2.33
Bundesallee 100
38176 Braunschweig
Germany

b) if the travelling standard will be sent to another participant laboratory**:**
Shipping address of the next participant (see Annex 1)

We confirm that we have included in both shipping containers, the accessories:

- ☐ 24 DC power supply
- ☐ Cable for PC read out of the RD22
- ☐ Datalogger for temperature / humidity

In any case, add the following information:

- flight number,
- airline,
- estimated time of arrival,
- air bill number and
- any other pertinent information about the shipment

Date: …….

CCEM-K5.2017 Key Comparison of 50/60 Hz Power

Report Draft B

Annex C

-

Participant Reports

Table of Contents

This Annex contains the reporting of all the participants in the comparison, including their measurement methods and uncertainty budgets. The reports are given in alphabetical order of the participants.

1. Comparison report of CENAM

CCEM-K5.2017

Key comparison of 50/60 Hz power

CENTRO NACIONAL DE METROLOGÍA, CENAM

TECHNICAL REPORT

May 8th, 2019

Centro Nacional de Metrología, CENAM.
May 8th, 2019.

Key comparison of 50/60 Hz of power measurement standards

Representatives: René Carranza López Padilla, Sergio A. Campos Montiel, and Marco A. Rodríguez Guerrero

The reference standards are two ultra stable wattmeters RD-22-332 with serial numbers 203409, and 206816, manufactured by Radian. The standards were received at CENAM on February 23th, 2018. After carrying out the measurements on the standards at CENAM, they were sent to the National Institute of Standards and Technology, NIST, on March 19th, 2018.

1. Reference measurement standard at CENAM.

The power reference standard used in CENAM is based on a digital sampling wattmeter. The power reference system consists of two 3458A digital sampling voltmeters (DSV) in synchronous master/slave configuration in the 1 V range for both voltage and current signals. The digital sampling process is compensated in bandwidth concerning the aperture time of the analog-to-digital converter in both DSVs. The master DSV synchronizes to the slave DSV through a continuous signal of dynamic width trigger pulses with a frequency close to 1 kHz. The characteristic hardware delay between DSVs in master/slave configuration is known, and its delay influence related to the measurement frequency signal is compensated to accurately determinate the reference phase angle between voltage and current signals.

The measurement of voltage consists of a master DSV and an AC coaxial resistive voltage divider with a 400:1 ratio. It was designed to measure both 120 V and 240 V ranges from DC to 10 kHz. For an input voltage signal of 120 V or 240 V, its nominal voltage output is 0.3 V and 0.6 V respectively. The measurement of current is made of a slave DSV and an AC coaxial current shunt, designed for 5 A from DC to 10 kHz. For an input current signal of 5 A, the shunt nominal voltage output is 0.8 V. The entire digital reference system is well known in amplitude and phase angle from DC to 10 kHz.

The AC RMS values of voltage and current are obtained by in house developed RMS measurement algorithm using digital techniques. The reference phase angle between voltage and current signals is computed by a in house method based on the power triangle properties. The measurement system is fully automated with NI LabView, the algorithm for computing the reference power was designed and developed entirely by the staff of the Power and Energy Laboratory at CENAM.

Figure 1 depicts a detailed schematic diagram of the main components of the reference measurement system described above.

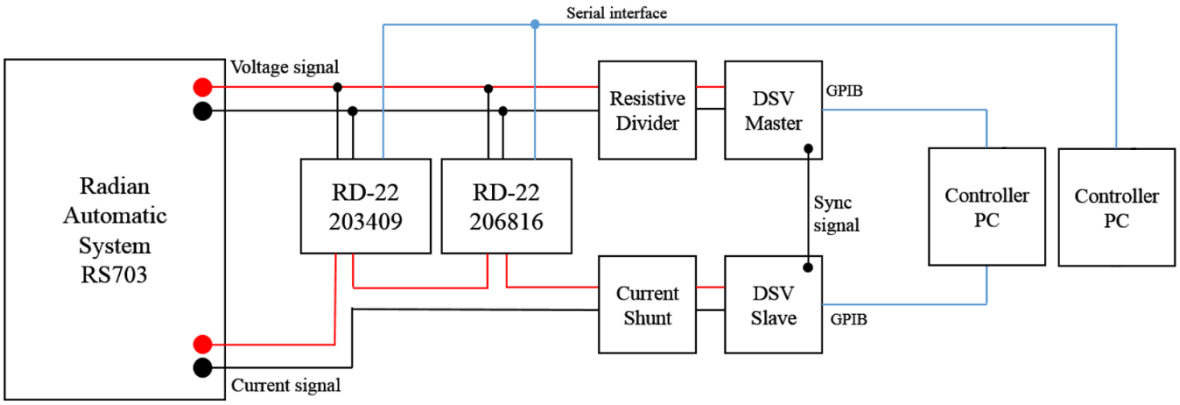

Fig. 1. Schematic diagram of CENAM's reference measurement system.

2. Measurement procedure followed at CENAM.

2.1 Measurement Arrangement.

Once the reference standards are in the power and energy laboratory at CENAM, and before starting the measurement process at CENAM, both RD-22-332 were energized by a period of four hours to allow them to reach thermal stability. Each meter was used with its own power supply.

The reset routine on each reference standard was executed before starting the measurements process as described in the protocol of this comparison.

A total of 50 sets of measurements were performed at every test point. A set of measurements consists of 100 independent measurements at each one of the test points. The overall measurement process is conducted in 10 days.

At each set of measurements, the traveling standards were deenergized for at least 30 seconds before performing the next set of measurements.

2.2 Environmental conditions during the measurements at CENAM.

The following are the average value of environmental conditions at the Power and Energy Laboratory at CENAM during the measurements. The internal temperature of the reference standards is reported.

Laboratory temperature: (23 ± 1) ºC

Laboratory relative humidity: (30 ± 10) % RH.

RD-22-332 s/n: 203409 internal temperature: (39.6 ± 0.5) ºC

RD-22-332 s/n: 206816 internal temperature: (38.7 ± 0.5) ºC

3. Measurement method at CENAM.

The reference standards RD-22-332 were compared against CENAM´s measurement standard of power and energy. A check standard (model: RD-22-231; s/n: 201512) of comparable metrological characteristics to the reference standards was used in the measurement circuit during all measurement process.

As shown on Figure , voltage and current signals from Radian RS703A power source were applied at the same time to both traveling standards RD-22-332, to CENAM's check standard RD-22-321, and to CENAM's digital sampling wattmeter for every set of measurements.

The measured values by both traveling standards RD-22-332 (voltage, current, frequency, phase angle, power factor, apparent power, active power, and reactive power) were recorded in a PC using the RS232 port of each standard. CENAM's digital sampling wattmeter was connected to an independent PC isolated with an optical interface based on GPIB.

4. Measurement error of Active Power.

The frequency of the measurement of power is 53 Hz.

The relative error of active power measured by the instrument under calibration was obtained according to the following expressions:

$$Active\ Power\ Error = \frac{Measured\ Active\ Power - Reference\ Active\ Power}{Apparent\ Power} \quad \left(\frac{\mu W}{VA}\right)$$

$$Apparent\ Power = Voltage \cdot Current \quad (VA)$$

5. Uncertainty of measurements of the reference standards RD-22-332.

The measurement uncertainty was estimated according to the Guide to the Expression of Uncertainty in Measurement, BIPM, IEC, IFCC, ISO, IUPAC, IUPAP, OIML (1995).

The expanded uncertainty reported in this comparison, includes the assessment associated with the type A uncertainty during the calibration of our reference standards and the instrument under calibration, which is estimated from an average of ten sets of measurements, with ten measurements in each set, and the type B uncertainty, which is associated with the known uncertainty of CENAM's reference standards.

The expanded uncertainty of measurement of both RD-22-332 is estimated to enclose a confidence interval higher than 95 % with a coverage factor equal to 2.0.

5.1. Type A and Type B measurement uncertainties RD-22-332 s/n: 203409

5.1.1. Measurement uncertainty of voltage.

Table 1. *Voltage: measurement uncertainties type A, B and expanded.*

Point	Current	Power Factor	Phase Angle	Frequency	Measured Voltage 203409	Reference Voltage	Error	Type A Uncertainty k = 2.0	Type B Uncertainty k = 2.0	Expanded Uncertainty k = 2.0
[n]	[A]		[°]	[Hz]	[V]	[V]	[μV/V]	[μV/V]	[μV/V]	[μV/V]
1	5	1	0	53	120.001 0	120.000 9	1	1	5	5
2	5	0.5 lead	60	53	120.000 8	120.000 7	0	1	5	5
3	5	0 lead	90	53	120.000 5	120.000 5	0	1	5	5
4	5	0.5 lag	-60	53	120.000 8	120.000 7	0	1	5	5
5	5	0 lag	-90	53	120.000 6	120.000 5	0	1	5	5
6	5	1	0	53	240.006 0	240.005 6	2	1	5	5
7	5	0.5 lead	60	53	240.005 4	240.005 1	1	1	5	5
8	5	0 lead	90	53	240.005 0	240.004 7	1	1	5	5
9	5	0.5 lag	-60	53	240.005 6	240.005 1	2	1	5	5
10	5	0 lag	-90	53	240.005 1	240.004 7	2	1	5	5

5.1.2. Measurement uncertainty of current.

Table 2. *Current: measurement uncertainties type A, B and expanded.*

Point	Voltage	Power Factor	Phase Angle	Frequency	Measured Current 203409	Reference Current	Error	Type A Uncertainty k = 2.0	Type B Uncertainty k = 2.0	Expanded Uncertainty k = 2.0
[n]	[V]		[°]	[Hz]	[A]	[A]	[μA/A]	[μA/A]	[μA/A]	[μA/A]
1	120	1	0	53	5.000 339	4.999 964	75	1	5	5
2	120	0.5 lead	60	53	5.000 338	4.999 963	75	1	5	5
3	120	0 lead	90	53	5.000 342	4.999 968	75	1	5	5
4	120	0.5 lag	-60	53	5.000 340	4.999 964	75	1	5	5
5	120	0 lag	-90	53	5.000 336	4.999 960	75	1	5	5
6	240	1	0	53	5.000 339	4.999 964	75	1	5	5
7	240	0.5 lead	60	53	5.000 339	4.999 964	75	1	5	5
8	240	0 lead	90	53	5.000 344	4.999 969	75	1	5	5
9	240	0.5 lag	-60	53	5.000 339	4.999 962	75	1	5	5
10	240	0 lag	-90	53	5.000 335	4.999 959	75	1	5	5

5.1.3. Measurement uncertainty of power factor.

Table 3. *Power factor: measurement uncertainties type A, B and expanded.*

Point	Voltage	Current	Power Factor	Frequency	Measured Power Factor 203409	Reference Power Factor	Error	Type A Uncertainty k = 2.0	Type B Uncertainty k = 2.0	Expanded Uncertainty k = 2.0
[n]	[V]	[A]		[Hz]			10^{-6}	10^{-6}	10^{-6}	10^{-6}
1	120	5	1	53	1.000 000	1.000 000	0	0.1	10	10
2	120	5	0.5 lead	53	0.500 037	0.500 002	35	0.1	10	10
3	120	5	0 lead	53	0.000 042	0.000 002	40	0.1	10	10
4	120	5	0.5 lag	53	0.499 970	0.500 004	-34	0.1	10	10
5	120	5	0 lag	53	-0.000 037	0.000 004	-41	0.1	10	10
6	240	5	1	53	1.000 000	1.000 000	0	0.1	10	10
7	240	5	0.5 lead	53	0.500 042	0.500 005	37	0.1	10	10
8	240	5	0 lead	53	0.000 048	0.000 007	40	0.1	10	10
9	240	5	0.5 lag	53	0.499 965	0.500 001	-36	0.1	10	10
10	240	5	0 lag	53	-0.000 042	0.000 001	-43	0.1	10	10

5.1.4 Active Power measurement uncertainty.

Table 4. *Active Power: measurement uncertainties type A, B and expanded.*

Point	Voltage	Current	Power Factor	Phase Angle	Frequency	Measured Active Power 203409	Reference Apparent Power	Reference Active Power	Error	Type A Uncertainty k = 2.0	Type B Uncertainty k = 2.0	Expanded Uncertainty k = 2.0
[n]	[V]	[A]		[°]	[Hz]	[W]	[VA]	[W]	[W/VA]	[µW/VA]	[µW/VA]	[µW/VA]
1	120	5	1	0	53	600.046 4	600.000 3	600.000 3	77	1	7	7
2	120	5	0.5 lead	60	53	300.044 3	599.999 2	300.000 8	73	1	10	10
3	120	5	0 lead	90	53	0.025 389	599.998 7	0.001 470	40	1	10	10
4	120	5	0.5 lag	-60	53	300.004 3	599.999 3	300.002 0	4	1	10	10
5	120	5	0 lag	-90	53	-0.022 026	599.997 8	0.002 596	-41	1	10	10
6	240	5	1	0	53	1 200.113	1 200.019	1 200.019	78	1	7	7
7	240	5	0.5 lead	60	53	600.104 2	1 200.017	600.014 0	75	1	10	10
8	240	5	0 lead	90	53	0.057 228	1 200.016	0.008 807	40	1	10	10
9	240	5	0.5 lag	-60	53	600.013 2	1 200.017	600.010 1	3	1	10	10
10	240	5	0 lag	-90	53	-0.050 146	1 200.014	0.001 522	-43	1	10	10

5.2. Type A and Type B measurement uncertainties RD-22-332 s/n: 206819

5.2.1. Measurement uncertainty of voltage.

Table 5. *Voltage: measurement uncertainties type A, B and expanded.*

Point	Current	Power Factor	Phase Angle	Frequency	Measured Voltage 206819	Reference Voltage	Error	Type A Uncertainty k = 2.0	Type B Uncertainty k = 2.0	Expanded Uncertainty k = 2.0
[n]	[A]		[°]	[Hz]	[V]	[V]	[µV/V]	[µV/V]	[µV/V]	[µV/V]
1	5	1	0	53	119.999 5	120.000 9	-12	1	5	5
2	5	0.5 lead	60	53	119.999 2	120.000 7	-13	1	5	5
3	5	0 lead	90	53	119.999 0	120.000 5	-13	1	5	5
4	5	0.5 lag	-60	53	119.999 3	120.000 7	-12	1	5	5
5	5	0 lag	-90	53	119.999 1	120.000 5	-12	1	5	5
6	5	1	0	53	240.002 6	240.005 6	-13	1	5	5
7	5	0.5 lead	60	53	240.001 9	240.005 1	-13	1	5	5
8	5	0 lead	90	53	240.001 4	240.004 7	-14	1	5	5
9	5	0.5 lag	-60	53	240.002 1	240.005 1	-13	1	5	5
10	5	0 lag	-90	53	240.001 6	240.004 7	-13	1	5	5

5.2.2. Measurement uncertainty of current.

Table 6. *Current: measurement uncertainties type A, B and expanded.*

Point	Voltage	Power Factor	Phase Angle	Frequency	Measured Current 206819	Reference Current	Error	Type A Uncertainty k = 2.0	Type B Uncertainty k = 2.0	Expanded Uncertainty k = 2.0
[n]	[V]		[°]	[Hz]	[A]	[A]	[µA/A]	[µA/A]	[µA/A]	[µA/A]
1	120	1	0	53	4.999 699	4.999 964	-53	1	5	5
2	120	0.5 lead	60	53	4.999 697	4.999 963	-53	1	5	5
3	120	0 lead	90	53	4.999 702	4.999 968	-53	1	5	5
4	120	0.5 lag	-60	53	4.999 701	4.999 964	-53	1	5	5
5	120	0 lag	-90	53	4.999 698	4.999 960	-53	1	5	5
6	240	1	0	53	4.999 700	4.999 964	-53	1	5	5
7	240	0.5 lead	60	53	4.999 698	4.999 964	-53	1	5	5
8	240	0 lead	90	53	4.999 702	4.999 969	-53	1	5	5
9	240	0.5 lag	-60	53	4.999 701	4.999 962	-52	1	5	5
10	240	0 lag	-90	53	4.999 697	4.999 959	-52	1	5	5

5.2.3. Measurement uncertainty of power factor.

Table 7. *Power factor: measurement uncertainties type A, B and expanded.*

Point	Voltage	Current	Power Factor	Frequency	Measured Power Factor 206819	Reference Power Factor	Error	Type A Uncertainty k = 2.0	Type B Uncertainty k = 2.0	Expanded Uncertainty k = 2.0
[n]	[V]	[A]		[Hz]			10^{-6}	10^{-6}	10^{-6}	10^{-6}
1	120	5	1	53	1.000 000	1.000 000	0	0.1	10	10
2	120	5	0.5 lead	53	0.499 975	0.500 002	-27	0.1	10	10
3	120	5	0 lead	53	-0.000 030	0.000 002	-32	0.1	10	10
4	120	5	0.5 lag	53	0.500 033	0.500 004	29	0.1	10	10
5	120	5	0 lag	53	0.000 036	0.000 004	32	0.1	10	10
6	240	5	1	53	1.000 000	1.000 000	0	0.1	10	10
7	240	5	0.5 lead	53	0.499 978	0.500 005	-27	0.1	10	10
8	240	5	0 lead	53	-0.000 027	0.000 007	-34	0.1	10	10
9	240	5	0.5 lag	53	0.500 031	0.500 001	29	0.1	10	10
10	240	5	0 lag	53	0.000 033	0.000 001	32	0.1	10	10

5.2.4 Active Power measurement uncertainty.

Table 8. *Active Power: measurement uncertainties type A, B and expanded.*

Point	Voltage	Current	Power Factor	Phase Angle	Frequency	Measured Active Power 206819	Reference Apparent Power	Reference Active Power	Error	Type A Uncertainty k = 2.0	Type B Uncertainty k = 2.0	Expanded Uncertainty k = 2.0
[n]	[V]	[A]		[°]	[Hz]	[W]	[VA]	[W]	[W/VA]	[µW/VA]	[µW/VA]	[µW/VA]
1	120	5	1	0	53	599.962 6	600.000 3	600.000 3	-63	1	7	7
2	120	5	0.5 lead	60	53	299.964 9	599.999 2	300.000 8	-60	1	10	10
3	120	5	0 lead	90	53	-0.017 894	599.998 7	0.001 470	-32	1	10	10
4	120	5	0.5 lag	-60	53	300.000 1	599.999 3	300.002 0	-3	1	10	10
5	120	5	0 lag	-90	53	0.021 597	599.997 8	0.002 596	32	1	10	10
6	240	5	1	0	53	1 199.943	1 200.019	1 200.019	-64	1	7	7
7	240	5	0.5 lead	60	53	599.941 6	1 200.017	600.014 0	-60	1	10	10
8	240	5	0 lead	90	53	-0.032 121	1 200.016	0.008 807	-34	1	10	10
9	240	5	0.5 lag	-60	53	600.006 0	1 200.017	600.010 1	-3	1	10	10
10	240	5	0 lag	-90	53	0.039 974	1 200.014	0.001 522	32	1	10	10

6. Results reporting laboratory: CENAM.

CENAM sent the resulting report (MS Excel doc) on 19th June, 2018 to the pilot laboratory.

The report of results sent complies with the format of the CCEM-K5.2017 protocol.

The identification name of the file sent was “CCEM-K5.2017 Results Reporting Laboratory CENAM.xlsx”

2. Comparison report of INMETRO

CCEM-K5.2017

Key comparison of 50/60 Hz power

MEASUREMENT REPORT

January 2021

BRAZIL – INMETRO

TABLE OF CONTENTS

1. INTRODUCTION

This report presents the information and results of the measurements performed for CCEM-K5 key comparison on 50/60 Hz electric power, in order to underpin the Mutual Recognition Arrangement as proposed by the Committee International of Weights and Measures, CIPM. Measurements were performed from 06 to 10 November 2020.

The measurements were performed in Electrical Energy Metrology Laboratory at Inmetro Brazil.

Laboratory representative: Rodrigo Simões Ribeiro.
Title: Head of Electrical Energy Metrology Laboratory.

2. REFERENCE STANDARDS

CCEM-K5 key comparison on 50/60 Hz electric power uses the following two power standards identified as:

Manufacturer: Radian Research
Model: RD-22-332S
Serial numbers: 206815 and 203409

3. PARTICIPANT LABORATORY

The Electrical Energy Metrology Laboratory is a laboratory of the Instituto Nacional de Metrologia, Qualidade e Tecnologia - INMETRO, responsible for the realization and maintenance of power (watt) and energy units (watt-hours) according to the "International System of Units" (SI), and for the dissemination of these units in Brazil.

3.1 Traceability Scheme

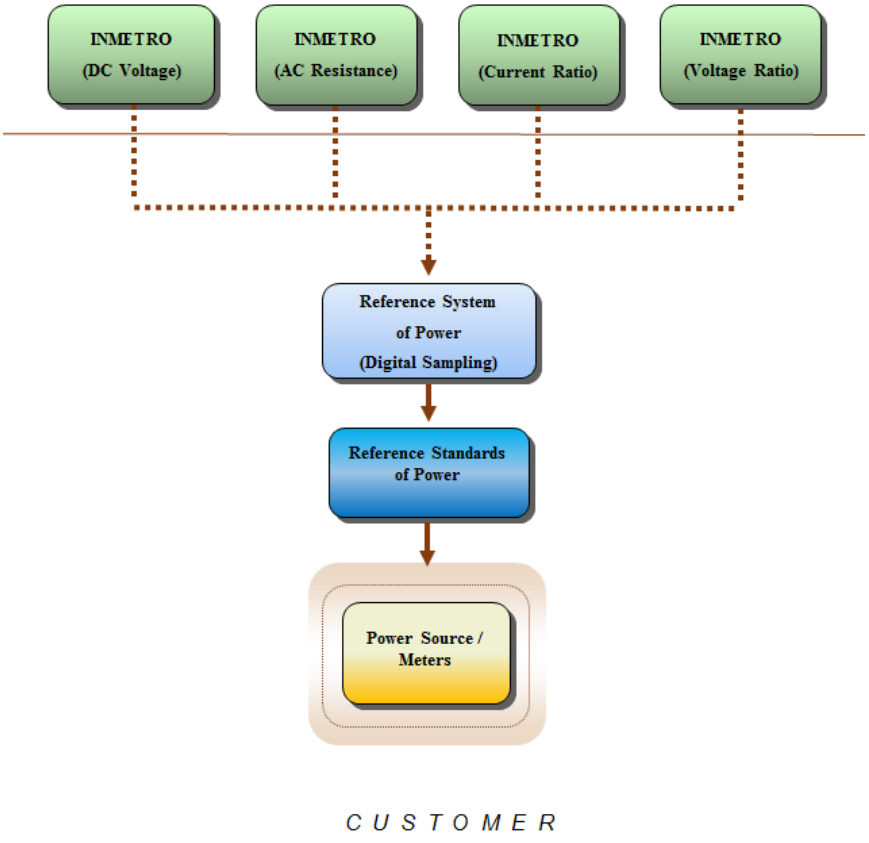

4. MEASUREMENT

4.1 Measurement set-up

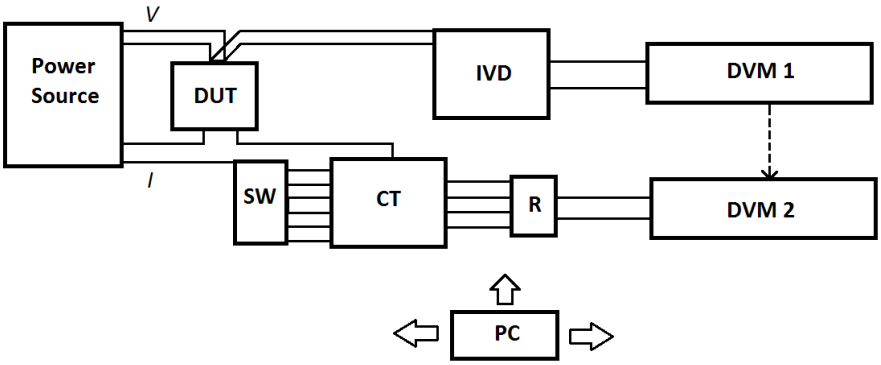

DUT: Device under test.

IVD: Inductive voltage divider.

DVM: Digital sampling voltmeter.

R: Shunt resistor.

CT: Two-stage current transformer.

SW: Automated switch.

4.2 Measurement procedure

The CCEM-K5 comparison traveling standards were calibrated by comparison with Inmetro´s reference system of power based on the digital sampling method, according to the instructions of the technical protocol CCEM-K5.2017. This reference system was also used by Inmetro in the SIM.EM-K5 key comparison on 50/60 Hz electric power in 2014.

Mean temperature during tests: (22.6 ± 0.5) °C
Mean relative humidity during tests: (56 ± 3) % RH.

The test points are listed in Table 1.

Table 1 – Points of measurements

Point	Voltage (V)	Current (A)	Power factor	Frequency (Hz)
1	120	5	1	53
2	120	5	0.5 lead	53
3	120	5	0 lead	53
4	120	5	0.5 lag	53
5	120	5	0 lag	53
6	240	5	1	53
7	240	5	0.5 lead	53
8	240	5	0 lead	53
9	240	5	0.5 lag	53
10	240	5	0 lag	53

4.3 Results

The measurement results refer to the mean value of five measurements and are shown in the Table 2 and Table 3.
The reported expanded uncertainties (U) of the measurements are declared as the standard uncertainties multiplied by the coverage factor k = 2, which corresponds to a coverage probability of 95.45%. The standard uncertainties of the measurements were evaluated in accordance with the "Evaluation of Measurement Data - Guide to the Expression of Uncertainty in Measurement - GUM 2008".

Table 2 – Measurement results for serial number: 206815

Point	Error (µW/VA)	U (µW/VA)	RMS voltage (V)	U (V)	RMS current (A)	U (A)	Phase angle (deg)	U (deg)	Frequency (Hz)	U (Hz)
1	-50	26	119.9983	0.0014	5.00148	0.00011	-0.0006	0.0015	52.999760	0.000053
2	-63	26	119.9957	0.0014	5.00142	0.00011	59.9974	0.0015	52.999725	0.000053
3	-44	26	119.9951	0.0014	5.00141	0.00011	89.9970	0.0015	52.999800	0.000053
4	12	26	119.9966	0.0014	5.00142	0.00011	-60.0019	0.0015	52.999740	0.000053
5	41	26	119.9964	0.0014	5.00140	0.00011	-90.0021	0.0015	52.999740	0.000053
6	-36	26	239.9982	0.0029	5.00141	0.00011	-0.0022	0.0015	52.999800	0.000053
7	-54	26	239.9954	0.0029	5.00141	0.00011	59.9964	0.0015	52.999800	0.000053
8	-41	26	239.9953	0.0029	5.00141	0.00011	89.9962	0.0015	52.999760	0.000053
9	17	26	239.9915	0.0029	5.00139	0.00011	-60.0048	0.0015	52.999760	0.000053
10	40	26	239.9938	0.0029	5.00139	0.00011	-90.0042	0.0015	52.999760	0.000053

Table 3 – Measurement results for serial number: 203049

Point	Error (µW/VA)	U (µW/VA)	RMS voltage (V)	U (V)	RMS current (A)	U (A)	Phase angle (deg)	U (deg)	Frequency (Hz)	U (Hz)
1	83	26	119.9981	0.0014	5.00153	0.00011	-0.0007	0.0015	52.999820	0.000053
2	65	26	119.9961	0.0014	5.00143	0.00011	59.9976	0.0015	52.999800	0.000053
3	28	26	119.9966	0.0014	5.00143	0.00011	89.9979	0.0015	52.999740	0.000053
4	17	26	119.9966	0.0014	5.00144	0.00011	-60.0019	0.0015	52.999775	0.000053
5	-30	26	119.9959	0.0014	5.00141	0.00011	-90.0024	0.0015	52.999760	0.000053
6	102	26	240.0002	0.0029	5.00141	0.00011	-0.0015	0.0015	52.999760	0.000053
7	84	26	239.9988	0.0029	5.00141	0.00011	59.9978	0.0015	52.999740	0.000053
8	38	26	239.9991	0.0029	5.00142	0.00011	89.9976	0.0015	52.999760	0.000053
9	18	26	239.9989	0.0029	5.00140	0.00011	-60.0020	0.0015	52.999740	0.000053
10	-39	26	239.9986	0.0029	5.00139	0.00011	-90.0024	0.0015	52.999800	0.000053

5. UNCERTAINTY

5.1 Uncertainty budget

Table 4 – Uncertainty Budget

Uncertainty components y_i	Standard uncertainty $u(y_i)$	Type method A or B of evaluation/probability distribution function	Sensitivity coefficient c_i	Uncertainty contribution $u(R_i)$	Degrees of freedom n_i
Standard deviation of the mean of the readings	$6.0 \cdot 10^{-4}$ W	Type A/ Normal	1	$6.0 \cdot 10^{-4}$ W	4
RMS voltage (@ DVM 1 input)	$1.5 \cdot 10^{-5}$ V	Type B / Normal	$100 \cos\theta$ A	$1.5 \cdot 10^{-3} \cos\theta$ W	inf.
RMS voltage (@ DVM 2 input)	$2.5 \cdot 10^{-6}$ V	Type B / Normal	$600 \cos\theta$ A	$1.5 \cdot 10^{-3} \cos\theta$ W	inf.
IVD ratio error	$1.1 \cdot 10^{-4}$ V/V	Type B / Normal	$30 \cos\theta$ W	$3.3 \cdot 10^{-3} \cos\theta$ W	inf.
CT ratio error	$5.0 \cdot 10^{-4}$ A/A	Type B / Normal	$12 \cos\theta$ W	$6.0 \cdot 10^{-3} \cos\theta$ W	inf.
Shunt resistor ac resistance	$5.0 \cdot 10^{-5}$ Ω	Type B / Normal	$-60 \cos\theta$ W/Ω	$-3.0 \cdot 10^{-3} \cos\theta$ W	inf.
Two-voltage phase displacement error (between DVM 1/ DVM 2 inputs)	$1.0 \cdot 10^{-5}$ rad	Type B / Normal	$-600 \sin\theta$ W	$-6.0 \cdot 10^{-3} \sin\theta$ W	inf.
IVD phase displacement	$4.6 \cdot 10^{-6}$ rad	Type B / Normal	$-600 \sin\theta$ W	$-2{,}8 \cdot 10^{-3} \sin\theta$ W	inf.
CT phase displacement	$6.5 \cdot 10^{-6}$ rad	Type B / Normal	$-600 \sin\theta$ W	$-3.9 \cdot 10^{-3} \sin\theta$ W	inf.
Shunt resistor phase angle	$1{,}7 \cdot 10^{-6}$ rad	Type B / Normal	$-600 \sin\theta$ W	$-1.0 \cdot 10^{-3} \sin\theta$ W	inf.
Root square sum of Type A standard uncertainties and effective degrees of freedom				$6.0 \cdot 10^{-4}$ W	4
Root square sum of Type B standard uncertainties and effective degrees of freedom				$7.8 \cdot 10^{-3}$ W	inf.
Combined standard uncertainty and effective degrees of freedom				$7.8 \cdot 10^{-3}$ W	inf.
Combined standard uncertainty (relative to apparent power) and effective degrees of freedom				13 μW/VA	inf.
Expanded uncertainty (95.45 % coverage factor) (relative to apparent power)				26 μW/VA	

6. DATES AND TIMES OF TRAVELING STANDARD

Table 5 – Dates and times of traveling standard

Serial Number	Date	Time	Condition
206815	06 November 2020	09:10 am	de-energized
206815	06 November 2020	09:11 am	energized
206815	06 November 2020	12:16 pm	de-energized
206815	06 November 2020	12:17 pm	energized
206815	06 November 2020	01:38 pm	de-energized
206815	06 November 2020	01:39 pm	energized
206815	06 November 2020	02:56 pm	de-energized
206815	06 November 2020	02:57 pm	energized
206815	09 November 2020	08:19 am	de-energized
206815	09 November 2020	08:20 am	energized
203409	09 November 2020	12:35 pm	de-energized
203409	09 November 2020	12:36 pm	energized
203409	09 November 2020	01:51 pm	de-energized
203409	09 November 2020	01:52 pm	energized
203409	09 November 2020	02:58 pm	de-energized
203409	09 November 2020	02:59 pm	energized
203409	10 November 2020	08:02 am	de-energized
203409	10 November 2020	08:03 am	energized
203409	10 November 2020	09:25 am	de-energized
203409	10 November 2020	09:26 am	energized

Brazil 25 January 2021

Rodrigo Simões Ribeiro
Head of the Electrical Energy Metrology Laboratory

3. Comparison report of LNE

LABORATOIRE NATIONAL DE MÉTROLOGIE ET D'ESSAIS
LABORATOIRE DE TRAPPES
29, avenue Roger Hennequin - 78197 Trappes Cedex
Tél : 01 30 69 10 00 - Fax : 01 30 69 12 34

RAPPORT DE COMPARAISON INTERLABORATOIRE
INTERLABORATORY COMPARISON REPORT
N° IN101242-DMSI-1

CCEM-K5.2017
Key comparison of 50/60 Hz power

DOMAINE : **AC power: single phase (frequencies below or equal to 400 Hz)**
Field

LABORATOIRES PILOTES : **VSL**, CENAM, PTB
Organizing laboratories **Thijsseweg 11,**
2629 JA Delft
The Netherlands

LABORATOIRE PARTICIPANT : **Laboratoire National de Métrologie et d'Essais (LNE)**
Participant laboratory **29 Avenue Roger Hennequin**
F-78197
Trappes
France

Ce document comprend 11 pages et 2 pages en annexe
This document includes 11 pages and 2 pages in appendix

Date d'émission : 28/11/2018
Date of issue : 28/11/2018

LE RESPONSABLE DU LABORATOIRE
The head of laboratory

Dominique FORTUNÉ

Summary

1. Identification of the travelling standard

The LNE laboratory performed the measurements on the following travelling standards:

RD-22-332S, serial number 206816;

RD-22-332S, serial number 203409.

2. Experimental Set-Up

The experimental set-up is shown in figure 1. A fictive power source provides voltages up to 1000 V and currents up to 20 A with a total harmonic distortion smaller than 0.02%. Voltage U and current I are applied simultaneously to the wattmeter under test (travelling standard), to a control wattmeter used for the good functioning of the primary standard and to the LNE Digital Sampling Wattmeter (DSWM) as primary standard.

DC output voltage of the travelling standard is measured using a digital voltmeter of high resolution (Agilent-HP 3458A).

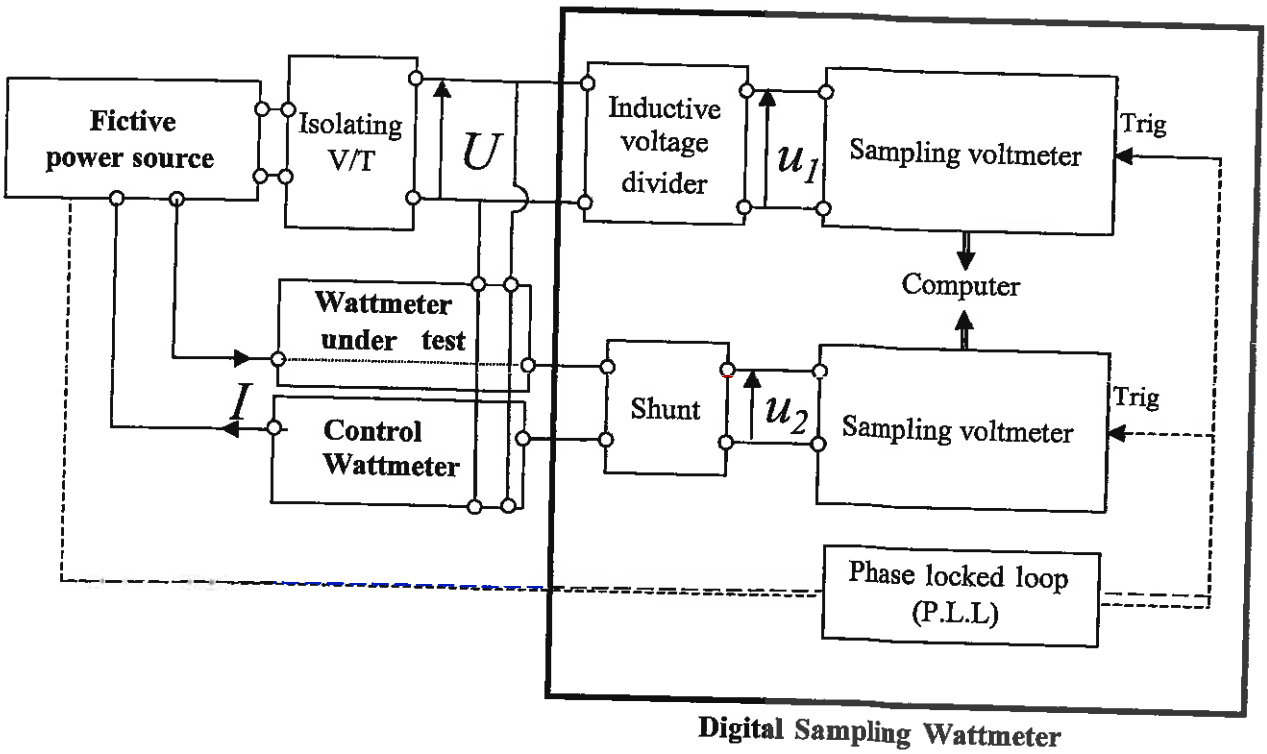

Figure 1 Experimental set-up

The basic measuring principle of the DSWM is to take simultaneous samples of the voltage and current inputs at equally spaced discrete instants covering an integer number of periods of the input waveforms. The total power is then calculated by discrete Fourier transform (DFT) of the sampled signals. The DSWM is composed of two high precision sampling voltmeters with ADC-capability (Agilent-HP 3458A) which are used in the DCV sampling mode to digitize the signals. A shunt is used to transform the current into a 0.8 V voltage signal and a separately excited three-stage inductive voltage divider (IVD) has been added to the voltage circuit to divide the test voltage, usually

up to 1000V, to a low-level signal that could be measured with better accuracy in the 1 V range. A voltage insulation transformer is used to prevent the IVD cores to be magnetized. To control the sampling process, a phase-lock circuit is used. The power source generating the sinusoidal waveforms provides a "sample reference" (TTL) to trigger the multi-meters. The TTL reference signal is a harmonic of the phase reference signal and is phase locked to it. Thus, the frequency of the power source and the sampling rate are synchronised, in order to sample an integer number of periods of the input waveforms.

Traceability

The traceability of our measurements to the SI is provided through the calibration of the digital voltmeters with reference to the French national standards, the shunt with reference to the SP standards, the Technical Research Institute of Sweden for the AC-DC difference and with reference to the French national standards for the DC value. The inductive voltage divider is calibrated with reference to the NMIA standards, the National Measurement Institute of Australia.

The used standards are:

- DC voltage laboratory standard (type Fluke 732B, SN° 6295011)
- Standard resistor (type CS2C, SP, SN° CS2C -0317)
- Inductive Voltage Divider (type NMIA, SN° 04001).

3. Results

The comparison was performed at 53 Hz for sinusoidal voltage and current signals. Ten points were selected to test the amplitude and phase measuring capabilities of the power standard: 120 V, 240 V and 5 A at power factors 1.0, 0.5 lead, 0.5 lag, 0.0 lead and 0.0 lag (where lead/lag indicates that the current waveform leads/lags the voltage waveform). Several test parameters that could influence the results have been recorded. These include voltage, current, power factor, temperature, humidity, zero offset and ± dc reference voltages of the traveling standard.

The procedure is the following:

- first step: The two Agilent-HP 3458 A are calibrated with a Zener-diode dc voltage standard immediately before the tests.

- second step: The travelling standard is de-energized during 1 minute followed by at least 15 minutes warm-up period. This period of warm-up is about the same on the primary standard.

After this period the register of the data starts at the same time on travelling and primary standard.

We measure during the same time P_{DSWM}, the active power of the DSWM and P_{TS}, the value given every minute by the travelling standard and its associated software.

The DSWM samples the voltage and current signals over 25 periods at a rate of 2.1 kHz. The procedure consists in taking 10 series of 10 measurements and for each series, one calculates P_k and the associated standard deviation σ_k :

$$P_k = \frac{1}{10}\sum_{i=1}^{10} U_i I_i cos\Phi_i,\ \sigma_k$$

$$\text{for } 1 \le k \le 10$$

The active power P_l is the average of the 10 series.

All these measurements are repeated 10 times.

At the same time, around 6000 values of P_{TS} are recorded from the travelling standard. Among this data, around 3000 values corresponding to 15 minutes of measurement have been kept and split in 10 series of consecutives values. For each series we calculate P_{TS100} and the experimental standard deviation.

The final values of P_{DSWM} and P_{TSf} and their standard deviations are finally defined by:

$$P_{DSWM} = \frac{1}{10}\sum_{l=1}^{10} P_l \text{ and } \sigma_{P_{DSWM}} = \sqrt{\frac{1}{10-1}\sum_{l=1}^{10}(P_l - P)^2}$$

$$P_{TSf} = \frac{1}{10}\sum_{i=1}^{10} P_{TS300} \text{ and } \sigma_{TSf} = \sqrt{\frac{1}{10-1}\sum_{i=1}^{10}(P_{TS100} - P_{TSf})^2}$$

The sequence above has been carried out two times for each set of point. Only the series with lower dispersion is kept.

Due to the used procedure it was not possible of de-energised the travelling standard during the measurements with primary standard. Nevertheless a series of 5 measurements for one measurement point has been carried out on each of the two travelling standards, according to the technical protocol, with another LNE power standard. Conclusion is that the action of de-energised the travelling standard between each series has negligible effect on the dispersion of the results.

A great number of measurements have been done during two weeks, in October 2018. The temperature of the laboratory was between 22.7°C and 22.9°C and the relative humidity varied from 40 % to 45 %.

All the results are presented in the following tables.

The mean error ε in terms of apparent power is defined by:

$$\varepsilon = \frac{P_{TSf} - P_{DSWM}}{UI}$$

Where P_{TSf} and P_{DSWM} stand for the active power measured respectively by the travelling standard and by the LNE Digital Sampling Wattmeter.

Point	Nominal set point					Measurement date	Error value ε [µW/VA]	Expanded uncertainty u_ε [µW/VA]
	Voltage [V]	Current [A]	Power factor	Phase angle [deg]	Frequency [Hz]			
1	120	5	1	0	53	19/09/2018	-56,7	26,0
2	120	5	0.5 lead	60	53	19/09/2018	-67,1	16,0
3	120	5	0 lead	90	53	20/09/2018	-45,0	11,0
4	120	5	0.5 lag	-60	53	19/09/2018	11,7	16,0
5	120	5	0 lag	-90	53	21/09/2018	43,5	11,0
6	240	5	1	0	53	07/09/2018	-55,7	26,0
7	240	5	0.5 lead	60	53	07/09/2018	-67,2	16,0
8	240	5	0 lead	90	53	11/09/2018	-44,6	12,0
9	240	5	0.5 lag	-60	53	10/09/2018	14,2	17,0
10	240	5	0 lag	-90	53	10/09/2018	45,0	11,0

Table 1 Error results for travelling standard n° 206816

Point	Applied RMS voltage V [V]	Expanded uncertainty u_V [V]	Applied RMS current I [A]	Expanded uncertainty u_I [A]	Power factor PF	Expanded uncertainty u_PF	Applied frequency f [Hz]	Expanded uncertainty u_f [Hz]
1	119.9339	1,2E-03	4,99870	1,2E-04	0,9999996	1,00E-08	53,00	0,01
2	119,9340	1,2E-03	4,99873	1,2E-04	0,5007599	9,00E-06	53,00	0,01
3	119,9339	1,2E-03	4,99872	1,2E-04	0,0008803	1,10E-05	53,00	0,01
4	119,9337	1,2E-03	4,99871	1,2E-04	0,4992394	9,00E-06	53,00	0,01
5	119,9341	1,2E-03	4,99874	1,2E-04	-0,0008803	1,10E-05	53,00	0,01
6	239,4415	2,5E-03	4,99865	1,2E-04	0,9999989	1,00E-08	53,00	0,01
7	239,4401	2,5E-03	4,99865	1,2E-04	0,5013099	9,00E-06	53,00	0,01
8	239,4401	2,5E-03	4,99870	1,2E-04	0,0015095	1,10E-05	53,00	0,01
9	239,4395	2,5E-03	4,99868	1,2E-04	0,4986893	9,00E-06	53,00	0,01
10	239,4387	2,5E-03	4,99868	1,2E-04	-0,0015129	1,10E-05	53,00	0,01

Table 2 Electrical conditions of measurements for travelling standard n° 206816

Environmental conditions for these measurements were:

Temperature : 22.8 °C ± 0.5 °C

Relative humidity : 43.0 ± 5.0 %

Point	Nominal set point					Measurement date	Error value ε [µW/VA]	Expanded uncertainty u_ε [µW/VA]
	Voltage [V]	Current [A]	Power factor	Phase angle [deg]	Frequency [Hz]			
1	120	5	1	0	53	13/09/2018	86,6	26,0
2	120	5	0.5 lead	60	53	13/09/2018	70,8	16,0
3	120	5	0 lead	90	53	17/09/2018	29,6	11,0
4	120	5	0.5 lag	-60	53	14/09/2018	16,7	16,0
5	120	5	0 lag	-90	53	17/09/2018	-32,2	11,0
6	240	5	1	0	53	11/09/2018	88,9	26,0
7	240	5	0.5 lead	60	53	11/09/2018	73,8	16,0
8	240	5	0 lead	90	53	12/09/2018	33,8	12,0
9	240	5	0.5 lag	-60	53	12/09/2018	16,2	16,0
10	240	5	0 lag	-90	53	12/09/2018	-35,9	11,0

Table 3 Error results for travelling standard n° 203409

Point	Applied RMS voltage V [V]	Expanded uncertainty u_V [V]	Applied RMS current I [A]	Expanded uncertainty u_I [A]	Power factor PF	Expanded uncertainty u_PF	Applied frequency f [Hz]	Expanded uncertainty u_f [Hz]
1	119,9339	1,2E-03	4,99870	1,2E-04	0,9999996	1,00E-08	53,00	0,01
2	119,9334	1,2E-03	4,99873	1,2E-04	0,5007544	9,00E-06	53,00	0,01
3	119,9340	1,2E-03	4,99873	1,2E-04	-0,0008735	1,10E-05	53,00	0,01
4	119,9333	1,2E-03	4,99873	1,2E-04	0,4992451	9,00E-06	53,00	0,01
5	119,9335	1,2E-03	4,99871	1,2E-04	-0,0008730	1,10E-05	53,00	0,01
6	239,4403	2,5E-03	4,99869	1,2E-04	0,9999989	1,00E-08	53,00	0,01
7	239,4393	2,5E-03	4,99870	1,2E-04	0,5013108	9,00E-06	53,00	0,01
8	239,4407	2,5E-03	4,998711	1,2E-04	0,0015104	1,10E-05	53,00	0,01
9	239,4402	2,5E-03	4,998688	1,2E-04	0,4986905	9,00E-06	53,00	0,01
10	239,4404	2,5E-03	4,99869	1,2E-04	-0,001512	1,10E-05	53,00	0,01

Table 4 Electrical conditions of measurements for travelling standard n° 203409

Environmental conditions for these measurements were:

Temperature : 22.8 °C ± 0.5 °C

Relative humidity :43.0 ± 5.0 %.

4. Uncertainty of measurement

Contribution to the errors of all components has been determined experimentally and/or calculated and applied as corrections. Taking into account all contributions, combined standard uncertainties (Table 5 Uncertainty at power factor 1Table 6 Uncertainty at power factor 0.5 Table 7 Uncertainty at power factor 0) range from 6 to 13.5 µW/W at 120V and 240 V, 5A, 53 Hz and at any power factors (see Annex 1 for details).

The type A contributions, named as "standard deviation of the calibration error of the travelling standard" and "measurement set-up" in the tables are taken in account with their maximum values for the considered power factor.

Main uncertainty components y_i	Standard uncertainty $u(y_i)$	Type method A or B of evaluation/probability distribution function	Sensitivity coefficient c_i	Uncertainty contribution $u(R_i)$	Degrees of freedom n_i
1) Standard deviation of the calibration error of the travelling standard	2	Type A pdf: Normal	1	2	9
2)Standard deviation due to measurement set-up	1.6	Type A pdf: Normal	1	1.6	9
3)DSWM-voltage (see annex 1)	5.0	Type B pdf: normal(see annex 1)	1	5.0	52
4)DSWM-current (see annex 1)	11.7	Type B pdf: normal(see annex 1)	1	11.7	122
5)DSWM-phase (see annex 1)	5.2	Type B pdf: normal(see annex 1)	0	0.0	-
3) Ambient conditions					
3.1) temperature 3.2) humidity	22.8 °C 43.0 %				
Root square sum of Type A standard uncertainties and effective degrees of freedom*				2.6	17
Root square sum of Type B standard uncertainties and effective degrees of freedom				12.7	158
Combined standard uncertainty and effective degrees of freedom				13.0	169
Expanded uncertainty (95.45 % coverage factor)				26.0	

Table 5 Uncertainty at power factor 1

Main uncertainty components y_i	Standard uncertainty $u(y_i)$ (µW/VA)	Type method A or B of evaluation/probability distribution function	Sensitivity coefficient c_i	Uncertainty contribution $u(R_i)$ (µW/VA)	Degrees of freedom n_i
1) Standard deviation of the calibration error of the travelling standard	2	Type A pdf: Normal	1	0.9	9
2)Standard deviation due to measurement set-up	1.6	Type A pdf: Normal	1	2.2	9
3)DSWM-voltage (see annex 1)	5.0	Type B pdf: normal(see annex 1)	0.5	2.5	52
4)DSWM-current (see annex 1)	11.7	Type B pdf: normal(see annex 1)	0.5	5.9	122
5)DSWM-phase (see annex 1)	5.2	Type B pdf: normal(see annex 1)	0.87	4.5	8130
3) Ambient conditions					
3.1) temperature 3.2) humidity	22.8 °C 43.0 %				
Root square sum of Type A standard uncertainties and effective degrees of freedom*				2.4	12
Root square sum of Type B standard uncertainties and effective degrees of freedom				7.8	357
Combined standard uncertainty and effective degrees of freedom				8.2	339
Expanded uncertainty (95.45 % coverage factor)				17.0	

Table 6 Uncertainty at power factor 0.5

Main uncertainty components y_i	Standard uncertainty $u(y_i)$	Type method A or B of evaluation/probability distribution function	Sensitivity coefficient c_i	Uncertainty contribution $u(R_i)$	Degrees of freedom n_i
1) Standard deviation of the calibration error of the travelling standard	2	Type A pdf: Normal	1	2.9	9
2)Standard deviation due to measurement set-up	1.6	Type A pdf: Normal	1	0.6	9
3)DSWM-voltage (see annex 1)	5.0	Type B pdf: normal(see annex 1)	0	0.0	-
4)DSWM-current (see annex 1)	11.7	Type B pdf: normal(see annex 1)	0	0.0	-
5)DSWM-phase (see annex 1)	5.2	Type B pdf: normal(see annex 1)	1	5.2	8130
3) Ambient conditions					
3.1) temperature 3.2) humidity	22.8 °C 43.0 %				
Root square sum of Type A standard uncertainties and effective degrees of freedom*				3.0	10
Root square sum of Type B standard uncertainties and effective degrees of freedom				5.2	8130
Combined standard uncertainty and effective degrees of freedom				6.0	161
Expanded uncertainty (95.45 % coverage factor)				12.0	

Table 7 Uncertainty at power factor 0

The expanded uncertainty at power factor 1 is 26 µW/VA relative the apparent power.

The expanded uncertainty at power factor 0.5 is 17 µW/VA relative the apparent power.

The expanded uncertainty at power factor 0 is 12 µW/VA relative the apparent power.

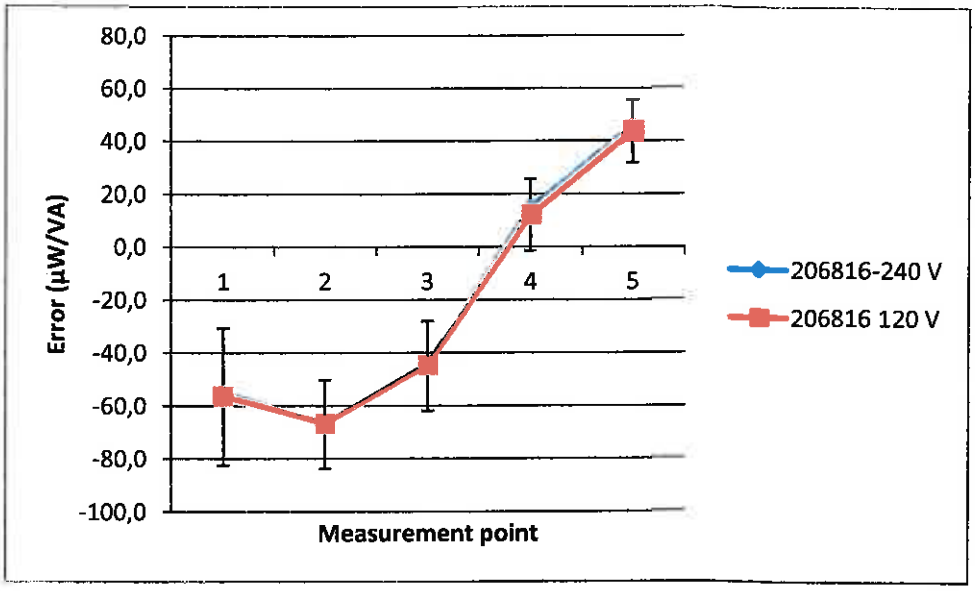

Figure 2 Error variation for RD22 206816

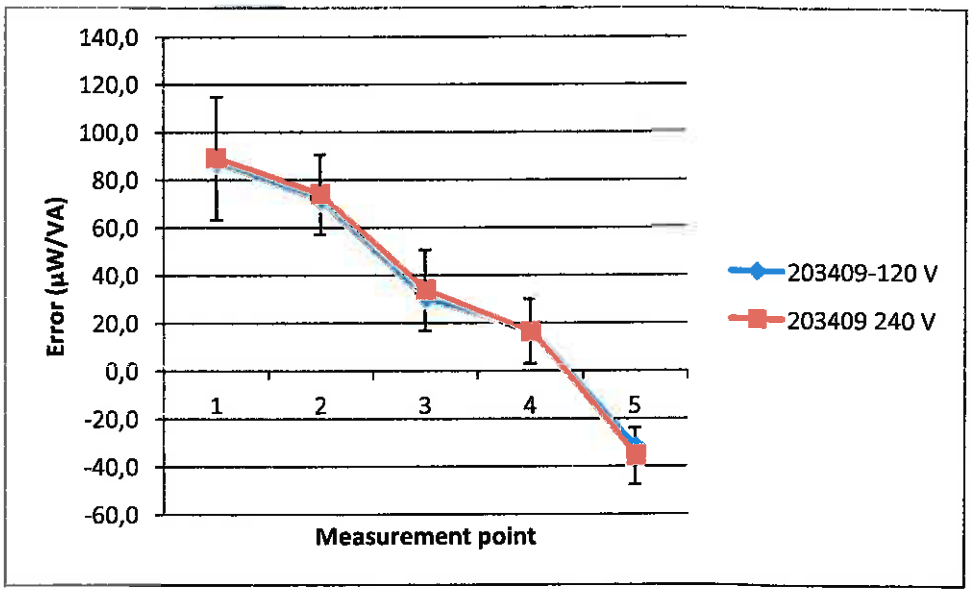

Figure 3 Error variation for RD22 203409

Annex 1

In the DSWM, the two independent measuring channels introduce errors in measuring the amplitude and phase angle difference between voltage and current signals.

The shunt resistors and the IVD are of high accuracy for ac power measurements and they have been calibrated respectively at the Swedish national laboratory (SP) and at the national measurement institute of Australia (NMIA).

Special efforts have been paid on evaluating the amplitude and phase angle errors introduced by the multimeters:

- The amplitude errors are a combination of the DC errors of the digitiser and the AC errors due to imperfections in the input channels of the voltmeters (limited bandwidths). Others sources of errors are the aperture time and the quantization noise.

Lots of experiments have been done to characterize the multimeters on the DCV digitising mode for the evaluation of the DC error contribution. The influence of aperture time, dead time, sampling frequency and auto-zero operation has been studied.

All the other parameters have been calculated.

- The phase angle errors are due to bandwidth differences of the two multimeters, trigger latency differences which can be defined as the difference of time delay between the trigger and the start of the measurement (dependent of the clock and internal timing circuits) and aperture time differences between the two multimeters. Another possible source of error is the sampling jitter. All these parameters have been evaluated experimentally.

Source of uncertainty	Type method A or B of evaluation/probability distribution function	Standard uncertainty (μW/VA)
Voltage measurement		
Calibration of multimeter in DCV mode	Type Br/pdf: Normal	5.00
Limitation in bandwidth	Type B/pdf: Rectangular	0.00
Sampling time aperture	Type B/pdf: Rectangular	0.10
Sampling jitter	Type A/pdf: Normal	0.30
Quantization noise	Type B/pdf: Rectangular	0.14
Multimeter resolution	Type B/pdf: Rectangular	0.40
Fluctuation of sample period	Type A/pdf: Normal	0,00
Calibration of inductive voltage divider	Type Br/pdf: Normal	0.10
Inductive voltage divider drift	Type B/pdf: Rectangular	0,01
TOTAL		**5.03**
Current measurement		
Calibration of multimeter in DCV mode	Type Br/pdf: Normal	5,00
Limitation in bandwidth	Type B/pdf: Rectangular	0,00
Sampling time aperture	Type B/pdf: Rectangular	0.10
Sampling jitter	Type A/pdf: Normal	0.30
Quantization noise	Type B/pdf: Rectangular	0.14
Multimeter resolution	Type B/pdf: Rectangular	0.40
Fluctuation of sample period	Type A/pdf: Normal	0,00
Calibration of shunt in DC	Type Br/pdf: Normal	1.50
Shunt drift	Type B/pdf: Rectangular	0.00
Shunt – AC/DC transfer difference	Type A/pdf: Normal	10.0
Shunt – AC/DC transfer difference-drift	Type B/pdf: Rectangular	2.90
TOTAL		**11.66**
Phase measurement		
Multimeter differences	Type A/pdf: Normal	5.00
Inductive voltage divider	Type Br/pdf: Normal	0.30
Shunt	Type Br/pdf: Normal	1.10
Quantization noise	Type B/pdf: Rectangular	0.2
Sampling jitter	Type A/pdf: Normal	1.00
TOTAL		**5.23**

4. Comparison report of NIM

CCEM Key Comparison CCEM-K5.2017 “Key comparison of 50/60 Hz power” Measurement Report by NIM, China

National Institute of Metrology, China
No.18 Bei San Hun Dong Rd., 100029 Beijing, China

Feb. 2020

1. Traveling standard

Manufacturer	Radians
Model	RD-22-332S
SN	206816，203409

2. Laboratory and its representative

Laboratory	Power/Energy Measurement Lab.
	National Institute of Metrology, China
Representative	Mr. Wang Lei

3. Measurement results

Measurement date	From June 10th, 2019 to June. 23rd, 2019	
Ambient conditions	Temperature:	23 °C ± 2 °C
	Humidity:	45 % ± 5 %

In this comparison NIM used primary standard and AC power measurement system based on program Josephson voltage standard (PJVS) to measure the traveling standard. During the measurement the RD-22-332S (SN. 203409) is not stable compared to the other one (SN. 206816) in the lag and lead angle tests.

Table 3.1 Calibration error, expanded uncertainty and degrees of freedom against primary standard SN. 206816

Applied values				Results	
Voltage [V]	Current [A]	Frequency [Hz]	Power Factor	Error [μW/VA]	Expanded uncertainty estimated at a 95% confidence level [μW/VA]
120	5	53	1	-60.7	12.0
			0.5L(lag)	9.8	12.0
			0.5C(Lead)	-70.4	12.0
			0L(lag)	44.8	10.0
			0L(Lead)	-46.2	10.0

240	5	53	1	-55.1	12.0
			0.5L(lag)	13.4	12.0
			0.5C(Lead)	-68.4	12.0
			0L(lag)	45.4	10.0
			0L(Lead)	-46.9	10.0

SN. 203409

Applied values				Results	
Voltage [V]	Current [A]	Frequency [Hz]	Power Factor	Error [μW/VA]	Expanded uncertainty estimated at a 95% confidence level [μW/VA]
120	5	53	1	69.7	16.0
			0.5L(lag)	7.7	16.0
			0.5C(Lead)	62.0	16.0
			0L(lag)	-33.2	10.0
			0L(Lead)	31.0	10.0
240	5	53	1	82.0	16.0
			0.5L(lag)	6.2	16.0
			0.5C(Lead)	75.5	16.0
			0L(lag)	-42.3	10.0
			0L(Lead)	40.0	10.0

Table 3.2 Calibration error, expanded uncertainty and degrees of freedom against AC power based on PJVS

SN. 206816

Applied values				Results	
Voltage [V]	Current [A]	Frequency [Hz]	Power Factor	Error [μW/VA]	Expanded uncertainty estimated at a 95% confidence level [μW/VA]
120	5	53	1	-61.6	10.4
			0.5L(lag)	11.8	12.2
			0.5C(Lead)	-74.6	12.2
			0L(lag)	48.2	6.8
			0L(Lead)	-48.9	6.8
240	5	53	1	-57.4	10.4
			0.5L(lag)	14.5	12.2

			0.5C(Lead)	-73.0	12.2
			0L(lag)	48.5	6.8
			0L(Lead)	-49.5	6.8

SN. 203409

Applied values				Results	
Voltage [V]	Current [A]	Frequency [Hz]	Power Factor	Error [μW/VA]	Expanded uncertainty estimated at a 95% confidence level [μW/VA]
120	5	53	1	79.9	10.6
			0.5L(lag)	17.4	18.8
			0.5C(Lead)	62.8	17.6
			0L(lag)	-27.6	17.2
			0L(Lead)	26.7	16.4
240	5	53	1	85.6	10.6
			0.5L(lag)	14.2	18.8
			0.5C(Lead)	70.0	17.6
			0L(lag)	-34.4	17.2
			0L(Lead)	33.0	16.4

4. Detailed measurement uncertainty budget

Table 4.1 Uncertainty budget of primary standard (power factor 1.0 53 Hz 120V and 240V)

Source of Uncertainty	type	Distribution	Standard uncertainty (μW/VA)	Sensitivity coefficient	Uncertainty contribution (μW/VA)	Degrees of freedom
Voltage transformer ratio	B	Normal	2.0	1	2.0	30
Current transformer ratio	B	Normal	2.0	1	2.0	30
DC Power	B	Normal	3.0	1	3.0	30
Compensation from emf	B	Normal	1.0	1	1.0	30
Synchronous with ac power stability	B	Normal	1.3	1	1.3	10
Ac/dc transfer error of power comparator	B	Normal	1.0	1	1.0	30

Temperature coefficient of UUT	B	Normal	2.0	1	2.0	30
Repeatability(53 Hz) SN. 206816	A	Normal	3.0	1	3.0	10
Repeatability(53 Hz) SN. 203409	A	Normal	6.0	1	6.0	10
Root square sum of Type A standard uncertainties and effective degrees of freedom (53 Hz) SN. 206816					3.0	10
Root square sum of Type A standard uncertainties and effective degrees of freedom (53 Hz) SN. 203409					6.0	10
Root square sum of Type B standard uncertainties and effective degrees of freedom					5.0	131
Combined standard uncertainty and effective degrees of freedom SN. 206816					5.8	89.8
Combined standard uncertainty and effective degrees of freedom SN. 203409					7.8	28
Coverage factor					2.0	
Expanded uncertainty SN. 206816					12.0 μW/VA	
Expanded uncertainty SN. 203409					16.0 μW/VA	

Table 4.2 Uncertainty budget of primary standard (power factor 0.5L 53 Hz 120V and 240V)

Source of Uncertainty	type	Distribution	Standard uncertainty (μW/VA)	Sensitivity coefficient	Uncertainty contribution (μW/VA)	Degrees of freedom
Voltage transformer ratio	B	Normal	2.0	1	2.0	30
Current transformer ratio	B	Normal	2.0	1	2.0	30
Voltage transformer angle	B	Normal	2.0	1	2.0	30
Current transformer angle	B	Normal	2.0	1	2.0	30
DC Power	B	Normal	2.0	1	2.0	30
Compensation from emf	B	Normal	1.0	1	1.0	30
Synchronous with ac power stability	B	Normal	1.3	1	1.3	10
Ac/dc transfer error of power comparator	B	Normal	1.0	1	1.0	30
Temperature coefficient of UUT	B	Normal	1.0	1	1.0	30
Repeatability(53 Hz) SN. 206816	A	Normal	2.5	1	2.5	10
Repeatability(53 Hz) SN. 203409	A	Normal	6.0	1	6.0	10
Root square sum of Type A standard uncertainties and effective degrees of freedom (53 Hz) SN. 206816					2.5	10
Root square sum of Type A standard uncertainties and effective degrees of freedom (53 Hz) SN. 203409					6.0	10
Root square sum of Type B standard uncertainties and effective degrees of freedom					5.0	199
Combined standard uncertainty and effective degrees of freedom SN. 206816					5.6	138
Combined standard uncertainty and effective degrees of freedom SN. 203409					7.8	28.0
Coverage factor					2.0	
Expanded uncertainty SN. 206816					12.0 μW/VA	
Expanded uncertainty SN. 203409					16.0 μW/VA	

Table 4.3 Uncertainty budget of primary standard (power factor 0.5C 53 Hz 120V and 240V)

Source of Uncertainty	type	Distribution	Standard uncertainty (μW/VA)	Sensitivity coefficient	Uncertainty contribution	Degrees of freedom

					(μW/VA)	
Voltage transformer ratio	B	Normal	2.0	1	2.0	30
Current transformer ratio	B	Normal	2.0	1	2.0	30
Voltage transformer angle	B	Normal	2.0	1	2.0	30
Current transformer angle	B	Normal	2.0	1	2.0	30
DC Power	B	Normal	2.0	1	2.0	30
Compensation from emf	B	Normal	1.0	1	1.0	30
Synchronous with ac power stability	B	Normal	1.3	1	1.3	10
Ac/dc transfer error of power comparator	B	Normal	1.0	1	1.0	30
Temperature coefficient of UUT	B	Normal	1.0	1	1.0	30
Repeatability(53 Hz) SN. 206816	A	Normal	3.0	1	3.0	10
Repeatability(53 Hz) SN. 203409	A	Normal	6.0	1	6.0	10
Root square sum of Type A standard uncertainties and effective degrees of freedom (53 Hz) SN. 206816					3.0	10
Root square sum of Type A standard uncertainties and effective degrees of freedom (53 Hz) SN. 203409					6.0	10
Root square sum of Type B standard uncertainties and effective degrees of freedom					5.0	199
Combined standard uncertainty and effective degrees of freedom SN. 206816					5.8	102
Combined standard uncertainty and effective degrees of freedom SN. 203409					7.8	28.0
Coverage factor					2.0	
Expanded uncertainty SN. 206816					12.0 μW/VA	
Expanded uncertainty SN. 203409					16.0 μW/VA	

Table 4.4 Uncertainty budget of primary standard (power factor 0L 53 Hz 120V and 240V)

Source of Uncertainty	type	Distribution	Standard uncertainty (μW/VA)	Sensitivity coefficient	Uncertainty contribution (μW/VA)	Degrees of freedom
Voltage transformer angle	B	Normal	2.0	1	2.0	30
Current transformer angle	B	Normal	2.0	1	2.0	30
Compensation from emf	B	Normal	1.0	1	1.0	30
Synchronous with ac power stability	B	Normal	1.3	1	1.3	10
Ac/dc transfer error of power comparator	B	Normal	1.0	1	1.0	30
Repeatability(53 Hz) SN. 206816	A	Normal	3.0	1	3.0	10
Repeatability(53 Hz) SN. 203409	A	Normal	3.0	1	3.0	10
Root square sum of Type A standard uncertainties and effective degrees of freedom (53 Hz) SN. 206816					3.0	10
Root square sum of Type A standard uncertainties and effective degrees of freedom (53 Hz) SN. 203409					3.0	10
Root square sum of Type B standard uncertainties and effective degrees of freedom					4.0	96
Combined standard uncertainty and effective degrees of freedom SN. 206816					5.0	58
Combined standard uncertainty and effective degrees of freedom SN. 203409					5.0	58
Coverage factor					2.0	
Expanded uncertainty SN. 206816					10.0 μW/VA	
Expanded uncertainty SN. 203409					10.0 μW/VA	

Table 4.5 Uncertainty budget of primary standard (power factor 0C 53 Hz 120V and 240V)

Source of Uncertainty	type	Distribution	Standard uncertainty (μW/VA)	Sensitivity coefficient	Uncertainty contribution (μW/VA)	Degrees of freedom
Voltage transformer angle	B	Normal	2.0	1	2.0	30
Current transformer angle	B	Normal	2.0	1	2.0	30

Compensation from emf	B	Normal	1.0	1	1.0	30
Synchronous with ac power stability	B	Normal	1.3	1	1.3	10
Ac/dc transfer error of power comparator	B	Normal	1.0	1	1.0	30
Repeatability(53 Hz) SN. 206816	A	Normal	3.0	1	3.0	10
Repeatability(53 Hz) SN. 203409	A	Normal	3.0	1	3.0	10
Root square sum of Type A standard uncertainties and effective degrees of freedom (53 Hz) SN. 206816					3.0	10
Root square sum of Type A standard uncertainties and effective degrees of freedom (53 Hz) SN. 203409					3.0	10
Root square sum of Type B standard uncertainties and effective degrees of freedom					4.0	96
Combined standard uncertainty and effective degrees of freedom SN. 206816					5.0	58
Combined standard uncertainty and effective degrees of freedom SN. 203409					5.0	58
Coverage factor					2.0	
Expanded uncertainty SN. 206816					10.0 μW/VA	
Expanded uncertainty SN. 203409					10.0 μW/VA	

Table 4.6 Uncertainty budget of AC power based on PJVS (power factor 1.0 53 Hz 120V and 240V)

Source of Uncertainty	type	Distribution	Standard uncertainty (μW/VA)	Sensitivity coefficient	Uncertainty contribution (μW/VA)	Degrees of freedom
Voltage divider ratio	B	Normal	3.1	1	3.1	30
I-V ratio	B	Normal	3.5	1	3.5	30
Synchronous with ac power stability	B	Normal	1.3	1	1.3	10
Sampling of PDM	B	Normal	1.0	1	1.0	30
Temperature coefficient of UUT	B	Normal	2.0	1	2.0	30
Repeatability(53 Hz) SN. 206816	A	Normal	1.5	1	1.5	10
Repeatability(53 Hz) SN. 203409	A	Normal	1.9	1	1.9	10
Root square sum of Type A standard uncertainties and effective degrees of freedom (53 Hz) SN. 206816					1.5	10
Root square sum of Type A standard uncertainties and effective degrees of freedom (53 Hz) SN. 203409					1.9	10
Root square sum of Type B standard uncertainties and effective degrees of freedom					5.0	91
Combined standard uncertainty and effective degrees of freedom SN. 206816					5.2	100
Combined standard uncertainty and effective degrees of freedom SN. 203409					5.3	100
Coverage factor					2.0	
Expanded uncertainty SN. 206816					10.4 μW/VA	
Expanded uncertainty SN. 203409					10.6 μW/VA	

Table 4.7 Uncertainty budget of AC power based on PJVS (power factor 0.5L 53 Hz 120V and 240V)

Source of Uncertainty	type	Distribution	Standard uncertainty (μW/VA)	Sensitivity coefficient	Uncertainty contribution (μW/VA)	Degrees of freedom
Voltage divider ratio	B	Normal	3.1	1	3.1	30
I-V ratio	B	Normal	3.5	1	3.5	30
Voltage divider angle	B	Normal	2.0	1	2.0	30
I-V angle	B	Normal	2.0	1	2.0	30
Synchronous with ac power stability	B	Normal	1.3	1	1.3	10
Sampling of PDM	B	Normal	1.0	1	1.0	30
Temperature coefficient of UUT	B	Normal	1.0	1	1.0	30
Repeatability(53 Hz) SN. 206816	A	Normal	1.3	1	1.3	10
Repeatability(53 Hz) SN. 203409	A	Normal	7.3	1	7.3	10
Root square sum of Type A standard uncertainties and effective degrees of freedom (53 Hz) SN. 206816					1.3	10
Root square sum of Type A standard uncertainties and effective degrees of freedom (53 Hz) SN. 203409					7.3	10
Root square sum of Type B standard uncertainties and effective degrees of freedom					6.0	118
Combined standard uncertainty and effective degrees of freedom SN. 206816					6.1	126
Combined standard uncertainty and effective degrees of freedom SN. 203409					9.4	27
Coverage factor					2.0	
Expanded uncertainty SN. 206816					12.2 μW/VA	
Expanded uncertainty SN. 203409					18.8 μW/VA	

Table 4.8 Uncertainty budget of AC power based on PJVS (power factor 0.5C 53 Hz 120V and 240V)

Source of Uncertainty	type	Distribution	Standard uncertainty (μW/VA)	Sensitivity coefficient	Uncertainty contribution (μW/VA)	Degrees of freedom

Voltage divider ratio	B	Normal	3.1	1	3.1	30
I-V ratio	B	Normal	3.5	1	3.5	30
Voltage divider angle	B	Normal	2.0	1	2.0	30
I-V angle	B	Normal	2.0	1	2.0	30
Synchronous with ac power stability	B	Normal	1.3	1	1.3	10
Sampling of PDM	B	Normal	1.0	1	1.0	30
Temperature coefficient of UUT	B	Normal	1.0	1	1.0	30
Repeatability(53 Hz) SN. 206816	A	Normal	1.3	1	1.3	10
Repeatability(53 Hz) SN. 203409	A	Normal	6.5	1	6.5	10
Root square sum of Type A standard uncertainties and effective degrees of freedom (53 Hz) SN. 206816					1.3	10
Root square sum of Type A standard uncertainties and effective degrees of freedom (53 Hz) SN. 203409					6.5	10
Root square sum of Type B standard uncertainties and effective degrees of freedom					6.0	118
Combined standard uncertainty and effective degrees of freedom SN. 206816					6.1	126
Combined standard uncertainty and effective degrees of freedom SN. 203409					8.8	32
Coverage factor					2.0	
Expanded uncertainty SN. 206816					10.2 μW/VA	
Expanded uncertainty SN. 203409					17.6 μW/VA	

Table 4.9 Uncertainty budget of AC power based on PJVS (power factor 0L 53 Hz 120V and 240V)

Source of Uncertainty	type	Distribution	Standard uncertainty (μW/VA)	Sensitivity coefficient	Uncertainty contribution (μW/VA)	Degrees of freedom
Voltage divider angle	B	Normal	2.0	1	2.0	30
I-V angle	B	Normal	2.0	1	2.0	30
Synchronous with ac power stability	B	Normal	1.3	1	1.3	10
Sampling of PDM	B	Normal	1.0	1	1.0	30
Repeatability(53 Hz) SN. 206816	A	Normal	1.0	1	1.0	10
Repeatability(53 Hz) SN. 203409	A	Normal	8.0	1	8.0	10
Root square sum of Type A standard uncertainties and effective degrees of freedom (53 Hz) SN. 206816					1.0	10
Root square sum of Type A standard uncertainties and effective degrees of freedom (53 Hz) SN. 203409					8.0	10
Root square sum of Type B standard uncertainties and effective degrees of freedom					3.2	82
Combined standard uncertainty and effective degrees of freedom SN. 206816					3.4	92
Combined standard uncertainty and effective degrees of freedom SN. 203409					8.6	13
Coverage factor					2.0	
Expanded uncertainty SN. 206816					6.8 μW/VA	
Expanded uncertainty SN. 203409					17.2 μW/VA	

Table 4.10 Uncertainty budget of AC power based on PJVS (power factor 0C 53 Hz 120V and 240V)

Source of Uncertainty	type	Distribution	Standard uncertainty (μW/VA)	Sensitivity coefficient	Uncertainty contribution (μW/VA)	Degrees of freedom
Voltage divider angle	B	Normal	2.0	1	2.0	30
I-V angle	B	Normal	2.0	1	2.0	30

Synchronous with ac power stability	B	Normal	1.3	1	1.3	10
Sampling of PDM	B	Normal	1.0	1	1.0	30
Repeatability(53 Hz) SN. 206816	A	Normal	1.0	1	1.0	10
Repeatability(53 Hz) SN. 203409	A	Normal	8.0	1	8.0	10
Root square sum of Type A standard uncertainties and effective degrees of freedom (53 Hz) SN. 206816					1.0	10
Root square sum of Type A standard uncertainties and effective degrees of freedom (53 Hz) SN. 203409					8.0	10
Root square sum of Type B standard uncertainties and effective degrees of freedom					3.2	82
Combined standard uncertainty and effective degrees of freedom SN. 206816					3.4	92
Combined standard uncertainty and effective degrees of freedom SN. 203409					8.6	13
Coverage factor					2.0	
Expanded uncertainty SN. 206816					6.8 μW/VA	
Expanded uncertainty SN. 203409					17.2 μW/VA	

5. Signature of the laboratory representative

Wang Lei

Power/Energy Measurement Lab.

National Institute of Metrology, China

APPENDIX Measurement method and circuit diagram of setup

The block diagram of the measurement setup of primary standard is shown in Fig. A.1. The “double bridge power comparator” (DBPC)[1] is adopted in the principle of the single phase energy primary standard. It compares the AC power to DC power directly by using two multijuction thermal converters.

The ac current and voltage signals are generated using a power source. The ac signals are applied to the UUT and the DBPC, the DC signal is only applied to the DBPC. When the double bridge power comparator is balanced, the AC power is equal to the DC power. The DC power is calculated by the DC voltage and DC resistor. In the measurement the remainder unbalanced value is get from the Nano voltage meter and compensated by the computer.

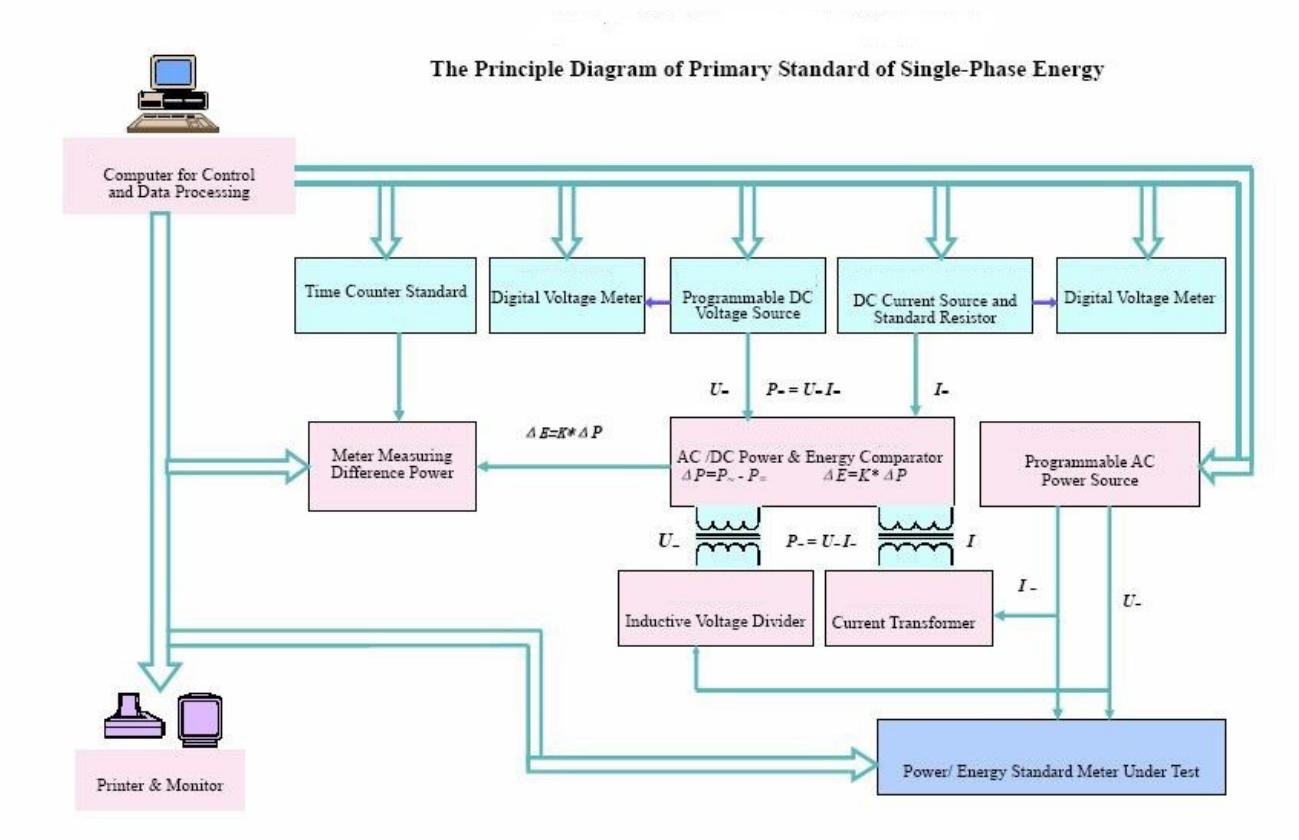

Fig. A.1 Block diagram of measurement setup

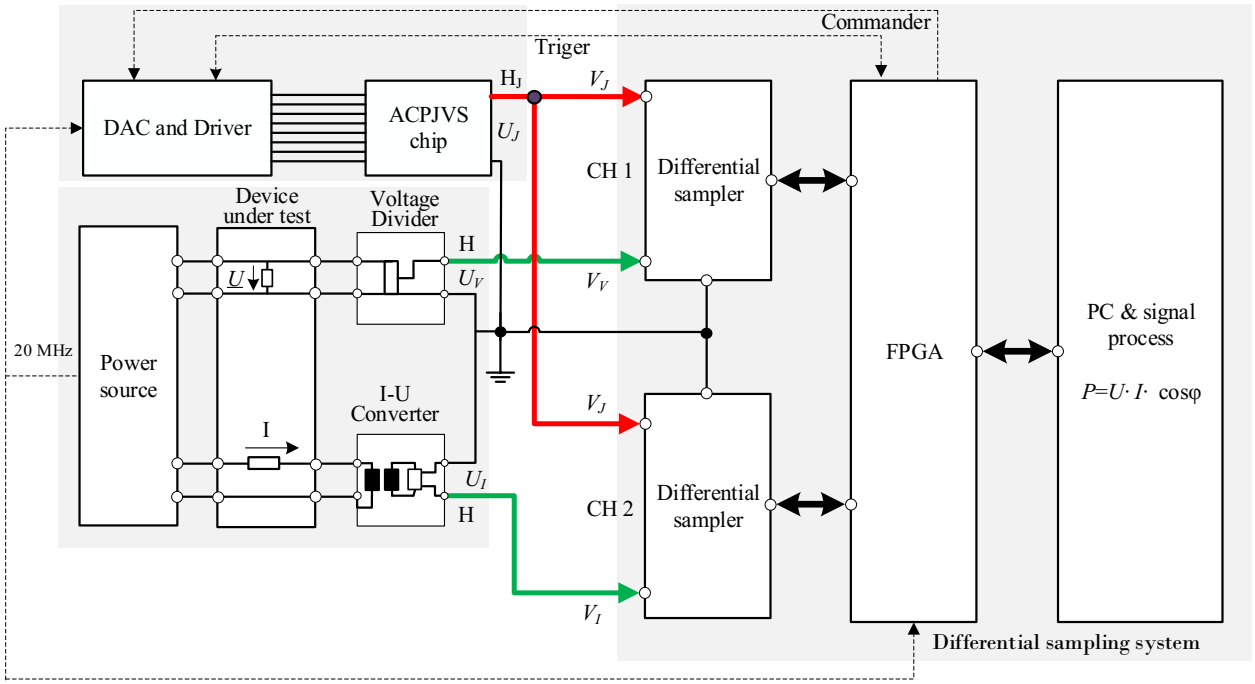

Fig. B.1 Block diagram of measurement setup

The block diagram of AC power measurement system based on program Josephson voltage standard (PJVS) is shown in the Fig B.1. A PJVS system is used in the system which can generate a quantum based stepwise signal. The power source generates voltage and current signals for the device under test, meanwhile the voltage and current will be transferred to 1 V voltage by a voltage divider and a I-U converter. Then the differential sampling system will acquire two differential signals between stepwise and AC voltage. After signal processing, we can calculate the quantum-based AC power. Then the difference of AC power between devise under test and quantum-based AC power can be calculated.

References

[l] D. Zhang et al., "A new power standard for audio-frequency measurements," IEEE Trans. lnstrument. Meas., IM 39, no. 3, pp. 545-547, 1990.

[2] Z. S. Jia et al., Precision AC Power Measurement System Based on AC Programmable Josephson Voltage Standards. IMEKO 2018 Conf. Digest.

5. Comparison report of NIST

CCEM-K5.2017 Measurement Report – NIST 2022 Tests

1. RD-22 Travelling Standards Serial No. 206816 and 203409

2. Results Submitted by: NIST
Tom Nelson, Bryan Waltrip
Quantum Measurement Division
100 Bureau Drive
Gaithersburg, MD 20899, USA
thomas.nelson@nist.gov, bryan.waltrip@nist.gov

3. **Measurement Setup and Traceability Scheme**

The RD-22 travelling standards were calibrated using a generation system of synthetic (or phantom) power that accurately relates the amplitudes and phases of the applied voltage and current signals to the piecewise-approximated sinewave signals produced by a dual-channel Programmable Josephson Voltage Standard (PJVS), as shown in Fig. 1.

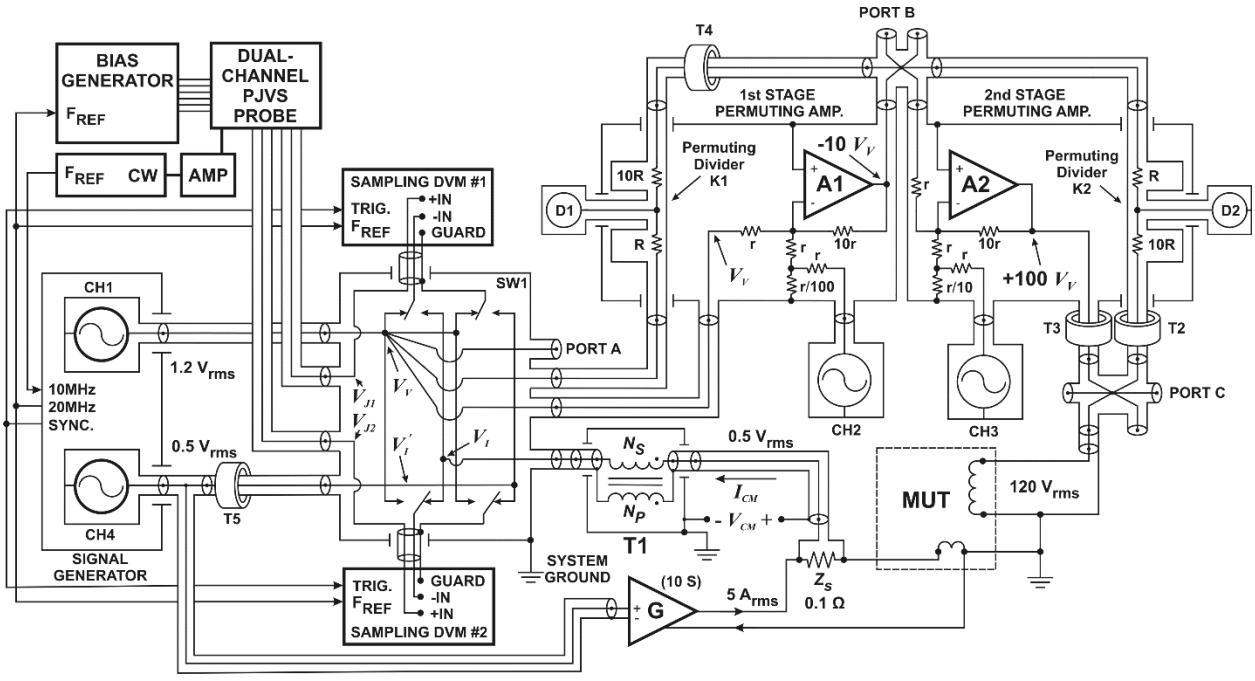

Fig. 1. Detailed diagram of the dual-channel PJVS-based power generation system.

The original system is described in [1], although significant improvements have been made to reduce uncertainties associated with the differential sampling technique [2] and the voltage amplification [3].

The single-channel PJVS of [1] has been replaced with a dual-channel version that eliminates the problem of ADC overloading caused by the required multiplexing of the scaled test voltage, V_V, and scaled test current, V_I, signals with the single PJVS signal, V_J. This allows for a significant improvement in measurement throughput and associated reduction in type A uncertainties of the V_V and V_I signals.

For an applied voltage and current of 120 V RMS and 5 A RMS, a custom designed multi-channel signal generator that is frequency locked to the 10 MHz frequency reference oscillator of the PJVS system is used to produce the sinusoidal 1.2 V RMS V_V and 0.5 V RMS V_I' signals with THD+N below -110 dB at the fundamental test frequency of 53 Hz. The type B uncertainties of the amplitudes and relative phases of the V_V and V_I signals are traceable to the SI Volt through the PJVS using a pair of sampling digital voltmeters (DVMs) and differential sampling techniques [2]. For this application, the type A and type B uncertainties associated with the PJVS are insignificant.

The 1.2 V RMS V_V signal is scaled to 120 V RMS using a two-stage voltage amplifier with a composite gain of 100 V/V. The amplifier consists of two -10:1 inverting amplifier stages, where the input and output of each stage are connected to a corresponding permuting voltage divider, i.e., an 11-element relay-switched array of 1 MΩ thin-film resistors with low temperature and voltage coefficients. These dividers are shown as dividers K1 and K2 in Fig. 1 and serve as voltage ratio references for the in-situ calibration and correction of the gain and phase errors of each amplifier stage [3]. The K1 and K2 dividers are regularly calibrated by comparing them to a reference permuting capacitance divider made up of 11 relay-switched nitrogen dielectric capacitors. For these calibrations, the reference divider is connected at either the PORT A and PORT B or PORT B and PORT C ports of Fig. 1. The traceability of the reference divider is through the NIST calculable capacitor [4], although only the relative values of the capacitance and loss vector, as well as the voltage coefficient [5], of the capacitive elements must be known. This technique of voltage ratio determination is discussed in [6].

For an applied voltage of 240 V RMS, the voltage amplifier of Fig. 1 includes a third -10:1 inverting amplifier stage (not shown) and associated permuting voltage divider, K3, resulting in an overall amplifier gain of -1000 V/V, resulting in an applied V_V signal of 0.24 V RMS.

The 5 A RMS current applied to the travelling standard meter under test (MUT of Fig. 1) is transformed to a 0.5 V RMS voltage using an ac current shunt, Z_S, with calculable ac resistance and time constant. The dc value of Z_S is traceable to the quantum Hall resistance and the ac response of Z_S is calculated using both theoretical and empirical means [7].

The common-mode voltage present at the output of Z_S, V_{CM}, is removed using T1, a 3-stage, amplifier-aided voltage transformer [8] operating as a common-mode choke.

4. **Measurement Procedure**

As described in the technical protocol for this comparison, the reference standards were allowed warm up for at least 4 hours after powering them with their 24 V DC power supply. Due to constraints between the allowed relationships between the generation and acquisition clocks of the NIST system, the fundamental frequency of the applied voltage and current for all tests was (53.074049 ± 0.000001) Hz.

At least 20 sets of readings of the relevant parameters measured by the reference standards were made at each test point over several days. At regular intervals over the measurement run, the reference standards were de-energized (applied power removed), voltage and current leads disconnected, re-initialized, re-connected, re-energized, and allowed to warm up for at least 15 minutes before continuing the measurement run.

For several reasons, the NIST system does not support the acquisition of applied frequency readings from the measurement standards. First, the applied frequency readings are observed on the front panel of the measurement standard when the instruments are initially set up at each test point to verify that the measured and applied frequency values are within 10 μHz/Hz. Second, previous observations of averaged frequency readings from RD-22 measurement standards have never shown 50 Hz to 60 Hz frequency measurement errors greater than 2 μHz/Hz. Finally, previous observations of the frequency response of RD-22 measurement standards over the 50 Hz to 60 Hz frequency range indicate that no appreciable frequency dependence occurs in the active power (or any other related parameter) readings for small (<1%) changes in the frequency of the applied voltage and current signals. For these reasons, the mean values of the frequency parameters measured by the reference standards are neither observed nor reported.

5. **Results**

The measurement results for each travelling standard are given in Table 1 to Table 20. In addition to the relevant parameters listed in Table 2 of the CCEM-K5.2017 Technical Protocol, the mean values of the phase measured by the reference standard are also included.

Table 1. RD-22 Serial # 203409, Active Power at 120 V, 5 A, 53 Hz, PF=1.000 (θ=0°)

a) Mean value of the calibration error of the reference standard (μW/VA)	87.1	
b) Expanded uncertainty (95.45 % coverage factor) (μW/VA) and degrees of freedom	6.3	82
c.1) Mean value of the voltage measured by the reference standard (V RMS)	120.00137	
c.2) Mean value of the current measured by the reference standard (A RMS)	5.000374	
c.3) Mean value of the power factor measured by the reference standard (dimensionless)	1.000000	
c.4) Mean value of the phase measured by the reference standard (degrees)	-0.00201	
d) Mean date of measurement	16-Aug-22	
e.1) Mean value and spread of temperature (degrees Celsius)	22.2	1.0
e.2) Mean value and spread of humidity (%)	35.5	3.4

Table 2. RD-22 Serial # 203409, Active Power at 120 V, 5 A, 53 Hz, PF=0.500 Lead (θ=60°)

a) Mean value of the calibration error of the reference standard (μW/VA)	76.5	
b) Expanded uncertainty (95.45 % coverage factor) (μW/VA) and degrees of freedom	6.4	113
c.1) Mean value of the voltage measured by the reference standard (V RMS)	120.00131	
c.2) Mean value of the current measured by the reference standard (A RMS)	5.000384	
c.3) Mean value of the power factor measured by the reference standard (dimensionless)	0.500033	
c.4) Mean value of the phase measured by the reference standard (degrees)	59.99832	

d) Mean date of measurement	16-Aug-22	
e.1) Mean value and spread of temperature (degrees Celsius)	22.2	1.0
e.2) Mean value and spread of humidity (%)	35.5	3.4

Table 3. RD-22 Serial # 203409, Active Power at 120 V, 5 A, 53 Hz, PF=0.000 Lead (θ=90°)

a) Mean value of the calibration error of the reference standard (µW/VA)	37.9	
b) Expanded uncertainty (95.45 % coverage factor) (µW/VA) and degrees of freedom	6.4	73
c.1) Mean value of the voltage measured by the reference standard (V RMS)	120.00130	
c.2) Mean value of the current measured by the reference standard (A RMS)	5.000391	
c.3) Mean value of the power factor measured by the reference standard (dimensionless)	0.000038	
c.4) Mean value of the phase measured by the reference standard (degrees)	89.99782	
d) Mean date of measurement	16-Aug-22	
e.1) Mean value and spread of temperature (degrees Celsius)	22.2	1.0
e.2) Mean value and spread of humidity (%)	35.5	3.4

Table 4. RD-22 Serial # 203409, Active Power at 120 V, 5 A, 53 Hz, PF=0.500 Lag (θ=-60°)

a) Mean value of the calibration error of the reference standard (µW/VA)	10.6	
b) Expanded uncertainty (95.45 % coverage factor) (µW/VA) and degrees of freedom	6.4	114
c.1) Mean value of the voltage measured by the reference standard (V RMS)	120.00133	
c.2) Mean value of the current measured by the reference standard (A RMS)	5.000367	
c.3) Mean value of the power factor measured by the reference standard (dimensionless)	0.499968	
c.4) Mean value of the phase measured by the reference standard (degrees)	-60.00213	
d) Mean date of measurement	16-Aug-22	
e.1) Mean value and spread of temperature (degrees Celsius)	22.2	1.0
e.2) Mean value and spread of humidity (%)	35.5	3.4

Table 5. RD-22 Serial # 203409, Active Power at 120 V, 5 A, 53 Hz, PF=0.000 Lag (θ=-90°)

a) Mean value of the calibration error of the reference standard (µW/VA)	-40.0	
b) Expanded uncertainty (95.45 % coverage factor) (µW/VA) and degrees of freedom	6.4	72
c.1) Mean value of the voltage measured by the reference standard (V RMS)	120.00134	
c.2) Mean value of the current measured by the reference standard (A RMS)	5.000363	
c.3) Mean value of the power factor measured by the reference standard (dimensionless)	-0.000040	
c.4) Mean value of the phase measured by the reference standard (degrees)	-90.00230	
d) Mean date of measurement	16-Aug-22	
e.1) Mean value and spread of temperature (degrees Celsius)	22.2	1.0
e.2) Mean value and spread of humidity (%)	35.5	3.4

Table 6. RD-22 Serial # 203409, Active Power at 240 V, 5 A, 53 Hz, PF=1.000 (θ=0°)

a) Mean value of the calibration error of the reference standard (µW/VA)	88.6	
b) Expanded uncertainty (95.45 % coverage factor) (µW/VA) and degrees of freedom	9.8	129
c.1) Mean value of the voltage measured by the reference standard (V RMS)	240.00310	
c.2) Mean value of the current measured by the reference standard (A RMS)	5.000376	
c.3) Mean value of the power factor measured by the reference standard (dimensionless)	1.000000	
c.4) Mean value of the phase measured by the reference standard (degrees)	-0.00250	
d) Mean date of measurement	16-Aug-22	
e.1) Mean value and spread of temperature (degrees Celsius)	22.2	1.0
e.2) Mean value and spread of humidity (%)	35.5	3.4

Table 7. RD-22 Serial # 203409, Active Power at 240 V, 5 A, 53 Hz, PF=0.500 Lead (θ=60°)

a) Mean value of the calibration error of the reference standard (µW/VA)	85.8	
b) Expanded uncertainty (95.45 % coverage factor) (µW/VA) and degrees of freedom	9.5	171
c.1) Mean value of the voltage measured by the reference standard (V RMS)	240.00307	
c.2) Mean value of the current measured by the reference standard (A RMS)	5.000395	
c.3) Mean value of the power factor measured by the reference standard (dimensionless)	0.500040	
c.4) Mean value of the phase measured by the reference standard (degrees)	59.99782	
d) Mean date of measurement	16-Aug-22	
e.1) Mean value and spread of temperature (degrees Celsius)	22.2	1.0
e.2) Mean value and spread of humidity (%)	35.5	3.4

Table 8. RD-22 Serial # 203409, Active Power at 240 V, 5 A, 53 Hz, PF=0.000 Lead (θ=90°)

a) Mean value of the calibration error of the reference standard (µW/VA)	47.9	
b) Expanded uncertainty (95.45 % coverage factor) (µW/VA) and degrees of freedom	9.0	96
c.1) Mean value of the voltage measured by the reference standard (V RMS)	240.00314	
c.2) Mean value of the current measured by the reference standard (A RMS)	5.000407	
c.3) Mean value of the power factor measured by the reference standard (dimensionless)	0.000048	
c.4) Mean value of the phase measured by the reference standard (degrees)	89.99726	
d) Mean date of measurement	16-Aug-22	
e.1) Mean value and spread of temperature (degrees Celsius)	22.2	1.0
e.2) Mean value and spread of humidity (%)	35.5	3.4

Table 9. RD-22 Serial # 203409, Active Power at 240 V, 5 A, 53 Hz, PF=0.500 Lag (θ=-60°)

a) Mean value of the calibration error of the reference standard (µW/VA)	1.4	
b) Expanded uncertainty (95.45 % coverage factor) (µW/VA) and degrees of freedom	9.1	160
c.1) Mean value of the voltage measured by the reference standard (V RMS)	240.00314	
c.2) Mean value of the current measured by the reference standard (A RMS)	5.000357	

c.3) Mean value of the power factor measured by the reference standard (dimensionless)	0.499959	
c.4) Mean value of the phase measured by the reference standard (degrees)	-60.00272	
d) Mean date of measurement	16-Aug-22	
e.1) Mean value and spread of temperature (degrees Celsius)	22.2	1.0
e.2) Mean value and spread of humidity (%)	35.5	3.4

Table 10. RD-22 Serial # 203409, Active Power at 240 V, 5 A, 53 Hz, PF=0.000 Lag (θ=-90°)

a) Mean value of the calibration error of the reference standard (µW/VA)	-51.7	
b) Expanded uncertainty (95.45 % coverage factor) (µW/VA) and degrees of freedom	9.0	96
c.1) Mean value of the voltage measured by the reference standard (V RMS)	240.00322	
c.2) Mean value of the current measured by the reference standard (A RMS)	5.000351	
c.3) Mean value of the power factor measured by the reference standard (dimensionless)	-0.000052	
c.4) Mean value of the phase measured by the reference standard (degrees)	-90.00297	
d) Mean date of measurement	16-Aug-22	
e.1) Mean value and spread of temperature (degrees Celsius)	22.2	1.0
e.2) Mean value and spread of humidity (%)	35.5	3.4

Table 11. RD-22 Serial # 206816, Active Power at 120 V, 5 A, 53 Hz, PF=1.000 (θ=0°)

a) Mean value of the calibration error of the reference standard (µW/VA)	-53.2	
b) Expanded uncertainty (95.45 % coverage factor) (µW/VA) and degrees of freedom	6.3	81
c.1) Mean value of the voltage measured by the reference standard (V RMS)	119.99987	
c.2) Mean value of the current measured by the reference standard (A RMS)	4.999733	
c.3) Mean value of the power factor measured by the reference standard (dimensionless)	1.000000	
c.4) Mean value of the phase measured by the reference standard (degrees)	0.00264	
d) Mean date of measurement	16-Aug-22	
e.1) Mean value and spread of temperature (degrees Celsius)	22.2	1.0
e.2) Mean value and spread of humidity (%)	35.5	3.4

Table 12. RD-22 Serial # 206816, Active Power at 120 V, 5 A, 53 Hz, PF=0.500 Lead (θ=60°)

a) Mean value of the calibration error of the reference standard (µW/VA)	-66.3	
b) Expanded uncertainty (95.45 % coverage factor) (µW/VA) and degrees of freedom	6.4	113
c.1) Mean value of the voltage measured by the reference standard (V RMS)	119.99976	
c.2) Mean value of the current measured by the reference standard (A RMS)	4.999731	
c.3) Mean value of the power factor measured by the reference standard (dimensionless)	0.499962	
c.4) Mean value of the phase measured by the reference standard (degrees)	60.00303	
d) Mean date of measurement	16-Aug-22	
e.1) Mean value and spread of temperature (degrees Celsius)	22.2	1.0
e.2) Mean value and spread of humidity (%)	35.5	3.4

Table 13. RD-22 Serial # 206816, Active Power at 120 V, 5 A, 53 Hz, PF=0.000 Lead (θ=90°)

a) Mean value of the calibration error of the reference standard (µW/VA)	-45.8	
b) Expanded uncertainty (95.45 % coverage factor) (µW/VA) and degrees of freedom	6.4	72
c.1) Mean value of the voltage measured by the reference standard (V RMS)	119.99973	
c.2) Mean value of the current measured by the reference standard (A RMS)	4.999736	
c.3) Mean value of the power factor measured by the reference standard (dimensionless)	-0.000046	
c.4) Mean value of the phase measured by the reference standard (degrees)	90.00262	
d) Mean date of measurement	16-Aug-22	
e.1) Mean value and spread of temperature (degrees Celsius)	22.2	1.0
e.2) Mean value and spread of humidity (%)	35.5	3.4

Table 14. RD-22 Serial # 206816, Active Power at 120 V, 5 A, 53 Hz, PF=0.500 Lag (θ=-60°)

a) Mean value of the calibration error of the reference standard (µW/VA)	13.4	
b) Expanded uncertainty (95.45 % coverage factor) (µW/VA) and degrees of freedom	6.4	114
c.1) Mean value of the voltage measured by the reference standard (V RMS)	119.99983	
c.2) Mean value of the current measured by the reference standard (A RMS)	4.999737	
c.3) Mean value of the power factor measured by the reference standard (dimensionless)	0.500040	
c.4) Mean value of the phase measured by the reference standard (degrees)	-59.99738	
d) Mean date of measurement	16-Aug-22	
e.1) Mean value and spread of temperature (degrees Celsius)	22.2	1.0
e.2) Mean value and spread of humidity (%)	35.5	3.4

Table 15. RD-22 Serial # 206816, Active Power at 120 V, 5 A, 53 Hz, PF=0.000 Lag (θ=-90°)

a) Mean value of the calibration error of the reference standard (µW/VA)	44.2	
b) Expanded uncertainty (95.45 % coverage factor) (µW/VA) and degrees of freedom	6.4	72
c.1) Mean value of the voltage measured by the reference standard (V RMS)	119.99982	
c.2) Mean value of the current measured by the reference standard (A RMS)	4.999735	
c.3) Mean value of the power factor measured by the reference standard (dimensionless)	0.000044	
c.4) Mean value of the phase measured by the reference standard (degrees)	-89.99747	
d) Mean date of measurement	16-Aug-22	
e.1) Mean value and spread of temperature (degrees Celsius)	22.2	1.0
e.2) Mean value and spread of humidity (%)	35.5	3.4

Table 16. RD-22 Serial # 206816, Active Power at 240 V, 5 A, 53 Hz, PF=1.000 (θ=0°)

a) Mean value of the calibration error of the reference standard (µW/VA)	-53.9	
b) Expanded uncertainty (95.45 % coverage factor) (µW/VA) and degrees of freedom	9.8	129
c.1) Mean value of the voltage measured by the reference standard (V RMS)	239.99959	
c.2) Mean value of the current measured by the reference standard (A RMS)	4.999734	

c.3) Mean value of the power factor measured by the reference standard (dimensionless)	1.000000	
c.4) Mean value of the phase measured by the reference standard (degrees)	0.00263	
d) Mean date of measurement	16-Aug-22	
e.1) Mean value and spread of temperature (degrees Celsius)	22.2	1.0
e.2) Mean value and spread of humidity (%)	35.5	3.4

Table 17. RD-22 Serial # 206816, Active Power at 240 V, 5 A, 53 Hz, PF=0.500 Lead (θ=60°)

a) Mean value of the calibration error of the reference standard (µW/VA)	-67.1	
b) Expanded uncertainty (95.45 % coverage factor) (µW/VA) and degrees of freedom	9.3	166
c.1) Mean value of the voltage measured by the reference standard (V RMS)	239.99950	
c.2) Mean value of the current measured by the reference standard (A RMS)	4.999729	
c.3) Mean value of the power factor measured by the reference standard (dimensionless)	0.499961	
c.4) Mean value of the phase measured by the reference standard (degrees)	60.00305	
d) Mean date of measurement	16-Aug-22	
e.1) Mean value and spread of temperature (degrees Celsius)	22.2	1.0
e.2) Mean value and spread of humidity (%)	35.5	3.4

Table 18. RD-22 Serial # 206816, Active Power at 240 V, 5 A, 53 Hz, PF=0.000 Lead (θ=90°)

a) Mean value of the calibration error of the reference standard (µW/VA)	-46.2	
b) Expanded uncertainty (95.45 % coverage factor) (µW/VA) and degrees of freedom	9.0	96
c.1) Mean value of the voltage measured by the reference standard (V RMS)	239.99952	
c.2) Mean value of the current measured by the reference standard (A RMS)	4.999738	
c.3) Mean value of the power factor measured by the reference standard (dimensionless)	-0.000046	
c.4) Mean value of the phase measured by the reference standard (degrees)	90.00265	
d) Mean date of measurement	16-Aug-22	
e.1) Mean value and spread of temperature (degrees Celsius)	22.2	1.0
e.2) Mean value and spread of humidity (%)	35.5	3.4

Table 19. RD-22 Serial # 206816, Active Power at 240 V, 5 A, 53 Hz, PF=0.500 Lag (θ=-60°)

a) Mean value of the calibration error of the reference standard (µW/VA)	12.2	
b) Expanded uncertainty (95.45 % coverage factor) (µW/VA) and degrees of freedom	9.1	160
c.1) Mean value of the voltage measured by the reference standard (V RMS)	239.99959	
c.2) Mean value of the current measured by the reference standard (A RMS)	4.999738	
c.3) Mean value of the power factor measured by the reference standard (dimensionless)	0.500039	
c.4) Mean value of the phase measured by the reference standard (degrees)	-59.99743	
d) Mean date of measurement	16-Aug-22	
e.1) Mean value and spread of temperature (degrees Celsius)	22.2	1.0
e.2) Mean value and spread of humidity (%)	35.5	3.4

Table 20. RD-22 Serial # 206816, Active Power at 240 V, 5 A, 53 Hz, PF=0.000 Lag (θ=-90°)

a) Mean value of the calibration error of the reference standard (μW/VA)	43.2	
b) Expanded uncertainty (95.45 % coverage factor) (μW/VA) and degrees of freedom	8.9	95
c.1) Mean value of the voltage measured by the reference standard (V RMS)	239.99960	
c.2) Mean value of the current measured by the reference standard (A RMS)	4.999736	
c.3) Mean value of the power factor measured by the reference standard (dimensionless)	0.000043	
c.4) Mean value of the phase measured by the reference standard (degrees)	-89.99752	
d) Mean date of measurement	16-Aug-22	
e.1) Mean value and spread of temperature (degrees Celsius)	22.2	1.0
e.2) Mean value and spread of humidity (%)	35.5	3.4

6. **Detailed Uncertainty Budget**

The synthetic power delivered to the MUT is given by:

$$P = \frac{V_V k_1 k_2 k_3 V_I \left(\frac{N_S}{N_P}\right)}{Z_S} \times \cos\left(\theta_{V_V} + \theta_{k_1} + \theta_{k_2} + \theta_{k_3} - \theta_{V_I} - \theta_{\frac{N_S}{N_P}} + \theta_{Z_S}\right) \qquad (1)$$

Where:

$V_V \angle \theta_{V_V}$ =The magnitude and phase of the voltage channel voltage generated by the signal generator that is multiplied by amplifiers A1 and A2, as shown in Fig. 1. The amplitude and phase of this voltage are driven by software to equal those of the PJVS using switch SW1 and sampling DVM #1(#2).

$k_1 \angle \theta_{k_1}$ = The gain and phase response of amplifier A1.

$k_2 \angle \theta_{k_2}$ = The gain and phase response of amplifier A2.

$k_3 \angle \theta_{k_3}$ = The gain and phase response of amplifier A3.

$V_I \angle \theta_{V_I}$ =The magnitude and phase of the voltage present at the Z_S shunt output. The amplitude and phase of this voltage are driven by software to equal those of the PJVS using switch SW1 and sampling DVM #1(#2).

$\frac{N_S}{N_P} \angle \theta_{\frac{N_S}{N_P}}$ = The gain and phase response of transformer T1.

$Z_S \angle \theta_{Z_S}$ = The magnitude and phase response of the shunt resistor Z_S.

From (1), we can express the combined uncertainty of the measured active power (in μW/VA) as [9]:

$$u^2_{P\frac{\mu W}{VA}} = \left\{ \begin{array}{l} \left[u^2_{V_V \frac{\mu V}{V}} + u^2_{k_1 \frac{\mu V}{V}} + u^2_{k_2 \frac{\mu V}{V}} + u^2_{k_3 \frac{\mu V}{V}} + u^2_{V_I \frac{\mu A}{A}} + u^2_{\frac{N_S}{N_P} \frac{\mu T}{T}} + u^2_{Z_S \frac{\mu \Omega}{\Omega}} \right] .. \\ \times \left[\cos\left(\theta_{V_V} + \theta_{k_1} + \theta_{k_2} + \theta_{k_3} - \theta_{V_I} - \theta_{\frac{N_S}{N_P}} + \theta_{Z_S} \right) \right]^2 .... \\ + \left[u^2_{\theta_{V_V} \mu rad} + u^2_{\theta_{k_1} \mu rad} + u^2_{\theta_{k_2} \mu rad} + u^2_{\theta_{k_3} \mu rad} + u^2_{\theta_{V_I} \mu rad} + u^2_{\theta_{\frac{N_S}{N_P}} \mu rad} + u^2_{\theta_{Z_S} \mu rad} \right] ... \\ \times \left[\sin\left(\theta_{V_V} + \theta_{k_1} + \theta_{k_2} + \theta_{k_3} - \theta_{V_I} - \theta_{\frac{N_S}{N_P}} + \theta_{Z_S} \right) \right]^2 \end{array} \right\} \quad (2)$$

In (2), we have the uncertainty of the constituent components of the measurand expressed in a parts in 10^6 format, such as $\frac{\mu V}{V}, \frac{\mu A}{A}, \frac{\mu \Omega}{\Omega}$, or μrad.

The detailed uncertainty budgets for active power for each travelling standard and test point are given in Table 21 to Table 40.

Table 21. NIST Uncertainty Components for RD-22 SN 203409, Active Power at 120 V, 5A, 53 Hz, PF=1.000 Lead

Main uncertainty components y_i	Standard uncertainty $u(y_i)$	Type method A or B of evaluation/probability distribution function	Sensitivity coefficient c_i	Uncertainty contribution $u(R_i)$	Degrees of freedom n_i
1) Standard deviation of the calibration error of the travelling standard	0.6	Type A / pdf: Normal	1	0.6	12
2) uncertainty components of the reference standard of the participant					
2.1) Magnitude of the voltage channel signal, $u(V_V)$, (μV/V)	0.1	Type A / pdf: Normal	cos(θ)=1.000	0.1	31
	1.2	Type B / pdf: Normal	cos(θ)=1.000	1.2	31
2.2) Phase of the voltage channel signal, θ(V_V), (μRad)	0.1	Type A / pdf: Normal	sin(θ)=0.000	0.0	31
	1.2	Type B / pdf: Normal	sin(θ)=0.000	0.0	31
2.3) Magnitude of the current channel signal, $u(V_I)$, (μV/V)	0.2	Type A / pdf: Normal	cos(θ)=1.000	0.2	31
	1.2	Type B / pdf: Normal	cos(θ)=1.000	1.2	31
2.4) Phase of the current channel signal, θ(V_I), (μRad)	0.2	Type A / pdf: Normal	sin(θ)=0.000	0.0	31
	1.2	Type B / pdf: Normal	sin(θ)=0.000	0.0	31
2.5) Magnitude of the voltage amplifier first stage, k_1, (μV/V)	0.3	Type A / pdf: Normal	cos(θ)=1.000	0.3	7
	1.2	Type B / pdf: Normal	cos(θ)=1.000	1.2	7
2.6) Phase of the voltage amplifier first stage, θ(k_1), (μRad)	0.3	Type A / pdf: Normal	sin(θ)=0.000	0.0	7
	1.3	Type B / pdf: Normal	sin(θ)=0.000	0.0	7
2.7) Magnitude of the voltage amplifier second stage, k_2, (μV/V)	0.3	Type A / pdf: Normal	cos(θ)=1.000	0.3	7
	1.2	Type B / pdf: Normal	cos(θ)=1.000	1.2	7
2.8) Phase of the voltage amplifier second stage, θ(k_2), (μRad)	0.3	Type A / pdf: Normal	sin(θ)=0.000	0.0	7
	1.3	Type B / pdf: Normal	sin(θ)=0.000	0.0	7
2.9) Magnitude of the shunt resistance, Z_S, (μΩ/Ω)	0.3	Type A / pdf: Normal	cos(θ)=1.000	0.3	99
	1.3	Type B / pdf: Normal	cos(θ)=1.000	1.3	99
2.10) Phase of the shunt resistance, θ(Z_S), (μRad)	0.3	Type A / pdf: Normal	sin(θ)=0.000	0.0	31
	1.3	Type B / pdf: Normal	sin(θ)=0.000	0.0	31
2.11) Ratio error of T_1 (parts in 10^6)	0.2	Type A / pdf: Normal	cos(θ)=1.000	0.2	3
	1.0	Type B / pdf: Normal	cos(θ)=1.000	1.0	3
2.12) Phase error of T_1 (μRad)	0.2	Type A / pdf: Normal	sin(θ)=0.000	0.0	3
	1.0	Type B / pdf: Normal	sin(θ)=0.000	0.0	3
3) Ambient conditions					
3.1) temperature	< 0.5	Type A / pdf: Normal	1	0.5	12
3.2) humidity	< 0.3			0.3	12
Root square sum of Type A standard uncertainties and effective degrees of freedom				1.0	56.7
Root square sum of Type B standard uncertainties and effective degrees of freedom				2.9	65.6
Combined standard uncertainty and effective degrees of freedom				3.1	81.7
Expanded uncertainty (95.45 % coverage factor) (μW/VA) and t-factor from the t-distribution				6.3	2.05

Table 22. NIST Uncertainty Components for RD-22 SN 203409, Active Power at 120 V, 5A, 53 Hz, PF=0.500 Lead

Main uncertainty components y_i	Standard uncertainty $u(y_i)$	Type method A or B of evaluation/probability distribution function	Sensitivity coefficient c_i	Uncertainty contribution $u(R_i)$	Degrees of freedom n_i
1) Standard deviation of the calibration error of the travelling standard	0.6	Type A / pdf: Normal	1	0.6	12
2) uncertainty components of the reference standard of the participant					
2.1) Magnitude of the voltage channel signal, $u(V_V)$, (μV/V)	0.1	Type A / pdf: Normal	cos(θ)=0.500	0.1	31
	1.2	Type B / pdf: Normal	cos(θ)=0.500	0.6	31
2.2) Phase of the voltage channel signal, θ(V_V), (μRad)	0.1	Type A / pdf: Normal	sin(θ)=0.866	0.1	31
	1.2	Type B / pdf: Normal	sin(θ)=0.866	1.0	31
2.3) Magnitude of the current channel signal, $u(V_I)$, (μV/V)	0.2	Type A / pdf: Normal	cos(θ)=0.500	0.1	31
	1.2	Type B / pdf: Normal	cos(θ)=0.500	0.6	31
2.4) Phase of the current channel signal, θ(V_I), (μRad)	0.2	Type A / pdf: Normal	sin(θ)=0.866	0.2	31
	1.2	Type B / pdf: Normal	sin(θ)=0.866	1.0	31
2.5) Magnitude of the voltage amplifier first stage, k_1, (μV/V)	0.3	Type A / pdf: Normal	cos(θ)=0.500	0.2	7
	1.2	Type B / pdf: Normal	cos(θ)=0.500	0.6	7
2.6) Phase of the voltage amplifier first stage, θ(k_1), (μRad)	0.3	Type A / pdf: Normal	sin(θ)=0.866	0.3	7
	1.3	Type B / pdf: Normal	sin(θ)=0.866	1.1	7
2.7) Magnitude of the voltage amplifier second stage, k_2, (μV/V)	0.3	Type A / pdf: Normal	cos(θ)=0.500	0.2	7
	1.2	Type B / pdf: Normal	cos(θ)=0.500	0.6	7
2.8) Phase of the voltage amplifier second stage, θ(k_2), (μRad)	0.3	Type A / pdf: Normal	sin(θ)=0.866	0.3	7
	1.3	Type B / pdf: Normal	sin(θ)=0.866	1.1	7
2.9) Magnitude of the shunt resistance, Z_S, (μΩ/Ω)	0.3	Type A / pdf: Normal	cos(θ)=0.500	0.2	99
	1.3	Type B / pdf: Normal	cos(θ)=0.500	0.7	99
2.10) Phase of the shunt resistance, θ(Z_S), (μRad)	0.3	Type A / pdf: Normal	sin(θ)=0.866	0.3	31
	1.3	Type B / pdf: Normal	sin(θ)=0.866	1.1	31
2.11) Ratio error of T_1 (parts in 10^6)	0.2	Type A / pdf: Normal	cos(θ)=0.500	0.1	3
	1.0	Type B / pdf: Normal	cos(θ)=0.500	0.5	3
2.12) Phase error of T_1 (μRad)	0.2	Type A / pdf: Normal	sin(θ)=0.866	0.2	3
	1.0	Type B / pdf: Normal	sin(θ)=0.866	0.9	3
3) Ambient conditions					
3.1) temperature	< 0.5	Type A / pdf: Normal	1	0.5	12
3.2) humidity	< 0.3			0.3	12
Root square sum of Type A standard uncertainties and effective degrees of freedom				1.0	61.7
Root square sum of Type B standard uncertainties and effective degrees of freedom				3.0	92.5
Combined standard uncertainty and effective degrees of freedom				3.1	113.3
Expanded uncertainty (95.45 % coverage factor) (μW/VA) and t-factor from the t-distribution				6.4	2.03

Table 23. NIST Uncertainty Components for RD-22 SN 203409, Active Power at 120 V, 5A, 53 Hz, PF=0.000 Lead

Main uncertainty components y_i	Standard uncertainty $u(y_i)$	Type method A or B of evaluation/probability distribution function	Sensitivity coefficient c_i	Uncertainty contribution $u(R_i)$	Degrees of freedom n_i
1) Standard deviation of the calibration error of the travelling standard	0.7	Type A / pdf: Normal	1	0.7	12
2) uncertainty components of the reference standard of the participant					
2.1) Magnitude of the voltage channel signal, $u(V_V)$, (µV/V)	0.1	Type A / pdf: Normal	cos(θ)=0.000	0.0	31
	1.2	Type B / pdf: Normal	cos(θ)=0.000	0.0	31
2.2) Phase of the voltage channel signal, θ(V_V), (µRad)	0.1	Type A / pdf: Normal	sin(θ)=1.000	0.1	31
	1.2	Type B / pdf: Normal	sin(θ)=1.000	1.2	31
2.3) Magnitude of the current channel signal, $u(V_I)$, (µV/V)	0.2	Type A / pdf: Normal	cos(θ)=0.000	0.0	31
	1.2	Type B / pdf: Normal	cos(θ)=0.000	0.0	31
2.4) Phase of the current channel signal, θ(V_I), (µRad)	0.2	Type A / pdf: Normal	sin(θ)=1.000	0.2	31
	1.2	Type B / pdf: Normal	sin(θ)=1.000	1.2	31
2.5) Magnitude of the voltage amplifier first stage, k_1, (µV/V)	0.3	Type A / pdf: Normal	cos(θ)=0.000	0.0	7
	1.2	Type B / pdf: Normal	cos(θ)=0.000	0.0	7
2.6) Phase of the voltage amplifier first stage, θ(k_1), (µRad)	0.3	Type A / pdf: Normal	sin(θ)=1.000	0.3	7
	1.3	Type B / pdf: Normal	sin(θ)=1.000	1.3	7
2.7) Magnitude of the voltage amplifier second stage, k_2, (µV/V)	0.3	Type A / pdf: Normal	cos(θ)=0.000	0.0	7
	1.2	Type B / pdf: Normal	cos(θ)=0.000	0.0	7
2.8) Phase of the voltage amplifier second stage, θ(k_2), (µRad)	0.3	Type A / pdf: Normal	sin(θ)=1.000	0.3	7
	1.3	Type B / pdf: Normal	sin(θ)=1.000	1.3	7
2.9) Magnitude of the shunt resistance, Z_S, (µΩ/Ω)	0.3	Type A / pdf: Normal	cos(θ)=0.000	0.0	99
	1.3	Type B / pdf: Normal	cos(θ)=0.000	0.0	99
2.10) Phase of the shunt resistance, θ(Z_S), (µRad)	0.3	Type A / pdf: Normal	sin(θ)=1.000	0.3	31
	1.3	Type B / pdf: Normal	sin(θ)=1.000	1.3	31
2.11) Ratio error of T_1 (parts in 10^6)	0.2	Type A / pdf: Normal	cos(θ)=0.000	0.0	3
	1.0	Type B / pdf: Normal	cos(θ)=0.000	0.0	3
2.12) Phase error of T_1 (µRad)	0.2	Type A / pdf: Normal	sin(θ)=1.000	0.2	3
	1.0	Type B / pdf: Normal	sin(θ)=1.000	1.0	3
3) Ambient conditions					
3.1) temperature	< 0.5	Type A / pdf: Normal	1	0.5	12
3.2) humidity	< 0.3			0.3	12
Root square sum of Type A standard uncertainties and effective degrees of freedom				1.1	52.0
Root square sum of Type B standard uncertainties and effective degrees of freedom				3.0	58.2
Combined standard uncertainty and effective degrees of freedom				3.2	72.6
Expanded uncertainty (95.45 % coverage factor) (µW/VA) and t-factor from the t-distribution				6.4	2.03

Table 24. NIST Uncertainty Components for RD-22 SN 203409, Active Power at 120 V, 5A, 53 Hz, PF=0.500 Lag

Main uncertainty components y_i	Standard uncertainty $u(y_i)$	Type method A or B of evaluation/probability distribution function	Sensitivity coefficient c_i	Uncertainty contribution $u(R_i)$	Degrees of freedom n_i
1) Standard deviation of the calibration error of the travelling standard	0.6	Type A / pdf: Normal	1	0.6	13
2) uncertainty components of the reference standard of the participant					
2.1) Magnitude of the voltage channel signal, $u(V_V)$, (µV/V)	0.1	Type A / pdf: Normal	cos(θ)=0.500	0.1	31
	1.2	Type B / pdf: Normal	cos(θ)=0.500	0.6	31
2.2) Phase of the voltage channel signal, θ(V_V), (µRad)	0.1	Type A / pdf: Normal	sin(θ)=-0.866	0.1	31
	1.2	Type B / pdf: Normal	sin(θ)=-0.866	1.0	31
2.3) Magnitude of the current channel signal, $u(V_I)$, (µV/V)	0.2	Type A / pdf: Normal	cos(θ)=0.500	0.1	31
	1.2	Type B / pdf: Normal	cos(θ)=0.500	0.6	31
2.4) Phase of the current channel signal, θ(V_I), (µRad)	0.2	Type A / pdf: Normal	sin(θ)=-0.866	0.2	31
	1.2	Type B / pdf: Normal	sin(θ)=-0.866	1.0	31
2.5) Magnitude of the voltage amplifier first stage, k_1, (µV/V)	0.3	Type A / pdf: Normal	cos(θ)=0.500	0.2	7
	1.2	Type B / pdf: Normal	cos(θ)=0.500	0.6	7
2.6) Phase of the voltage amplifier first stage, θ(k_1), (µRad)	0.3	Type A / pdf: Normal	sin(θ)=-0.866	0.3	7
	1.3	Type B / pdf: Normal	sin(θ)=-0.866	1.1	7
2.7) Magnitude of the voltage amplifier second stage, k_2, (µV/V)	0.3	Type A / pdf: Normal	cos(θ)=0.500	0.2	7
	1.2	Type B / pdf: Normal	cos(θ)=0.500	0.6	7
2.8) Phase of the voltage amplifier second stage, θ(k_2), (µRad)	0.3	Type A / pdf: Normal	sin(θ)=-0.866	0.3	7
	1.3	Type B / pdf: Normal	sin(θ)=-0.866	1.1	7
2.9) Magnitude of the shunt resistance, Z_S, (µΩ/Ω)	0.3	Type A / pdf: Normal	cos(θ)=0.500	0.2	99
	1.3	Type B / pdf: Normal	cos(θ)=0.500	0.7	99
2.10) Phase of the shunt resistance, θ(Z_S), (µRad)	0.3	Type A / pdf: Normal	sin(θ)=-0.866	0.3	31
	1.3	Type B / pdf: Normal	sin(θ)=-0.866	1.1	31
2.11) Ratio error of T_1 (parts in 10^6)	0.2	Type A / pdf: Normal	cos(θ)=0.500	0.1	3
	1.0	Type B / pdf: Normal	cos(θ)=0.500	0.5	3
2.12) Phase error of T_1 (µRad)	0.2	Type A / pdf: Normal	sin(θ)=-0.866	0.2	3
	1.0	Type B / pdf: Normal	sin(θ)=-0.866	0.9	3
3) Ambient conditions					
3.1) temperature	< 0.5	Type A / pdf: Normal	1	0.5	13
3.2) humidity	< 0.3			0.3	13
Root square sum of Type A standard uncertainties and effective degrees of freedom				1.0	64.3
Root square sum of Type B standard uncertainties and effective degrees of freedom				3.0	92.5
Combined standard uncertainty and effective degrees of freedom				3.1	113.8
Expanded uncertainty (95.45 % coverage factor) (µW/VA) and t-factor from the t-distribution				6.4	2.03

Table 25. NIST Uncertainty Components for RD-22 SN 203409, Active Power at 120 V, 5A, 53 Hz, PF=0.000 Lag

Main uncertainty components y_i	Standard uncertainty $u(y_i)$	Type method A or B of evaluation/probability distribution function	Sensitivity coefficient c_i	Uncertainty contribution $u(R_i)$	Degrees of freedom n_i
1) Standard deviation of the calibration error of the travelling standard	0.6	Type A / pdf: Normal	1	0.6	12
2) uncertainty components of the reference standard of the participant					
2.1) Magnitude of the voltage channel signal, $u(V_V)$, (μV/V)	0.1 1.2	Type A / pdf: Normal Type B / pdf: Normal	cos(θ)=0.000 cos(θ)=0.000	0.0 0.0	31 31
2.2) Phase of the voltage channel signal, θ(V_V), (μRad)	0.1 1.2	Type A / pdf: Normal Type B / pdf: Normal	sin(θ)=-1.000 sin(θ)=-1.000	0.1 1.2	31 31
2.3) Magnitude of the current channel signal, $u(V_I)$, (μV/V)	0.2 1.2	Type A / pdf: Normal Type B / pdf: Normal	cos(θ)=0.000 cos(θ)=0.000	0.0 0.0	31 31
2.4) Phase of the current channel signal, θ(V_I), (μRad)	0.2 1.2	Type A / pdf: Normal Type B / pdf: Normal	sin(θ)=-1.000 sin(θ)=-1.000	0.2 1.2	31 31
2.5) Magnitude of the voltage amplifier first stage, k_1, (μV/V)	0.3 1.2	Type A / pdf: Normal Type B / pdf: Normal	cos(θ)=0.000 cos(θ)=0.000	0.0 0.0	7 7
2.6) Phase of the voltage amplifier first stage, θ(k_1), (μRad)	0.3 1.3	Type A / pdf: Normal Type B / pdf: Normal	sin(θ)=-1.000 sin(θ)=-1.000	0.3 1.3	7 7
2.7) Magnitude of the voltage amplifier second stage, k_2, (μV/V)	0.3 1.2	Type A / pdf: Normal Type B / pdf: Normal	cos(θ)=0.000 cos(θ)=0.000	0.0 0.0	7 7
2.8) Phase of the voltage amplifier second stage, θ(k_2), (μRad)	0.3 1.3	Type A / pdf: Normal Type B / pdf: Normal	sin(θ)=-1.000 sin(θ)=-1.000	0.3 1.3	7 7
2.9) Magnitude of the shunt resistance, Z_S, (μΩ/Ω)	0.3 1.3	Type A / pdf: Normal Type B / pdf: Normal	cos(θ)=0.000 cos(θ)=0.000	0.0 0.0	99 99
2.10) Phase of the shunt resistance, θ(Z_S), (μRad)	0.3 1.3	Type A / pdf: Normal Type B / pdf: Normal	sin(θ)=-1.000 sin(θ)=-1.000	0.3 1.3	31 31
2.11) Ratio error of T_1 (parts in 10^6)	0.2 1.0	Type A / pdf: Normal Type B / pdf: Normal	cos(θ)=0.000 cos(θ)=0.000	0.0 0.0	3 3
2.12) Phase error of T_1 (μRad)	0.2 1.0	Type A / pdf: Normal Type B / pdf: Normal	sin(θ)=-1.000 sin(θ)=-1.000	0.2 1.0	3 3
3) Ambient conditions					
3.1) temperature 3.2) humidity	< 0.5 < 0.3	Type A / pdf: Normal	1	0.5 0.3	12 12
Root square sum of Type A standard uncertainties and effective degrees of freedom				1.0	57.9
Root square sum of Type B standard uncertainties and effective degrees of freedom				3.0	58.2
Combined standard uncertainty and effective degrees of freedom				3.2	71.6
Expanded uncertainty (95.45 % coverage factor) (μW/VA) and t-factor from the t-distribution				6.4	2.03

Table 26. NIST Uncertainty Components for RD-22 SN 203409, Active Power at 240 V, 5A, 53 Hz, PF=1.000 Lead

Main uncertainty components y_i	Standard uncertainty $u(y_i)$	Type method A or B of evaluation/probability distribution function	Sensitivity coefficient c_i	Uncertainty contribution $u(R_i)$	Degrees of freedom n_i
1) Standard deviation of the calibration error of the travelling standard	2.3	Type A / pdf: Normal	1	2.3	43
2) uncertainty components of the reference standard of the participant					
2.1) Magnitude of the voltage channel signal, $u(V_V)$, (µV/V)	0.5	Type A / pdf: Normal	cos(θ)=1.000	0.5	31
	1.2	Type B / pdf: Normal	cos(θ)=1.000	1.2	31
2.2) Phase of the voltage channel signal, θ(V_V), (µRad)	0.5	Type A / pdf: Normal	sin(θ)=0.000	0.0	31
	1.2	Type B / pdf: Normal	sin(θ)=0.000	0.0	31
2.3) Magnitude of the current channel signal, $u(V_I)$, (µV/V)	0.2	Type A / pdf: Normal	cos(θ)=1.000	0.2	31
	1.2	Type B / pdf: Normal	cos(θ)=1.000	1.2	31
2.4) Phase of the current channel signal, θ(V_I), (µRad)	0.2	Type A / pdf: Normal	sin(θ)=0.000	0.0	31
	1.2	Type B / pdf: Normal	sin(θ)=0.000	0.0	31
2.5) Magnitude of the voltage amplifier first stage, k_1, (µV/V)	1.4	Type A / pdf: Normal	cos(θ)=1.000	1.4	7
	1.2	Type B / pdf: Normal	cos(θ)=1.000	1.2	7
2.6) Phase of the voltage amplifier first stage, θ(k_1), (µRad)	1.4	Type A / pdf: Normal	sin(θ)=0.000	0.0	7
	1.3	Type B / pdf: Normal	sin(θ)=0.000	0.0	7
2.7) Magnitude of the voltage amplifier second stage, k_2, (µV/V)	1.4	Type A / pdf: Normal	cos(θ)=1.000	1.4	7
	1.2	Type B / pdf: Normal	cos(θ)=1.000	1.2	7
2.8) Phase of the voltage amplifier second stage, θ(k_2), (µRad)	1.4	Type A / pdf: Normal	sin(θ)=0.000	0.0	7
	1.3	Type B / pdf: Normal	sin(θ)=0.000	0.0	7
2.9) Magnitude of the voltage amplifier third stage, k_3, (µV/V)	1.4	Type A / pdf: Normal	cos(θ)=1.000	1.4	7
	1.2	Type B / pdf: Normal	cos(θ)=1.000	1.2	7
2.10) Phase of the voltage amplifier third stage, θ(k_3), (µRad)	1.4	Type A / pdf: Normal	sin(θ)=0.000	0.0	7
	1.6	Type B / pdf: Normal	sin(θ)=0.000	0.0	7
2.11) Magnitude of the shunt resistance, Z_S, (µΩ/Ω)	0.3	Type A / pdf: Normal	cos(θ)=1.000	0.3	99
	1.3	Type B / pdf: Normal	cos(θ)=1.000	1.3	99
2.12) Phase of the shunt resistance, θ(Z_S), (µRad)	0.3	Type A / pdf: Normal	sin(θ)=0.000	0.0	31
	1.3	Type B / pdf: Normal	sin(θ)=0.000	0.0	31
2.13) Ratio error of T_1 (parts in 10^6)	0.2	Type A / pdf: Normal	cos(θ)=1.000	0.2	3
	1.0	Type B / pdf: Normal	cos(θ)=1.000	1.0	3
2.14) Phase error of T_1 (µRad)	0.2	Type A / pdf: Normal	sin(θ)=0.000	0.0	3
	1.0	Type B / pdf: Normal	sin(θ)=0.000	0.0	3
3) Ambient conditions					
3.1) temperature	< 0.5	Type A / pdf: Normal	1	0.5	43
3.2) humidity	< 0.3			0.3	43
Root square sum of Type A standard uncertainties and effective degrees of freedom				3.4	61.7
Root square sum of Type B standard uncertainties and effective degrees of freedom				3.1	70.6
Combined standard uncertainty and effective degrees of freedom				4.7	129.0
Expanded uncertainty (95.45 % coverage factor) (µW/VA) and t-factor from the t-distribution				9.8	2.11

Table 27. NIST Uncertainty Components for RD-22 SN 203409, Active Power at 240 V, 5A, 53 Hz, PF=0.500 Lead

Main uncertainty components y_i	Standard uncertainty $u(y_i)$	Type method A or B of evaluation/probability distribution function	Sensitivity coefficient c_i	Uncertainty contribution $u(R_i)$	Degrees of freedom ν_i
1) Standard deviation of the calibration error of the travelling standard	2.1	Type A / pdf: Normal	1	2.1	43
2) uncertainty components of the reference standard of the participant					
2.1) Magnitude of the voltage channel signal, $u(V_V)$, (μV/V)	0.5	Type A / pdf: Normal	cos(θ)=0.500	0.3	31
	1.2	Type B / pdf: Normal	cos(θ)=0.500	0.6	31
2.2) Phase of the voltage channel signal, $\theta(V_V)$, (μRad)	0.5	Type A / pdf: Normal	sin(θ)=0.866	0.4	31
	1.2	Type B / pdf: Normal	sin(θ)=0.866	1.0	31
2.3) Magnitude of the current channel signal, $u(V_I)$, (μV/V)	0.2	Type A / pdf: Normal	cos(θ)=0.500	0.1	31
	1.2	Type B / pdf: Normal	cos(θ)=0.500	0.6	31
2.4) Phase of the current channel signal, $\theta(V_I)$, (μRad)	0.2	Type A / pdf: Normal	sin(θ)=0.866	0.2	31
	1.2	Type B / pdf: Normal	sin(θ)=0.866	1.0	31
2.5) Magnitude of the voltage amplifier first stage, k_1, (μV/V)	1.4	Type A / pdf: Normal	cos(θ)=0.500	0.7	7
	1.2	Type B / pdf: Normal	cos(θ)=0.500	0.6	7
2.6) Phase of the voltage amplifier first stage, $\theta(k_1)$, (μRad)	1.4	Type A / pdf: Normal	sin(θ)=0.866	1.2	7
	1.3	Type B / pdf: Normal	sin(θ)=0.866	1.1	7
2.7) Magnitude of the voltage amplifier second stage, k_2, (μV/V)	1.4	Type A / pdf: Normal	cos(θ)=0.500	0.7	7
	1.2	Type B / pdf: Normal	cos(θ)=0.500	0.6	7
2.8) Phase of the voltage amplifier second stage, $\theta(k_2)$, (μRad)	1.4	Type A / pdf: Normal	sin(θ)=0.866	1.2	7
	1.3	Type B / pdf: Normal	sin(θ)=0.866	1.1	7
2.9) Magnitude of the voltage amplifier third stage, k_3, (μV/V)	1.4	Type A / pdf: Normal	cos(θ)=1.000	0.7	7
	1.2	Type B / pdf: Normal	cos(θ)=1.000	0.6	7
2.10) Phase of the voltage amplifier third stage, $\theta(k_3)$, (μRad)	1.4	Type A / pdf: Normal	sin(θ)=0.000	1.2	7
	1.6	Type B / pdf: Normal	sin(θ)=0.000	1.4	7
2.11) Magnitude of the shunt resistance, Z_S, (μΩ/Ω)	0.3	Type A / pdf: Normal	cos(θ)=0.500	0.2	99
	1.3	Type B / pdf: Normal	cos(θ)=0.500	0.7	99
2.12) Phase of the shunt resistance, $\theta(Z_S)$, (μRad)	0.3	Type A / pdf: Normal	sin(θ)=0.866	0.3	31
	1.3	Type B / pdf: Normal	sin(θ)=0.866	1.1	31
2.13) Ratio error of T_1 (parts in 10^6)	0.2	Type A / pdf: Normal	cos(θ)=0.500	0.1	3
	1.0	Type B / pdf: Normal	cos(θ)=0.500	0.5	3
2.14) Phase error of T_1 (μRad)	0.2	Type A / pdf: Normal	sin(θ)=0.866	0.2	3
	1.0	Type B / pdf: Normal	sin(θ)=0.866	0.9	3
3) Ambient conditions					
3.1) temperature	< 0.5	Type A / pdf: Normal	1	0.5	43
3.2) humidity	< 0.3			0.3	43
Root square sum of Type A standard uncertainties and effective degrees of freedom				3.3	82.5
Root square sum of Type B standard uncertainties and effective degrees of freedom				3.3	88.9
Combined standard uncertainty and effective degrees of freedom				4.7	171.2
Expanded uncertainty (95.45 % coverage factor) (μW/VA) and t-factor from the t-distribution				9.5	2.03

Table 28. NIST Uncertainty Components for RD-22 SN 203409, Active Power at 240 V, 5A, 53 Hz, PF=0.000 Lead

Main uncertainty components y_i	Standard uncertainty $u(y_i)$	Type method A or B of evaluation/probability distribution function	Sensitivity coefficient c_i	Uncertainty contribution $u(R_i)$	Degrees of freedom n_i
1) Standard deviation of the calibration error of the travelling standard	1.2	Type A / pdf: Normal	1	1.2	43
2) uncertainty components of the reference standard of the participant					
2.1) Magnitude of the voltage channel signal, $u(V_V)$, (μV/V)	0.5	Type A / pdf: Normal	cos(θ)=0.000	0.0	31
	1.2	Type B / pdf: Normal	cos(θ)=0.000	0.0	31
2.2) Phase of the voltage channel signal, $\theta(V_V)$, (μRad)	0.5	Type A / pdf: Normal	sin(θ)=1.000	0.5	31
	1.2	Type B / pdf: Normal	sin(θ)=1.000	1.2	31
2.3) Magnitude of the current channel signal, $u(V_I)$, (μV/V)	0.2	Type A / pdf: Normal	cos(θ)=0.000	0.0	31
	1.2	Type B / pdf: Normal	cos(θ)=0.000	0.0	31
2.4) Phase of the current channel signal, $\theta(V_I)$, (μRad)	0.2	Type A / pdf: Normal	sin(θ)=1.000	0.2	31
	1.2	Type B / pdf: Normal	sin(θ)=1.000	1.2	31
2.5) Magnitude of the voltage amplifier first stage, k_1, (μV/V)	1.4	Type A / pdf: Normal	cos(θ)=0.000	0.0	7
	1.2	Type B / pdf: Normal	cos(θ)=0.000	0.0	7
2.6) Phase of the voltage amplifier first stage, $\theta(k_1)$, (μRad)	1.4	Type A / pdf: Normal	sin(θ)=1.000	1.4	7
	1.3	Type B / pdf: Normal	sin(θ)=1.000	1.3	7
2.7) Magnitude of the voltage amplifier second stage, k_2, (μV/V)	1.4	Type A / pdf: Normal	cos(θ)=0.000	0.0	7
	1.2	Type B / pdf: Normal	cos(θ)=0.000	0.0	7
2.8) Phase of the voltage amplifier second stage, $\theta(k_2)$, (μRad)	1.4	Type A / pdf: Normal	sin(θ)=1.000	1.4	7
	1.3	Type B / pdf: Normal	sin(θ)=1.000	1.3	7
2.9) Magnitude of the voltage amplifier third stage, k_3, (μV/V)	1.4	Type A / pdf: Normal	cos(θ)=1.000	0.0	7
	1.2	Type B / pdf: Normal	cos(θ)=1.000	0.0	7
2.10) Phase of the voltage amplifier third stage, $\theta(k_3)$, (μRad)	1.4	Type A / pdf: Normal	sin(θ)=0.000	1.4	7
	1.6	Type B / pdf: Normal	sin(θ)=0.000	1.6	7
2.11) Magnitude of the shunt resistance, Z_S, (μΩ/Ω)	0.3	Type A / pdf: Normal	cos(θ)=0.000	0.0	99
	1.3	Type B / pdf: Normal	cos(θ)=0.000	0.0	99
2.12) Phase of the shunt resistance, $\theta(Z_S)$, (μRad)	0.3	Type A / pdf: Normal	sin(θ)=1.000	0.3	31
	1.3	Type B / pdf: Normal	sin(θ)=1.000	1.3	31
2.13) Ratio error of T_1 (parts in 10^6)	0.2	Type A / pdf: Normal	cos(θ)=0.000	0.0	3
	1.0	Type B / pdf: Normal	cos(θ)=0.000	0.0	3
2.14) Phase error of T_1 (μRad)	0.2	Type A / pdf: Normal	sin(θ)=1.000	0.2	3
	1.0	Type B / pdf: Normal	sin(θ)=1.000	1.0	3
3) Ambient conditions					
3.1) temperature	< 0.5	Type A / pdf: Normal	1	0.5	43
3.2) humidity	< 0.3			0.3	43
Root square sum of Type A standard uncertainties and effective degrees of freedom				2.8	38.6
Root square sum of Type B standard uncertainties and effective degrees of freedom				3.4	57.3
Combined standard uncertainty and effective degrees of freedom				4.4	95.9
Expanded uncertainty (95.45 % coverage factor) (μW/VA) and t-factor from the t-distribution				9.0	2.03

Table 29. NIST Uncertainty Components for RD-22 SN 203409, Active Power at 240 V, 5A, 53 Hz, PF=0.500 Lag

Main uncertainty components y_i	Standard uncertainty $u(y_i)$	Type method A or B of evaluation/probability distribution function	Sensitivity coefficient c_i	Uncertainty contribution $u(R_i)$	Degrees of freedom n_i
1) Standard deviation of the calibration error of the travelling standard	1.6	Type A / pdf: Normal	1	1.6	43
2) uncertainty components of the reference standard of the participant					
2.1) Magnitude of the voltage channel signal, $u(V_V)$, (µV/V)	0.5	Type A / pdf: Normal	cos(θ)=0.500	0.3	31
	1.2	Type B / pdf: Normal	cos(θ)=0.500	0.6	31
2.2) Phase of the voltage channel signal, θ(V_V), (µRad)	0.5	Type A / pdf: Normal	sin(θ)=-0.866	0.4	31
	1.2	Type B / pdf: Normal	sin(θ)=-0.866	1.0	31
2.3) Magnitude of the current channel signal, $u(V_I)$, (µV/V)	0.2	Type A / pdf: Normal	cos(θ)=0.500	0.1	31
	1.2	Type B / pdf: Normal	cos(θ)=0.500	0.6	31
2.4) Phase of the current channel signal, θ(V_I), (µRad)	0.2	Type A / pdf: Normal	sin(θ)=-0.866	0.2	31
	1.2	Type B / pdf: Normal	sin(θ)=-0.866	1.0	31
2.5) Magnitude of the voltage amplifier first stage, k_1, (µV/V)	1.4	Type A / pdf: Normal	cos(θ)=0.500	0.7	7
	1.2	Type B / pdf: Normal	cos(θ)=0.500	0.6	7
2.6) Phase of the voltage amplifier first stage, θ(k_1), (µRad)	1.4	Type A / pdf: Normal	sin(θ)=-0.866	1.2	7
	1.3	Type B / pdf: Normal	sin(θ)=-0.866	1.1	7
2.7) Magnitude of the voltage amplifier second stage, k_2, (µV/V)	1.4	Type A / pdf: Normal	cos(θ)=0.500	0.7	7
	1.2	Type B / pdf: Normal	cos(θ)=0.500	0.6	7
2.8) Phase of the voltage amplifier second stage, θ(k_2), (µRad)	1.4	Type A / pdf: Normal	sin(θ)=-0.866	1.2	7
	1.3	Type B / pdf: Normal	sin(θ)=-0.866	1.1	7
2.9) Magnitude of the voltage amplifier third stage, k_3, (µV/V)	1.4	Type A / pdf: Normal	cos(θ)=1.000	0.7	7
	1.2	Type B / pdf: Normal	cos(θ)=1.000	0.6	7
2.10) Phase of the voltage amplifier third stage, θ(k_3), (µRad)	1.4	Type A / pdf: Normal	sin(θ)=0.000	1.2	7
	1.6	Type B / pdf: Normal	sin(θ)=0.000	1.4	7
2.11) Magnitude of the shunt resistance, Z_S, (µΩ/Ω)	0.3	Type A / pdf: Normal	cos(θ)=0.500	0.2	99
	1.3	Type B / pdf: Normal	cos(θ)=0.500	0.7	99
2.12) Phase of the shunt resistance, θ(Z_S), (µRad)	0.3	Type A / pdf: Normal	sin(θ)=-0.866	0.3	31
	1.3	Type B / pdf: Normal	sin(θ)=-0.866	1.1	31
2.13) Ratio error of T_1 (parts in 10^6)	0.2	Type A / pdf: Normal	cos(θ)=0.500	0.1	3
	1.0	Type B / pdf: Normal	cos(θ)=0.500	0.5	3
2.14) Phase error of T_1 (µRad)	0.2	Type A / pdf: Normal	sin(θ)=-0.866	0.2	3
	1.0	Type B / pdf: Normal	sin(θ)=-0.866	0.9	3
3) Ambient conditions					
3.1) temperature	< 0.5	Type A / pdf: Normal	1	0.5	43
3.2) humidity	< 0.3			0.3	43
Root square sum of Type A standard uncertainties and effective degrees of freedom				3.0	71.2
Root square sum of Type B standard uncertainties and effective degrees of freedom				3.3	88.9
Combined standard uncertainty and effective degrees of freedom				4.5	160.1
Expanded uncertainty (95.45 % coverage factor) (µW/VA) and t-factor from the t-distribution				9.1	2.03

Table 30. NIST Uncertainty Components for RD-22 SN 203409, Active Power at 240 V, 5A, 53 Hz, PF=0.000 Lag

Main uncertainty components y_i	Standard uncertainty $u(y_i)$	Type method A or B of evaluation/probability distribution function	Sensitivity coefficient c_i	Uncertainty contribution $u(R_i)$	Degrees of freedom n_i
1) Standard deviation of the calibration error of the travelling standard	1.2	Type A / pdf: Normal	1	1.2	43
2) uncertainty components of the reference standard of the participant					
2.1) Magnitude of the voltage channel signal, $u(V_V)$, (µV/V)	0.5	Type A / pdf: Normal	cos(θ)=0.000	0.0	31
	1.2	Type B / pdf: Normal	cos(θ)=0.000	0.0	31
2.2) Phase of the voltage channel signal, θ(V_V), (µRad)	0.5	Type A / pdf: Normal	sin(θ)=-1.000	0.5	31
	1.2	Type B / pdf: Normal	sin(θ)=-1.000	1.2	31
2.3) Magnitude of the current channel signal, $u(V_I)$, (µV/V)	0.2	Type A / pdf: Normal	cos(θ)=0.000	0.0	31
	1.2	Type B / pdf: Normal	cos(θ)=0.000	0.0	31
2.4) Phase of the current channel signal, θ(V_I), (µRad)	0.2	Type A / pdf: Normal	sin(θ)=-1.000	0.2	31
	1.2	Type B / pdf: Normal	sin(θ)=-1.000	1.2	31
2.5) Magnitude of the voltage amplifier first stage, k_1, (µV/V)	1.4	Type A / pdf: Normal	cos(θ)=0.000	0.0	7
	1.2	Type B / pdf: Normal	cos(θ)=0.000	0.0	7
2.6) Phase of the voltage amplifier first stage, θ(k_1), (µRad)	1.4	Type A / pdf: Normal	sin(θ)=-1.000	1.4	7
	1.3	Type B / pdf: Normal	sin(θ)=-1.000	1.3	7
2.7) Magnitude of the voltage amplifier second stage, k_2, (µV/V)	1.4	Type A / pdf: Normal	cos(θ)=0.000	0.0	7
	1.2	Type B / pdf: Normal	cos(θ)=0.000	0.0	7
2.8) Phase of the voltage amplifier second stage, θ(k_2), (µRad)	1.4	Type A / pdf: Normal	sin(θ)=-1.000	1.4	7
	1.3	Type B / pdf: Normal	sin(θ)=-1.000	1.3	7
2.9) Magnitude of the voltage amplifier third stage, k_3, (µV/V)	1.4	Type A / pdf: Normal	cos(θ)=1.000	0.0	7
	1.2	Type B / pdf: Normal	cos(θ)=1.000	0.0	7
2.10) Phase of the voltage amplifier third stage, θ(k_3), (µRad)	1.4	Type A / pdf: Normal	sin(θ)=0.000	1.4	7
	1.6	Type B / pdf: Normal	sin(θ)=0.000	1.6	7
2.11) Magnitude of the shunt resistance, Z_S, (µΩ/Ω)	0.3	Type A / pdf: Normal	cos(θ)=0.000	0.0	99
	1.3	Type B / pdf: Normal	cos(θ)=0.000	0.0	99
2.12) Phase of the shunt resistance, θ(Z_S), (µRad)	0.3	Type A / pdf: Normal	sin(θ)=-1.000	0.3	31
	1.3	Type B / pdf: Normal	sin(θ)=-1.000	1.3	31
2.13) Ratio error of T_1 (parts in 10^6)	0.2	Type A / pdf: Normal	cos(θ)=0.000	0.0	3
	1.0	Type B / pdf: Normal	cos(θ)=0.000	0.0	3
2.14) Phase error of T_1 (µRad)	0.2	Type A / pdf: Normal	sin(θ)=-1.000	0.2	3
	1.0	Type B / pdf: Normal	sin(θ)=-1.000	1.0	3
3) Ambient conditions					
3.1) temperature	< 0.5	Type A / pdf: Normal	1	0.5	43
3.2) humidity	< 0.3			0.3	43
Root square sum of Type A standard uncertainties and effective degrees of freedom				2.9	38.8
Root square sum of Type B standard uncertainties and effective degrees of freedom				3.4	57.3
Combined standard uncertainty and effective degrees of freedom				4.4	96.1
Expanded uncertainty (95.45 % coverage factor) (µW/VA) and t-factor from the t-distribution				9.0	2.03

Table 31. NIST Uncertainty Components for RD-22 SN 206816, Active Power at 120 V, 5A, 53 Hz, PF=1.000 Lead

Main uncertainty components y_i	Standard uncertainty $u(y_i)$	Type method A or B of evaluation/probability distribution function	Sensitivity coefficient c_i	Uncertainty contribution $u(R_i)$	Degrees of freedom n_i
1) Standard deviation of the calibration error of the travelling standard	0.6	Type A / pdf: Normal	1	0.6	12
2) uncertainty components of the reference standard of the participant					
2.1) Magnitude of the voltage channel signal, $u(V_V)$, (µV/V)	0.1 1.2	Type A / pdf: Normal Type B / pdf: Normal	cos(θ)=1.000 cos(θ)=1.000	0.1 1.2	31 31
2.2) Phase of the voltage channel signal, θ(V_V), (µRad)	0.1 1.2	Type A / pdf: Normal Type B / pdf: Normal	sin(θ)=0.000 sin(θ)=0.000	0.0 0.0	31 31
2.3) Magnitude of the current channel signal, $u(V_I)$, (µV/V)	0.2 1.2	Type A / pdf: Normal Type B / pdf: Normal	cos(θ)=1.000 cos(θ)=1.000	0.2 1.2	31 31
2.4) Phase of the current channel signal, θ(V_I), (µRad)	0.2 1.2	Type A / pdf: Normal Type B / pdf: Normal	sin(θ)=0.000 sin(θ)=0.000	0.0 0.0	31 31
2.5) Magnitude of the voltage amplifier first stage, k_1, (µV/V)	0.3 1.2	Type A / pdf: Normal Type B / pdf: Normal	cos(θ)=1.000 cos(θ)=1.000	0.3 1.2	7 7
2.6) Phase of the voltage amplifier first stage, θ(k_1), (µRad)	0.3 1.3	Type A / pdf: Normal Type B / pdf: Normal	sin(θ)=0.000 sin(θ)=0.000	0.0 0.0	7 7
2.7) Magnitude of the voltage amplifier second stage, k_2, (µV/V)	0.3 1.2	Type A / pdf: Normal Type B / pdf: Normal	cos(θ)=1.000 cos(θ)=1.000	0.3 1.2	7 7
2.8) Phase of the voltage amplifier second stage, θ(k_2), (µRad)	0.3 1.3	Type A / pdf: Normal Type B / pdf: Normal	sin(θ)=0.000 sin(θ)=0.000	0.0 0.0	7 7
2.9) Magnitude of the shunt resistance, Z_S, (µΩ/Ω)	0.3 1.3	Type A / pdf: Normal Type B / pdf: Normal	cos(θ)=1.000 cos(θ)=1.000	0.3 1.3	99 99
2.10) Phase of the shunt resistance, θ(Z_S), (µRad)	0.3 1.3	Type A / pdf: Normal Type B / pdf: Normal	sin(θ)=0.000 sin(θ)=0.000	0.0 0.0	31 31
2.11) Ratio error of T_1 (parts in 10^6)	0.2 1.0	Type A / pdf: Normal Type B / pdf: Normal	cos(θ)=1.000 cos(θ)=1.000	0.2 1.0	3 3
2.12) Phase error of T_1 (µRad)	0.2 1.0	Type A / pdf: Normal Type B / pdf: Normal	sin(θ)=0.000 sin(θ)=0.000	0.0 0.0	3 3
3) Ambient conditions					
3.1) temperature 3.2) humidity	< 0.5 < 0.3	Type A / pdf: Normal	1	0.5 0.3	12 12
Root square sum of Type A standard uncertainties and effective degrees of freedom				1.0	57.8
Root square sum of Type B standard uncertainties and effective degrees of freedom				2.9	65.6
Combined standard uncertainty and effective degrees of freedom				3.1	81.5
Expanded uncertainty (95.45 % coverage factor) (µW/VA) and t-factor from the t-distribution				6.3	2.05

Table 32. NIST Uncertainty Components for RD-22 SN 206816, Active Power at 120 V, 5A, 53 Hz, PF=0.500 Lead

Main uncertainty components y_i	Standard uncertainty $u(y_i)$	Type method A or B of evaluation/probability distribution function	Sensitivity coefficient c_i	Uncertainty contribution $u(R_i)$	Degrees of freedom n_i
1) Standard deviation of the calibration error of the travelling standard	0.6	Type A / pdf: Normal	1	0.6	12
2) uncertainty components of the reference standard of the participant					
2.1) Magnitude of the voltage channel signal, $u(V_V)$, (μV/V)	0.1 1.2	Type A / pdf: Normal Type B / pdf: Normal	cos(θ)=0.500 cos(θ)=0.500	0.1 0.6	31 31
2.2) Phase of the voltage channel signal, $\theta(V_V)$, (μRad)	0.1 1.2	Type A / pdf: Normal Type B / pdf: Normal	sin(θ)=0.866 sin(θ)=0.866	0.1 1.0	31 31
2.3) Magnitude of the current channel signal, $u(V_I)$, (μV/V)	0.2 1.2	Type A / pdf: Normal Type B / pdf: Normal	cos(θ)=0.500 cos(θ)=0.500	0.1 0.6	31 31
2.4) Phase of the current channel signal, $\theta(V_I)$, (μRad)	0.2 1.2	Type A / pdf: Normal Type B / pdf: Normal	sin(θ)=0.866 sin(θ)=0.866	0.2 1.0	31 31
2.5) Magnitude of the voltage amplifier first stage, k_1, (μV/V)	0.3 1.2	Type A / pdf: Normal Type B / pdf: Normal	cos(θ)=0.500 cos(θ)=0.500	0.2 0.6	7 7
2.6) Phase of the voltage amplifier first stage, $\theta(k_1)$, (μRad)	0.3 1.3	Type A / pdf: Normal Type B / pdf: Normal	sin(θ)=0.866 sin(θ)=0.866	0.3 1.1	7 7
2.7) Magnitude of the voltage amplifier second stage, k_2, (μV/V)	0.3 1.2	Type A / pdf: Normal Type B / pdf: Normal	cos(θ)=0.500 cos(θ)=0.500	0.2 0.6	7 7
2.8) Phase of the voltage amplifier second stage, $\theta(k_2)$, (μRad)	0.3 1.3	Type A / pdf: Normal Type B / pdf: Normal	sin(θ)=0.866 sin(θ)=0.866	0.3 1.1	7 7
2.9) Magnitude of the shunt resistance, Z_S, (μΩ/Ω)	0.3 1.3	Type A / pdf: Normal Type B / pdf: Normal	cos(θ)=0.500 cos(θ)=0.500	0.2 0.7	99 99
2.10) Phase of the shunt resistance, $\theta(Z_S)$, (μRad)	0.3 1.3	Type A / pdf: Normal Type B / pdf: Normal	sin(θ)=0.866 sin(θ)=0.866	0.3 1.1	31 31
2.11) Ratio error of T_1 (parts in 10^6)	0.2 1.0	Type A / pdf: Normal Type B / pdf: Normal	cos(θ)=0.500 cos(θ)=0.500	0.1 0.5	3 3
2.12) Phase error of T_1 (μRad)	0.2 1.0	Type A / pdf: Normal Type B / pdf: Normal	sin(θ)=0.866 sin(θ)=0.866	0.2 0.9	3 3
3) Ambient conditions					
3.1) temperature 3.2) humidity	< 0.5 < 0.3	Type A / pdf: Normal	1	0.5 0.3	12 12
Root square sum of Type A standard uncertainties and effective degrees of freedom				1.0	63.8
Root square sum of Type B standard uncertainties and effective degrees of freedom				3.0	92.5
Combined standard uncertainty and effective degrees of freedom				3.1	112.9
Expanded uncertainty (95.45 % coverage factor) (μW/VA) and t-factor from the t-distribution				6.4	2.03

Table 33. NIST Uncertainty Components for RD-22 SN 206816, Active Power at 120 V, 5A, 53 Hz, PF=0.000 Lead

Main uncertainty components y_i	Standard uncertainty $u(y_i)$	Type method A or B of evaluation/probability distribution function	Sensitivity coefficient c_i	Uncertainty contribution $u(R_i)$	Degrees of freedom n_i
1) Standard deviation of the calibration error of the travelling standard	0.6	Type A / pdf: Normal	1	0.6	12
2) uncertainty components of the reference standard of the participant					
2.1) Magnitude of the voltage channel signal, $u(V_V)$, (μV/V)	0.1	Type A / pdf: Normal	cos(θ)=0.000	0.0	31
	1.2	Type B / pdf: Normal	cos(θ)=0.000	0.0	31
2.2) Phase of the voltage channel signal, θ(V_V), (μRad)	0.1	Type A / pdf: Normal	sin(θ)=1.000	0.1	31
	1.2	Type B / pdf: Normal	sin(θ)=1.000	1.2	31
2.3) Magnitude of the current channel signal, $u(V_I)$, (μV/V)	0.2	Type A / pdf: Normal	cos(θ)=0.000	0.0	31
	1.2	Type B / pdf: Normal	cos(θ)=0.000	0.0	31
2.4) Phase of the current channel signal, θ(V_I), (μRad)	0.2	Type A / pdf: Normal	sin(θ)=1.000	0.2	31
	1.2	Type B / pdf: Normal	sin(θ)=1.000	1.2	31
2.5) Magnitude of the voltage amplifier first stage, k_1, (μV/V)	0.3	Type A / pdf: Normal	cos(θ)=0.000	0.0	7
	1.2	Type B / pdf: Normal	cos(θ)=0.000	0.0	7
2.6) Phase of the voltage amplifier first stage, θ(k_1), (μRad)	0.3	Type A / pdf: Normal	sin(θ)=1.000	0.3	7
	1.3	Type B / pdf: Normal	sin(θ)=1.000	1.3	7
2.7) Magnitude of the voltage amplifier second stage, k_2, (μV/V)	0.3	Type A / pdf: Normal	cos(θ)=0.000	0.0	7
	1.2	Type B / pdf: Normal	cos(θ)=0.000	0.0	7
2.8) Phase of the voltage amplifier second stage, θ(k_2), (μRad)	0.3	Type A / pdf: Normal	sin(θ)=1.000	0.3	7
	1.3	Type B / pdf: Normal	sin(θ)=1.000	1.3	7
2.9) Magnitude of the shunt resistance, Z_S, (μΩ/Ω)	0.3	Type A / pdf: Normal	cos(θ)=0.000	0.0	99
	1.3	Type B / pdf: Normal	cos(θ)=0.000	0.0	99
2.10) Phase of the shunt resistance, θ(Z_S), (μRad)	0.3	Type A / pdf: Normal	sin(θ)=1.000	0.3	31
	1.3	Type B / pdf: Normal	sin(θ)=1.000	1.3	31
2.11) Ratio error of T_1 (parts in 10^6)	0.2	Type A / pdf: Normal	cos(θ)=0.000	0.0	3
	1.0	Type B / pdf: Normal	cos(θ)=0.000	0.0	3
2.12) Phase error of T_1 (μRad)	0.2	Type A / pdf: Normal	sin(θ)=1.000	0.2	3
	1.0	Type B / pdf: Normal	sin(θ)=1.000	1.0	3
3) Ambient conditions					
3.1) temperature	< 0.5	Type A / pdf: Normal	1	0.5	12
3.2) humidity	< 0.3			0.3	12
Root square sum of Type A standard uncertainties and effective degrees of freedom				1.0	56.1
Root square sum of Type B standard uncertainties and effective degrees of freedom				3.0	58.2
Combined standard uncertainty and effective degrees of freedom				3.2	71.9
Expanded uncertainty (95.45 % coverage factor) (μW/VA) and t-factor from the t-distribution				6.4	2.03

Table 34. NIST Uncertainty Components for RD-22 SN 206816, Active Power at 120 V, 5A, 53 Hz, PF=0.500 Lag

Main uncertainty components y_i	Standard uncertainty $u(y_i)$	Type method A or B of evaluation/probability distribution function	Sensitivity coefficient c_i	Uncertainty contribution $u(R_i)$	Degrees of freedom n_i
1) Standard deviation of the calibration error of the travelling standard	0.6	Type A / pdf: Normal	1	0.6	13
2) uncertainty components of the reference standard of the participant					
2.1) Magnitude of the voltage channel signal, $u(V_V)$, (µV/V)	0.1	Type A / pdf: Normal	cos(θ)=0.500	0.1	31
	1.2	Type B / pdf: Normal	cos(θ)=0.500	0.6	31
2.2) Phase of the voltage channel signal, θ(V_V), (µRad)	0.1	Type A / pdf: Normal	sin(θ)=-0.866	0.1	31
	1.2	Type B / pdf: Normal	sin(θ)=-0.866	1.0	31
2.3) Magnitude of the current channel signal, $u(V_I)$, (µV/V)	0.2	Type A / pdf: Normal	cos(θ)=0.500	0.1	31
	1.2	Type B / pdf: Normal	cos(θ)=0.500	0.6	31
2.4) Phase of the current channel signal, θ(V_I), (µRad)	0.2	Type A / pdf: Normal	sin(θ)=-0.866	0.2	31
	1.2	Type B / pdf: Normal	sin(θ)=-0.866	1.0	31
2.5) Magnitude of the voltage amplifier first stage, k_1, (µV/V)	0.3	Type A / pdf: Normal	cos(θ)=0.500	0.2	7
	1.2	Type B / pdf: Normal	cos(θ)=0.500	0.6	7
2.6) Phase of the voltage amplifier first stage, θ(k_1), (µRad)	0.3	Type A / pdf: Normal	sin(θ)=-0.866	0.3	7
	1.3	Type B / pdf: Normal	sin(θ)=-0.866	1.1	7
2.7) Magnitude of the voltage amplifier second stage, k_2, (µV/V)	0.3	Type A / pdf: Normal	cos(θ)=0.500	0.2	7
	1.2	Type B / pdf: Normal	cos(θ)=0.500	0.6	7
2.8) Phase of the voltage amplifier second stage, θ(k_2), (µRad)	0.3	Type A / pdf: Normal	sin(θ)=-0.866	0.3	7
	1.3	Type B / pdf: Normal	sin(θ)=-0.866	1.1	7
2.9) Magnitude of the shunt resistance, Z_S, (µΩ/Ω)	0.3	Type A / pdf: Normal	cos(θ)=0.500	0.2	99
	1.3	Type B / pdf: Normal	cos(θ)=0.500	0.7	99
2.10) Phase of the shunt resistance, θ(Z_S), (µRad)	0.3	Type A / pdf: Normal	sin(θ)=-0.866	0.3	31
	1.3	Type B / pdf: Normal	sin(θ)=-0.866	1.1	31
2.11) Ratio error of T_1 (parts in 10^6)	0.2	Type A / pdf: Normal	cos(θ)=0.500	0.1	3
	1.0	Type B / pdf: Normal	cos(θ)=0.500	0.5	3
2.12) Phase error of T_1 (µRad)	0.2	Type A / pdf: Normal	sin(θ)=-0.866	0.2	3
	1.0	Type B / pdf: Normal	sin(θ)=-0.866	0.9	3
3) Ambient conditions					
3.1) temperature	< 0.5	Type A / pdf: Normal	1	0.5	13
3.2) humidity	< 0.3			0.3	13
Root square sum of Type A standard uncertainties and effective degrees of freedom				1.0	64.8
Root square sum of Type B standard uncertainties and effective degrees of freedom				3.0	92.5
Combined standard uncertainty and effective degrees of freedom				3.1	113.7
Expanded uncertainty (95.45 % coverage factor) (µW/VA) and t-factor from the t-distribution				6.4	2.03

Table 35. NIST Uncertainty Components for RD-22 SN 206816, Active Power at 120 V, 5A, 53 Hz, PF=0.000 Lag

Main uncertainty components y_i	Standard uncertainty $u(y_i)$	Type method A or B of evaluation/probability distribution function	Sensitivity coefficient c_i	Uncertainty contribution $u(R_i)$	Degrees of freedom n_i
1) Standard deviation of the calibration error of the travelling standard	0.6	Type A / pdf: Normal	1	0.6	12
2) uncertainty components of the reference standard of the participant					
2.1) Magnitude of the voltage channel signal, $u(V_V)$, (µV/V)	0.1	Type A / pdf: Normal	cos(θ)=0.000	0.0	31
	1.2	Type B / pdf: Normal	cos(θ)=0.000	0.0	31
2.2) Phase of the voltage channel signal, θ(V_V), (µRad)	0.1	Type A / pdf: Normal	sin(θ)=-1.000	0.1	31
	1.2	Type B / pdf: Normal	sin(θ)=-1.000	1.2	31
2.3) Magnitude of the current channel signal, $u(V_I)$, (µV/V)	0.2	Type A / pdf: Normal	cos(θ)=0.000	0.0	31
	1.2	Type B / pdf: Normal	cos(θ)=0.000	0.0	31
2.4) Phase of the current channel signal, θ(V_I), (µRad)	0.2	Type A / pdf: Normal	sin(θ)=-1.000	0.2	31
	1.2	Type B / pdf: Normal	sin(θ)=-1.000	1.2	31
2.5) Magnitude of the voltage amplifier first stage, k_1, (µV/V)	0.3	Type A / pdf: Normal	cos(θ)=0.000	0.0	7
	1.2	Type B / pdf: Normal	cos(θ)=0.000	0.0	7
2.6) Phase of the voltage amplifier first stage, θ(k_1), (µRad)	0.3	Type A / pdf: Normal	sin(θ)=-1.000	0.3	7
	1.3	Type B / pdf: Normal	sin(θ)=-1.000	1.3	7
2.7) Magnitude of the voltage amplifier second stage, k_2, (µV/V)	0.3	Type A / pdf: Normal	cos(θ)=0.000	0.0	7
	1.2	Type B / pdf: Normal	cos(θ)=0.000	0.0	7
2.8) Phase of the voltage amplifier second stage, θ(k_2), (µRad)	0.3	Type A / pdf: Normal	sin(θ)=-1.000	0.3	7
	1.3	Type B / pdf: Normal	sin(θ)=-1.000	1.3	7
2.9) Magnitude of the shunt resistance, Z_S, (µΩ/Ω)	0.3	Type A / pdf: Normal	cos(θ)=0.000	0.0	99
	1.3	Type B / pdf: Normal	cos(θ)=0.000	0.0	99
2.10) Phase of the shunt resistance, θ(Z_S), (µRad)	0.3	Type A / pdf: Normal	sin(θ)=-1.000	0.3	31
	1.3	Type B / pdf: Normal	sin(θ)=-1.000	1.3	31
2.11) Ratio error of T_1 (parts in 10^6)	0.2	Type A / pdf: Normal	cos(θ)=0.000	0.0	3
	1.0	Type B / pdf: Normal	cos(θ)=0.000	0.0	3
2.12) Phase error of T_1 (µRad)	0.2	Type A / pdf: Normal	sin(θ)=-1.000	0.2	3
	1.0	Type B / pdf: Normal	sin(θ)=-1.000	1.0	3
3) Ambient conditions					
3.1) temperature	< 0.5	Type A / pdf: Normal	1	0.5	12
3.2) humidity	< 0.3			0.3	12
Root square sum of Type A standard uncertainties and effective degrees of freedom				1.0	58.1
Root square sum of Type B standard uncertainties and effective degrees of freedom				3.0	58.2
Combined standard uncertainty and effective degrees of freedom				3.2	71.6
Expanded uncertainty (95.45 % coverage factor) (µW/VA) and t-factor from the t-distribution				6.4	2.03

Table 36. NIST Uncertainty Components for RD-22 SN 206816, Active Power at 240 V, 5A, 53 Hz, PF=1.000 Lead

Main uncertainty components y_i	Standard uncertainty $u(y_i)$	Type method A or B of evaluation/probability distribution function	Sensitivity coefficient c_i	Uncertainty contribution $u(R_i)$	Degrees of freedom n_i
1) Standard deviation of the calibration error of the travelling standard	2.3	Type A / pdf: Normal	1	2.3	43
2) uncertainty components of the reference standard of the participant					
2.1) Magnitude of the voltage channel signal, $u(V_V)$, (µV/V)	0.5	Type A / pdf: Normal	cos(θ)=1.000	0.5	31
	1.2	Type B / pdf: Normal	cos(θ)=1.000	1.2	31
2.2) Phase of the voltage channel signal, θ(V_V), (µRad)	0.5	Type A / pdf: Normal	sin(θ)=0.000	0.0	31
	1.2	Type B / pdf: Normal	sin(θ)=0.000	0.0	31
2.3) Magnitude of the current channel signal, $u(V_I)$, (µV/V)	0.2	Type A / pdf: Normal	cos(θ)=1.000	0.2	31
	1.2	Type B / pdf: Normal	cos(θ)=1.000	1.2	31
2.4) Phase of the current channel signal, θ(V_I), (µRad)	0.2	Type A / pdf: Normal	sin(θ)=0.000	0.0	31
	1.2	Type B / pdf: Normal	sin(θ)=0.000	0.0	31
2.5) Magnitude of the voltage amplifier first stage, k_1, (µV/V)	1.4	Type A / pdf: Normal	cos(θ)=1.000	1.4	7
	1.2	Type B / pdf: Normal	cos(θ)=1.000	1.2	7
2.6) Phase of the voltage amplifier first stage, θ(k_1), (µRad)	1.4	Type A / pdf: Normal	sin(θ)=0.000	0.0	7
	1.3	Type B / pdf: Normal	sin(θ)=0.000	0.0	7
2.7) Magnitude of the voltage amplifier second stage, k_2, (µV/V)	1.4	Type A / pdf: Normal	cos(θ)=1.000	1.4	7
	1.2	Type B / pdf: Normal	cos(θ)=1.000	1.2	7
2.8) Phase of the voltage amplifier second stage, θ(k_2), (µRad)	1.4	Type A / pdf: Normal	sin(θ)=0.000	0.0	7
	1.3	Type B / pdf: Normal	sin(θ)=0.000	0.0	7
2.9) Magnitude of the voltage amplifier third stage, k_3, (µV/V)	1.4	Type A / pdf: Normal	cos(θ)=1.000	1.4	7
	1.2	Type B / pdf: Normal	cos(θ)=1.000	1.2	7
2.10) Phase of the voltage amplifier third stage, θ(k_3), (µRad)	1.4	Type A / pdf: Normal	sin(θ)=0.000	0.0	7
	1.6	Type B / pdf: Normal	sin(θ)=0.000	0.0	7
2.11) Magnitude of the shunt resistance, Z_S, (µΩ/Ω)	0.3	Type A / pdf: Normal	cos(θ)=1.000	0.3	99
	1.3	Type B / pdf: Normal	cos(θ)=1.000	1.3	99
2.12) Phase of the shunt resistance, θ(Z_S), (µRad)	0.3	Type A / pdf: Normal	sin(θ)=0.000	0.0	31
	1.3	Type B / pdf: Normal	sin(θ)=0.000	0.0	31
2.13) Ratio error of T_1 (parts in 10^6)	0.2	Type A / pdf: Normal	cos(θ)=1.000	0.2	3
	1.0	Type B / pdf: Normal	cos(θ)=1.000	1.0	3
2.14) Phase error of T_1 (µRad)	0.2	Type A / pdf: Normal	sin(θ)=0.000	0.0	3
	1.0	Type B / pdf: Normal	sin(θ)=0.000	0.0	3
3) Ambient conditions					
3.1) temperature	< 0.5	Type A / pdf: Normal	1	0.5	43
3.2) humidity	< 0.3			0.3	43
Root square sum of Type A standard uncertainties and effective degrees of freedom				3.4	61.1
Root square sum of Type B standard uncertainties and effective degrees of freedom				3.1	70.6
Combined standard uncertainty and effective degrees of freedom				4.7	128.5
Expanded uncertainty (95.45 % coverage factor) (µW/VA) and t-factor from the t-distribution				9.8	2.11

Table 37. NIST Uncertainty Components for RD-22 SN 206816, Active Power at 240 V, 5A, 53 Hz, PF=0.500 Lead

Main uncertainty components y_i	Standard uncertainty $u(y_i)$	Type method A or B of evaluation/probability distribution function	Sensitivity coefficient c_i	Uncertainty contribution $u(R_i)$	Degrees of freedom n_i
1) Standard deviation of the calibration error of the travelling standard	1.9	Type A / pdf: Normal	1	1.9	43
2) uncertainty components of the reference standard of the participant					
2.1) Magnitude of the voltage channel signal, $u(V_V)$, (µV/V)	0.5	Type A / pdf: Normal	cos(θ)=0.500	0.3	31
	1.2	Type B / pdf: Normal	cos(θ)=0.500	0.6	31
2.2) Phase of the voltage channel signal, θ(V_V), (µRad)	0.5	Type A / pdf: Normal	sin(θ)=0.866	0.4	31
	1.2	Type B / pdf: Normal	sin(θ)=0.866	1.0	31
2.3) Magnitude of the current channel signal, $u(V_I)$, (µV/V)	0.2	Type A / pdf: Normal	cos(θ)=0.500	0.1	31
	1.2	Type B / pdf: Normal	cos(θ)=0.500	0.6	31
2.4) Phase of the current channel signal, θ(V_I), (µRad)	0.2	Type A / pdf: Normal	sin(θ)=0.866	0.2	31
	1.2	Type B / pdf: Normal	sin(θ)=0.866	1.0	31
2.5) Magnitude of the voltage amplifier first stage, k_1, (µV/V)	1.4	Type A / pdf: Normal	cos(θ)=0.500	0.7	7
	1.2	Type B / pdf: Normal	cos(θ)=0.500	0.6	7
2.6) Phase of the voltage amplifier first stage, θ(k_1), (µRad)	1.4	Type A / pdf: Normal	sin(θ)=0.866	1.2	7
	1.3	Type B / pdf: Normal	sin(θ)=0.866	1.1	7
2.7) Magnitude of the voltage amplifier second stage, k_2, (µV/V)	1.4	Type A / pdf: Normal	cos(θ)=0.500	0.7	7
	1.2	Type B / pdf: Normal	cos(θ)=0.500	0.6	7
2.8) Phase of the voltage amplifier second stage, θ(k_2), (µRad)	1.4	Type A / pdf: Normal	sin(θ)=0.866	1.2	7
	1.3	Type B / pdf: Normal	sin(θ)=0.866	1.1	7
2.9) Magnitude of the voltage amplifier third stage, k_3, (µV/V)	1.4	Type A / pdf: Normal	cos(θ)=1.000	0.7	7
	1.2	Type B / pdf: Normal	cos(θ)=1.000	0.6	7
2.10) Phase of the voltage amplifier third stage, θ(k_3), (µRad)	1.4	Type A / pdf: Normal	sin(θ)=0.000	1.2	7
	1.6	Type B / pdf: Normal	sin(θ)=0.000	1.4	7
2.11) Magnitude of the shunt resistance, Z_S, (µΩ/Ω)	0.3	Type A / pdf: Normal	cos(θ)=0.500	0.2	99
	1.3	Type B / pdf: Normal	cos(θ)=0.500	0.7	99
2.12) Phase of the shunt resistance, θ(Z_S), (µRad)	0.3	Type A / pdf: Normal	sin(θ)=0.866	0.3	31
	1.3	Type B / pdf: Normal	sin(θ)=0.866	1.1	31
2.13) Ratio error of T_1 (parts in 10^6)	0.2	Type A / pdf: Normal	cos(θ)=0.500	0.1	3
	1.0	Type B / pdf: Normal	cos(θ)=0.500	0.5	3
2.14) Phase error of T_1 (µRad)	0.2	Type A / pdf: Normal	sin(θ)=0.866	0.2	3
	1.0	Type B / pdf: Normal	sin(θ)=0.866	0.9	3
3) Ambient conditions					
3.1) temperature	< 0.5	Type A / pdf: Normal	1	0.5	43
3.2) humidity	< 0.3			0.3	43
Root square sum of Type A standard uncertainties and effective degrees of freedom				3.2	77.6
Root square sum of Type B standard uncertainties and effective degrees of freedom				3.3	88.9
Combined standard uncertainty and effective degrees of freedom				4.6	166.5
Expanded uncertainty (95.45 % coverage factor) (µW/VA) and t-factor from the t-distribution				9.3	2.03

Table 38. NIST Uncertainty Components for RD-22 SN 206816, Active Power at 240 V, 5A, 53 Hz, PF=0.000 Lead

Main uncertainty components y_i	Standard uncertainty $u(y_i)$	Type method A or B of evaluation/probability distribution function	Sensitivity coefficient c_i	Uncertainty contribution $u(R_i)$	Degrees of freedom n_i
1) Standard deviation of the calibration error of the travelling standard	1.2	Type A / pdf: Normal	1	1.2	43
2) uncertainty components of the reference standard of the participant					
2.1) Magnitude of the voltage channel signal, $u(V_V)$, (µV/V)	0.5	Type A / pdf: Normal	cos(θ)=0.000	0.0	31
	1.2	Type B / pdf: Normal	cos(θ)=0.000	0.0	31
2.2) Phase of the voltage channel signal, θ(V_V), (µRad)	0.5	Type A / pdf: Normal	sin(θ)=1.000	0.5	31
	1.2	Type B / pdf: Normal	sin(θ)=1.000	1.2	31
2.3) Magnitude of the current channel signal, $u(V_I)$, (µV/V)	0.2	Type A / pdf: Normal	cos(θ)=0.000	0.0	31
	1.2	Type B / pdf: Normal	cos(θ)=0.000	0.0	31
2.4) Phase of the current channel signal, θ(V_I), (µRad)	0.2	Type A / pdf: Normal	sin(θ)=1.000	0.2	31
	1.2	Type B / pdf: Normal	sin(θ)=1.000	1.2	31
2.5) Magnitude of the voltage amplifier first stage, k_1, (µV/V)	1.4	Type A / pdf: Normal	cos(θ)=0.000	0.0	7
	1.2	Type B / pdf: Normal	cos(θ)=0.000	0.0	7
2.6) Phase of the voltage amplifier first stage, θ(k_1), (µRad)	1.4	Type A / pdf: Normal	sin(θ)=1.000	1.4	7
	1.3	Type B / pdf: Normal	sin(θ)=1.000	1.3	7
2.7) Magnitude of the voltage amplifier second stage, k_2, (µV/V)	1.4	Type A / pdf: Normal	cos(θ)=0.000	0.0	7
	1.2	Type B / pdf: Normal	cos(θ)=0.000	0.0	7
2.8) Phase of the voltage amplifier second stage, θ(k_2), (µRad)	1.4	Type A / pdf: Normal	sin(θ)=1.000	1.4	7
	1.3	Type B / pdf: Normal	sin(θ)=1.000	1.3	7
2.9) Magnitude of the voltage amplifier third stage, k_3, (µV/V)	1.4	Type A / pdf: Normal	cos(θ)=1.000	0.0	7
	1.2	Type B / pdf: Normal	cos(θ)=1.000	0.0	7
2.10) Phase of the voltage amplifier third stage, θ(k_3), (µRad)	1.4	Type A / pdf: Normal	sin(θ)=0.000	1.4	7
	1.6	Type B / pdf: Normal	sin(θ)=0.000	1.6	7
2.11) Magnitude of the shunt resistance, Z_S, (µΩ/Ω)	0.3	Type A / pdf: Normal	cos(θ)=0.000	0.0	99
	1.3	Type B / pdf: Normal	cos(θ)=0.000	0.0	99
2.12) Phase of the shunt resistance, θ(Z_S), (µRad)	0.3	Type A / pdf: Normal	sin(θ)=1.000	0.3	31
	1.3	Type B / pdf: Normal	sin(θ)=1.000	1.3	31
2.13) Ratio error of T_1 (parts in 10^6)	0.2	Type A / pdf: Normal	cos(θ)=0.000	0.0	3
	1.0	Type B / pdf: Normal	cos(θ)=0.000	0.0	3
2.14) Phase error of T_1 (µRad)	0.2	Type A / pdf: Normal	sin(θ)=1.000	0.2	3
	1.0	Type B / pdf: Normal	sin(θ)=1.000	1.0	3
3) Ambient conditions					
3.1) temperature	< 0.5	Type A / pdf: Normal	1	0.5	43
3.2) humidity	< 0.3			0.3	43
Root square sum of Type A standard uncertainties and effective degrees of freedom				2.9	39.2
Root square sum of Type B standard uncertainties and effective degrees of freedom				3.4	57.3
Combined standard uncertainty and effective degrees of freedom				4.4	96.5
Expanded uncertainty (95.45 % coverage factor) (µW/VA) and t-factor from the t-distribution				9.0	2.03

Table 39. NIST Uncertainty Components for RD-22 SN 206816, Active Power at 240 V, 5A, 53 Hz, PF=0.500 Lag

Main uncertainty components y_i	Standard uncertainty $u(y_i)$	Type method A or B of evaluation/probability distribution function	Sensitivity coefficient c_i	Uncertainty contribution $u(R_i)$	Degrees of freedom n_i
1) Standard deviation of the calibration error of the travelling standard	1.6	Type A / pdf: Normal	1	1.6	43
2) uncertainty components of the reference standard of the participant					
2.1) Magnitude of the voltage channel signal, $u(V_V)$, (µV/V)	0.5	Type A / pdf: Normal	cos(θ)=0.500	0.3	31
	1.2	Type B / pdf: Normal	cos(θ)=0.500	0.6	31
2.2) Phase of the voltage channel signal, θ(V_V), (µRad)	0.5	Type A / pdf: Normal	sin(θ)=-0.866	0.4	31
	1.2	Type B / pdf: Normal	sin(θ)=-0.866	1.0	31
2.3) Magnitude of the current channel signal, $u(V_I)$, (µV/V)	0.2	Type A / pdf: Normal	cos(θ)=0.500	0.1	31
	1.2	Type B / pdf: Normal	cos(θ)=0.500	0.6	31
2.4) Phase of the current channel signal, θ(V_I), (µRad)	0.2	Type A / pdf: Normal	sin(θ)=-0.866	0.2	31
	1.2	Type B / pdf: Normal	sin(θ)=-0.866	1.0	31
2.5) Magnitude of the voltage amplifier first stage, k_1, (µV/V)	1.4	Type A / pdf: Normal	cos(θ)=0.500	0.7	7
	1.2	Type B / pdf: Normal	cos(θ)=0.500	0.6	7
2.6) Phase of the voltage amplifier first stage, θ(k_1), (µRad)	1.4	Type A / pdf: Normal	sin(θ)=-0.866	1.2	7
	1.3	Type B / pdf: Normal	sin(θ)=-0.866	1.1	7
2.7) Magnitude of the voltage amplifier second stage, k_2, (µV/V)	1.4	Type A / pdf: Normal	cos(θ)=0.500	0.7	7
	1.2	Type B / pdf: Normal	cos(θ)=0.500	0.6	7
2.8) Phase of the voltage amplifier second stage, θ(k_2), (µRad)	1.4	Type A / pdf: Normal	sin(θ)=-0.866	1.2	7
	1.3	Type B / pdf: Normal	sin(θ)=-0.866	1.1	7
2.9) Magnitude of the voltage amplifier third stage, k_3, (µV/V)	1.4	Type A / pdf: Normal	cos(θ)=1.000	0.7	7
	1.2	Type B / pdf: Normal	cos(θ)=1.000	0.6	7
2.10) Phase of the voltage amplifier third stage, θ(k_3), (µRad)	1.4	Type A / pdf: Normal	sin(θ)=0.000	1.2	7
	1.6	Type B / pdf: Normal	sin(θ)=0.000	1.4	7
2.11) Magnitude of the shunt resistance, Z_S, (µΩ/Ω)	0.3	Type A / pdf: Normal	cos(θ)=0.500	0.2	99
	1.3	Type B / pdf: Normal	cos(θ)=0.500	0.7	99
2.12) Phase of the shunt resistance, θ(Z_S), (µRad)	0.3	Type A / pdf: Normal	sin(θ)=-0.866	0.3	31
	1.3	Type B / pdf: Normal	sin(θ)=-0.866	1.1	31
2.13) Ratio error of T_1 (parts in 10^6)	0.2	Type A / pdf: Normal	cos(θ)=0.500	0.1	3
	1.0	Type B / pdf: Normal	cos(θ)=0.500	0.5	3
2.14) Phase error of T_1 (µRad)	0.2	Type A / pdf: Normal	sin(θ)=-0.866	0.2	3
	1.0	Type B / pdf: Normal	sin(θ)=-0.866	0.9	3
3) Ambient conditions					
3.1) temperature	< 0.5	Type A / pdf: Normal	1	0.5	43
3.2) humidity	< 0.3			0.3	43
Root square sum of Type A standard uncertainties and effective degrees of freedom				3.0	70.9
Root square sum of Type B standard uncertainties and effective degrees of freedom				3.3	88.9
Combined standard uncertainty and effective degrees of freedom				4.5	159.8
Expanded uncertainty (95.45 % coverage factor) (µW/VA) and t-factor from the t-distribution				9.1	2.03

Table 40. NIST Uncertainty Components for RD-22 SN 206816, Active Power at 240 V, 5A, 53 Hz, PF=0.000 Lag

Main uncertainty components y_i	Standard uncertainty $u(y_i)$	Type method A or B of evaluation/probability distribution function	Sensitivity coefficient c_i	Uncertainty contribution $u(R_i)$	Degrees of freedom n_i
1) Standard deviation of the calibration error of the travelling standard	1.2	Type A / pdf: Normal	1	1.2	43
2) uncertainty components of the reference standard of the participant					
2.1) Magnitude of the voltage channel signal, $u(V_V)$, (µV/V)	0.5	Type A / pdf: Normal	cos(θ)=0.000	0.0	31
	1.2	Type B / pdf: Normal	cos(θ)=0.000	0.0	31
2.2) Phase of the voltage channel signal, θ(V_V), (µRad)	0.5	Type A / pdf: Normal	sin(θ)=-1.000	0.5	31
	1.2	Type B / pdf: Normal	sin(θ)=-1.000	1.2	31
2.3) Magnitude of the current channel signal, $u(V_I)$, (µV/V)	0.2	Type A / pdf: Normal	cos(θ)=0.000	0.0	31
	1.2	Type B / pdf: Normal	cos(θ)=0.000	0.0	31
2.4) Phase of the current channel signal, θ(V_I), (µRad)	0.2	Type A / pdf: Normal	sin(θ)=-1.000	0.2	31
	1.2	Type B / pdf: Normal	sin(θ)=-1.000	1.2	31
2.5) Magnitude of the voltage amplifier first stage, k_1, (µV/V)	1.4	Type A / pdf: Normal	cos(θ)=0.000	0.0	7
	1.2	Type B / pdf: Normal	cos(θ)=0.000	0.0	7
2.6) Phase of the voltage amplifier first stage, θ(k_1), (µRad)	1.4	Type A / pdf: Normal	sin(θ)=-1.000	1.4	7
	1.3	Type B / pdf: Normal	sin(θ)=-1.000	1.3	7
2.7) Magnitude of the voltage amplifier second stage, k_2, (µV/V)	1.4	Type A / pdf: Normal	cos(θ)=0.000	0.0	7
	1.2	Type B / pdf: Normal	cos(θ)=0.000	0.0	7
2.8) Phase of the voltage amplifier second stage, θ(k_2), (µRad)	1.4	Type A / pdf: Normal	sin(θ)=-1.000	1.4	7
	1.3	Type B / pdf: Normal	sin(θ)=-1.000	1.3	7
2.9) Magnitude of the voltage amplifier third stage, k_3, (µV/V)	1.4	Type A / pdf: Normal	cos(θ)=1.000	0.0	7
	1.2	Type B / pdf: Normal	cos(θ)=1.000	0.0	7
2.10) Phase of the voltage amplifier third stage, θ(k_3), (µRad)	1.4	Type A / pdf: Normal	sin(θ)=0.000	1.4	7
	1.6	Type B / pdf: Normal	sin(θ)=0.000	1.6	7
2.11) Magnitude of the shunt resistance, Z_S, (µΩ/Ω)	0.3	Type A / pdf: Normal	cos(θ)=0.000	0.0	99
	1.3	Type B / pdf: Normal	cos(θ)=0.000	0.0	99
2.12) Phase of the shunt resistance, θ(Z_S), (µRad)	0.3	Type A / pdf: Normal	sin(θ)=-1.000	0.3	31
	1.3	Type B / pdf: Normal	sin(θ)=-1.000	1.3	31
2.13) Ratio error of T_1 (parts in 10^6)	0.2	Type A / pdf: Normal	cos(θ)=0.000	0.0	3
	1.0	Type B / pdf: Normal	cos(θ)=0.000	0.0	3
2.14) Phase error of T_1 (µRad)	0.2	Type A / pdf: Normal	sin(θ)=-1.000	0.2	3
	1.0	Type B / pdf: Normal	sin(θ)=-1.000	1.0	3
3) Ambient conditions					
3.1) temperature	< 0.5	Type A / pdf: Normal	1	0.5	43
3.2) humidity	< 0.3			0.3	43
Root square sum of Type A standard uncertainties and effective degrees of freedom				2.8	37.5
Root square sum of Type B standard uncertainties and effective degrees of freedom				3.4	57.3
Combined standard uncertainty and effective degrees of freedom				4.4	94.7
Expanded uncertainty (95.45 % coverage factor) (µW/VA) and t-factor from the t-distribution				8.9	2.03

7. **Date and Time When Reference Standards are Initialized**

Both reference standards were rebooted (de-energized and simultaneously energized approximately 15 minutes later). The dates that the instruments were de-energized and energized are given in Table 41.

Table 41. Reboot Dates

8/15/2022, 17:22:28
8/15/2022, 21:36:09
8/16/2022, 03:53:39
8/16/2022, 10:10:57
8/16/2022, 14:22:37
8/16/2022, 18:04:30
8/17/2022, 10:35:26
8/18/2022, 05:52:09
8/19/2022, 06:37:10
8/20/2022, 18:23:31

REFERENCES

[1] B. Waltrip, B. Gong, T. Nelson, Y. Wang, C. Burroughs, A. Rüfenacht, S. Benz, and P. Dresselhaus, "AC power standard using a programmable Josephson voltage standard," *IEEE Trans. Instrum. Meas*., vol. 58, no. 4, pp. 1041–1048, Apr. 2009.

[2] A. Rüfenacht *et al.*, "Precision differential sampling measurements of low-frequency voltages synthesized with an AC programmable Josephson voltage standard," *IEEE Trans. Instrum. Meas.*, vol. 58, no. 4, pp. 809-815, Apr. 2009.

[3] B. Waltrip, O. Laug, and T. Nelson, "A 600-V AC voltage amplifier for power measurements," *IEEE Trans. Instrum. Meas.*, vol. 64, no. 6, pp. 1373-1377, Jun. 2015.

[4] R. Cutkosky, "New NBS measurements of the absolute Farad and Ohm," *IEEE Trans. Instrum. Meas.*, vol. IM-23, no. 4, pp. 305-309, Dec. 1974.

[5] J. Shields, "Voltage dependence of precision air capacitors," *J. Res. NBS*, vol. 69C, no. 4, Oct.-Dec. 1965.

[6] R. Cutkosky and J. Shields, "The precision measurement of transformer ratios," *IRE Trans. Instrum*., vol. I-9, pp. 243-250, Sept. 1960.

[7] O. Laug, T. Souders, B. Waltrip, "A four-terminal current shunt with calculable AC response," *NIST Tech. Note 1462*, August 2004.

[8] P. Miljanic, E. So, W. Moore, "An electronically enhanced magnetic core for current transformers," *IEEE Trans. Instrum. Meas.*, vol. 40, no. 2, pp. 410-414, April 1991.

[9] *American National Standard for Expressing Uncertainty – U.S. Guide to the Expression of Uncertainty in Measurement*, ANSI/NCSL Std Z540-2-1997.

Measurements performed by:

Bryan C. Waltrip, Electronics Engineer
Quantum Measurement Division

Reviewed by,

Thomas Nelson, Group Leader
Quantum Measurement Division

6. Comparison report of NMIA

Australian Government
Department of Industry, Science, Energy and Resources

National Measurement Institute

Our Ref.: RN190637
File No.: CB/19/0064

27 May 2021

The Manager
Centro Nacional de Metrología (CENAM)
km. 4.5 Carretera los Cues
76246 El Marques, Queretaro
MEXICO

Attention: Dr Rene Carranza

Dear Rene,

Subject: Measurement Report RN190637

Enclosed is Measurement Report RN190637 on two energy meters, Radian model RD-22-332S, s/n: 206816, 203409, submitted to this institute for examination as a part of CCEM-K5 intercomparison.

Yours sincerely,

Dr Ilya Budovsky
Section Manager: Electricity
(Encl.)

Australian Government
Department of Industry, Innovation and Science

National Measurement Institute

MEASUREMENT REPORT ON

Two energy meters

Model RD-22-332S

Serial numbers 206816 and 203409

The National Measurement Institute is responsible for Australia's units and standards of measurement.
The measurement results presented in this report are traceable to Australia's primary standards.

Headquarters
36 Bradfield Road
West Lindfield NSW 2070
Australia

GPO Box 2013
Canberra ACT 2601
Australia

Telephone: +61 2 8467 3600
Facsimile: +61 2 8467 3610

For further information contact: Mr V Balakrishnan *telephone* + 61 2 8467 3539
facsimile + 61 2 8467 3783
email vasu.balakrishnan@measurement.gov.au

Ref: RN190637 File: CB//19/0064 Checked: DG Date: 11 May 2021

For	**:** Centro Nacional de Metrología (CENAM) km. 4.5 Carretera los Cues 76246 El Marques, Queretaro MEXICO
Reference	**:** CCEMK5-2017
Manufacturer	**:** Radian Research Inc. USA
Description	**:** Auto-ranging Primary Transfer Standard
Model	**:** RD-22-332S
Serial numbers	**:** 206816, 203409
Ranges	**:** Voltages: 40 to 600 V auto ranging Currents: 0.2 to 125 A auto ranging
Duration of tests	**:** 8 March 2019 to 26 March 2019
Type of tests	**:** Ac calibration of active and reactive energy and power factor
Waveform	**:** Sinusoidal
Test method	**:** PM-LFS-8.2.3
Mean dates of tests:	s/n 206815 – 23 March 2019 s/n 203409 – 21 March 2019
Air temperature	**:** (23.1 ± 0.7) °C
Relative humidity	**:** (51 ± 4) %

Note: The calibration was conducted at NMI, Bradfield Road, West Lindfield, NSW 2070.

Test conditions:

a**:** The instruments were switched on for 24 hours prior to the commencement of testing. A further period of 30 minutes was allowed for stabilsiation after the application of each test load.

b: The instruments were de-energised for one minute between each set of measurements, followed by at least 15-minute warm-up period.

c: Instrument readings were obtained remotely using the RS-232 interface.

d: During all tests, the "AUX. POWER" terminals were supplied from its 24V dc supply.

e: Test voltage was applied to the potential terminals with the terminal marked "O" earthed.

f: Test current was applied to the current input terminals marked "A" for all test points. The low current terminal was earthed.

Test parameters:

Table 1: Mean Test Parameters

Mean Test Voltage (V)	Mean Test Current (A)	Mean Test Power factor	Mean Test Frequency (Hz)
120.0008 ± 0.0002	5.0001 ± 0.0001	1.00000 ± 0.00002	52.9993 ± 0.0001
120.0008 ± 0.0002	5.0001 ± 0.0001	0.49994 ± 0.00002	52.9993 ± 0.0001
120.0008 ± 0.0002	5.0001 ± 0.0001	– 0.00007± 0.00002	52.9993 ± 0.0001
120.0008 ± 0.0002	5.0001 ± 0.0001	0.50005 ± 0.00002	52.9993 ± 0.0001
120.0008 ± 0.0002	5.0001 ± 0.0001	0.00006 ± 0.00002	52.9993 ± 0.0001
240.0076 ± 0.001	5.0001 ± 0.0001	1.00000 ± 0.00002	52.9993 ± 0.0001
240.0076 ± 0.001	5.0001 ± 0.0001	0.50004 ± 0.00002	52.9993 ± 0.0001
240.0076 ± 0.001	5.0001 ± 0.0001	0.00004 ± 0.00002	52.9993 ± 0.0001
240.0076 ± 0.001	5.0001 ± 0.0001	0.49995 ± 0.00002	52.9993 ± 0.0001
240.0076 ± 0.001	5.0001 ± 0.0001	– 0.00005± 0.00002	52.9993 ± 0.0001

Measurement setup:

The measurement setup [1] is shown in Figure 1. The test voltage $U_{\sim}$ and test current $I_{\sim}$ are supplied from a Rotek 8100 phantom power source. The test voltage is scaled using a NMIA precision Inductive Voltage Divider (IVD) [2] and is defined at the voltage input terminals of the instrument under test (IUT). The test current is applied to the NMIA Multi-range Current Transformer (MCT) [3,4] and the current input of the IUT. The output voltage $U_{u\sim}$ of the IVD and output voltage of the MCT $U_{i\sim}$ are applied to the Digital Power Comparator (DPC), which is formed by two digital voltmeters in a master-slave arrangement, driven by sampling software [5]. Both voltmeters operate on the 1.0 V range for maximum accuracy. The MCT output voltage is obtained from a series combination of three 10 Ω current shunts R_{S1} to R_{S3}, with precision current shunt R_{S1} determining the relevant uncertainty contribution.

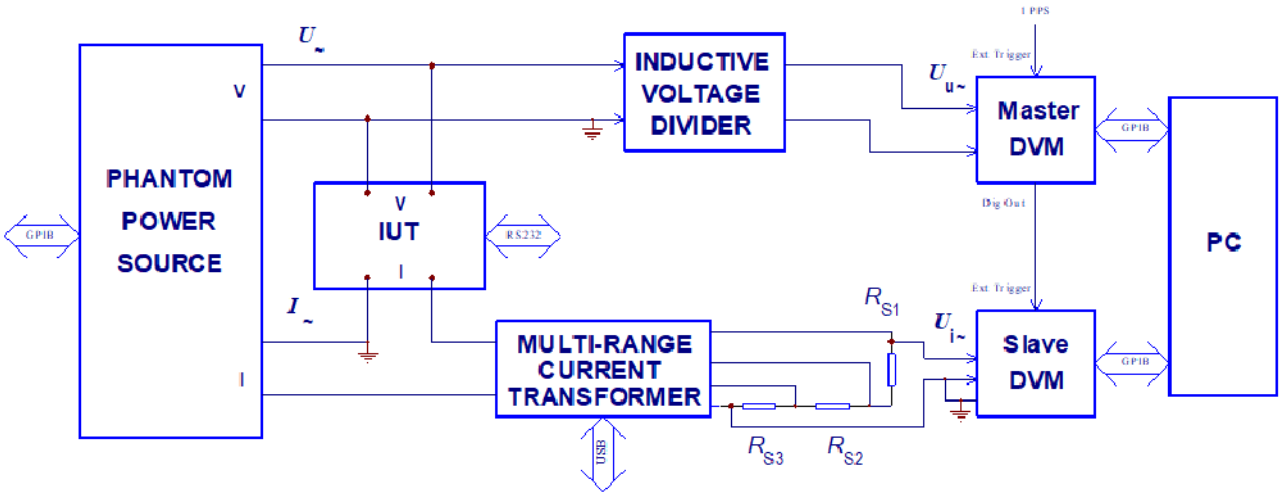

Figure 1. Measurement Setup

Measurement Procedure:

The RD22's readings were obtained remotely using the RS-232 remote interface and compared with the reference value obtained from the DPC. At least ten sets of measurements were averaged for each test point on each day of measurement.

Traceability scheme:

The ratio errors of NMIA IVD have been obtained through a build-up calibration using Thompson's method [6-8]. The Multi-range current transformer is traceable to NMIA current ratio standards and calculable micropotentiometer resistors [9, 10]. The precision current shunt is traceable to NMIA primary standards of resistance and to the micropotentiometer resistors [9, 11]. The dc traceability of the DPC is to NMIA primary standard of voltage based on the Josephson effect. The ac traceability of the DPC is to NMIA primary ac-dc transfer standards [12,13] and the NMIA Thermal Power Comparator [1,14].

Results:

Table 2: Serial number: 206816

Applied Voltage *(V)*	*Applied Current* *(A)*	*Power factor*	*Error* *(μW/VA)*	*Uncertainty* *(μW/VA)*
120	5	1	– 55.7	± 4.4
120	5	0.5 C	– 66.9	± 2.8
120	5	0 C	– 45.5	± 2.9
120	5	0.5 L	+ 11.7	± 2.8
120	5	0 L	+ 43.7	± 2.9
240		1	– 50.8	± 4.4
240	5	0.5 C	– 65.3	± 2.8
240	5	0 C	– 46.1	± 2.9
240	5	0.5 L	+ 14.5	± 2.8
240	5	0 L	+ 44.4	± 2.9

Table 3: Serial number: 203409

Applied Voltage *(V)*	**Applied Current** *(A)*	**Power factor**	**Error** *(µW/VA)*	**Uncertainty** *(µW/VA)*
120	5	1	+ 82.4	± 4.4
120	5	0.5 C	+ 65.8	± 2.8
120	5	0 C	+ 28.0	± 2.9
120	5	0.5 L	+ 16.8	± 2.8
120	5	0 L	– 30.5	± 2.9
240	5	1	+ 87.3	± 4.4
240	5	0.5 C	+ 71.4	± 2.8
240	5	0 C	+ 32.0	± 2.9
240	5	0.5 L	+ 15.7	± 2.8
240	5	0 L	– 34.3	± 2.9

Interpretation of errors:

The errors given in Tables 2 and 3 are to be subtracted from the respective indicated value to obtain the true value.

Uncertainties: The uncertainties stated in this Report have been calculated in accordance with the principles in *JCGM 100:2008 - Evaluation of measurement data - Guide to the expression of uncertainty in measurement*, and gives an interval estimated to have a level of confidence of 95%.

The uncertainties apply at the time of measurement only and take no account of any drift or other effects that may apply afterwards. When estimating uncertainty at any later time, other relevant information should also be considered, including, where possible, the history of the performance of the instrument and the manufacturer's specifications.

Uncertainty budgets:

Table 4. Uncertainty budget at power factor = 1

Component *(i=1,2,...16)*	Distribution	U_i *(ppm)*	k_i	c_i	u_i (ppm)	$c_i u_i$ (ppm)	υ_i
1 DPC Calibration uncertainty	Normal	1.70	1	1.0	1.7	1.70	50
2 DPC Stability	Normal	0.40	2	1.0	0.2	0.20	12.5
3 DPC Linearity	Normal	0.50	2	1.0	0.3	0.25	12.5
4 DPC Uncancelled loading	Rectangular	0.60	1.73	0.0	0.0	0.00	12.5
5 DVMu calibration uncertainty	Normal	0.40	2	1.0	0.2	0.20	50
6 DVMi calibration uncertainty	Normal	0.40	2	1.0	0.2	0.20	50
7 IUT stability	Normal	1.00	1.4	1.0	0.7	0.71	2
8 MCT calibration uncertainty (in-phase)	Normal	1.98	2.1	1.0	0.9	0.94	12.5
9 MCT calibration uncertainty (quadrature)	Normal	1.84	2	0.0	0.0	0.00	30
10 MCT stability (in-phase)	Normal	0.20	2	1.0	0.1	0.10	12.5
11 MCT calibration uncertainty (quadrature)	Normal	0.30	2	0.0	0.0	0.00	12.5
12 Shunt dc calibration uncertainty	Normal	1.10	2.6	1.0	0.4	0.42	4
13 Shunt dc stability	Normal	0.20	2	1.0	0.1	0.10	4
14 Shunt ac-dc difference calibration uncertainty	Normal	1.00	2	1.0	0.5	0.50	4
15 Shunt phase angle calibration uncertainty	Normal	1.10	2	0.0	0.0	0.00	4
16 IVD correction uncertainty	Normal	0.01	2	1.0	0.0	0.01	4

Combined Standard Uncertainty, u_c (μW/VA)	2.2
Effective degr.of freedom, u_{eff}	63
Coverage Factor, k	2.0
Expanded Uncertainty $U = ku_c$ (μW/VA)	4.4

Table 5. Uncertainty budget at power factor = 0.5

Component *(i=1,2,...16)*	Distribution	U_i *(ppm)*	k_i	c_i	u_i (ppm)	$c_i u_i$ (ppm)	υ_i
1 DPC Calibration uncertainty	Normal	1.70	1	0.50	0.9	0.43	50
2 DPC Stability	Normal	0.40	2	0.50	0.1	0.05	12.5
3 DPC Linearity	Normal	1.00	2	1	0.5	0.50	12.5
4 DPC Uncancelled loading	Rectangular	0.60	1.73	0.87	0.3	0.26	12.5
5 DVMu calibration uncertainty	Normal	0.40	2	0.50	0.1	0.05	50
6 DVMi calibration uncertainty	Normal	0.40	2	0.50	0.1	0.05	50
7 IUT stability	Normal	1.00	1.4	1	0.7	0.71	2
8 MCT calibration uncertainty (in-phase)	Normal	1.98	2.1	0.50	0.5	0.24	12.5
9 MCT calibration uncertainty (quadrature)	Normal	1.84	2	0.87	0.8	0.69	30
10 MCT stability (in-phase)	Normal	0.20	2	0.50	0.1	0.03	12.5
11 MCT calibration uncertainty (quadrature)	Normal	0.30	2	0.87	0.1	0.11	12.5
12 Shunt dc calibration uncertainty	Normal	1.10	2.6	0.50	0.2	0.11	4
13 Shunt dc stability	Normal	0.20	2	0.50	0.1	0.03	4
14 Shunt ac-dc difference calibration uncertainty	Normal	1.00	2	0.50	0.3	0.13	4
15 Shunt phase angle calibration uncertainty	Normal	1.10	2	0.87	0.5	0.41	4
16 IVD correction uncertainty	Normal	0.01	2	1	0.0	0.01	4

Combined Standard Uncertainty, u_c (μW/VA)	1.3
Effective degr.of freedom, u_{eff}	20
Coverage Factor, k	2.1
Expanded Uncertainty $U = ku_c$ (μW/VA)	2.8

Table 6. Uncertainty budget at power factor = 0

Component *(i=1,2,...16)*	Distribution	U_i *(ppm)*	k_i	c_i	u_i (ppm)	$c_i u_i$ (ppm)	υ_i
1 DPC Calibration uncertainty	Normal	1.70	1	0.00	0.0	0.00	50
2 DPC Stability	Normal	0.40	2	0.00	0.0	0.00	12.5
3 DPC Linearity	Normal	1.00	2	1	0.5	0.50	12.5
4 DPC Uncancelled loading	Rectangular	0.60	1.73	1.00	0.3	0.35	12.5
5 DVMu calibration uncertainty	Normal	0.40	2	0.00	0.0	0.00	50
6 DVMi calibration uncertainty	Normal	0.40	2	0.00	0.0	0.00	50
7 IUT stability	Normal	1.00	1.4	1	0.7	0.71	4
8 MCT calibration uncertainty (in-phase)	Normal	1.98	2.1	0.00	0.0	0.00	12.5
9 MCT calibration uncertainty (quadrature)	Normal	1.84	2	1.00	0.9	0.92	30
10 MCT stability (in-phase)	Normal	0.20	2	0.00	0.0	0.00	12.5
11 MCT calibration uncertainty (quadrature)	Normal	0.30	2	1.00	0.2	0.15	12.5
12 Shunt dc calibration uncertainty	Normal	1.10	2.6	0.00	0.0	0.00	4
13 Shunt dc stability	Normal	0.20	2	0.00	0.0	0.00	4
14 Shunt ac-dc difference calibration uncertainty	Normal	1.00	2	0.00	0.0	0.00	4
15 Shunt phase angle calibration uncertainty	Normal	1.10	2	1.00	0.6	0.55	4
16 IVD correction uncertainty	Normal	0.01	2	1	0.0	0.01	4

Combined Standard Uncertainty, u_c (μW/VA)	1.4
Effective degr.of freedom, u_{eff}	36
Coverage Factor, k	2.0
Expanded Uncertainty $U = ku_c$ (μW/VA)	2.9

References

[1] I. Budovsky, T. Hagen and D. Arthur, "New standard of power at NMIA," *CPEM 2014 Conf. Digest.*, pp. 410-411, Aug. 2014.

[2] G. W. Small, I. F. Budovsky, A. M. Gibbes and J. R. Fiander, "Precision three-stage 1000 V/50 Hz inductive voltage divider*", IEEE Trans. Instrum. Meas.*, 54, pp. 600- 603, 2005.

[3] I. Budovsky, T. Hagen, F. Emms, H.L. Johnson, L. Marais and V. Balakrishnan, Precision multi-range current transformer for the automation of electrical power standards," *CPEM 2014 Conf .Digest*, pp. 412 – 413, August 2014.

[4] I. Budovsky, L. Marais and L. Willems van Beveren, "Precision characterisation of current transformers and shunts in the audio frequency range," *CPEM 2018 Conf. Digest*, July 2018.

[5] G. Gubler and E. Z. Shapiro, "Implementation of sampling measurement system for new VNIIM power standard," *CPEM 2012 Conf. Digest*, p. 294, July 2012

[6] A. Thompson, "Precise calibration of ratio transformers," *IEEE Trans. Instrum. Meas*., vol 32, pp. 47 – 50, 1983.

[7] I.F. Budovsky, G.W. Small, A.M. Gibbes and J.R. Fiander, "Calibration of 1000V/ 50 Hz inductive voltage dividers and ratio transformers," *CPEM'04 Digest*, June 2004, pp. 322-323.

[8] H. L. Johnson and R Xie, "A young person's guide to Thompson's method for the precise measurement of voltage ratio," *Metrology Society of Australia Biennial Conf. Digest*, pp. 93-100, 2011

[9] I. Budovsky, "A micropotentiometer-based system for low voltage calibration 0f alternating voltage current standards," *IEEE Trans. Instrum. Meas*., vol 46, pp. 356 – 360, 1997.

[10] Ilya Budovsky, 'Measurement of Phase Angle Errors of Precision Current Shunts in the Frequency Range From 40 Hz to 200 kHz, " IEEE Trans. Instrum. Meas, Vol. 56, Issue 2, pp. 284 – 288, 2007

[11] I. Budovsky, "Calibration of precision current transformers and ac resistors by comparison using Two Sampling Digital Voltmeters," CPEM 2020 Conf. Digest, July 2020.

[12] I. Budovsky and B D Inglis, "High-Frequency AC-DC Differences of NML Single-Junction Thermal Voltage Converters at Frequencies," IEEE Trans. Instrum. Meas., Vol. 50, No1, February 2001, pp 101-105.

[13] T. Hagen and I. Budovsky, "Single –junction thermal voltage converters with reduced uncertainties at frequencies up to 1 MHz," ," IEEE Trans. Instrum. Meas., Vol. 58, No 2, April 2009, pp.848-852.

[14] I. Budovsky, A M Gibbes and D C Arthur, "A high-frequency thermal power comparator," IEEE Trans. Instrum. Meas., Vol. 48, N2, April 1999, pp 427-430.

ooooooo0ooooooo

Dr I F Budovsky
for Dr R B Warrington
Chief Metrologist

7. Comparison report of NMISA

NMISA-20-00087

Report on Measurements for CCEM-K5.2017 Key comparison of 50/60 Hz power

5 October 2020

Approval Sheet

		Signature	Date
Prepared for	National Metrology Institute of South Africa		
Contract (Project)	Maintenance of DCLF-RF NMS: AC Power NMS		
Prepared by	P.J. Prinsloo		2020-12-04
Checked by	E. Golovins		2020-12-04
Approved by	L. Magagula		2020-12-05

Contact Persons:

P.J. Prinsloo

Telephone Details:

+27 12 841 3013

+27 84 400 4775

Distribution List

Internal	**External**
DCLF & RF Section	Dr. Gert Rietveld VSL, Netherlands Thijsseweg 11, 2629 JA Delft The Netherlands
NMISA Registry	Email: grietveld@vsl.nl

Table of Contents

1. Introduction

NMISA participated in the CCEM-K5.2017 key comparison for 50/60 Hz ac power. The laboratory received the traveling standard on 14 February 2020. The measurements were carried out from 26 February until 19 March 2020. During this period measurements were interrupted due to laboratory temperature conditions going out of tolerance.

The global pandemic caused by COVID-19 resulted in lockdown conditions in many countries. Operation of courier services and ports were uncertain, and it was decided not to send the traveling standard to the next participant but rather keep it safe in the NMISA laboratory until conditions improve. With COVID-19 infection rates reducing and lockdown conditions easing, arrangements were made to send the traveling standard to the next laboratory so that circulation could continue. The traveling standard was dispatched to the next laboratory on 9 October 2020.

2. Traveling Standard

The traveling standard comprised of two Radian RD-22-332S reference standards, serial numbers 203409 and 206815.

Both reference standards were energised on 18 February 2020, left for approximately 24 hours, de-energised, and energised again before measurements commenced.

3. Measurement setup and traceability scheme

The measurements were performed using a Digital Simultaneous Sampling Technique (DSST) system implemented in 2019 [1]. Amplitudes of the voltage and current signals are scaled down to approximately 0,8 V and then digitised by two Keysight 3458A digital multi-meters [2].

The measurement setup used is shown in Figure 1.

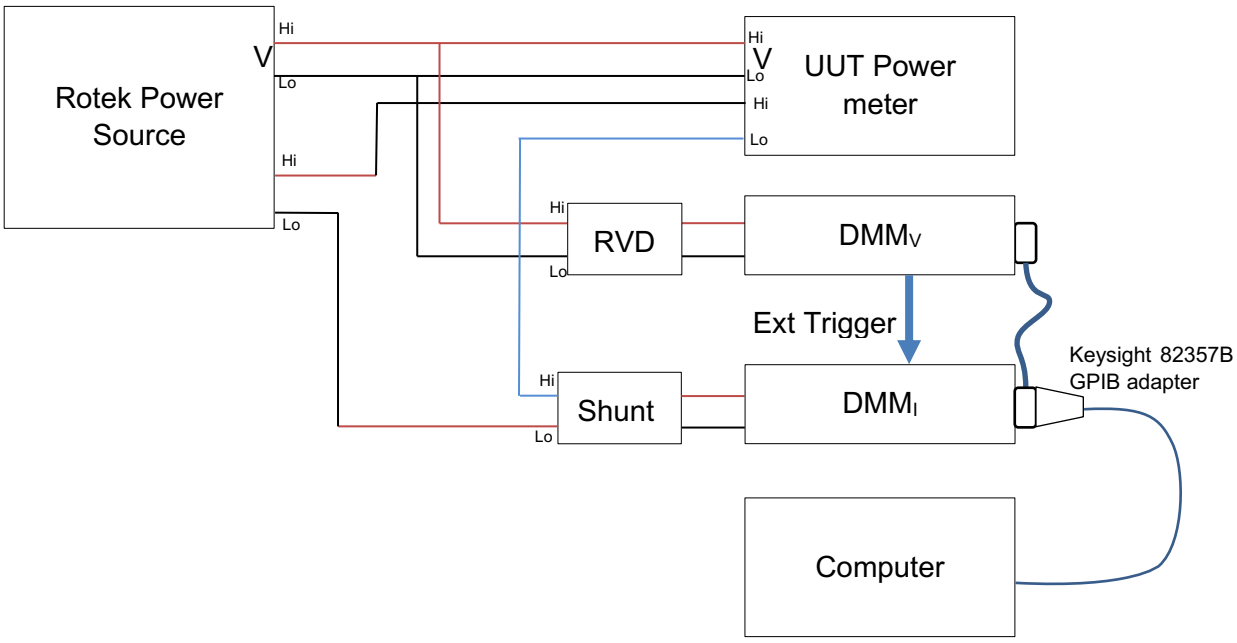

Figure 1: Measurement setup

Traceability for the system is obtained for voltage, current and phase as shown in Table 1.

Table 1: Traceability for ac power constituent quantities

Parameter	Equipment	Description
Voltage	DC voltage calibrator Fluke 5790B measurement standard Resistive Voltage Divider (RVD)	The ac voltage ratio magnitude of the RVD was calibrated using the Fluke 5790B measurement standard, which was calibrated using the NMISA National Measurement Standards (NMS) for ac-dc difference voltage thermal transfer
Current	DC resistance standards Ac-dc thermal transfer standards for ac current Current Shunt	The current shunt was calibrated for dc resistance using the NMISA current-comparator bridge NMS and for ac-dc difference - using the thermal transfer standards for current
Phase	Primary method for phase source calibration [3] Clarke-Hess 5500 Phase Angle Standard	Phase displacement was characterised for the RVD and digital multi-meters (DMM) using the Clarke-Hess phase standard [4]. The contribution of current phase shift in the shunt was incorporated into the phase measurement uncertainty using the manufacturer's accuracy specification data

4. Measurement Method

The system implements a comparison method where the source voltage is applied in parallel to the RVD and UUT voltage input, and the source current flows through a series connection of the current shunt and UUT current input.

The RVD and current shunt are used to scale the input signals to approximately 0,8 V to be measured on the 1 V ranges of the DMMs.

The computer performs a DFT on this data to obtain the magnitude and phase information about the signals.

The ac ratio of the RVD is applied to calculate the magnitude of the input voltage, and dc resistance and ac-dc difference of the shunt are applied to calculate the magnitude of the input current.

The ac voltage at the input of the RVD is calculated as:

$$U = U_{dmmV} U_r \tag{1}$$

where: U_{dmmV} is the measured voltage on the voltage DMM (V)

U_r Is the ratio of the RVD input ac voltage to the output ac voltage

The ac current at the input of the shunt is calculated as:

$$I = \frac{U_{dmm\_ac}}{R_{dc}}(1 + \delta_I) \quad (2)$$

where:

U_{dmm_ac} is the voltage measured across the shunt (V)

δ_I is the ac-dc difference of the shunt (A/A)

R_{dc} is the dc resistance of the shunt (Ω)

The phase difference between the input voltage of the RVD and input current of the shunt is calculated as:

$$\emptyset = \emptyset_{dsst} + \emptyset_{\varepsilon} + \emptyset_{s} \quad (3)$$

Where:

$\emptyset_{dsst}$ is the calculated phase difference after DFT of DMM inputs

$\emptyset_{\varepsilon}$ is the calibrated phase error of the DSST system including RVD

$\emptyset_{s}$ is the phase displacement specification of the current shunt

Power is calculated using formula (4).

$$P = U\ I\ cos\emptyset \quad (4)$$

Where: P is the active power (W)

U is the rms voltage (V)

I is the rms current (A)

$\emptyset$ is the phase angle between the input voltage and current

5. Summary of Results

5.1 Active power calibration error

The table below contains the mean value and expanded uncertainty (95,45%) of the calibration error of the UUTs.

Measurement Point	Calibration Error (µW/VA)		Uncertainty (± µW/VA)
	Sn. 203409	Sn. 206815	
120V, 5A, 0°, 53Hz	103	-60	55
120V, 5A, 60°, 53Hz	98	-33	49
120V, 5A, 90°, 53Hz	69	-8	52
120V, 5A, -60°, 53Hz	-24	-3	49
120V, 5A, -90°, 53 Hz	-56	5	52
240V, 5A, 0°, 53Hz	103	-44	60
240V, 5A, 60°, 53Hz	113	-29	52

Measurement Point	Calibration Error (μW/VA)		Uncertainty (± μW/VA)
	Sn. 203409	Sn. 206815	
240V, 5A, 90°, 53Hz	78	-23	51
240V, 5A, -60°, 53Hz	7	4	52
240V, 5A, -90°, 53Hz	-83	32	51

5.2 Parameters measured by reference standards

The tables below contain the mean value of relevant parameters measured by the UUTs.

Sn. 203409

Measurement Point	Voltage (V)	Current (I)	Power Factor	Frequency (Hz)
120V, 5A, 0°, 53Hz	120.0095	5.001169	0.999988	53.0449
120V, 5A, 60°, 53Hz	120.0096	5.001054	0.499956	53.0438
120V, 5A, 90°, 53Hz	120.0101	5.001040	-0.000476	53.0377
120V, 5A, -60°, 53Hz	120.0097	5.001017	0.501391	53.0464
120V, 5A, -90°, 53 Hz	120.0099	5.000966	0.001829	53.0344
240V, 5A, 0°, 53Hz	239.9855	5.001032	0.999993	53.0660
240V, 5A, 60°, 53Hz	239.9858	5.000721	0.500062	53.0638
240V, 5A, 90°, 53Hz	239.9869	5.000730	-0.000388	53.0643
240V, 5A, -60°, 53Hz	239.9850	5.001163	0.500180	53.0624
240V, 5A, -90°, 53Hz	239.9865	5.001279	0.000446	53.0643

Sn. 206815

Measurement Point	Voltage (V)	Current (I)	Power Factor	Frequency (Hz)
120V, 5A, 0°, 53Hz	120.0079	5.000509	0.999988	53.0355
120V, 5A, 60°, 53Hz	120.0080	5.000396	0.499889	53.0416
120V, 5A, 90°, 53Hz	120.0084	5.000382	-0.000552	53.0485
120V, 5A, -60°, 53Hz	120.0080	5.000323	0.501475	53.0391
120V, 5A, -90°, 53 Hz	120.0082	5.000366	0.001886	53.0471
240V, 5A, 0°, 53Hz	239.9801	5.000342	0.999993	53.0626
240V, 5A, 60°, 53Hz	239.9812	5.000034	0.499987	53.0650
240V, 5A, 90°, 53Hz	239.9822	5.000058	-0.000469	53.0701
240V, 5A, -60°, 53Hz	239.9809	5.000540	0.500250	53.0669
240V, 5A, -90°, 53Hz	239.9852	5.000713	0.000505	53.0753

5.3 Ambient conditions

The tables below contain the mean value and uncertainties of the temperature and humidity measurements during calibration of each UUT.

Sn. 203409

Measurement Point	Date of measurement	Temperature (°C)	Uncertainty (°C)	Relative Humidity (%)	Uncertainty (%)
120V, 5A, 0°, 53Hz	18/03/2020	24.3	0.6	52.3	3.5
120V, 5A, 60°, 53Hz	18/03/2020	24.4	0.6	52.2	3.5
120V, 5A, 90°, 53Hz	19/03/2020	23.8	0.6	52.0	3.5
120V, 5A, -60°, 53Hz	19/03/2020	23.8	0.6	51.6	3.5
120V, 5A, -90°, 53 Hz	19/03/2020	23.9	0.6	52.2	3.5
240V, 5A, 0°, 53Hz	18/03/2020	23.7	0.6	51.8	3.5
240V, 5A, 60°, 53Hz	18/03/2020	24.0	0.6	52.3	3.5
240V, 5A, 90°, 53Hz	18/03/2020	24.3	0.6	52.0	3.5
240V, 5A, -60°, 53Hz	18/03/2020	24.5	0.6	52.3	3.5
240V, 5A, -90°, 53Hz	18/03/2020	24.4	0.6	51.9	3.5

Sn. 206815

Measurement Point	Date of measurement	Temperature (°C)	Uncertainty (°C)	Relative Humidity (%)	Uncertainty (%)
120V, 5A, 0°, 53Hz	19/03/2020	23.9	0.6	51.5	3.5
120V, 5A, 60°, 53Hz	19/03/2020	24.0	0.6	50.2	3.5
120V, 5A, 90°, 53Hz	19/03/2020	24.1	0.6	48.2	3.5
120V, 5A, -60°, 53Hz	19/03/2020	24.1	0.6	49.2	3.5
120V, 5A, -90°, 53 Hz	20/03/2020	24.0	0.6	50.8	3.5
240V, 5A, 0°, 53Hz	17/03/2020	23.8	0.6	50.0	3.5
240V, 5A, 60°, 53Hz	17/03/2020	23.9	0.6	50.1	3.5
240V, 5A, 90°, 53Hz	17/03/2020	24.0	0.6	50.1	3.5
240V, 5A, -60°, 53Hz	17/03/2020	23.9	0.6	50.2	3.5
240V, 5A, -90°, 53Hz	18/03/2020	23.7	0.6	51.4	3.5

6. Uncertainty Evaluation

Uncertainties were determined according to the Guide to the expression of uncertainty in measurement [5]. Refer to Appendix A for detailed uncertainty budgets.

Uncertainties are calculated in separate budgets for different parts of the system, and after that combined to calculate the final uncertainty for active power.

6.1 Type A uncertainty

$$\delta_{sd} = \sqrt{\frac{\sum_{i=1}^{n}(x_i - \bar{x})^2}{n-1}} \tag{5}$$

where: δ_{sd} is the standard deviation

x_i Is the i th measured value

n is the number of measured values

$$\delta_{ESDM} = \frac{\delta_{sd}}{\sqrt{n}} \tag{6}$$

where: δ_{ESDM} Type A uncertainty evaluation of repeated measurements expressed as the estimated standard deviation of the mean

6.2 DMM amplitude contributors

$$V_{dmm} = V_{fft} + \Delta_{dcV} + \Delta_l + \Delta_q \tag{7}$$

where: V_{dmm} is the true value of the rms voltage at the input of the DMM (V)

V_{fft} is the measured rms voltage calculated through FFT (V)

Δ_{dcV} is the correction for the dc voltage accuracy calibration error on the 1V range (V)

Δ_l is the correction for the voltage nonlinearity on the 1V range (V)

Δ_q is the correction for the digitiser's quantisation error for the selected DMM range (V)

6.3 AC Voltage contributors

$$V = V_{dmmV}(RVD_{ratio} + \delta_{ratio}) \tag{8}$$

where: V is the true value of the rms voltage at the input of the RVD (V)

RVD_{rat} is the measured/certified input to output ratio of the RVD (V/V)

δ_{rat} is the correction for the error of the RVD ratio (V/V)

6.4 AC Current contributors

$$I = \frac{V_{dmmI}}{(R_{shunt} + \Delta_{RS} + \Delta_{st})}(1 + \delta_I + \delta_{acdc}) \tag{9}$$

where: I is the true value of the rms current flowing through the shunt (A)

δ_I is the certified ac-dc difference of the shunt (A/A)

R_{shunt} is the certified dc resistance of the shunt (Ω)

Δ_{RS} is the correction for the resistance accuracy calibration error of the shunt (Ω)

δ_{acdc} is the correction for the ac-dc difference accuracy calibration error of the shunt (A/A)

Δ_{st} is the correction for the long-term resistance drift of the shunt (Ω)

6.5 Power factor contributors

$$PF = cos\left(\emptyset_{VI} + \Delta_{dsst} + \Delta_{Sp}\right) \quad (10)$$

where:

PF	is the true value of the power factor
$\emptyset_{VI}$	is the measured phase difference between the voltage and current at the RVD and shunt inputs (deg)
Δ_{dsst}	is the correction for the RVD phase error and reference phase misalignment between the two DMMs (calibrated as one system with the Clarke-Hess 5500 phase standard) (deg)
Δ_{Sp}	is the correction for the phase displacement error of the current shunt (deg)

6.6 AC Power contributors

$$P = \frac{(V_{dmmV} + \Delta_{dmmV})(RVD_{rat} + \delta_{rat})(V_{dmmI} + \Delta_{dmmI})(1 + \delta_I + \delta_{acdc})\cos\left(\emptyset_{VI} + \Delta_{\emptyset_{VI}}\right)}{R_{shunt} + \Delta_{shunt}} \quad (11)$$

where:

P	is the true value of the power at the input of the RVD and current shunt (W)
$\Delta_{shunt} = \Delta_{RS} + \Delta_{st}$	is the correction for the error due to ac current contributors in 6.4 (Ω)
$\Delta_{dmmV} = \Delta_{dcV} + \Delta_l + \Delta_q$	is the correction for the error due to DMM contributors in 6.2 (V)
$\Delta_{dmmI} = \Delta_{dcV} + \Delta_l + \Delta_q$	is the correction for the error due to DMM contributors in 6.2 (V)
$\Delta_{\emptyset_{VI}} = \Delta_{dsst} + \Delta_{Sp}$	is the correction for the error due to power factor contributors in 6.5 (deg)

7. References

[1] DCLF\P-0005, “Operation of Dgitizing power standard at NMISA”.

[2] Agilent Technologies 3458A Multimeter, User’s Guide, Manual Part Number: 03458-90014.

[3] K. K. C. a. D. T. Hess, “Phase Measurement, Traceability, and Verification Theory and Practice,” *IEEE Transactions on Instrumentation and Measurement,* vol. 39, no. 1, p. 52 to 55, 1990.

[4] clarke-hess 5500-2, Phase calibration standards & phase measurement techniques.

[5] JCGM 100:2008, “Evaluation of measurement data — Guide to the expression of uncertainty in measurement”.

Appendix A - Uncertainty budgets

120V			PF 1		PF 0.5		PF 0		
Main uncertainty components Estimated	**Type**	**Standard uncertainty**	**Sensitivity coefficient**	**Uncertainty contribution $u(R_i)$**	**Sensitivity coefficient**	**Uncertainty contribution $u(R_i)$**	**Sensitivity coefficient**	**Uncertainty contribution $u(R_i)$**	**Degrees of freedom**
y_i		$u(y_i)$	c_i	µW/VA	c_i	µW/VA	c_i	µW/VA	n_i
ESDM of the calibration error of the UUT	A		1	3.3	1	5.3	1	12.3	4
DMM (V) uncertainty	B	4.5	1	4.5	0.5	2.3	0	0.0	infinite
DMM (I) uncertainty	B	4.5	1	4.5	0.5	2.3	0	0.0	infinite
RVD input to output ratio calibration	B	19.0	1	19.0	0.5	9.5	0	0.0	infinite
Shunt dc resistance calibration (0.16Ω)	B	0.5	1	0.5	0.5	0.3	0	0.0	infinite
Shunt ac-dc difference calibration	B	14.7	1	14.7	0.5	7.4	0	0.0	infinite
Shunt dc resistance 12 month stability	B	10.4	1	10.4	0.5	5.2	0	0.0	infinite
RVD + DSST meters phase calibration	B	20.2	0.000	0.0	0.866	17.5	1.000	20.2	infinite
Shunt phase displacement accuracy	B	10.4	0.000	0.0	0.866	9.0	1.000	10.4	infinite
Combined standard uncertainty and effective degrees of freedom:				27.1		24.4		25.8	infinite
Expanded uncertainty (95.45 % coverage factor):				55		49		52	

240V			PF 1		PF 0.5		PF 0		
Main uncertainty components Estimated	**Type**	**Standard uncertainty**	**Sensitivity coefficient**	**Uncertainty contribution $u(R_i)$**	**Sensitivity coefficient**	**Uncertainty contribution $u(R_i)$**	**Sensitivity coefficient**	**Uncertainty contribution $u(R_i)$**	**Degrees of freedom**
y_i		$u(y_i)$	c_i	µW/VA	c_i	µW/VA	c_i	µW/VA	n_i
ESDM of the calibration error of the UUT	A		1	4.8	1	7.6	1	10.9	4
DMM (V) uncertainty	B	4.5	1	4.5	0.5	2.3	0	0.0	infinite
DMM (I) uncertainty	B	4.5	1	4.5	0.5	2.3	0	0.0	infinite
RVD input to output ratio calibration	B	22.0	1	22.0	0.5	11.0	0	0.0	infinite
Shunt dc resistance calibration (0.16Ω)	B	0.5	1	0.5	0.5	0.3	0	0.0	infinite
Shunt ac-dc difference calibration	B	14.7	1	14.7	0.5	7.4	0	0.0	infinite
Shunt dc resistance 12 month stability	B	10.4	1	10.4	0.5	5.2	0	0.0	infinite
RVD + DSST meters phase calibration	B	20.2	0.000	0.0	0.866	17.5	1.000	20.2	infinite
Shunt phase displacement accuracy	B	10.4	0.000	0.0	0.866	9.0	1.000	10.4	infinite
Combined standard uncertainty and effective degrees of freedom:				29.5		25.6		25.2	infinite
Expanded uncertainty (95.45 % coverage factor):				60		52		51	

8. Comparison report of PTB

Physikalisch-Technische Bundesanstalt
Nationales Metrologieinstitut

Measurement Report on
Key Comparison of 50/60 Hz Power
(CCEM-K5.2017)

Matthias Schmidt, Kristian Dauke

Contents

1 Introduction

This report describes the calibration of the two reference standards from Radian Research RD-22-332S with the serial numbers 203409 and 206816, which was used for this key comparison (CCEM-K5.2015), as well as their results and the uncertainty balance when measuring active power.
The measurements were performed within the time schedule given in the Technical Protocol distributed by the organizing laboratories (VSL, Netherlands, PTB, Germany, CENAM, Mexico).

2 Basic Operating Principle

The scheme of the basic PTB ac power sampling standard is shown in figure 1.
The key to reach low uncertainties is due to the use of a single clock f_{Clock}, which is derived from a highly precise digital sampling voltmeter (DVM). It serves as master clock for the sampling process and for the generation of the test signals with a two-channel ac waveform synthesizer. This synthesizer generates two sinusoidal voltages U_A and U_B with very low distortion (< -100 dBc), high stability (< 10^{-6} / hour) and any phase angle γ within ± 180°. The very low distortion voltage and transconductance amplifiers generate the test signals U and I. These quantities are fed to the device under test, to a calibrated voltage divider and a two-stage current transformer with its ac shunt, respectively. The output voltages U_1 and U_2 of the instrument transformers are voltages proportional to the test quantities U and I defining the power to be measured. The DVM samples the voltages U_1 and U_2 alternately via the signal switch. This fully synchronized operation eliminates sampling errors of the measurement process, as it allows to set the sampling frequency of the DVM equal to an exact integer multiple of the signal frequency. Under the condition that the Nyquist theorem is fulfilled and an integer number of periods of the signals are measured, the complex voltages U_1 and U_2 of the fundamental signal frequency can exactly be reconstructed from the sampled dataset using the discrete Fourier transform (DFT). With the ratio of the voltage divider $F_u = U_1 / U$ and the ratio of the current-to-voltage transducer $F_i = U_2 / I$, the power quantities P (active power) can be calculated according to:

$$\underline{S} = \underline{U} \cdot \underline{I^*} = \frac{U_1 \cdot U_2}{F_u \cdot F_i} \cdot cos\left(\varphi_1 - \varphi_2 - arg(F_u) + arg(F_i)\right)$$

$$P = Re\{S\} = \frac{U_1 \cdot U_2}{F_u \cdot F_i} \cdot cos\left(\varphi_1 - \varphi_2 - arg(F_u) + arg(F_i)\right)$$

where $\underline{I^*}$ stands for the complex conjugate current I, and the arg expressions describe the phase displacements of the transducers.

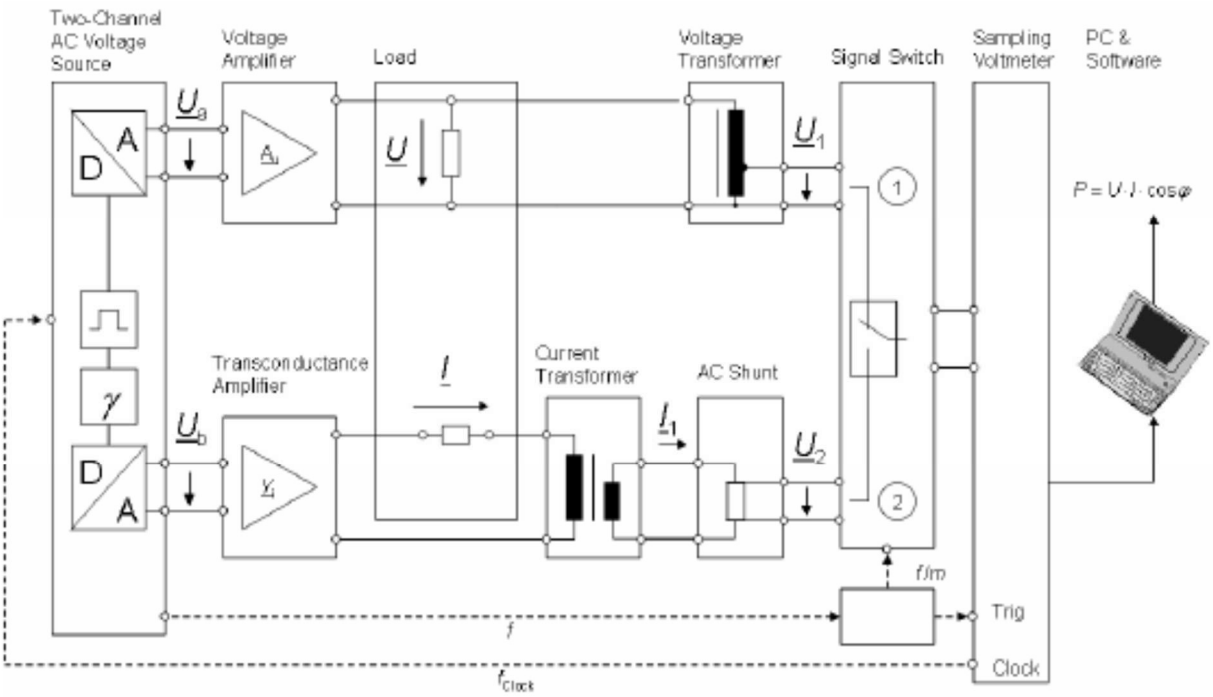
Two-Channel
AC Voltage
Source
Voltage
Amplifier
Load
Voltage
Transformer
Signal Switch
Sampling
Voltmeter
PC &
Software
D
A
$\underline{U}_a$
A_u
$\underline{U}$
$\underline{U}_1$
1
$P = U \cdot I \cdot \cos\varphi$
γ
Transconductance
Amplifier
$\underline{I}$
Current
Transformer
AC Shunt
$\underline{I}_1$
$\underline{U}_2$
2
$\underline{U}_b$
Y_t
f/m
Trig
f
Clock
f_{Clock}

Figure 1

3 Measurement Results

3.1 RD22 with serial number 203409

U_{set} [V]	I_{Set} [A]	PF	ΔP in µW/VA
			07.01.2020
120	5	1	82
120	5	0.5 lead	64
120	5	0 lead	27
120	5	0.5 lag	17
120	5	0 lag	-30
240	5	1	88
240	5	0.5 lead	68
240	5	0 lead	29
240	5	0.5 lag	20
240	5	0 lag	-31

3.2 RD22 with serial number 206816

U_{set} [V]	I_{Set} [A]	PF	ΔP in µW/VA
			07.01.2020
120	5	1	-56
120	5	0.5 lead	-65
120	5	0 lead	-42
120	5	0.5 lag	9
120	5	0 lag	40
240	5	1	-52
240	5	0.5 lead	-64
240	5	0 lead	-43
240	5	0.5 lag	12
240	5	0 lag	42

3.3 Ambient conditions

The measurements were carried out according to the scenario described in the CCEM K5 Draft, Chapter 4.3.
The temperature in the Lab is controlled in a range of (23 +/-1) °C.
The humidity is less than 40%.

4 Measurement uncertainty

Main uncertainty components y_i	Standard uncertainty $u(y_i)$	Type method A or B of evaluation/probability distribution function	Sensitivity coefficient c_i	Uncertainty contribution $u(R_i)$	Degrees of freedom n_i
Standard deviation of the calibration error of the travelling standard	1,0E-06	A	1	1,0E-06	9
Voltage transformer	3,0E-06	B	1	3,0E-06	∞
Current transformer	2,0E-06	B	1	2,0E-06	∞
AC Shunt	2,0E-06	B	1	2,0E-06	∞
Sampling and DFT	5,0E-07	B	1	5,0E-07	∞
RMS Voltmeter	2,0E-06	B	1,4	2,8E-06	∞
Root square sum of Type A standard uncertainties and effective degrees of freedom				1,0E-06	9
Root square sum of Type B standard uncertainties and effective degrees of freedom				5,0E-06	∞
Combined standard uncertainty and effective degrees of freedom, µW/VA				5,1E-06	6126
Expanded uncertainty (95.45 %, k = 2 - coverage factor), µW/VA				1,0E-05	

9. Comparison report of RISE

REPORT

Contact person RISE
Stefan Svensson
Measurement Science and Technology
+46 10 516 54 15
stefan.svensson@ri.se

Euramet

CCEM K5 Power comparison - Sweden

Identification of the travelling standards

Two devices were tested.

DUT 1: Radian Research RD-22-332S, snbr 206816.

DUT 2: Radian Research RD-22-332S snbr 203409.

Identification of the participant laboratory and its representative

Laboratory: RISE Research Institutes of Sweden

Representative: Stefan Svensson, Safety and transport division, Measurement department

Measurement set-up and traceability scheme

Set-up

A phantom power source is set up by two Fluke 5700 calibrators (snbr 5775307 and 6450605), phase-locked to a Keysight 33520B Arbitrary waveform generator (AWG), together with a transconductance amplifier Datron D4600 (snbr 20017-1).

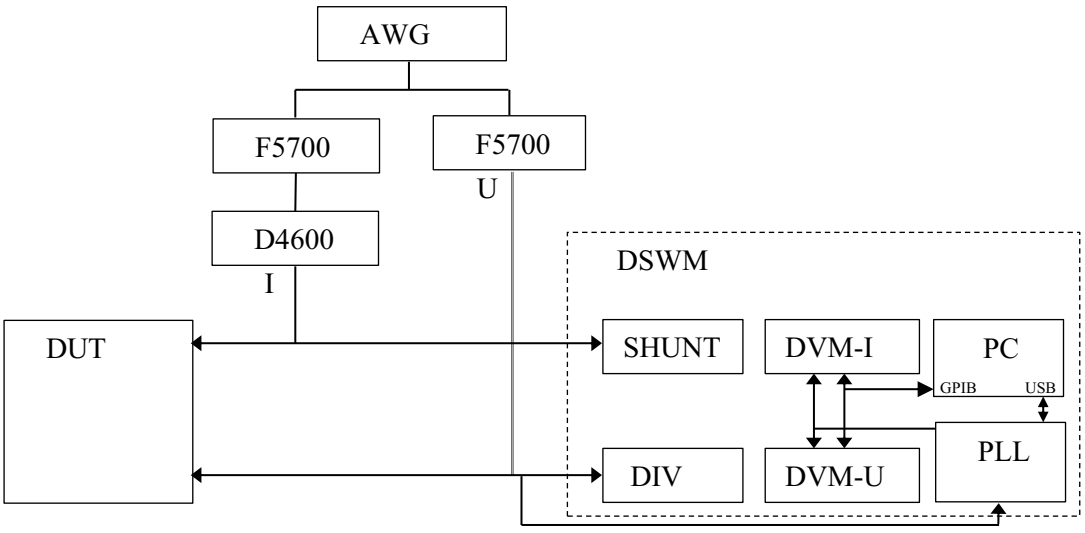

Figure 1. Calibration set-up

As reference standard, the Digital sampling wattmeter system (DSWM) of RISE were used with a 120 V to 0,8 V (Snbr VD4-1611) and a 240 to 0.8 V(Snbr VD4X-1612) resistive divider

and 5A resistive coaxial current shunt(ID 503242), DVM-U HP3458A(ID 501243), DVM-I HP3458A (ID 501244) and PLL unit PLT-5 (Snbr 130108/2).

Traceability scheme

The reference standard for power at RISE is the Digital Sampling Wattmeter (DSWM) [1][2]. The traceability of the DSWM is achieved by calibrating the voltage and current channels by comparison to the ac voltage and current standards of RISE and by calibrating the phase angle deviation between the two sampling voltmeters and for the voltage dividers[3] and current shunts [4][11].

Voltage channel

The complete voltage channel of the DSWM (divider, coaxial output cable and sampling voltmeter) is calibrated by an ac-voltage simultaneously measured by RISE reference standards. The comparison is made using RISE ac-dc transfer system where ac and dc voltage can be applied consecutively using a fast switch, Figure . To have a well-defined reference plane an X-connector is used to connect the input of the DSWM voltage channel, a reference thermal voltage converter (TVC) and a dc digital voltmeter (DVM) in parallel. During a sequence of applied voltages DC+, AC and DC- the ac-dc difference of the applied ac and dc voltages is measured by the TVC and the two dc voltages are measured by the DVM. From these measured values the value of the ac voltage can be calculated. During the AC part of the sequence the DSWM also measures the applied ac voltage. Hence, the error of the DSWM voltage channel can be determined.

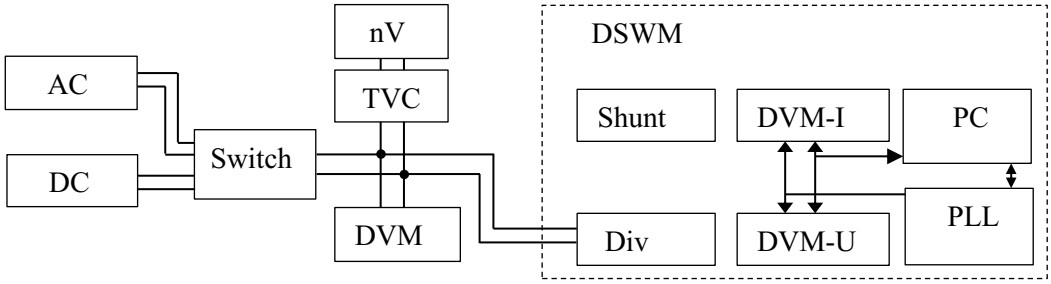

Figure 2. Volage channel calibration set-up

E.g. at 120 V an ac-dc transfer is made and measured by RISE TVC and the dc voltage is measured by a calibrated DVM. Then it is possible to calculate the ac-voltage which is at the same time measured by the voltage channel of DSWM. As the bandwidths of the TVC and the DVM on dc range are very different it is important to use a “clean” dc-voltage. There must be no significant power in noise/spurious of the dc voltage source (or from the DVM input or DSWM input) above the bandwidth of the DVM dc range.

This measurement was made before and after the measurement of the CCEM-K5 travelling standard to verify the stability of the DSWM voltage channel.

The traceability of ac voltage at RISE

The ac-dc voltage transfer difference at the primary level (1 V – 3 V) at RISE is based on a group of 3d multijunction thermal converters (MJTCs) and HF single junction thermal voltage converters (HF-TVCs). The realization of the ac-dc voltage transfer difference is made by three different methods depending on the frequency band. At medium frequencies around 1 kHz the realization is based on the fast reversed dc method (FRDC). Around 1 kHz the ac-dc voltage transfer difference of a MJTC is assumed to depend only on the dc-effects due to Peltier and Thomson [5]. At low frequencies the ac-ac(1 kHz) transfer difference of MJTC is determined by a special comparison to a resistor with large thermal time constant [6]. At high

frequencies the ac-ac(1 kHz) voltage transfer difference is based on the VSL modelling of HF-TVCs [7].

At higher voltages combinations of series resistors and Planar Multijunction Thermal Converters (PMJTC) are used and at frequencies of 1 kHz and higher the ac-dc voltage transfer differences of the resistor/PMJTC combinations are determined by a step-up procedure comparing adjacent ranges. The low frequency behavior is determined by the ac-ac(1 kHz) transfer difference of the PMJTC by the method mentioned above [6]. The step-up procedure has been verified by a measuring system that allows comparison of TVCs with a ratio of 2:1 without introducing any error due to level dependence with good agreement at frequencies up to 100 kHz [8].

The traceability for dc voltage up to 10 V is based on our Josephson standard and at higher voltages by using the Reference step method [8].

Current channel

In a similar way the complete current channel of the DSWM (shunt, coaxial output cable and sampling voltmeter) is calibrated by an ac-current simultaneously measured by an intermediate standard, traceable RISE reference standard. The comparison is made using RISE ac-dc transfer system where ac and dc voltage can be applied consecutively to a transconductance amplifier via a fast switch, Figure 3.

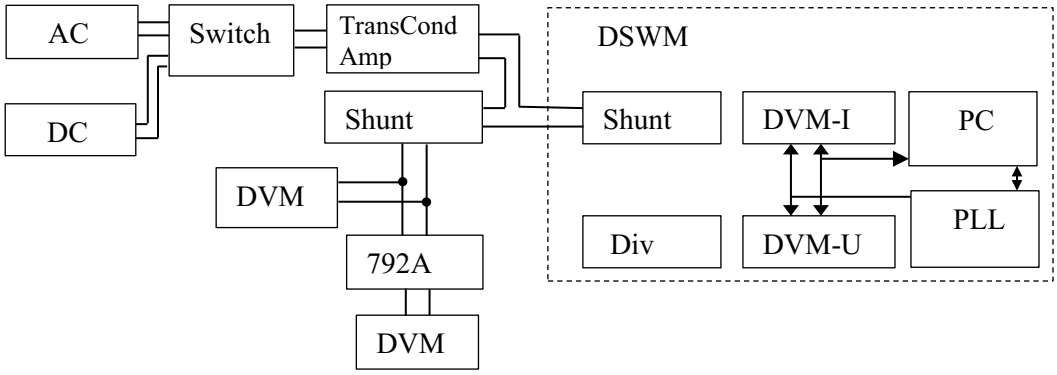

Figure 3. Current channel calibration set-up.

The intermediate standard consisting of a 5 A current shunt and a Fluke 792A was calibrated by comparison to RISE reference current shunt and PMJTC before the calibration of the DSWM current channel.

A special current T-connector is used to connect the input of the DSWM current channel and the current shunt combined with Fluke 792A. The dc DVM is connected at the output of the current shunt in parallel with the Fluke 792A. During a sequence of applied currents DC+, AC and DC- the ac-dc difference of the applied ac and dc currents is measured by the shunt/792 combination and the two dc voltages are measured by the DVM. From these measured values and the dc resistance of the reference current shunt the value of the ac current can be calculated. During the AC part of the sequence the DSWM also measures the applied ac current. Hence, the error of the DSWM current channel can be determined.

It was verified that the dc DVM measuring the output of the reference current shunt had an insignificant influence on the measured ac-dc difference. This was done in a separate test by measuring the ac-dc current difference between the shunt/792, with and without the dc DVM, and a shunt/PMJTC.

The stability of DSWM current channel was monitored by calibrating the dc resistance of its current shunt before and after the measurement of the CCEM-K5.

The traceability of ac current at RISE

The RISE realization of ac-dc current transfer difference at the primary level 10 mA is based on three different methods depending on the frequency band. At medium frequencies around 1 kHz the realization is based on the fast reversed dc method (FRDC). Around 1 kHz the ac-dc current transfer difference of a MJTC is assumed to depend only on the dc-effects due to Peltier and Thomson [5]. At low frequencies the ac-ac(1 kHz) transfer difference of MJTC is determined by a special comparison to a resistor with large thermal time constant [6]. At high frequencies the ac-ac(1 kHz) transfer difference of single junction converters (SJTC) are modelled by their reactive and loss components [10].

At higher currents combinations of current shunts and Planar Multijunction Thermal Converters (PMJTC) are used and at frequencies of 1 kHz and higher the ac-dc transfer difference of the shunt/PMJTC combinations are determined by a step-up procedure comparing adjacent ranges. The low frequency behavior is determined by the ac-ac(1 kHz) transfer difference of the PMJTC by the method mentioned above [3]. Some steps have been checked by a measuring system that allows comparison of thermal current converters with a ratio of 2:1 without introducing any error due to level dependence with good agreement at frequencies up to 1 kHz [11].

The measured dc resistance of the refence current shunt is traceable to QHR and the traceability for dc voltage up to 10 V is based on our Josephson standard.

Phase angle error and traceability

The phase angle error between the DSWMs two sampling voltmeters at zero phase is determined by connecting the same voltage to both inputs and then measure the phase difference. Traceability is achieved as this is a true zero phase standard. The accuracy at other measured phase angles is based on the inherent characteristics of the FFT algorithm used and equal spaced and phase-locked sampling used.

The linearity of the phase angle measurements has once been verified by comparison to a zero-power factor standard [12].

Traceability of the phase angle errors of dividers are achieved by a step-up method using the DSWMs two sampling voltmeters. The phase angle error of the current shunts is based on the measured inductance, capacitance and resistance and then calculated, based on model.

Traceability of inductance in pH range is realized by comparison of three current shunts designed to have equal inductance but different resistance. The measurement is made by LCR-meter measurement or by comparison between the shunts in high frequency DSWM [13]. Capacitance is traceable to our QHR via a quadrature bridge and resistance is as mentioned above traceable to our QHR. The capacitance is measured on a shunt prototype without resistors, capacitance of input cable, output coax and the input of the sampling voltmeter need to be included.

Measurement procedure

All instrument were powered up and connected in accordance with the set-up section above, in a climate-controlled laboratory..

The instrument were left powered on overnight, and the travelling standard was cycled power-off/power-on according to the instructions before each set of measurements. After each change of settings a waiting period of at least 20 minutes were inserted before start of measurements.

Each measurement was done as an 20 s average, by approximately simultaneous measurements, by readings with the Radian Research software Pcsuite and with DSWM software.

Three measurements of each of the ten measurement points were made and this was repeated three times which gives a total of nine measurement at each of the ten points.

Measurement on DUT 1 was performed on 2018-10-19 and 2018-10-22. Measurement on DUT 2 was performed on 2018-10-23.

Results

Calibration errors DUT 1 id 206816

Voltage [V]	Current [A]	Power factor	Phase angle [deg]	Error value ε [µW/VA]	Expanded uncertainty u_ε [µW/VA]
120	5	1	0	-53.3	9.9
120	5	0.5 lead	60	-63.4	9.1
120	5	0 lead	90	-40.8	9.1
120	5	0.5 lag	-60	9.3	9.1
120	5	0 lag	-90	40.4	9.1
240	5	1	0	-51.8	9.9
240	5	0.5 lead	60	-63.7	9.1
240	5	0 lead	90	-43.7	9.1
240	5	0.5 lag	-60	12.0	9.1
240	5	0 lag	-90	42.1	9.1

Calibration errors DUT 2, id 203409

Voltage [V]	Current [A]	Power factor	Phase angle [deg]	Error value ε [µW/VA]	Expanded uncertainty u_ε [µW/VA]
120	5	1	0	88.3	9.9
120	5	0.5 lead	60	71.1	9.1
120	5	0 lead	90	32.6	9.1
120	5	0.5 lag	-60	15.8	9.1
120	5	0 lag	-90	-33.2	9.1
240	5	1	0	90.9	9.9
240	5	0.5 lead	60	75.3	9.1
240	5	0 lead	90	34.4	9.1
240	5	0.5 lag	-60	15.2	9.1
240	5	0 lag	-90	-35.9	9.1

Parameters measured by the reference standard: voltage, current, power factor, frequency

Item	Nominal value	Mean value
Voltage	120 V	120.00
	240 V	240.00
Current	5 A	4.9985
Power factor	1	1.00000
	0.5 lead	0.49999
	0 lead	-0.00001
	0.5 lag	0.50007
	0 lag	0.00001
Frequency	53 Hz	53,000*

* Not measured during calibration.

Ambient conditions

Mean temperature: 23.2 degrees Celsius (22.9 to 23.5)

Mean humidity: 40,2 % (40.0 to 40.5)

Report using the template xls file

The measurement results are also reported using the template xls file that was given.

Detailed uncertainty budget

The basic power calculation equation is

$P = U \cdot I \cdot cos\varphi$

The error of the DUT is to be given in W/VA, that is in relation to apparent power. The sensitivity coefficients for voltage, current and phase angle are then given by

$$\frac{\Delta P}{S} = cos\varphi \frac{\Delta U}{U}, \qquad \frac{\Delta P}{S} = cos\varphi \frac{\Delta I}{I}, \qquad \frac{\Delta P}{S} = -sin\varphi \cdot \Delta\varphi$$

Table 1. Uncertainty budget for PF=1

Main uncertainty components y_i	Standard uncertainty $u(y_i)$	Type method A or B of evaluation/probability distribution function	Sensitivity coefficient c_i	Uncertainty contribution $u(R_i)$	Degrees of freedom n_i
1) Standard deviation of the calibration error of the travelling standard	1.5 µW/VA	Type A pdf: Normal	1.0	1.5 µW/VA	8
2.1)Traceability of the voltage channel of the reference standard, PF=1	2.5 µW/VA	Type B pdf: Normal	1.0	2.5 µW/VA	∞
2.2)Traceability of the current channel of the reference standard, PF=1	3.0 µW/VA	Type B pdf: Normal	1.0	3.0 µW/VA	∞
2.3)Traceability of the phase angle of the reference standard, PF=0	2.0 µW/VA	Type B pdf: Normal	0.0	0.0 µW/VA	∞
2.4) One month stability of the reference standard of the participant PF=1	1.5 µW/VA	Type B pdf: Normal	1.0	1.5 µW/VA	∞
2.5) One month stability of the reference standard of the participant PF=0	2.0 µW/VA	Type B pdf: Normal	0.0	0.0 µW/VA	∞
2.3) Measurement setup of the reference standard of the participant, PF=1	1.5 µW/VA	Type B pdf: Normal	1.0	1.5 µW/VA	∞
2.3) Measurement setup of the reference standard of the participant, PF=0	2.0 µW/VA	Type B pdf: Normal	0.0	0.0 µW/VA	∞
3.1) Temperature	0.5 K	Type B pdf: Normal	1.0 µW/VA/K	0.5 µW/VA	∞
3.2) Humidity	3.0 %	Type B pdf: Normal	0.5 µW/VA/%	1.5 µW/VA	∞
Root square sum of Type A standard uncertainties and effective degrees of freedom				1.5 µW/VA	∞
Root square sum of Type B standard uncertainties and effective degrees of freedom				4.7 µW/VA	∞
Combined standard uncertainty and effective degrees of freedom				4.9 µW/VA	∞
Expanded uncertainty (95.45 % coverage factor)				9.9 µW/VA	∞

Table 2. Uncertainty budget for PF= 0.5

Main uncertainty components y_i	Standard uncertainty $u(y_i)$	Type method A or B of evaluation/probability distribution function	Sensitivity coefficient c_i	Uncertainty contribution $u(R_i)$	Degrees of freedom n_i
1) Standard deviation of the calibration error of the travelling standard	2.0 µW/VA	Type A pdf: Normal	1.00	2.0 µW/VA	8
2.1)Traceability of the voltage channel of the reference standard, PF=1	2.5 µW/VA	Type B pdf: Normal	0.50	1.3 µW/VA	∞
2.2)Traceability of the current channel of the reference standard, PF=1	3.0 µW/VA	Type B pdf: Normal	0.50	1.5 µW/VA	∞
2.3)Traceability of the phase angle of the reference standard, PF=0	2.0 µW/VA	Type B pdf: Normal	0.87	1.7 µW/VA	∞
2.4) One month stability of the reference standard of the participant PF=1	1.5 µW/VA	Type B pdf: Normal	0.50	0.8 µW/VA	∞
2.5) One month stability of the reference standard of the participant PF=0	2.0 µW/VA	Type B pdf: Normal	0.87	1.7 µW/VA	∞
2.3) Measurement setup of the reference standard of the participant, PF=1	1.5 µW/VA	Type B pdf: Normal	0.50	0.8 µW/VA	∞
2.3) Measurement setup of the reference standard of the participant, PF=0	2.0 µW/VA	Type B pdf: Normal	0.87	1.7 µW/VA	∞
3.1) Temperature	0.5 K	Type B pdf: Normal	1.0 µW/VA/K	0.5 µW/VA	∞
3.2) Humidity	3.0 %	Type B pdf: Normal	0.5 µW/W/%	1.5 µW/VA	∞
Root square sum of Type A standard uncertainties and effective degrees of freedom				2.0 µW/VA	∞
Root square sum of Type B standard uncertainties and effective degrees of freedom				4.1 µW/VA	∞
Combined standard uncertainty and effective degrees of freedom				4.5 µW/VA	∞
Expanded uncertainty (95.45 % coverage factor)				9.1 µW/VA	∞

Table 3. Uncertainty budget for PF=0.

Main uncertainty components y_i	Standard uncertainty $u(y_i)$	Type method A or B of evaluation/probability distribution function	Sensitivity coefficient c_i	Uncertainty contribution $u(R_i)$	Degrees of freedom n_i
1) Standard deviation of the calibration error of the travelling standard	2.5 µW/VA	Type A pdf: Normal	1.00	2.5 µW/VA	8
2.1)Traceability of the voltage channel of the reference standard, PF=1	2.5 µW/VA	Type B pdf: Normal	0.00	0.0 µW/VA	∞
2.2)Traceability of the current channel of the reference standard, PF=1	3.0 µW/VA	Type B pdf: Normal	0.00	0.0 µW/VA	∞
2.3)Traceability of the phase angle of the reference standard, PF=0	2.0 µW/VA	Type B pdf: Normal	1.00	2.0 µW/VA	∞
2.4) One month stability of the reference standard of the participant PF=1	1.5 µW/VA	Type B pdf: Normal	0.00	0.0 µW/VA	∞
2.5) One month stability of the reference standard of the participant PF=0	2.0 µW/VA	Type B pdf: Normal	1.00	2.0 µW/VA	∞
2.3) Measurement setup of the reference standard of the participant, PF=1	1.5 µW/VA	Type B pdf: Normal	0.00	0.0 µW/VA	∞
2.3) Measurement setup of the reference standard of the participant, PF=0	2.0 µW/VA	Type B pdf: Normal	1.00	2.0 µW/VA	∞
3.1) Temperature	0.5 K	Type B pdf: Normal	1.0 µW/VA/K	0.5 µW/VA	∞
3.2) Humidity	3.0 %	Type B pdf: Normal	0.5 µW/W/%	1.5 µW/VA	∞
Root square sum of Type A standard uncertainties and effective degrees of freedom				2.5 µW/VA	∞
Root square sum of Type B standard uncertainties and effective degrees of freedom				3.8 µW/VA	∞
Combined standard uncertainty and effective degrees of freedom				4.6 µW/VA	∞
Expanded uncertainty (95.45 % coverage factor)				9.1 µW/VA	∞

Date and time when the reference standard is de-energized and energized.

The travelling standard DUT 1 was energized and de-energized according to this approximate scheme.

Standard	De-energised - Energised
DUT 1	2018-10-18 14:00*
	2018-10-19 13:45
	2018-10-19 17:15
	2018-10-22 08:40
	2018-10-22 13:30
	2018-10-22 17:00**
DUT 2	2018-10-22 18:00*
	2018-10-23 08:30
	2018-10-23 11:00
	2018-10-23 16:30
	2018-10-23 19:20**

* Energizing only ** de-energizing only

References

[1] S. Svensson and K.-E. Rydler, “A measuring system for the calibration of power analyzers,” IEEE Trans. Instrum. Meas., vol. 44, pp. 316-317, Apr. 1995.

[2] Svensson, S., Rydler, K.-E. & Tarasso, V., “Upgrade of accuracy and traceability the SP Sampling Wattmeter,” Dig. Conf. Prec. Electrom. Meas., CPEM 2016, Ottawa, Canada, July 2016.

[3] K.-E. Rydler, S. Svensson, and V. Tarasso, “Voltage dividers with low phase angle errors for a wideband power measuring system, ”Dig. Conf. Prec. Electrom. Meas., CPEM 2002, Ottawa, Canada, pp. 382-383, June 2002.

[4] S. Svensson, K.-E. Rydler, and V. Tarasso, “Improved model and phase-angle verification of current shunts for ac and power measurements,” CPEM 2004 Conf. Digest, p. 82, June 2004.

[5] K. Takahashi, M. Klonz, H. Sasaki, B.D. Inglis, "Determination of the Time Constants of Thermoelectric Effects in Thermal Converters using a Fast-Reversed DC, " IEEE Trans. Instrum. Meas., vol. 46, pp. 377-381, April 1997.

[6] K.-E. Rydler and V. Tarasso, “A method to determine the low frequency behaviour of thermal converters,” Dig. Conf. Prec. Electrom. Meas., CPEM 2002, Ottawa, Canada, pp. 358-359, June 2002.

[7] C.J. van Mullem, W.J.G.D. Janssen, and J.P.M. de Vreede, “Evaluation of the Calculable High Frequency Ac-dc Standard,” IEEE Trans. Instrum. Meas., vol. 46, pp. 361-364, April 1997.

[8] P. Simonson and K.-E. Rydler, "Level dependence of ac-dc transfer devices," IEEE Trans. Instrum. Meas., vol. 48, pp. pp. 395-398, April 1999.

[9] M. D. Early, M. Šíra, B.-O. Andersson, L. A. Christian, O. Gunnarsson, K.-E. Rydler and J. Streit. “A Simple Build-Up Method for the DC Voltage Scale of a Source”, IEEE Trans. on Instrum. and Meas., vol. 62, no. 6, pp. 1600-1607, June 2013; also Erratum, IEEE Trans. on Instrum. and Meas., vol. 63, no. 1, p. 246, Jan 2014.

[10] K.-E. Rydler and V. Tarasso, “Realization of ac-dc current transfer difference to 1 MHz,” Dig. Conf. Prec. Electrom. Meas., CPEM 2008, Boulder, USA, pp. 406-407, June 2008.

[11] V. Tarasso, and K.-E. Rydler, “A measuring system for determination of level dependence of current ac-dc tranfer devices,” Dig. Conf. Prec. Electrom. Meas., CPEM 2006, Turino, Italy, pp. 242-243, July 2006.

[12] P. Simonson, S. Svensson and K.-E. Rydler, “A comparison of power measuring systems,” IEEE Trans. Instrum. Meas., vol. 46, pp. 423-425, Apr. 1997.

[13] K.-E. Rydler, T. Bergsten and V. Tarasso, “Determination of phase angle errors of current shunts for wideband power measurement,” Dig. Conf. Prec. Electrom. Meas., CPEM 2012, Washington, USA, pp 284-285, July 2012.

RISE Research Institutes of Sweden AB
Measurement Science and Technology - High Voltage

Performed and reviewed by

Signed by: Stefan Svensson
Date & Time: 2021-11-16 15:39:56 +01:00

Stefan Svensson

10. Comparison report of VSL

VSL Results

CCEM K5 2017

Key Comparison of 50/60 Hz Power

Measuring period: 23-2-2021 / 4-3-2021

Reporting date: 15-11-2021

Measurements executed by: E. Houtzager

Report written by: E. Houtzager

Report Checked by: G. Rietveld

Contents

Arrival of standards

The traveling standards arrived on 26 November 2020 at the VSL premises.

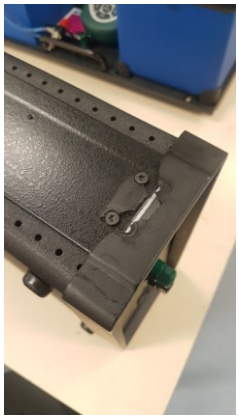

On arrival one of the power supplies was damaged but still functional.

Identification of the travelling standard: RD-22

Below the pictures of both travelling standards. The protocol states that the comparison contains an RD22 with serial number 206815. The received standard had serial number 206 816

Figure 1: reference standard: RD-22-332S, serial number: 206 816

Figure 2: reference standard: RD-22-332S, serial number: 203 409

Measurement set-up and traceability scheme

The VSL Primary Power set-up that is used to calibrate the travelling standard in this comparison consists of two HP3458A's with extended memory, synchronized to a power calibrator (Fluke 6105A). A phantom method is used to calibrate the traveling standard in which the current and voltage have two different circuits (see the figure below). One HP3458A is used to measure a voltage which is scaled by an inductive voltage divider to the 0.8 V level and the other HP3458A is used to measure the current which is converted to 0.9 V voltage by using a 0.18 Ω wideband current shunt (JV design). The phase relation between the voltage measurement and the current measurement is created by an external trigger which is supplied to both HP3458A meters from the power calibrator and a trigger unit.

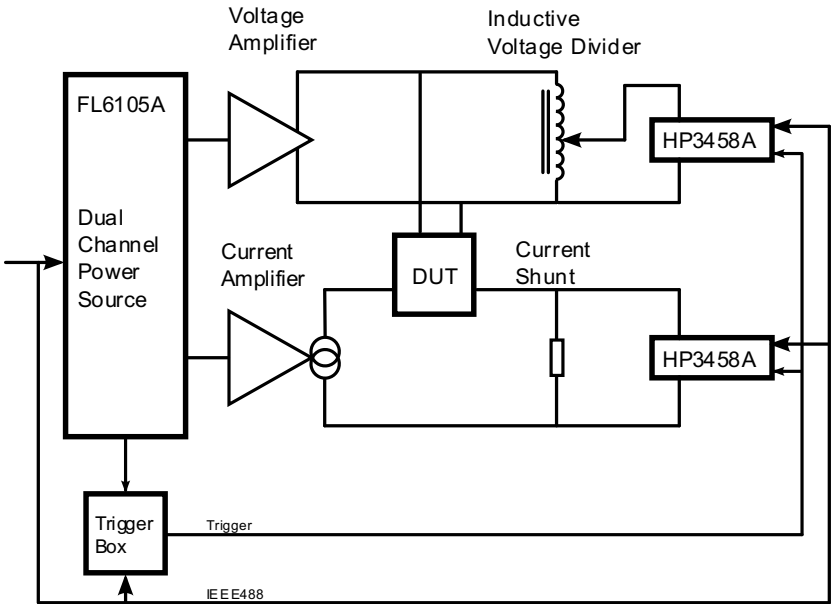

The traceability of the setup comes from several sources.

The absolute DC voltage of the two HP3458's is derived from an external Zener calibrated against the Josephson standard. The AC/DC error is determined for both HP3458's by comparison against an ACDC reference standard. The ratio error and phase displacement of the inductive voltage divider is determined by comparison against a reference voltage divider with known errors. Finally, the resistance and power coefficient of the wideband current shunt are determined using a high-accuracy DC resistance bridge. Based on the very small AC/DC error of the shunt at 100 kHz, the phase of the wideband current shunt is estimated to be less than 2 µrad at powerline frequencies. This is verified by comparing different wideband shunts against each other.

Measurement procedure

The standard was unpacked and checked for visual damage. No damage was found on the standard apart from the power supply damage.

After testing the power supply, everything was placed on the workbench where the travelling standard remained during its visit to VSL.

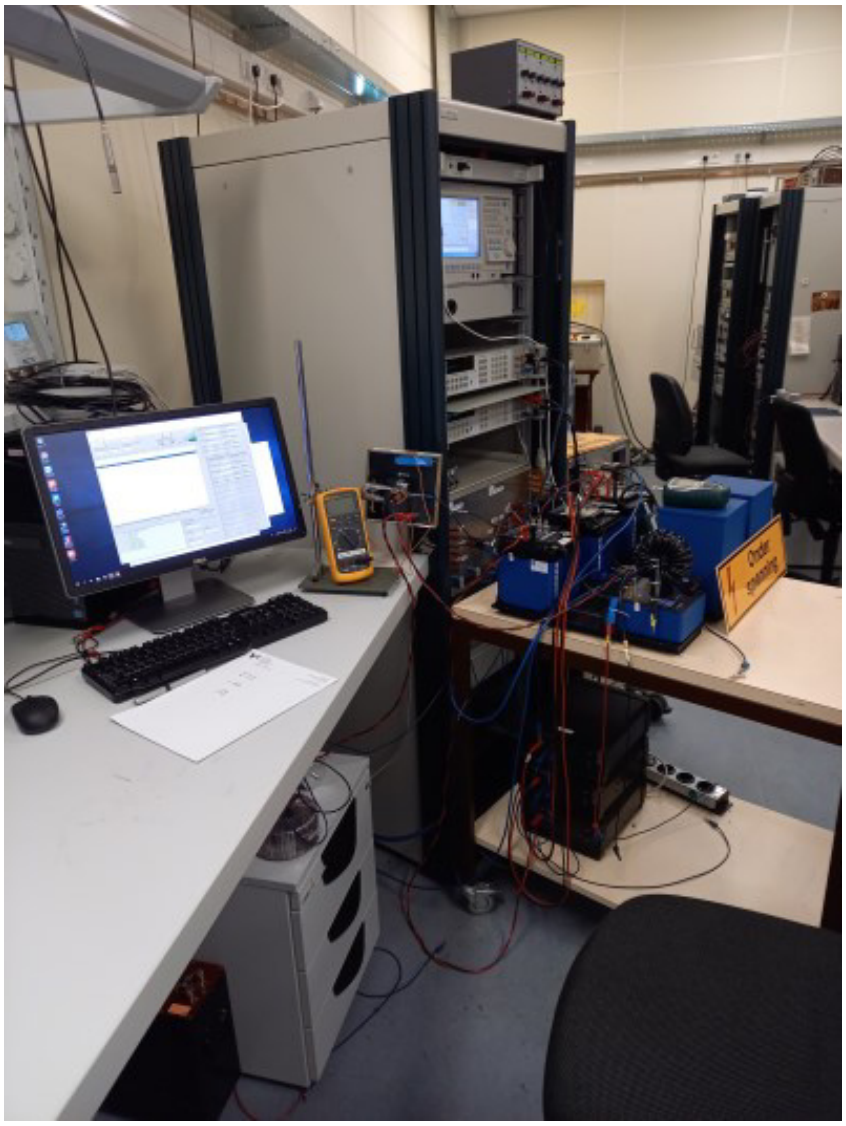

Figure 2. Travelling standards connected to the VSL primary power reference setup.

Both the ground plate of the RD22 and one of the ground terminals (Black) of the power supply were connected to the central grounding point. The entire setup, both the reference and travelling

standard were powered from an artificial mains 230 V at a frequency of 65 Hz to minimize interference between the power supply and the measurement signals.

In the connection scheme both the Lo of the voltage and current were at ground potential.

Before each measurement, the RD22 is reset (while being warm), to start the internal RD22 calibration routine. Both voltage and current were supplied to the RD22 for at least 10 minutes before starting the automated measurement sequence. This is done to let both the voltage circuit of the RD22 warm-up as well as the current shunt used in the reference setup.

The measurements were controlled by a computer which both reads the traveling standard as well as the reference setup. All setpoints were automatically measured and the results were stored in a file.

In several independent measurement runs were done which led to the results reported in the results section.

After sending the traveling standards to the next participant a thorough analysis of the data was performed. The analysis is done using a script written in “R” where all the corrections are done on the raw measurement data and finally aggregated and summarized to the desired data format.

Since we use the HP3458A with AZERO off, the importance of the lo terminal really being at zero volt is crucial. During the first arming of the HP3458 it still takes a sample of the low voltage terminal and subtracts this from all sequential samples. Because we did not measure synchronous to the generated waveform, this effect results in extra noise in both magnitude and phase.

Results

The final calibration results of the power meter are indicated in the table below:

RD22 serial number: 203409

Point	Voltage [V]	Current [A]	Power factor	Phase angle [deg]	Frequency [Hz]	Measurement date	Error value ε [µW/VA]	Expanded uncertainty u_ε [µW/VA]
1	120	5	1	0	53	26/02/2021	73	10
2	120	5	0.5 lead	60	53	26/02/2021	66	8
3	120	5	0 lead	90	53	26/02/2021	34	7
4	120	5	0.5 lag	-60	53	26/02/2021	6	8
5	120	5	0 lag	-90	53	26/02/2021	-37	6
6	240	5	1	0	53	26/02/2021	79	10
7	240	5	0.5 lead	60	53	26/02/2021	74	7
8	240	5	0 lead	90	53	26/02/2021	39	6
9	240	5	0.5 lag	-60	53	26/02/2021	5	7
10	240	5	0 lag	-90	53	26/02/2021	-42	6

RD22 serial number: 206815

Point	Voltage [V]	Current [A]	Power factor	Phase angle [deg]	Frequency [Hz]	Measurement date	Error value ε [µW/VA]	Expanded uncertainty u_ε [µW/VA]
1	120	5	1	0	53	26/02/2021	-65	10
2	120	5	0.5 lead	60	53	26/02/2021	-70	8
3	120	5	0 lead	90	53	26/02/2021	-44	7
4	120	5	0.5 lag	-60	53	26/02/2021	5	8
5	120	5	0 lag	-90	53	26/02/2021	41	6
6	240	5	1	0	53	26/02/2021	-64	10
7	240	5	0.5 lead	60	53	26/02/2021	-71	7
8	240	5	0 lead	90	53	26/02/2021	-45	6
9	240	5	0.5 lag	-60	53	26/02/2021	6	7
10	240	5	0 lag	-90	53	26/02/2021	42	6

For the full results see the submitted Excel file.

Uncertainty budget

Two uncertainty budgets are given, one for power factor 1 and for power factor 0. A summary of the individual uncertainty components is given below.

Uncertainty Components

The uncertainty components that were taken into account in the uncertainty analysis of the VSL primary power reference setup are:

P_{DUT}:	Reading of the travelling standard (type A contribution)
$U_{HP3458A}$:	The raw measurement voltage of the HP 3458A measuring the voltage
$Ratio_{Vtrans}$:	Ratio of the voltage transformer
HP_{Vacdc}:	AC/DC error @ 53 Hz of the HP3458 measuring voltage
$HP_{VDCcalibration}$:	DC calibration of the HP3458A measuring the voltage
$I_{HP3458A}$:	The raw measurement voltage of the HP 3458A measuring the current
R_{shunt}:	The Resistance value of the used wideband current shunt
R_{Iacdc}:	AC/DC error @ 53 Hz of the wideband current shunt
R_{pc}:	Change in current shunt value due to the power coefficient of the shunt
HP_{Iacdc}:	AC/DC error @ 53 Hz of the HP3458 measuring the current
$HP_{IDCcalibration}$:	DC calibration of the HP3458A measuring the current
ϕ_{HPDiff}:	Phase error between the HP3458As
$\phi_{voltagetransformer}$:	Phase error in the voltage transformer
$\phi_{currentshunt}$:	Phase error in the current shunt

PF=1

Main uncertainty Components y_i	Standard Uncertainty $u(y_i)$	Type method A or B of evaluation/probability distribution function	Sensitivity Coefficient c_i	Uncertainty Contribution $u(R_i)$ [W/VA]	Degrees of freedom n_i
P_{DUT}	$1 \cdot 10^{-6}$ W/VA	A normal	1	$1.0 \cdot 10^{-6}$	7
$U_{HP3458A}$	$1.60 \cdot 10^{-6}$ V	A normal	1.2	$2.0 \cdot 10^{-6}$	20
$Ratio_{Vtrans}$	$333 \cdot 10^{-6}$ -	B normal	$6.0 \cdot 10^{-3}$	$2.0 \cdot 10^{-6}$	20
HP_{Vacdc}	$2.00 \cdot 10^{-6}$ V/V	B normal	1.0	$2.0 \cdot 10^{-6}$	20
$HPV_{DCcalibration}$	$1.00 \cdot 10^{-6}$ V/V	B normal	1.0	$1.0 \cdot 10^{-6}$	20
$I_{HP3458A}$	$1.60 \cdot 10^{-6}$ V	A normal	1.2	$2.0 \cdot 10^{-6}$	20
R_{shunt}	$180 \cdot 10^{-9}$ W	B normal	5.6	$1.0 \cdot 10^{-6}$	20
R_{Iacdc}	$50.0 \cdot 10^{-9}$ Ω/Ω	B normal	1.0	$50 \cdot 10^{-9}$	20
R_{pc}	$500 \cdot 10^{-9}$ Ω/Ω /W	B normal	3.6	$1.8 \cdot 10^{-6}$	20
HP_{Iacdc}	$2.00 \cdot 10^{-6}$ V/V	B normal	1.0	$2.0 \cdot 10^{-6}$	20
$HPI_{DCcalibration}$	$1.00 \cdot 10^{-6}$ V/V	B normal	1.0	$1.0 \cdot 10^{-6}$	20
ϕ_{HPDiff}	$1.00 \cdot 10^{-6}$ rad	A normal	0.0	0.0	20
$\phi_{voltagetransformer}$	$2.00 \cdot 10^{-6}$ rad	B normal	0.0	0.0	20
$\phi_{currentshunt}$	$2.00 \cdot 10^{-6}$ rad	B normal	0.0	0.0	20

Quantity	Expanded Uncertainty	Coverage factor	Coverage
δP	$10 \cdot 10^{-6}$ W/VA	2.00	95% (normal)

PF=0

Main uncertainty Components y_i	Standard Uncertainty $u(y_i)$	Type method A or B of evaluation/probability distribution function	Sensitivity Coefficient c_i	Uncertainty Contribution $u(R_i)$ [W/VA]	Degrees of freedom n_i
P_{DUT}	$0.5 \cdot 10^{-6}$ W/VA	A normal	1	$0.5 \cdot 10^{-6}$	7
$U_{HP3458A}$	$1.60 \cdot 10^{-6}$ V	A normal	0	0.0	20
$Ratio_{Vtrans}$	$417 \cdot 10^{-6}$ -	B normal	0	0.0	20
HP_{Vacdc}	$2.00 \cdot 10^{-6}$ V/V	B normal	0	0.0	20
$HPV_{DCcalibration}$	$1.00 \cdot 10^{-6}$ V/V	B normal	0	0.0	20
$I_{HP3458A}$	$1.60 \cdot 10^{-6}$ V	A normal	0	0.0	20
R_{shunt}	$180 \cdot 10^{-9}$ W	B normal	0	0.0	20
R_{Iacdc}	$50.0 \cdot 10^{-9}$ Ω/Ω	B normal	0	0.0	20
R_{pc}	$500 \cdot 10^{-9}$ Ω/Ω/W	B normal	0	0.0	0.0
HP_{Iacdc}	$2.00 \cdot 10^{-6}$ V/V	B normal	0	0.0	20
$HPI_{DCcalibration}$	$1.00 \cdot 10^{-6}$ V/V	B normal	0	0.0	20
ϕ_{HPDiff}	$1.00 \cdot 10^{-6}$ rad	A normal	1.0	$1.0 \cdot 10^{-6}$	20
$\phi_{voltagetransformer}$	$2.00 \cdot 10^{-6}$ rad	B normal	1.0	$2.0 \cdot 10^{-6}$	20
$\phi_{currentshunt}$	$2.00 \cdot 10^{-6}$ rad	B normal	1.0	$2.0 \cdot 10^{-6}$	20

Quantity	Expanded Uncertainty	Coverage factor	Coverage
δP	$6 \cdot 10^{-6}$ W/VA	2.00	95% (normal)

CCEM-K5.2017 Key Comparison of 50/60 Hz Power

Report Draft B

Annex D

-

Read-me file to digital supplement

Annex E

In order to facilitate further analysis and uptake of the intercomparison measurement data and computed results, the main parts of this analysis have been made available in the form of a digital, machine-readable supplement. The main data structures of interest have been encoded in JSON format which is available in the form of .json file as Annex E. This also includes the bilateral degrees of equivalence d'_{ij} and the uncertainties $u(d'_{ij})$ which have not been presented in this report. The values of d'_{ij} are stored in the variable Calc.bildoe_per_lab_lab_pnt, whereas the values of $u(d'_{ij})$ are stored in the variable Calc.ubildoe_per_lab_lab_pnt.

Furthermore, the full covariance matrices of the corrected measurement results and of the DoEs are given as well as matrices with sensitivity coefficients, which can be of use when linking regional (RMO) comparisons to this CIPM comparison.

The data structure is split into three parts:

- 'Gen' contains some general variables;
- 'Stab' contains the measurement results of the stability measurements;
- 'Meas' contains the provided measurement results by the participating laboratories;
- 'Calc' contains the computed results as presented in the main part of this document1.

More details on the variables stored in the digital supplement Annex E can be found in Table 1.

Table 1: Explanation of the variables stored in the digital supplement Annex E.

Variable name	**Explanation**	**Reference in report**
General variables (Gen)		
• n_pnts	Number of test points (= 10)	Table 2
• n_labs	Number of participating laboratories (= 10)	Table 1
• n_ts	Number of travelling standards (= 2)	Section 3
• meas_pnt_defs_per_pnt	Definition of test points	Table 2
• laboratory_name_per_lab	Names of the participating laboratories	Table 1
• extended_laboratory_name_ per_extlab	Names of the participating laboratories with an additional postfix -A or -B depending on the travelling standard being reported on	Table 1
• rho_measurement_uncertainty	Assumed correlation coefficient between provided measurement results by the same laboratory for the same nominal quantity (= 0.8)	Equation (3)

Variable name	**Explanation**	**Reference in report**
Stability measurement data (Stab)		
• lab_name	The name of the laboratory performing the stability measurements (= PTB)	Table 1
• date_per_rep_ts_pnt	The measurement dates of the stability measurements for each repeated measurement, traveling standard and test point	Table 3 and Table 4
• y_per_rep_ts_pnt	The measured values of the stability measurements	Table 3 and Table 4
• uy_per_rep_ts_pnt	The standard uncertainties of the stability measurements	Table 3 and Table 4
Provided measurement data (Meas)		
• date_per_labext_pnt	Matrix containing the measurement dates for each laboratory (with postfixes -A and -B) and each test point	Table 1
• y_per_labext_pnt	Matrix containing the provided measurement values for each laboratory (with postfix -A or -B) and each test point	Annex A – Table 1 and Table 2
• uy_per_labext_pnt	Matrix containing the provided standard uncertainty for each laboratory (with postfix -A or -B) and each test point	Annex A – Table 1 and Table 2
Calculated results (Calc)		
• ycor_per_labext_pnt	Matrix containing the corrected measurement values for each laboratory (with postfix -A or -B) and each test point	Equation (8)
• vycor_per_labext_labext_pnt	3D-matrix whereby each 2D-slice (per test point, 3rd dimension) contains the covariance matrix of the corrected measurement values for each pair of laboratories (with postfix -A or -B)	Equation (9)
• kcrv_per_ts_pnt	Matrix containing the computed KCRVs for each of the TSs for each test point	Equation (10)
• vkcrv_per_ts_ts_pnt	3D-matrix whereby each 2D-slice (per test point, 3rd dimension) contains the covariance matrix of the computed KCRVs for each pair of TSs	Equation (10)

Variable name	Explanation	Reference in report
• sens_kcrv_ycor_per_ts_labext_pnt	3D-matrix whereby each 2D-slice (per test point, 3rd dimension) contains the sensitivity coefficients or weights for each of the KCRVs w.r.t. each of the provided measurement values	Equation (10)
• doe_ts_per_labext_pnt	Matrix containing the DoE-TSs before merging for each laboratory (with postfix -A or -B) and for each test point	Equation (11)
• vdoe_ts_per_labext_labext_pnt	3D-matrix whereby each 2D-slice (per test point, 3rd dimension) contains the covariance matrix of the DoEs for each pair of laboratories (with postfix -A or -B)	Equation (12)
• doe_per_lab_pnt	Matrix containing the merged DoEs for each laboratory per test point	Equation (14)
• vdoe_per_lab_lab_pnt	3D-matrix whereby each 2D-slice (per test point, 3rd dimension) contains the covariance matrix of the merged DoEs for each pair of laboratories	Equation (16)
• sens_doe_ycor_per_lab_labext_pnt	3D-matrix whereby each 2D-slice (per test point, 3rd dimension) contains the sensitivity coefficients of the merged DoE for each of the laboratories w.r.t. each of the provided measurement values	Product based on Equations (10), (11) and (15)
• bildoe_per_lab_lab_pnt	3D-matrix whereby each 2D-slice (per test point, 3rd dimension) contains the bilateral DoEs (for the merged DoEs) for each pair of laboratories	Equation (17)
• ubildoe_per_lab_lab_pnt	3D-matrix whereby each 2D-slice (per test point, 3rd dimension) contains the standard uncertainty of the bilateral DoEs (for the merged DoEs) for each pair of laboratories	Equation (18)